

Design, development and evaluation of formulations of poorly water soluble drugs intended for oral delivery

A thesis submitted to the University of Dhaka in partial fulfillment of the degree of Doctor of Philosophy

By

Md. Rezowanur Rahman

March, 2022



DEPARTMENT OF PHARMACEUTICAL TECHNOLOGY
FACULTY OF PHARMACY
UNIVERSITY OF DHAKA

Declaration

This is to certify that Md. Rezowanur Rahman has carried out his thesis work entitled “Design, development and evaluation of formulations of poorly water soluble drugs intended for oral delivery” under our joint supervision for the degree of Doctor of Philosophy in the Department of Pharmaceutical Technology, Faculty of Pharmacy, University of Dhaka. This work, thereof, has not been submitted in substance anywhere for any other degree or award.

(Prof. Dr. Abu Shara Shamsur Rouf)
Supervisor
Department of Pharmaceutical Technology
Faculty of Pharmacy
University of Dhaka.

(Prof. Dr. Sitesh Chandra Bachar)
Co-Supervisor
Department of Pharmacy &
Dean
Faculty of Pharmacy
University of Dhaka.

Dedicated to my beloved wife, Rebeka, my son Raiyan, my
parents and all members of my family

Acknowledgement

First of all, I want to submit my sincere respect and earnest gratitude go to my honorable supervisor, Professor Dr. Abu Shara Samsur Rouf, Department of Pharmaceutical Technology, Faculty of Pharmacy, University of Dhaka for his motivating, knowledgeable, fervent guidance and outstanding supervision that encouraged me to complete the research work successfully. I consider myself privileged to have the chance to work with a very dynamic and competent professor like him.

I also want to give my warmest thanks to my co-supervisor, Professor Dr. Sitiesh Chandra Bachar, Department of Pharmaceutical Technology, Faculty of Pharmacy, University of Dhaka for his support, motivation and guidance.

Abstract

Ledipasvir and Daclatasvir, belonging to the BCS class 2, and Velpatasvir, belonging to the BCS class 4, are directly acting anti-viral agents used to treat Hepatitis C virus infections. Owing to poor aqueous solubility and oral bioavailability, development of effective delivery system for these drugs has been enormously challenging. Moreover, suitable dosage forms for pediatric and geriatric patients and patients having difficulty in swallowing as well pose added burden. Therefore, the aim of the present study was to develop a nanosuspension, via solid dispersion technique, based liquid oral suspension using Quality by Design (QbD) approach. Primarily, the compatible polymers for Ledipasvir were screened using FTIR and DSC, and finally the polymers - Poloxamer 188, Poloxamer 407, HPC and HMPC were selected, considering their ability to convert the API into amorphous state in solid dispersions. Design of formulation and analysis with the D-Optimal design using Design Expert[®] software revealed that Poloxamer 188 and Poloxamer 407 in 0.3:0.7 ratio of Ledipasvir:Polymer produced the optimized nanosuspension formulations with a statistically significant mathematical model. Subsequently, the formulations were stabilized using suspension vehicle optimized via Box Behnken Design using the amount of xanthan gum (gm), avicel[®] RC-591 (gm) and citric acid monohydrate (gm) as independent variables whereas viscosity (cp) and zeta potential (mv) as responses. The dissolution profiles revealed that the prepared suspensions of Ledipasvir had much faster dissolution than pure API, suspensions prepared with micronized and non-micronized API, and the market products available as tablet dosage form. *In-vivo* simulation studies using PKSolver[®] suggested that the absorption of drug from the formulated suspensions was comparable to that of market product up to single dose level (90mg) and superseded in triplicate dose level (270 mg). The formulated suspensions were found to be stable over three- and six-months periods, identified via accelerated stability studies. Interestingly, dissolution profile of the stabilized suspensions was found to be similar after six months. An RP-HPLC method to determine the assay content of Ledipasvir in the finished product has also been developed using 3² full factorial design with a Diphenyl column (250 mm X 4.6 mm, 5 μm), the detection wavelength of 330 nm and the injection volume of 20 μL. The optimized method consisted a mobile phase of buffer:acetonitrile at 48:52 ratio and flow rate of 1.7 ml/min. A simple and rapid UV method was developed simultaneously to analyze Ledipasvir and shown to be equivalent to the developed RP-HPLC method. To determine the content of the residual solvent in

Ledipasvir solid dispersions, a GC method was developed using the same 3^2 full factorial design and fused silica GC capillary column (30-m x 0.32-mm x 1.8- μ m), Nitrogen with 14.0 psi through head space as carrier gas. Validation of all the developed methods were carried out by following ICH Q2 (R1) guideline.

The best results were found with Poloxamer 188 in the Ledipasvir study at a drug:polymer ratio of 0.7:1.3 in terms of *in-vivo* simulation. Therefore, both Daclatasvir and Velpatasvir were further studied to develop solid dispersion based nanosuspensions and finally a stabilized oral suspension using Poloxamer 188. In case of Daclatasvir, the drug failed to produce amorphous solid dispersion and hence, was not further evaluated for nanosuspension preparation. On contrary, Velpatasvir produced amorphous solid dispersion and thus, nanosuspension was prepared using the same approach applied for Ledipasvir. Afterward, the nanosuspension of Velpatasvir were stabilized using the same method used to stabilize Ledipasvir nanosuspension. The study of the dissolution profiles revealed that stabilized suspension of Velpatasvir had much faster dissolution than its market product available as tablet dosage form. Finally, *in-vivo* simulation study revealed that single dose of formulated suspension gave the comparable absorption profile to that of the market product.

Key words: D-Optimal, Design Expert[®], Box Behnken, PKSolver[®], RP-HPLC, GC, Validation

Table of Contents

Chapter No.	Tittle	Page
1	General Introduction	1-25
1.1	Oral drug delivery system	1
1.1.1	Advantages of the oral route of drug administration	1
1.1.2	Disadvantages of the oral route of drug administration	1
1.1.3	Different oral dosage forms	1
1.2	Poorly water soluble drugs	6
1.3	Biopharmaceutical classification system (BCS)	6
1.3.1	Solubility	6
1.3.2	Permeability	6
1.3.3	Dissolution	7
1.4	Bioavailability	7
1.5	Challenges of newly developed drugs	7
1.6	Taxonomy	8
1.6.1	Taxonomy of Ledipasvir	8
1.6.2	Taxonomy of Daclatasvir	8
1.6.3	Taxonomy of Velpatasvir	9
1.7	Physical properties	9
1.7.1	Physical properties of Ledipasvir	9
1.7.2	Physical properties of Daclatasvir	9
1.7.3	Physical properties of Velpatasvir	10
1.8	Chemical properties	10
1.8.1	Chemical properties of Ledipasvir	10
1.8.2	Chemical properties of Daclatasvir	11
1.8.3	Chemical properties of Velpatasvir	12
1.9	Pharmacokinetics	12
1.9.1	Pharmacokinetics of Ledipasvir	12
1.9.2	Pharmacokinetics of Daclatasvir	13
1.9.3	Pharmacokinetics of Velpatasvir	13
1.10	Pharmacodynamics and mechanism of action	14

Chapter No.	Title	Page
1.10.1	Pharmacodynamics and mechanism of action of Ledipasvir	14
1.10.2	Pharmacodynamics and mechanism of action of Daclatasvir	14
1.10.3	Pharmacodynamics and mechanism of action of Velpatasvir	14
1.11	Solid dispersion	15
1.11.1	Methods of preparation of solid dispersions	15
1.11.2	Characterization of Solid Dispersion	16
1.12	Nanosuspension approach	17
1.12.1	Mechanism of improvement of dissolution	17
1.13	Advantages of nanosuspension over traditional approach	18
1.14	Method of preparation of nanosuspension	18
1.14.1	Bottom-Up Technology	18
1.14.2	Top-Down Technology	19
1.15	Characterization of nanosuspension	21
1.15.1	Particle size and polydispersity index	21
1.15.2	Crystalline state and particle morphology	22
1.15.3	Particle charge (zeta potential)	22
1.15.4	Sedimentation Volume	23
1.15.5	Redispersibility	23
1.15.6	Stability	23
1.16	Analytical methods	24
1.16.1	RP-HPLC method	24
1.16.2	UV method	24
1.16.3	Residual solvent determination	24
1.17	Generalized objective of the research	25
2	<i>Materials and Methods</i>	26-67
2.1	Materials	26
2.1.1	Drug Profile	27
2.1.2	Excipients Profile	28
2.1.3	Equipment	32
2.2	Methods	33

Chapter No.	Tittle	Page
2.2.1	Suspension with non-micronized and micronized Ledipasvir	33
2.2.2	Characterization of suspensions with non-micronized and micronized Ledipasvir	34
2.2.3	Solubility study of Ledipasvir	34
2.2.4	Solution stability study of Ledipasvir in different solvents	35
2.2.5	Drug-excipients compatibility study	36
2.2.6	Preparation of solid dispersions	37
2.2.7	Preparation of nanosuspensions	38
2.2.8	Characterization of nanosuspensions	41
2.2.9	Stabilization of nanosuspensions	43
2.2.10	Dissolution Method	46
2.2.11	Dissolution profile comparison	52
2.2.12	Drug Release Kinetics	52
2.2.13	<i>In-vivo</i> simulation study	52
2.2.14	Stability study of the formulated suspensions	55
2.2.15	Analytical method for analysis of Ledipasvir in pharmaceutical dosage forms	55
2.2.16	Method of analysis for Velpatasvir content in pharmaceutical dosage forms	61
2.2.17	Development and validation of GC headspace method for Ledipasvir	62
2.2.18	Residual solvent determination	66
3	<i>Results and Discussion</i>	68-237
3.1	Challenges with delivery of Ledipasvir, Daclatasvir and Velpatasvir	68
3.1.1	Absorption and Dissolution	68
3.1.2	Difficulty for paediatric and geriatric patients	68
3.2	Objective of the study	68
3.3	Results and discussion	69
3.3.1	Characterization of suspensions prepared with non-micronized and micronized Ledipasvir	69

Chapter No.	Title	Page
3.3.2	Solubility Study	71
3.3.3	Solution stability	73
3.3.4	Drug-excipients compatibility study	78
3.3.5	Characterization of prepared solid dispersions	93
3.3.6	Characterization of prepared nanosuspensions	97
3.3.7	QbD for preparation of Ledipasvir nanosuspension	111
3.3.8	Stabilization of prepared nanosuspension	124
3.3.9	Comparative dissolution profiles and kinetics study	147
3.3.10	<i>In-vivo</i> simulation study	162
3.3.11	Stability Study	171
3.3.12	Development and validation of analytical methods for Ledipasvir	178
3.3.13	Validation of developed RP-HPLC analytical method	189
3.3.14	Development and validation of UV method for analysis of Ledipasvir	199
3.3.15	Equivalency between UV and HPLC method	207
3.3.16	Development of GC method	214
3.3.17	Validation of developed GC method	225
3.3.18	Residual solvent determination of SD formulations	233
4	<i>Conclusion and Future Direction</i>	238-242
4.1	Discussion on formulation	238
4.2	Discussion on analytical method development and validation	241
4.3	Future direction	242
5	<i>References</i>	243-257

List of Tables

Table No.	Title of Table	Page
1.1	Taxonomy of Ledipasvir	8
1.2	Taxonomy of Daclatasvir	8

Table No.	Title of Table	Page
1.3	Taxonomy of Velpatasvir	9
1.4	Physical properties of Ledipasvir	9
1.5	Physical properties of Daclatasvir	9
1.6	Physical properties of Velpatasvir	10
1.7	Chemical properties of Ledipasvir	10
1.8	Chemical properties of Daclatasvir	11
1.9	Chemical properties of Velpatasvir	12
2.1	List of ingredients used in the present study	26
2.2	List of instruments used in the present study	32
2.3	Composition of suspensions with non-micronized and micronized API	33
2.4	Solubility study design of ledipasvir in methanol, ethanol, dichloromethane and acetone	35
2.5	Solution stability study design of ledipasvir in methanol, ethanol, dichloromethane and acetone	36
2.6	Formulation for solid dispersions of Ledipasvir	38
2.7	Formulation for solid dispersions of Daclatasvir and Velpatasvir	38
2.8	Ratios of API and polymers for the D-Optimal mixture design	40
2.9	Solid dispersion (SD) formulation with different ratios of Ledipasvir and polymer	40
2.10	Solid dispersion (SD) formulation with different ratios of Velpatasvir and polymer	41
2.11	Preparation of sample solution for accuracy	48
2.12	Standard and placebo for accuracy study (HPLC)	59
3.1	Assay of Ledipasvir in suspensions prepared with non-micronized and micronized API	69
3.2	Dissolution profiles of suspensions prepared with non-micronized and micronized API	70
3.3	Solubility data of Ledipasvir in methanol, ethanol, dichloromethane and acetone	71
3.4	Solution stability study of the solution of Ledipasvir in methanol	74

Table No.	Title of Table	Page
3.5	Solution stability study of the solution of Ledipasvir in ethanol	75
3.6	Solution stability study of the solution of Ledipasvir in dichloromethane	76
3.7	Solution stability study of the solution of Ledipasvir in acetone	77
3.8	DSC characteristics of Ledipasvir, polymers and the physical mixtures	86
3.9	PSD of different SD suspensions	99
3.10	PDI of different nanosuspensions	100
3.11	Viscosity of all SD suspensions	101
3.12	Zeta Potential of different SD suspensions	102
3.13	PSD of different SD suspensions of Velpatasvir	105
3.14	PDI of different nanosuspensions of Velpatasvir	106
3.15	Zeta Potential of SD suspensions of Velpatasvir	106
3.16	Results of visual observation of prepared LDV SD suspensions at week 1, 2, 3 and 4	107
3.17	Fit summary for response 1 (PSD) of NSF1	111
3.18	ANOVA for linear model of response 1 (PSD) of NSF1	111
3.19	Fit summary for response 2 (PDI) of NSF1	112
3.20	ANOVA for linear model of response 2 (PDI) of NSF1	112
3.21	Constraints for optimization of NSF1	114
3.22	Solution for optimized formulation	114
3.23	Fit summary for response 1 (PSD) of NSF2	115
3.24	ANOVA for linear model of response 1 (PSD) of NSF2	115
3.25	Fit summary for response 2 (PDI) of NSF2	116
3.26	ANOVA for linear model of response 2 (PDI) of NSF2	116
3.27	Constraints for optimization of NSF2	118
3.28	Optimized solution for NSF2	118
3.29	Fit Summary for response 1 (PSD) of NSF4	119
3.30	ANOVA for linear model of response 1 (PSD) of NSF4	119
3.31	Fit summary for response 2 (PDI) of NSF4	120

Table No.	Title of Table	Page
3.32	ANOVA for mean model of response 2 (PDI) of NSF4	120
3.33	Fit summary for response 1 (PSD) of NSF5	121
3.34	ANOVA for linear model of response 1 (PSD) of NSF5	121
3.35	Fit summary for response 2 (PDI) of NSF5	122
3.36	ANOVA for linear model of response 2 (PDI) of NSF5	122
3.37	Independent variables for designing of suspension vehicle	124
3.38	Designed runs using Box-Behnken design and experimental observation of responses f	124
3.39	Fit summary for response 1 for optimization of suspension vehicle	125
3.40	ANOVA for linear model for response 1 for optimization of suspension vehicle	126
3.41	Fit summary for response 2 for optimization of suspension vehicle	129
3.42	ANOVA for quadratic model for response 2 for optimization of suspension vehicle	129
3.43	Optimization criteria for optimization of responses	132
3.44	Constraints for optimization of design	132
3.45	Final formulation for the suspension vehicle for stabilization of prepared nanosuspension	133
3.46	Composition of stabilized suspensions of Ledipasvir	134
3.47	Composition of stabilized suspensions of Velpatasvir	135
3.48	Zeta Potential of the suspension vehicle	135
3.49	PSD of the suspension vehicle	136
3.50	Zeta potential of the stabilized Ledipasvir suspensions	136
3.51	Zeta potential of the stabilized Velpatasvir suspension	137
3.52	Sedimentation volumes of FNSF1a and FNSF2a at different time points	138
3.53	Assay of Ledipasvir in the stabilized nanosuspensions	140
3.54	Assay of Velpatasvir in the stabilized suspension	141
3.55	Dissolution profiles of the stabilized suspension, FNSF1a (Individual samples)	142

Table No.	Title of Table	Page
3.56	Dissolution profiles of the stabilized suspension, FNSF2a (Individual samples)	143
3.57	Dissolution profiles of the stabilized suspension, FNSF1a and FNSF2a (average)	145
3.58	Dissolution profiles of the stabilized suspension, VFNSF1a	146
3.59	Dissolution profiles of different preparations of Ledipasvir	147
3.60	Dissolution profile comparison with similarity factor (f2), difference factor (f1)	148
3.61	Dissolution profiles of different preparations of Velpatasvir	149
3.62	Dissolution profile comparison with similarity factor (f2), difference factor (f1)	150
3.63	Data for zero order plot	151
3.64	Data for first order plot	152
3.65	Data for Korsmeyer-Peppas plot	152
3.66	Data for Higuchi plot	154
3.67	Data for Hixson plot	155
3.68	R2 values of different mathematical models obtained for studied preparations	156
3.69	Data for zero order plot	156
3.70	Data for first order plot	157
3.71	Data for Korsmeyer-Peppas plot	158
3.72	Data for Higuchi plot	159
3.73	Data for Hixson plot	160
3.74	R2 values of different mathematical models obtained for studied preparations	161
3.75	Amount of Ledipasvir released from market product 1 (MP1) (90mg dose)	162
3.76	Predicted blood conc. of Ledipasvir from <i>in-vitro</i> dissolution data from MP1 (90mg dose) MP1	163
3.77	Predicted PK parameters for MP1 along with %PE	164

Table No.	Title of Table	Page
3.78	Drug conc. calculated from dissolution profiles for FNSF1a and FNSF2a for a dose of 90mg	164
3.79	Predicted PK parameters for FNSF1a and FNSF2a suspensions for 90mg dose	165
3.80	Dissolution profiles of MP1, FNSF1a, FNSF2a (270mg dose)	166
3.81	Drug conc. calculated from dissolution profiles for MP1, FNSF1a and FNSF2a for a dose of 270mg	167
3.82	Predicted pharmacokinetic parameters for MP1, FNSF1a and FNSF2a for a dose of 270mg	168
3.83	Drug conc. calculated from dissolution profiles for VFNSF1a	169
3.84	Predicted PK parameters for VFNSF1a suspension	170
3.85	Zeta potential of the formulated suspensions of Ledipasvir, FNSF1a and FNSF2a after 3 and 6 months at accelerated conditions	171
3.86	Assay content of the formulated suspensions of Ledipasvir, FNSF1a and FNSF2a after 3 and 6 months at accelerated conditions	172
3.87	ANOVA table for assay results of FNSF1(a)	173
3.88	ANOVA table for assay results of FNSF2(a)	174
3.89	Dissolution profiles of Ledipasvir of the final formulations after 6 months at accelerated conditions	175
3.90	Dissolution profile comparison with similarity factor (f2), difference factor (f1)	177
3.91	Fit summary for response 1 (Retention time) for development of RP-HPLC method	179
3.92	ANOVA for quadratic model for response 1 (Retention time) for development of RP-HP	179
3.93	Fit summary for response 2 (Tailing factor) for development of RP-HPLC method	182
3.94	ANOVA for quadratic model for response 2 (Tailing factor) for development of RP-HP	182
3.95	Fit summary for response 3 (Theoretical plate count) for development of RP-HPLC me	185

Table No.	Title of Table	Page
3.96	ANOVA for quadratic model for response 3 (Theoretical plate count) for development	185
3.97	Constraints for optimization of developed RP-HPLC method	188
3.98	Solution for optimized method	188
3.99	Result of linearity and range for validation of RP-HPLC method	190
3.100	Result of accuracy study for validation of RP-HPLC method	191
3.101	Result of repeatability study for validation of RP-HPLC method	192
3.102	Result of intermediate precision study for validation of RP-HPLC method	193
3.103	Result of robustness study for validation of RP-HPLC method	194
3.104	Result of system suitability test for validation of RP-HPLC method	195
3.105	Result of solution stability study (Standard) for validation of RP-HPLC method	196
3.106	Result of solution stability study (Sample) for validation of RP-HPLC method	197
3.107	Result of filter compatibility study for validation of RP-HPLC method	198
3.108	Result of Linearity and Range	201
3.109	Result of repeatability study for UV method validation	202
3.110	Result of intermediate precision study for UV method validation	203
3.111	Result of accuracy study for UV method validation	204
3.112	Result of robustness study for UV method validation	204
3.113	Result of solution stability study (standard) for UV method validation	205
3.114	Result of solution stability study (sample) for UV method validation	206
3.115	Results of the regression analysis of data for the quantitation of Ledipasvir	208
3.116	Comparison of repeatability and intermediate precision for HPLC and UV assay method	209
3.117	Comparison of accuracy for HPLC and UV assay methods	210

Table No.	Title of Table	Page
3.118	Comparison of solution stability study for HPLC and UV assay methods (standard solution)	210
3.119	Comparison of solution stability study for HPLC and UV assay methods (sample solution)	211
3.120	% Recovery of Ledipasvir from HPLC and UV method	212
3.121	ANOVA table for comparing % recovery of Ledipasvir from HPLC and UV method	212
3.122	Paired t-test for comparing % recovery of Ledipasvir from HPLC and UV method	213
3.123	Paired equivalence test for comparing % recovery of Ledipasvir from HPLC and UV method	214
3.124	Fit summary for response 1 for GC method development	215
3.125	ANOVA for quadratic model for response 1 (Retention time) GC method development	218
3.126	Fit summary for response 2 (Tailing factor) for GC method development	218
3.127	ANOVA for 2FI model for response 2 (Tailing factor) for GC method development	221
3.128	Fit summary for response 3 (Theoretical plate count) for GC method development	221
3.129	ANOVA for 2FI model for response 3 (Theoretical plate count) for GC method development	224
3.130	Constraints for optimization of developed GC method	224
3.131	Solutions for optimization of developed GC method	225
3.132	Result of linearity and range for GC method validation	225
3.133	Repeatability result of dichloromethane for GC method validation	226
3.134	Intermediate precision result of dichloromethane for GC method validation	227
3.135	Accuracy result of dichloromethane for GC method validation	228
3.136	Result of robustness study for GC method validation	230
3.137	Result of system suitability for GC method validation	231

Table No.	Title of Table	Page
3.138	% LODs for of F1SD, F2SD, F3SD, F4SD, F5SD, F6SD, F7SD and F8SD after 1 hour of secondary drying	233
3.139	% LODs of F3SD after different hours of secondary drying	233
3.140	% LODs of F1SD, F2SD, F3SD, F4SD, F5SD, F6SD, F7SD and F8SD after 24 hours of secondary drying	234
3.141	Dichloromethane content of F5SD and F8SD after 1 hour of secondary drying	235
3.142	Dichloromethane content of F5SD after different hours of secondary drying	236
3.143	Dichloromethane content of F5SD and F8SD after 24 hours of secondary drying	237

List of Figures

Figure No.	Figure Caption	Page
1.1	Structure of Ledipasvir	11
1.2	Structure of Daclatasvir	11
1.3	Structure of Velpatasvir	12
2.1	(a) Particle size distribution of non-micronized ledipasvir; (b) Particle size distribution of micronized Ledipasvir	34
2.2	a) Disposable Zeta; b) Cell Disposable Sizing Cuvette	42
2.3	Schematic representation of deconvolution and convolution processes.	53
3.1	Assay of Ledipasvir in the suspensions prepared with non-micronized and micronized API	70
3.2	Dissolution profiles of suspensions prepared with non-micronized and micronized API	71
3.3	Solubility data for Ledipasvir solution in methanol, ethanol, dichloromethane and acetone	72

Figure No.	Figure Caption	Page
3.4	(a) Detection of λ_{\max} of Ledipasvir in methanol; (b) Standard curve of Ledipasvir in methanol; (c) Detection of λ_{\max} of Ledipasvir in ethanol; (d) Standard curve of Ledipasvir in ethanol; (e) Detection of λ_{\max} of Ledipasvir in dichloromethane; (f) Standard curve of Ledipasvir in dichloromethane; (g) Detection of λ_{\max} of Ledipasvir in acetone; (h) Standard curve of Ledipasvir in acetone	73
3.5	UV spectra of the solution of Ledipasvir in methanol. at 0, 6, 12 and 24 hour and blank (methanol)	74
3.6	UV spectra of the solution of Ledipasvir in ethanol at 0, 6, 12 and 24 hour and blank (Ethanol)	75
3.7	UV spectra of the solution of Ledipasvir in dichloromethane at 0, 6, 12 and 24 hour and blank (dichloromethane)	76
3.8	UV spectra of the solution of Ledipasvir in acetone at 0, 6, 12 and 24 hour and blank (acetone)	77
3.9	FTIR spectrum of Ledipasvir	80
3.10	a) FTIR spectrum of Ledipasvir, Poloxamer 188 and binary mixture of Ledipasvir and Ploxamer 188 (D11=LDV, D21=Poloxamer 188, D141=LDV+Poloxamer 188 mixture); b) FTIR Spectrum of Ledipasvir, Poloxamer 407 and binary mixture of Ledipasvir and Ploxamer 407 (D11=LDV, D31=Poloxamer 407, D151=LDV+Poloxamer 407 mixture); c) FTIR spectrum of Ledipasvir, Klucel EF and binary mixture of Ledipasvir and Klucel EF (D11=LDV, D42=Klucel EF, D162=LDV+Klucel EF mixture); d) FTIR spectrum of Ledipasvir, Klucel EXF and binary mixture of Ledipasvir and Klucel EXF (D11=LDV, D51=Klucel EXF, D172=LDV+Klucel EXF mixture); e) FTIR spectrum of Ledipasvir, HPMC 5cps and binary mixture of Ledipasvir and HPMC 5cps (D11=LDV, D61=HPMC 5cps, D182=LDV+ HPMC 5cps mixture); f) FTIR spectrum of Ledipasvir, Povidone K17 and binary mixture of Ledipasvir and Povidone K17 (D11=LDV,	81

Figure No.	Figure Caption	Page
	D81=Povidone K17, D202=LDV+ Povidone K17 mixture); g) FTIR spectrum of Ledipasvir, Povidone K30 and binary mixture of Ledipasvir and Povidone K30 (D11=LDV, D101=Povidone K30, D222=LDV+ Povidone K30 mixture); h) FTIR spectrum of Ledipasvir, CMC Sodium and binary mixture of Ledipasvir and CMC Sodium (D11=LDV, D121= CMC Sodium , D232=LDV+ CMC Sodium mixture)	
3.11	FTIR spectrum of Daclatasvir	82
3.12	FTIR spectrum of Daclatasvir and binary mixture of Daclatasvir and Poloxamer 188	83
3.13	FTIR spectrum of Velpatasvir	83
3.14	FTIR spectrum of Velpatasvir and binary mixture of Velpatasvir and Poloxamer 188	84
3.15	a) DSC thermogram of Ledipasvir; b) DSC thermogram of Poloxamer 188; c) DSC thermogram of physical mixture of Ledipasvir and Poloxamer 188; d) DSC thermogram of Poloxamer 407; e) DSC thermogram of physical mixture of Ledipasvir and Poloxamer 407; f) DSC thermogram of Klucel EF; g) DSC thermogram of physical mixture of Ledipasvir and Klucel EF; h) DSC thermogram of Klucel EXF ; i) DSC curve of physical thermogram of physical mixture of Ledipasvir and Povidone K17; n) DSC thermogram of Povidone K30; o) DSC thermogram of physical mixture of Ledipasvir and Povidone K30; p) DSC thermogram of CMC Sodium (7MF); q) DSC thermogram of physical mixture of Ledipasvir and CMC Sodium mixture of Ledipasvir and Klucel EXF; j) DSC thermogram of HPMC 5 cps; k) DSC thermogram of physical mixture of Ledipasvir and HPMC 5cps; l) DSC thermogram of Povidone K17; m) DSC	90
3.16	DSC thermogram of Daclatasvir	90
3.17	a) DSC thermogram of Poloxamer 188; b) DSC thermogram of physical mixture of Daclatasvir and Poloxamer 188	91

Figure No.	Figure Caption	Page
3.18	DSC thermogram of Velpatasvir	91
3.19	DSC thermogram of physical mixture of Velpatasvir and Poloxamer 188	92
3.20	a) DSC curve of F1 SD (Ledipasvir-Poloxamer 188 solid dispersion); b) DSC curve of F2 SD (Ledipasvir-Poloxamer 407 solid dispersion); c) DSC curve of F3 SD (Ledipasvir-Klucel EF solid dispersion); d) DSC curve of F4 SD (Ledipasvir-Klucel EXF solid dispersion); e) DSC curve of F5 SD (Ledipasvir-HPMC 5cps solid dispersion); f) DSC curve of F6 SD (Ledipasvir-PVP K17 solid dispersion); g) DSC curve of F7 SD (Ledipasvir-PVP K30 solid dispersion); h) DSC curve of F8 SD (Ledipasvir-CMC Sodium solid dispersion)	95
3.21	DSC curve of DF1SD (Daclatasvir-Poloxamer 188 solid dispersion)	96
3.22	DSC curve of VF1SD (Velpatasvir-Poloxamer 188 solid dispersion)	97
3.23	Particle size distribution of formulated different nanosuspensions	98
3.24	a) Particle size distribution of NSF1; b) Particle size distribution of NSF1b; c) Particle size distribution of NSF1c; d) Particle size distribution of NSF2a; e) Particle size distribution of NSF2b; f) Particle size distribution of NSF2c; g) Particle size distribution of NSF4a; h) Particle size distribution of NSF4b; i) Particle size distribution of NSF4c; j) Particle size distribution of NSF5a; k) Particle size distribution of NSF5b; l) Particle size distribution of NSF5c	99
3.25	PDI of different nanosuspensions	100
3.26	Viscosity of all SD suspensions	102
3.27	Zeta potential of different SD suspensions	103

Figure No.	Figure Caption	Page
3.28	a) Zeta potential distribution of NSF1a SD suspension; b) NSF1b SD suspension; c) NSF1c SD suspension; d) NSF2a SD suspension; e) NSF2b SD suspension; f) NSF2c SD suspension; g) NSF4a SD suspension; h) NSF4b SD suspension; i) NSF4c SD suspension; j) NSF5a SD suspension; k) NSF5b SD suspension; l) NSF5c SD suspension.	104
3.29	Particle size distribution of VNSF1a	105
3.30	Zeta potential distribution of VNSF1a SD suspension	107
3.31	(a) Two component mix plots, (b) Predicted vs Actual plot for response 1 (PSD); (c) Two component mix plot, (d) Predicted vs Actual plot for response 2 (PDI) of formulation NSF1	113
3.32	Optimization plot for NSF1 formulation	114
3.33	(a) Two component mix plot, (b) Predicted vs Actual plot for response 1; (c) Two component mix plot, (d) Predicted vs Actual plot for response 2 of formulation NSF2	117
3.34	Optimization plot for NSF2 formulation	118
3.35	(a) Two component mix plot, (b) Predicted vs Actual plot for response 1 (PSD); (c) Two component mix plot, (d) Predicted vs Actual plot for response 2 (PDI) of formulation NSF4	120
3.36	(a) Two component mix plot, (b) Predicted vs Actual plot for response 1 (PSD); (c) Two component mix plot, (d) Predicted vs Actual plot for response 2 (PDI) of formulation NSF5	123
3.37	(a) Box-Cox plot; (b) Predicted vs Actual plot and; (c) Cubic plot for response 1 for optimization of suspension vehicle	127
3.38	(a) Contour plot; (b) 3D response surface plot for response 1 (Viscosity) for optimization of suspension vehicle	128
3.39	(a) Box-Cox plot; (b) Predicted vs Actual plot and; (c) Cubic plot for response 2 (Zeta potential) for optimization of suspension vehicle	130

Figure No.	Figure Caption	Page
3.40	(a) Contour plot; (b) 3D response surface plot for response 2 (Zeta potential) for optimization of suspension vehicle	131
3.41	Zeta potential distribution of the optimized suspension vehicle a) run 1 b) run 2 c) run 3	135
3.42	PSD of the optimized suspension vehicle a) run 1 b) run 2 c) run 3	136
3.43	Zeta potential of the stabilized suspensions a) FNSF1a b) FNSF2a	137
3.44	Zeta potential of the stabilized suspension VFNSF1a	137
3.45	Sedimentation volume FNSF1a and FNSF2a at a) day 0 b) at day 30 c) day 60 d) day 90 e) day 120 f) day 150 and g) day 180	139
3.46	Sedimentation volume profiles of FNSF1a and FNSF2a suspensions at day 0, 30, 60, 90, 120, 150 and 180	139
3.47	Assay of Ledipasvir in the stabilized suspensions	140
3.48	Dissolution profiles of the stabilized suspension, FNSF1a (Individual samples)	144
3.49	Dissolution profiles of the stabilized suspension, FNSF2a (Individual samples)	144
3.50	Dissolution profiles of the stabilized suspension, FNSF1a and FNSF2a (average)	145
3.51	Dissolution profiles of the stabilized suspension, VFNSF1a	146
3.52	Dissolution profiles of different preparations of Ledipasvir	148
3.53	Dissolution profiles of different preparations of Velpatasvir	150
3.54	Zero order plot of market product 1 and 2 and formulated suspensions NSF1a and NSF2a	151
3.55	First order plot of market product 1 and 2 and formulated suspensions FNSF1a and FNSF2a	152
3.56	Korsmeyer-Peppas plot of market product 1 and 2 and formulated suspensions FNSF1a and FNSF2a	153
3.57	Higuchi plot of market product 1 and 2 and formulated suspensions FNSF1a and FNSF2a	154

Figure No.	Figure Caption	Page
3.58	Hixson plot of market product 1 and 2 and formulated suspensions FNSF1a and FNSF2a	155
3.59	Zero order plot of market product 3 and formulated suspension VNSF1a	157
3.60	First order plot of market product 3 and formulated suspension VNSF1a	158
3.61	Korsmeyer-Peppas plot of market product 3 and formulated suspension VNSF1a	159
3.62	Higuchi plot of market product 3 and formulated suspension VNSF1a	160
3.63	Hixson plot of market product 3 and formulated suspension VNSF1a	161
3.64	Drug concentration profiles calculated from dissolution profiles for MP1, FNSF1a and FNSF2a for a dose of 90mg	165
3.65	Dissolution profiles of MP1, FNSF1a, FNSF2a (270mg dose)	167
3.66	Drug concentration profiles calculated from dissolution profiles for MP1, FNSF1a and FNSF2a for a dose of 270 mg	168
3.67	Drug concentration profiles calculated from dissolution profiles for MP3 and VNSF1a	170
3.68	Zeta potential of the FNSF1(a) formulation after 3 months at accelerated conditions; (b) formulations after 6 months at accelerated conditions.	171
3.69	Zeta potential of the FNSF2(a) formulations after 3 months at accelerated conditions; (b) formulations after 6 months at accelerated conditions.	172
3.70	Dissolution profiles of Ledipasvir of the final formulations after 3 and 6 months at accelerated conditions	176
3.71	3D response surface plot for standard error of design for development of RP-HPLC method	178

Figure No.	Figure Caption	Page
3.72	(a) Normal plot of residuals; (b) Box-Cox plot for power transform; (c) Predicted vs Actual plot; (d) Perturbation plot for response 1 (Retention time)	180
3.73	(a) Contour plot; (b) 3D response surface plot for response 1 (Retention time) for development of RP-HPLC method	181
3.74	(a) Normal plot of residuals; (b) Box-Cox plot for power transform; (c) Predicted vs Actual plot; (d) Perturbation plot for response 2 (Tailing factor)	183
3.75	(a) Contour plot; (b) 3D response surface plot for response 2 (Tailing factor) for development of RP-HPLC method	184
3.76	(a) Normal plot of residuals; (b) Box-Cox plot for power transform; (c) Predicted vs Actual plot; (d) Perturbation plot for response 3 (Theoretical	186
3.77	(a) Contour plot; (b) 3D response surface plot for response 3 (Theoretical plate count) for development of RP-HPLC method	187
3.78	Optimization of developed RP-HPLC method for analysis of Ledipasvir	188
3.79	Chromatograms of specificity study for analysis of Ledipasvir	189
3.80	Linearity and range study for RP-HPLC method of Ledipasvir	190
3.81	Chromatograms of robustness study of Ledipasvir (a) at pH 5.8; (b) at pH 6.2	194
3.82	Chromatograms of filter compatibility study of Ledipasvir analysis (a) Unfiltered Standard; (b) Unfiltered Sample	197
3.83	Maximum absorbance (λ_{max}) for Ledipasvir	199
3.84	Specificity of blank, placebo, standard and sample (from bottom to upwards)	200
3.85	Linearity and Range study of Ledipasvir for UV method validation	202
3.86	(a) Standard calibration curve of ledipasvir for HPLC method; (b) Standard calibration curve of ledipasvir for UV method	207

Figure No.	Figure Caption	Page
3.87	(a) Predicted vs actual plot; (b) Box-Cox plot; (c) Perturbation plot; (d) Interaction plot for response 1 (Retention time) of GC method development	216
3.88	(a) Contour plot; (b) 3D response surface plot for response 1 (Retention time) of GC method development	217
3.89	(a) Predicted vs actual plot; (b) Box-Cox plot; (c) Perturbation plot; (d) Interaction plot for response 2 (Tailing factor) of GC method development	219
3.90	(a) Contour plot; (b) 3D response surface plot for response 2 (Tailing factor) of GC method development	220
3.91	(a) Predicted vs actual plot; (b) Box-Cox plot; (c) Perturbation plot; (d) Interaction plot for response 3 (Theoretical plate count) of GC method de	222
3.92	(a) Contour plot; (b) 3D response surface plot for response 3 (Theoretical plate count) of GC method development	223
3.93	3D response surface plot for optimization of developed GC method	224
3.94	Linearity and range study for GC method validation	226
3.95	Chromatograms for specificity study of GC method (a) Blank; (b) Placebo; (c) Standard; (d) Sample	229
3.96	Chromatograms for robustness study for GC method validation (a) at Detector Temperature 245°C; (b) at Detector Temperature 255°C; (c) at Changed of	232
3.97	% LODs of F3SD after different hours of secondary drying	234
3.98	% LODs of F1SD, F2SD, F3SD, F4SD, F5SD, F6SD, F7SD and F8SD after 24 hours of secondary drying	235
3.99	Dichloromethane content of F5SD after different hours of secondary drying	236
3.100	Dichloromethane content of F5SD and F8SD after 24 hours of secondary drying	237

Chapter 1: General Introduction

1.1 Oral drug delivery system

The most acceptable route of drug administration is the oral route due to ease of administration, noninvasiveness, highly compliant for the patient, economic, easy to handle, safety and highly flexible on dosages (Hasan et al., 2021; Zamani et al., 2017).

Orally taken drugs are swallowed after placing inside the mouth. Almost all the drugs taken orally are swallowed although a few orally taken drugs are envisioned to dissolve in the mouth, the majority of oral drugs are administered for the systemic actions resulting from absorption through the different surfaces along the GIT. Among the oral drugs, a few drugs (e.g. antacids), are swallowed or chewed for their local action in the GIT (Pharmapproach, 2020).

1.1.1 Advantages of the oral route of drug administration

- Simple and safe
- Suitable for repetitive and long-term application.
- Can be administered by the patients themselves.
- Devoid of pain.
- Cost effective.
- No sterile safety measures are needed.
- Minimal chance of serious drug reaction.
- No special knowledge is needed.
- No special devices (e.g. syringes, needles) are needed.

1.1.2 Disadvantages of the oral route of drug administration

- Comparatively slow onset of action and hence, not appropriate in case of emergency.
- Not appropriate for unconscious patients.
- Not suitable for patients with difficulty to swallow.
- Cooperation from the patients is needed for administering the drugs (Pharmapproach, 2020).

1.1.3 Different oral dosage forms

There are different dosage forms available for oral administration such as solid (e.g. tablets, capsules, granules etc.) and liquid forms (e.g. solutions, suspensions, syrups and emulsions etc.) (Batchelor & Marriott, 2015).

1.1.3.1 Tablets

Tablet is a type of solid dosage form in which the active pharmaceutical ingredient (API) is mixed with other additives and then compressed to obtain the final form. Among all the dosage forms, tablets are most extensively used. Tablets are compressed by giving high pressures to granules or powder mix in the tablet compression machine with the help of stainless-steel (SS) die-punch sets. The tablets can be of different dimensions, shapes and ID marks on the surface. The tablets which are capsule shaped are commonly known as caplets. Customized tablet compression machines may be needed to prepare the tablets with special features like multiple layers or osmotic tablets or with specially prepared core tablets placed inside of the final dosage form. These customized tablet presentations can modify drug release or physically isolate APIs which are incompatible. Coating of the tablets may be done by using different technologies for unpleasant taste and odor masking, protection of the APIs, modify release or inimitable look (USP, 2021).

1.1.3.2 Capsules

Capsules are a type of solid dosage forms where API and additives are bounded within a soluble shell. Considering the type of shells, capsules may be classified as the hard-shell or the soft-shell. Usually, the hard-shell capsules contain two parts, a body and a cap and the soft-shell may be of a single piece. Generally, gelatin is the main excipient for capsule shells. Nevertheless, cellulose or other suitable ingredients may be used for the manufacturing of capsule shells. The majority of the capsules are orally administered (USP, 2021).

1.1.3.3 Granules

Granules are solid pharmaceutical dosage forms which are composed of aggregates or clusters of small particles. These are used to provide flexibility of dosing for orally given drugs as granules or as suspensions, stabilize the drug, mask unwanted taste or odor or facilitate ease of administration to children or elderly population. Usually, the reconstitution of the granules is done to a suspension with the help of provided liquid diluent/water immediately before administering. Effervescent granules are designed to give effervescence reaction where they cause evolution of carbon dioxide bubble when water is added to the formulation (e.g. antacid granules, vitamin and mineral supplementation preparations etc.). Antibiotics, different cough preparations with more than active substances are examples of some of the common therapeutic group which may be formulated as granules (USP, 2021).

1.1.3.4 Solution

A solution is a one phase liquid dosage form in which one or more active pharmaceutical ingredients and additives are dissolved in an appropriate solvent or combination of commonly miscible solvents. Uniformity and precision of dosing can be accomplished upon administration because the API is dispersed in solution at a molecular level in a uniform way. Materials in solutions are subjected to more chemical instability than they are in the solid state. Most commonly, solution dosage forms may be administered through oral, parenteral, inhalation, ocular, the mucosal, otic, topical/dermal, and gastrointestinal routes. Oral Solutions may contain flavoring and coloring agents to make them acceptable and palatable for the patients. Sometimes, they are formulated with stabilizers to prevent instability issues and anti-microbial preservatives to prevent growth of the microorganisms (USP, 2021).

1.1.3.5 Suspension

A suspension is a two-phase preparation composed of insoluble solid particles dispersed throughout a liquid phase. In general, the particle size of the dispersed solid is more than 0.5 micron (R. Santosh & T. Naga Satya, 2016). Suspension may be formulated for different routes of administration such oral, topical etc. Liquid suspensions are ready to administer and others are prepared as powder or granules for reconstitution. Some that are intended for parenteral or ophthalmic application, are manufactured as sterile.

One of the main causes to select a suspension dosage form is the poor aqueous solubility of the active ingredients. Solutions are chemically less stable than Suspensions. Suspensions may provide taste masking and hence, may improve patient acceptance. In ideal situation, small particles of a suspension should be suspended in a uniform manner and should be readily redispersible upon shaking. Usually, the solid particles in a suspension may settle to the lower most part of the bottle at undisturbed condition apart from the colloidal ones. Sometimes caking (hardening of the sediment) and difficulty in redispersion may happen. In order to evade such issues, a gelling network may be incorporated or viscosity and degree of flocculation may be increased by adding appropriate ingredients like suspending agents, wetting agents, polyols, polymers, sugars etc. (USP, 2021).

The viscosity and the ease of removing the dose from the bottle are influenced by temperature. Temperature cycling may alter the particle size of the dispersed particles because of Ostwald ripening. Therefore, cycle conditions (freeze/thaw) should be studied to

investigate temperature effects during the stability study of the suspensions. Anti-microbial preservatives may be incorporated in suspensions to evade growth of the microorganisms growth (USP, 2021).

1.1.3.6 Syrup

Syrup refers to a solution having high concentrations of sucrose (usually 60 to 80%) (Reeves, Philip T., Camille Roesch, 2017). It is a common term applied for compounding pharmacy (USP, 2021).

1.1.3.7 Emulsion

Emulsions for oral administration are composed of two immiscible liquids, where one liquid (dispersed phase) is dispersed throughout the other (continuous phase) as fine droplets. The droplet size of the dispersed phase may vary from 0.1 to 100 micron. Because of their nature of instability, emulsifiers are used to stabilize them by averting coalescence of the dispersed droplets. Emulsion may also contain other additives such as buffers, antioxidants, and preservatives (Reeves, Philip T., Camille Roesch, 2017). Emulsions are mainly of two types based on the type of the two phases i.e. oil in water and water in oil (Naturespharmacy, 2018). Emulsions for oral administration are usually oil in water and they help in the administration of oily substances (e.g. mineral oil) in a more acceptable manner (Reeves, Philip T., Camille Roesch, 2017).

1.1.4 Advantages of solid dosage form

- Highly precise, lowest variability, stable and accurate dosing.
- Simpler formulation than liquid and semi-solid dosage forms.
- Strong onset of action.
- Administration of multiple doses can be avoided by combining several medicines and excipients.
- By using a capsule shell, the liquid can be converted into a solid form.
- Flexibility of dosing.
- Ease of packaging and transportation.
- Usually, no special storage conditions are required.
- It is easy to swallow and can be attractive to pediatric and geriatric population.
- Easy to administer (e.g. can be swallowed with water only)
- Suitable for partial and divided dosing.

- Unlikely to harm the gastrointestinal tract as it is easy and rapidly digested.
- Masking of unpleasant taste and odor is possible.
- Can be manufactured in custom sizes, shapes, and colors as needed.
- API can be protected from atmospheric conditions such as moisture, temperature, and light, etc.
- Chemical, physically and microbiologically stable (Chrominfo, 2020).

1.1.5 Disadvantages of solid dosage form

- Not easy to swallow, particularly for geriatric and pediatric population.
- Not possible to administer in patients with unconsciousness.
- Difficult to prepare the dosage form when the API is poorly water soluble.
- Administration of some drugs as tablets or capsules may result in gastric irritation.
- Difficult to formulate hygroscopic and deliquescent drugs.
- Sometimes patients may not prefer to take it because of unpleasant taste and odor.
- Relatively expensive due to lengthy manufacturing process.

1.1.6 Advantages of liquid dosage forms

- Suitable for children and elderly population also for patients with difficulty to swallow solid dosage.
- High aesthetic value.
- Sweetening, flavoring and coloring agents can be added for drugs having unsatisfactory taste and odor.
- Flexible dosing.
- Accurate dosing can be done rapidly with ease by computing multiple volumes.
- Rapidly absorbed and hence, a rapid onset of action.
- Suitable for moisture sensitive drugs for which other dosage forms are not feasible.
- Adsorbents and antacids have better efficacy as liquid (Pharmapproach, 2020).

1.1.7 Disadvantages of liquid dosage forms

- More sensitive to chemical degradation than solid medicaments.
- Inconvenient to transport or store because of large volume.
- The whole dosage form may be lost due to accidental breakage or damage of the container.

- Much shorter shelf life due to low chemical stability.
- Preservative may be added to the formulation due to it is prone to microbial growth.
- Some liquid medicaments like vaccines, insulin etc. may require special arrangement for storage.
- Unpleasant taste of an API remains predominant in case of solution dosage form (Pharmapproach, 2020).

1.2 Poorly water soluble drugs

The capacity of a drug to be soluble in aqueous media plays a predominant part to establish its extent of dissolution (Zishan et al., 2017). Very slightly soluble drugs are those having solubility from 1g/L to 1g/10L; insoluble or practically insoluble drugs have from solubility of smaller than 1g/10L (Mirza R Baig, 2018). BCS defines a drug as poorly soluble when its maximum strength is not dissolved in 250 mL of aqueous media between the physiologic pH of 1 to 6.8. Bioavailability of an immediate release (IR) oral solid drug is not limited by dissolution if the dissolution is more than 85% in fifteen minutes in 0.1 N HCl (CDER/FDA, 2015). Aqueous solubility of 1g/100 mL or more is must to avoid potential solubility limited absorption problems (Zishan et al., 2017). Drugs having water solubility less than 1g/10L may lead to dissolution limitations to absorption (Hörter & Dressman, 1997; Kaplan, 1972).

1.3 Biopharmaceutical classification system (BCS):

The BCS is a science-based outline based on which drug substances are classified according to their aqueous solubility and intestinal permeability. Dissolution, solubility and intestinal permeability are the main factors controlling the rate and extent of drug absorption from immediate release (IR) solid oral dosage forms (CDER/FDA, 2015).

As per BCS, drug substances can be classified into following 4 classes (CDER/FDA, 2015):

Class 1: Highly Soluble – Highly Permeable

Class 2: Poorly Soluble – Highly Permeable

Class 3: Highly Soluble – Poorly Permeable

Class 4: Highly Soluble – Poorly Permeable

1.3.1 Solubility

If the maximum strength of a drug is soluble in 250 mL or less of aqueous media between the physiologic pH range of 1 - 6.8, then it is called a highly soluble drug. 250 mL volume is based on conventional bioequivalence study protocols where it is advised to give a drug

product with an eight fluid ounce glass of water to fasting condition of healthy human volunteers (CDER/FDA, 2015).

1.3.2 Permeability

The permeability depends passively on the amount of absorption (fraction of dose absorbed) in humans and actively on the rate of mass transfer through human intestinal membrane. Instead, *in-vitro* epithelial cell culture methods, in situ animal or any other method able to forecast the extent of drug absorption in humans may be used. If a drug substance has eighty five percent or more systemic bioavailability or the amount of absorption in humans for a given dose according to mass balance or compared to a reference dose given intravenously, then it may be referred as highly permeable drug (CDER/FDA, 2015).

1.3.3 Dissolution

An IR drug product is known as rapidly dissolving when average of eighty five percent or more of the administered dose is dissolved in thirty minutes when using standard dissolution conditions as mention in USP <711> in pH 1.2, 4.5 and 6.8 buffers. (CDER/FDA, 2015).

1.4 Bioavailability

Bioavailability is the extent and rate at which the active substance from the finished product is absorbed and reaches the site of action (Chow, 2014). Comparative bioavailability is the comparison of bioavailabilities of different formulations of the same drug or different drug products (Chow, 2014). Absolute bioavailability is defined as the fraction of drug absorbed into the systemic circulation (Allam et al., 2011).

1.5 Challenges of newly developed drugs

Approximately forty percent of the newly developed molecules exhibit poor solubility in aqueous media (Heimbach et al., 2007). Owing to low aqueous solubility and poor dissolution rate, a significant number of medicaments exhibit low drug concentrations at the site of absorption and hence, poor oral bioavailability (Leuner & Dressman, 2000). According to BCS, dissolution is the rate limiting step for absorption of BCS class 2 and 4 drugs after oral administration (Sareen et al., 2012).

In the recent years, several tactics have been adopted to improve the dissolution of such drugs with the help of surface-active agents, permeability boosters, particle size reduction by

micronizing the drug, salt preparation, nanosuspension and solid dispersions (Kumar et al., 2010).

Development of nanosuspension can be a lucrative and prospective approach to resolve the issues of low solubility and bioavailability of BCS class 2 drugs (Agrawal & Patel, 2011). Drug nanoparticles can improve the solubility of BCS class 2 and 4 drugs (Attari et al., 2016). Preparation of nanosuspension is easy and can be applied to most of the drugs which are water insoluble. A nanosuspension drives away the problems of low solubility and bioavailability. At the same time, it can also change the pharmacokinetics and hence, safety and efficacy of the drug is improved.

Globally, approximately fifty eight million people are infected with chronic hepatitis C virus whereas around one and a half million people are getting newly infected each year (WHO, 2021). Therefore, three anti-hepatitis C virus drugs, Ledipasvir, Daclatasvir and Velpatasvir were selected for this study where Ledipasvir (European Medicines Agency, 2014) and Daclatasvir are BCS class 2 drugs (Bharate, 2021) and Velpatasvir is a BCS class 4 drug (European Medicines Agency, 2016).

1.6 Taxonomy

1.6.1 Taxonomy of Ledipasvir

Taxonomy of Ledipasvir is mentioned below (Drugbank, 2014):

Table 1.1: Taxonomy of Ledipasvir

Kingdom	Organic compounds
Super Class	Benzenoids
Class	Fluorenes
Direct Parent	Fluorenes
Molecular Framework	Aromatic heteropolycyclic compounds

1.6.2 Taxonomy of Daclatasvir

Taxonomy of Daclatasvir is mentioned below (Drugbank, 2015):

Table 1.2: Taxonomy of Daclatasvir

Kingdom	Organic compounds
Super Class	Organic acids and derivatives

Class	Carboxylic acids and derivatives
Direct Parent	Valine and derivatives
Molecular Framework	Aromatic heteromonocyclic compounds

1.6.3 Taxonomy of Velpatasvir

Taxonomy of Velpatasvir is mentioned below (Drugbank, 2016):

Table 1.3: Taxonomy of Velpatasvir

Kingdom	Organic compounds
Super Class	Organoheterocyclic compounds
Class	Naphopyrans
Direct Parent	Fluorenes
Molecular Framework	Aromatic heteropolycyclic compounds

1.7 Physical properties

1.7.1 Physical properties of Ledipasvir

Physical properties of Ledipasvir are highlighted below.

Table 1.4: Physical properties of Ledipasvir

Appearance	Ledipasvir is a slightly hygroscopic white to tan or yellow crystalline powder (European Medicines Agency, 2014).
Water Solubility	Ledipasvir has slight solubility below pH 2.3 and practical insolubility from pH range 3.0 to 7.5 (Gilead Sciences, 2014).
LogP	3.8 (Drugbank, 2014)
pka	pka1 is 4.0 and pka2 is 5.0 (Drugbank, 2014)

1.7.2 Physical properties of Daclatasvir

Physical properties of Daclatasvir are highlighted below:

Table 1.5: Physical properties of Daclatasvir

Appearance	Daclatasvir is a non-hygroscopic white to yellow solid (Bristol-Myers Squibb Company, 2017).
Water Solubility	Daclatasvir has poor solubility in water having strongly pH-dependent solubility. If the pH is acidic, then Daclatasvir

	Dihydrochloride has a solubility of 20 g/L and if the pH increases then the solubility decreases e.g. at pH 5.0 the solubility was 110mg/L and at pH 7.0 the solubility was 15 mg/L (Bharate, 2021).
LogP	4.18 (Drugbank, 2015)
pka	pka1 is 6.09 and pka2 is 11.15 (Drugbank, 2015)

1.7.3 Physical properties of Velpatasvir

Physical properties of Velpatasvir are highlighted below:

Table 1.6: Physical properties of Velpatasvir

Appearance	Velpatasvir is a hygroscopic white to tan or yellow crystalline solid (Gilead Sciences, 2016).
Water Solubility	Velpatasvir has poor water solubility with pH reliant solubility. it is practically insoluble at pH over 5.0, sparingly soluble if pH is 2.0 and soluble if pH is 1.2 (Gilead Sciences, 2016).
LogP	1.62 (Gilead Sciences, 2016)
pka	pka1 is 3.2 and pka2 is 4.6 (Gilead Sciences, 2016)

1.8 Chemical properties

1.8.1 Chemical properties of Ledipasvir

Chemical properties of Ledipasvir are highlighted below:

Table 1.7: Chemical properties of Ledipasvir

IUPAC Name	Methyl N-[(2S)-1-[(6S)-6-[4-(9,9-difluoro-7-{2-[(1R,3S,4S)-2-[(2S)-2-[(methoxycarbonyl)amino]-3-methylbutanoyl]-2-azabicyclo[2.2.1]heptan-3-yl]-1H-1,3-benzodiazol-5-yl}-9H-fluoren-2-yl)-1H-imidazol-2-yl]-5-azaspiro[2.4]heptan-5-yl]-3-methyl-1-oxobutan-2-yl]carbamate (Drugbank, 2014)
Molecular Formula	C ₄₉ H ₅₄ F ₂ N ₈ O ₆ (Drugbank, 2014)
Molecular Weight	889 (Drugbank, 2014)

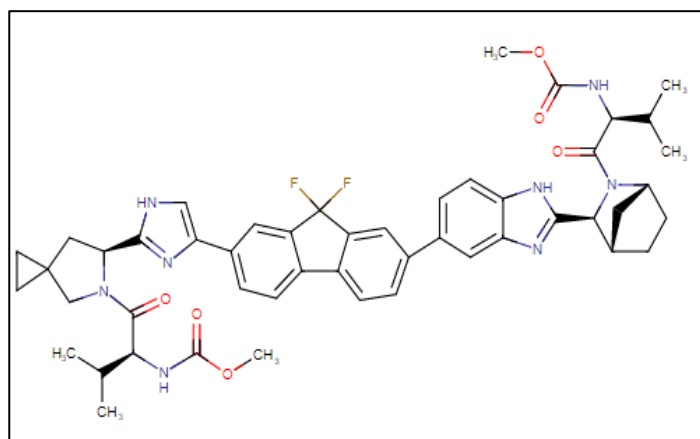


Figure 1.1: Structure of Ledipasvir (Drugbank, 2014)

1.8.2 Chemical properties of Daclatasvir

Chemical properties of Daclatasvir are highlighted below-

Table 1.8: Chemical properties of Daclatasvir

IUPAC Name	Methyl N-[(2S)-1-[(2S)-2-[5-(4'-{2-[(2S)-1-[(2S)-2-[(methoxycarbonyl)amino]-3-methylbutanoyl]pyrrolidin-2-yl]-1H-imidazol-5-yl}]-1,1'-biphenyl]-4-yl)-1H-imidazol-2-yl]pyrrolidin-1-yl]-3-methyl-1-oxobutan-2-yl]carbamate (Drugbank, 2015)
Molecular Formula	C ₄₀ H ₅₀ N ₈ O ₆ (Drugbank, 2015)
Molecular Weight	738.89 (Drugbank, 2015)

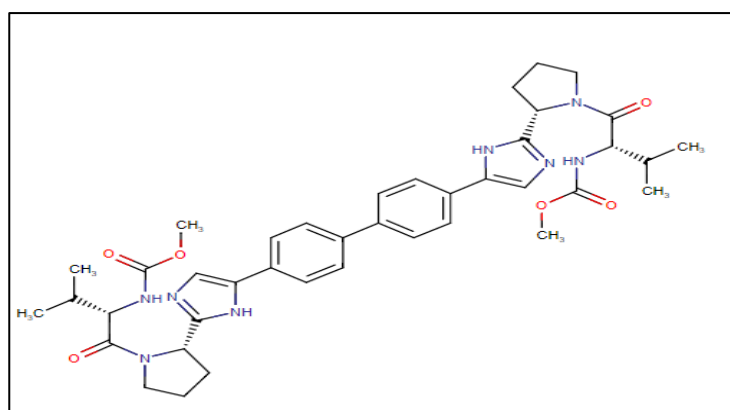


Figure 1.2: Structure of Daclatasvir (Drugbank, 2015)

1.8.3 Chemical properties of Velpatasvir

Chemical properties of Velpatasvir are highlighted below-

Table 1.9: Chemical properties of Velpatasvir

IUPAC Name	Methyl N-[(1R)-2-[(2S,4S)-2-(5-{6-[(2S,5S)-1-[(2S)-2-[(methoxycarbonyl)amino]-3-methylbutanoyl]-5-methylpyrrolidin-2-yl]-21-oxa-5,7-diazapentacyclo[11.8.0.0 ^{3,11} .0 ^{4,8} .0 ^{14,19}]}henicos-1,3(11),4(8),6,9,12,14,16,18-nonaen-17-yl)-1H-imidazol-2-yl)-4-(methoxymethyl)pyrrolidin-1-yl]-2-oxo-1-phenylethyl]carbamate (Drugbank, 2016)
Molecular Formula	C ₄₉ H ₅₄ N ₈ O ₈ (Drugbank, 2016)
Molecular Weight	883.02 (Drugbank, 2016)

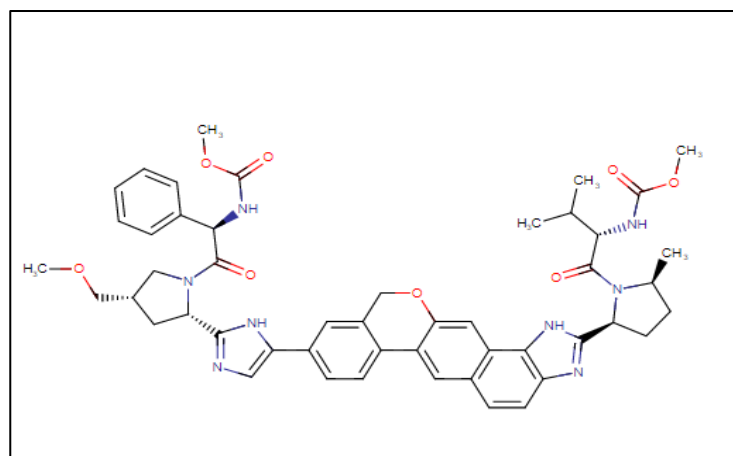


Figure 1.3: Structure of Velpatasvir (Drugbank, 2016)

1.9 Pharmacokinetics

1.9.1 Pharmacokinetics of Ledipasvir

Absorption: When given orally, it takes about 4 to 4.5 hours for Ledipasvir to reach its peak plasma concentration with a peak concentration (C_{max}) of 323ng/mL. Ledipasvir may be given without regard for food (Drugbank, 2014).

Protein Binding: The degree to which drugs attach to proteins within the blood is known as plasma protein binding. The degree of protein binding of a drug may affect its efficiency

(pharmacy180.com, 2019). Ledipasvir exhibits more than 99.8% protein binding capacity to human plasma (Drugbank, 2014).

Metabolism: Ledipasvir exhibits sluggish oxidative metabolism. The systemic exposure of Ledipasvir was almost complete compared to the original drug (greater than 98%) after a single oral dose of 90mg, the majority of the dose was present in faeces as unchanged drug (Drugbank, 2014).

Routes of Elimination: Approximately 70% of the dose excreted in faeces and approximately 2.2% was the oxidative metabolite. Therefore, Ledipasvir is mainly eliminated through biliary excretion in unchanged form along with insignificant renal excretion (almost 1%) (Drugbank, 2014).

Half-life: 47 hours (Drugbank, 2014).

1.9.2 Pharmacokinetics of Daclatasvir

Absorption: The time required to achieve maximum plasma concentrations is 2 hours following oral administration of multiple doses of daclatasvir between 1 - 100 mg once daily. Steady state is attained in around 4 days. Absolute bioavailability of Daclatasvir tablet is about 67% (Drugbank, 2015).

Protein Binding: Daclatasvir exhibits about 99% protein binding capacity (Drugbank, 2015).

Metabolism: CYP3A enzymes act on Daclatasvir where its metabolism is predominantly mediated by CYP3A4 isoform. Most the drug (>97%) is in the plasma as unchanged form (Drugbank, 2015).

Route of Elimination: High proportion of the total dose (about 88%) of Daclatasvir is excreted into bile and feces where a significant percentage (about 53%) stays as unchanged form, at the same time, a minor amount (about 6.6%) is excreted unchanged in the urine (Drugbank, 2015).

Half-life: 12 to 15 hours (Drugbank, 2015).

1.9.3 Pharmacokinetics of Velpatasvir

Absorption: Velpatasvir has an oral bioavailability of 25-30% (Drugbank, 2016).

Protein Binding: Velpatasvir exhibits about more than 99.5% protein binding capacity (Drugbank, 2016).

Metabolism: Velpatasvir is metabolized by CYP2B6, CYP2C8 and CYP3A4 to some extent (Drugbank, 2016).

Route of Elimination: High proportion (94%) of Velpatasvir is eliminated in feces with where a significant percentage (77%) stays as unchanged form, a minor proportion (0.4%) eliminated in urine (Drugbank, 2016).

Half-life: 15 hours (Drugbank, 2016).

1.10 Pharmacodynamics and mechanism of action

1.10.1 Pharmacodynamics and mechanism of action of Ledipasvir

Ledipasvir is an inhibitor of the hepatitis C virus (HCV) non-structural protein 5A (NS5A) replication complex, with potential activity against HCV which is available for oral administration. After giving orally and being available at cellular level, Ledipasvir stops the activity of the NS5A protein by binding with it. As a result, the replication complex of viral RNA is ruptured and inhibits the production of HCV RNA and blocks the viral replication. (Drugbank, 2014).

1.10.2 Pharmacodynamics and mechanism of action of Daclatasvir

Daclatasvir targets the NS5A and causes a reduction in serum HCV RNA levels. It stops the replication of HCV by blocking the activity of NS5A protein in the replication complex. Daclatasvir downregulates the hyperphosphorylation of NS5A and interfere with the function of new HCV replication complexes. It inhibits both intracellular viral RNA synthesis and virion assembly *in-vivo* (Drugbank, 2015).

1.10.3 Pharmacodynamics and mechanism of action of Velpatasvir

The mechanism of action of Velpatasvir is similar to Daclatasvir and Ledipasvir. Velpatasvir binds with domain I of NS5A which contains amino acids 33 to 202 and thus, blocks the replication of HCV RNA. NS5A plays a significant part in RNA replication by unknown mechanism (Drugbank, 2016).

1.11 Solid dispersion

Solid dispersion (SD) is the dispersion of hydrophobic drug(s) at molecular level in inert and hydrophilic carrier polymer(s). In the SD, the drug can be dispersed as amorphous or crystalline particles. The first work of solid dispersion was done in the beginning of 1960s, (Sekiguchi & Obi, 1961). To prepared SD, the drug is dispersed in a hydrophilic carrier at solid state. Examples of water soluble carriers include methylcellulose, polyvinyl pyrrolidone (Povidone), polyethylene glycols, surface-active agents such as polysorbate 80, poloxamer 188, poloxamer 407 and sodium dodecyl sulfate etc. (Abdul-Fattah & Bhargava, 2002; Gupta et al., 2004; Sinha et al., 2010).

1.11.1 Methods of preparation of solid dispersions

1.11.1.1 Solvent evaporation method: This technique involves solubilization of both API and polymer in a mutual organic solvent. The solvent is evaporated to form the solid preparation at low temperature (Jagadeesan & Radhakrishnan, 2013).

Advantage: Thermal degradation of API can be avoided (Karanth et al., 2006).

Disadvantage: Long process as residual solvent has to be removed below acceptable limit (Karanth et al., 2006).

1.11.1.2 Modified solvent evaporation method: The API is solubilized in organic solvent while the carrier is dispersed as suspension in water. Then the solution of API solution all together is poured in the carrier suspension and the solvent is fully removed upon drying (Rane et al., 2007).

1.11.1.3 Melting/Fusion method: This technique involves the incorporation of API in the melted polymer matrix. Solid solution will be produced if the API is highly soluble in the polymer by remaining dissolved in the solid state. An ice batch is used to solidify the melt with continuous stirring, then it is grounded and sized. (Kannao, 2014).

1.11.1.4 Melt solvent evaporation technique: The API is solubilized in an organic solvent and mixed with the melted polymer. The resultant preparation is grounded and sized after full removal of the solvent (Kannao, 2014).

1.11.1.5 Melt extrusion method: In this technique, SD is prepared with the help of a twin-screw hot melt extruder where only thermo stable components are relevant. The extruder

consists of barrel, a hopper, a mixing screw, a die and heaters. The dry mix of the API and the carrier is put inside the hopper which is advanced by feed screw and eventually, is extruded from the die. (Kannao, 2014).

1.11.1.6 Lyophilization (freeze drying): Lyophilization is a technique in which the API and polymer are solubilized together in a mutual solvent, frozen and sublimed to obtain a dried molecular dispersion. It causes exchange of heat and mass to and from the product under preparation. (Kannao, 2014).

1.11.1.7 Melt agglomeration method: This technique involves the incorporation of API in the matrix either by heating the binder and API, other additives to a temperature higher than the binder's melting point or spray of dispersed API in molten binder on the preheated additives with the help of a high shear mixer (Kannao, 2014).

1.11.2 Characterization of solid dispersion

1.11.2.1 Detection of crystallinity in solid dispersions

1.11.2.1.1 Powder X-ray Diffraction Study (XRD)

Materials with long range order can be identified qualitatively using X-ray diffraction study. More crystalline materials are indicated by sharper diffraction peaks. Recent X-ray diffractometers are semi-quantitative (Leuner & Dressman, 2000; A. N. Patil et al., 2017).

1.11.2.1.2 Fourier Transformed Infrared (FTIR)

The difference in the energy of vibration for the interactions between API and polymer can be identified by FTIR (Forster et al., 2010). Usually, crystallinity is indicated by sharp vibrational peaks whereas amorphicity is addressed by a broad hump owing to disorder in arrangements of molecules (Broman et al., 2001).

1.11.2.1.3 Microscopic Technique

Microscopic techniques can measure the variation in the mechanical properties between amorphous and crystalline states. Percentage of crystallinity can affect elasticity modulus and viscosity which can be determined by density measurement using cross polarized microscopes. This microscopy may be applied to have idea about the kinetics of crystallization and the stability of amorphous systems (Taylor & Zografi, 1997; Yu, 2001). This microscopy can differentiate between amorphous and crystalline substances as crystalline materials exhibit birefringence (Broman et al., 2001).

1.11.2.1.4 Differential Scanning Calorimetry (DSC)

DSC is the most applied thermodynamic method for characterization of SD. Usually, the method of measurement is to heat the reference and test samples at an identical temperature. The energy of the phase transition quantified from the record of additional heat requirement. Conversion of a polymorph to a more stable polymorph (i.e. exothermic transitions) can also be detected. The presence of a sharp melting peak indicates that the drug is present in crystalline state in the SD whereas the absence of a melting peak means that the drug is present in amorphous state in the SD (Kerč & Srčić, 1995; Leuner & Dressman, 2000).

1.12 Nanosuspension approach

Poorly water-soluble drugs are conventionally formulated with the help of different excipients to improve dissolution percentage and stability upon storage. Excipients (e.g. co-solvents, surface-active agents, disintegrating agents etc.) increase % drug release by increasing the surface area of the molecule when coming in touch with dissolution media (Yadollahi et al., 2015).

Nevertheless, drawbacks such as toxicity of surface-active agents applied to keep drug in the dispersed state and limitation of drug loading have been recognized (Rao et al., 2004). Milling or micronizing the API with the help of ball mill or jet mills to reduce the particle size is another approach used to increase drug solubility. The resultant particle size varies in the range from 1 micron to 25 micron and very minor proportion of drug particles is found smaller than 1 micron (Müller, R. H., Peters, K., Becker, R., & Kruss, 1995). Converting micron size drug particles into nano size was the next development stage (Liversidge, G. G., Cundy, K. C., Bishop, J. F., & Czekai, 1992).

At early stage, drug nanoparticles were prepared using a precipitation method (Gassmann et al., 1994). The constraint with this method is that the API must be solubilized in minimum one solvent and that solvent has to be miscible with a nonsolvent (Müller et al., 2001). In order to get the better of these limitations, nanosuspensions were prepared by using dispersion method (Müller, R. H., Peters, K., Becker, R., & Kruss, 1995). These researchers have proved that pure drug particles within the size range of 10 to 1000nm were stable in the presence of surface-active agents and polymers. After their work, nanosuspensions have been defined as drug carriers with particle size ranging from 10 to 1000nm.

1.12.1 Mechanism of improvement of dissolution

The reasons for improved dissolution from nanosuspension are -

- increased surface area provided by the nanoparticles
- decrease in particle size
- availability of drug in amorphous form (M. P. Patil et al., 2020)

1.13 Advantages of nanosuspension over traditional approach

- By increasing % drug release, the drawbacks of BCS class 2 and 4 can be solved (Yadollahi et al., 2015).
- Higher drug loading can be done.
- Drug stability can be increased.
- Can be fused in different dosage forms like tablets, pellets and capsules.
- Bioavailability of drug can be increased.
- Reduction of dose is possible (Zhang et al., 2007).
- Reduction of adverse effects due to reduced dose.
- Cost effective.
- Provides a passive drug targeting.
- Production methods are very simple and less time consuming.
- Nanosuspension provides lower fed/fast variability.

1.14 Method of preparation of nanosuspension

1.14.1 Bottom-Up Technology

It starts from the molecular level and goes via molecular association to the formation of a solid particle. It is basically precipitation method in which the solvent amount is decreased, such as, by incorporating the solvent into a nonsolvent or altering the temperature or a mixture of both (Shid et al., 2013).

Advantages:

- Easy and economic technique.
- Higher saturation solubility.

Disadvantages:

- The API has to be soluble in at least one solvent.
- The solvent has to be miscible with minimum one nonsolvent.
- Residual solvent has to be removed or reduced to an acceptable level.

1.14.2 Top-Down Technology

Top down technologies include Media milling and high-pressure homogenization.

1.14.2.1 Media milling

Nanosuspensions can be prepared by using high-shear media mills or bead mill. The parts of the mill are a milling chamber, milling shaft and a recirculation chamber. An aqueous suspension of the materials is then fed into the mill containing small grinding beads or balls. These beads impact against the sample on the opposite wall while rotating at a very high shear rate. Significant decrease in particle size can be obtained because of both friction and impact together. The beads are manufactured of ceramic-sintered aluminum oxide or zirconium oxide etc. which are non-abrasive in nature. Example of such equipment is Bead mill (DYNO® MILL, WAB, Germany). Zn-Insulin nanosuspension was manufactured by the wet milling having an average particle size of 150 nm (Shid et al., 2013).

Advantages

- Easy and economic technique.
- Large-scale production is possible.

Disadvantages

- Chance of product contamination due to erosion from the milling material.
- Lengthy process.
- Chance of microbial growth.

1.14.2.2 High pressure homogenization:

1.14.2.2.1 Dissocubes: This technique involves passing of the drug suspension through a small hole resulting in a decrease in static pressure lower than the boiling pressure of water, so the water boils and gas bubbles are formed. The bubbles collapse and the nearby suspension having the drug particles run to the center when the suspension leaves the gap and normal air pressure is attained again. During this process, the particles collide and a decrease in the particle size results. More than one passes may be required through the homogenizer to obtain the target particle size and uniformity. High pressure homogenization is suitable for diluted and concentrated suspensions and aseptic manufacturing (Shid et al., 2013).

1.14.2.2.2 Nanopure: In this technique, the API is dispersed in the non- aqueous medium and homogenized at zero degree Celsius or below the freezing point. It can be selected for substances which are sensitive to heat (Shid et al., 2013).

1.14.2.2.3 Nanoedge™: It is a mixture of precipitation and homogenization process. It is possible to obtain smaller particle size and higher stability in short period of time. Growth of crystals can be stopped by this method (Shid et al., 2013).

1.14.2.3 Emulsion diffusion method

This technology involves emulsion as templates for nanosuspension preparation of APIs where the APIs are soluble in organic solvent or partially water-miscible solvent. These solvents will play the role of dispersed phase for the emulsion. An organic solvent (e.g. methanol, ethanol etc.) or mixture of solvents containing the API is dispersed in the aqueous phase encumbered with suitable surface-active agents and stirred prepare an emulsion. This emulsion may be further homogenized through high pressure homogenization (Shid et al., 2013).

Advantages

- No need of high-tech equipment.
- Control of particle size can easily be done easily.
- Convenient to scale-up for optimized formulation.

Disadvantages

- Not suitable for drugs that have poor solubility in both aqueous and organic solvents.
- Costly and long process.
- Use of high concentration of surfactant can be a safety concern.
- Ultrafiltration is needed for purification which may render the nanosuspension.

1.14.2.4 Micro emulsion Template

This technique is same as emulsion diffusion method where microemulsion is formed in place of emulsion. Microemulsion has a particle size in nanometers whereas the same for the coarse emulsion is in micrometers (Ita, 2020).

1.14.2.5 Supercritical fluid method

The commonly used super critical fluid technique is rapid expansion of supercritical solution process (RESS). In RESS, supercritical fluid loaded with drugs is passed through a nozzle,

reusing in the precipitation of the nanoparticles by removal of solvents. A nanoparticle of cyclosporine was produced having a particle size of 400 to 700 nm (Shid et al., 2013).

Disadvantages

- Safety concerns due to use of hazardous solvents, high concentration of surfactants.
- Chance of polymorphic conversion due to high super saturation.

1.14.2.6 Melt emulsification method

This method involves the production of emulsion by suspending the API in the aqueous solution of stabilizer and heating above the melting point of the API followed by homogenization (Shid et al., 2013).

Advantage

- Green method as organic solvent is not needed.

1.14.2.7 Dry Co-Grinding method

In this technique, API with poor solubility are dry-grinded with soluble polymers and copolymers after suspending in a liquid media. Examples of such polymers include are Povidone, hydroxypropyl methylcellulose (HPMC) etc. (Shid et al., 2013).

1.15 Characterization of nanosuspension

1.15.1 Particle size and polydispersity index

Two of the most important characteristics of nanosuspensions are particle size distribution (PSD) and polydispersity index (PDI). The following properties of nanosuspensions are governed by particle size (Gao et al., 2008) -

- drug saturation solubility
- physical stability
- dissolution rate and bioavailability.

As per the equation of Noyes-Whitney, reduction of particle size leads to increment in surface area of the particles which eventually, enhance the solubility of drugs owing to improved dissolution rate (Bosselmann & Williams, 2012; Patravale et al., 2010).

$$dM/dt = D(C_{\text{Bulk}} - C_{\text{Eq}})/h$$

where dM/dt is the rate of dissolution, D is the mean diffusion coefficient, A is the surface area of the solid, C_{Bulk} is the concentration of drug in the bulk solution, C_{Eq} is the

concentration of drug in the diffusion layer surrounding the drug, and h is the diffusion layer thickness.

PSD of nanosuspension can be determined by Brownian movement of particles against time. In general, smaller particles move with higher velocity than larger particles. Photon Correlation Spectroscopy (PCS) or Dynamic Light Scattering (DLS). This method can also be used for measuring PI of nanosuspension. DLS can measure the particle size between 3nm to 3 microns with accuracy. If PSD is more than 3 microns, this method cannot produce precise results. To measure the PSD above 3 micron, Laser Diffraction (LD) is implemented to measure the particle size (Gao et al., 2008). SEM (Scanning Electron Microscopy) can also be used for PSD determination (Gaumet et al., 2008; Teeranachaideekul et al., 2008).

The width of PSD is known as polydispersity index (PDI) that describes Low value of PDI is needed for prolonged stability of nanosuspension (Gumustas et al., 2017). Polydispersity describes the extent of non-uniformity of a PSD. PDI can be measured by DLS method. If PDI value is more than 0.7, it means that the sample has a very broad PSD and may not be appropriate to be measured by the DLS methodology (Yadollahi et al., 2015).

1.15.2 Crystalline state and particle morphology

The solubility of amorphous form is higher than that of its crystalline form as amorphous form has higher Gibbs free energy than the stable crystalline form (Graeser et al., 2010).

Drugs having amorphous form gives better dissolution and higher bioavailability from the formulation (Fakes et al., 2009). Nevertheless, upon storage of nanosuspension, this amorphous form can be converted to crystalline one which is one of the significant points to contemplate. XRPD or DSC or combination of both can be used to determine amorphous and crystalline states (Van Eerdenbrugh et al., 2007).

1.15.3 Particle charge (zeta potential)

Particle charge exerts a vital influence for obtaining stabilized nanosuspensions. Electric charge and electrostatic repulsion inhibit the particles to aggregate and precipitate. The difference of potential across phase boundaries between solids and liquids is known as zeta potential. It measures the electrical charge of particles that are dispersed in liquid (Anne Marie Helmenstine, 2019). In general, zeta potential of $\pm 30\text{mV}$ is needed for electrostatic stabilisation. However, in case of electrostatic stabilisation joined with stabilisation (with the help of proper polymer), zeta potential of $\pm 20\text{mV}$ can be proved

enough to stop particles from aggregating and precipitating (Jacobs & Müller, 2002). Zeta potential is usually measured with the help of Helmholtz-Smoluchowski equation (Deshiikan & Papadopoulos, 1998). Zeta sizer is an example of equipment that works on the principle of dynamic light scattering and can be used for measuring zeta potential.

1.15.4 Sedimentation Volume

The equation for calculating sedimentation volume (F) is, $F = V_u/V_o$

Where, V_u is the volume of sediment at time zero and V_o is the volume of the final sediment and the after vigorous shaking (Abood, 2016).

If F is equal to 1, then the flocculation can be considered stable and not settling is visible. The greater the F value, the more stable the flocculated system will be and therefore, is the more stable suspension (Mahato & Narang, 2011).

Sedimentation volume (F) gives a qualitative idea of the quantum of settling taking place in a suspension. F is less than one in case of settling down of the particles while F is greater than 1 in case of swallowing of particles (Michael E. Aulton & Kevin M. G. Taylor, 2017).

1.15.5 Redispersibility

Pharmaceutical suspensions should be uniformly dispersed before taking a dose for ensuring proper dosing. In some cases, it is a pharmacopoeial requisite for suspensions to be redispersed by shaking (Deicke & Süverkrüp, 1999). Redispersibility may refer to the capacity of suspensions to disperse in a uniform manner upon agitation after standing for some time (Patel, 2010). The suspension should be easily redispersible to gain better acceptability.

1.15.6 Stability

In case of particle size reduction, surface energy of particles is increased because of larger number of unstable surface atoms and molecules leading to destabilisation of the suspension. This is why sometimes, stabilizers are used to evade the agglomeration of particle and the chance of Ostwald ripening (Charurasia et al., 2012). Examples of some such stabilizers may be polysorbates, povidones, poloxamer etc. (Quintanar-Guerrero et al., 1998). For prolonged stabilization of nanosuspensions, both surfactants and polymers can also be used combinedly (Jacob et al., 2020; Kocbek et al., 2006; Muller & Keck, 2004). Polymers and surface-active agents inhibit the intimate interaction between particles. Surface-active agents can elevate the electrostatic repulsion and stabilize the particles by changing the zeta

potential. Precipitation of particles is another point to anticipate while preparing stabilized nanosuspension. The increase in the uniformity of particle sizes through centrifugation will increase the nanosuspension stability (Yadollahi et al., 2015).

1.16 Analytical methods

1.16.1 RP-HPLC method

Chromatography is a prevalent method applied in analytical field. High pressure liquid chromatography (HPLC) separates mixture of compounds passing through a separation column using high pressure. In case of Reverse Phase HPLC (RP-HPLC), a polar mobile phase is used with a non-polar stationary phase. Separation is obtained by hydrophobic interaction of molecules with the stationary phase. The advantages of RP-HPLC system is that most of the drug molecules can be solubilized in polar mobile phase (Hashim, 2019).

1.16.2 UV method

Ultra-Visible spectrophotometers used in UV analysis works by measuring the absorbance of light of sample in response to blank solution. As it is easy, fast and cost effective, UV method has become a popular technique in analyzing pharmaceutical dosage forms (Behera, 2012; Nayon et al., 2013). UV spectrophotometry is based on Beer -Lambert law which states that the absorbance is directly proportional to concentration of the sample when the pathlength for absorption is fixed (Behera, 2012).

1.16.3 Residual solvent determination

Residual solvents are organic volatile substances which are utilized or produced in the preparation of drug products, API or excipients. The solvents are not completely removed by practical manufacturing techniques. Residual solvents exert no therapeutic action. Hence, these solvents should be removed to an acceptable limit., good manufacturing practices, or other quality-based requirements. Class 1 solvents are toxic to an unacceptable level and should not be utilized in manufacturing. Example of such solvent is benzene with an acceptable limit of 2 ppm. Class 2 solvents exert less severe toxicity and should be utilized in manufacturing at a minimal level to evade possible side effects. Example of such solvent is methylene chloride with an acceptable limit of 600 ppm. Class 3 solvents are less toxic and should be utilized where possible (ICH, 2019).

Presence of higher level of residual solvent can significantly impact the dissolution behavior of the drug product. Moreover, higher level of residual solvent can adversely affect the

stability of the product (Kachrimanis et al., 2008). Therefore, it is very important to control the residual solvent of the drug product which are manufactured using organic solvents to find out proper dissolution behavior and also to ensure the maximum stability of the products. Gas chromatographic (GC) methods are applied to analyze residual solvents in pharmaceutical products routinely (Battu & Reddy, 2009).

In this study, a static GC Headspace method was selected to develop the method for determination residual solvent content of the Ledipasvir preparations because of the below advantages (Penton, 1992) -

- Simple.
- Robust.
- Negligible carry-over.
- Inert sample path.
- Accurate and precise.
- Admirable repeatability.

1.17 Generalized objective of the research

In this research study it was aimed to develop a solid dispersion based nanosuspension and eventually, a stabilized liquid oral suspension of Ledipasvir, Daclatasvir and Velpatasvir for increasing their solubility and oral bioavailability.

Chapter 2: Materials and Methods

2.1 Materials

The list of materials used for the current study is given below:

Table 2.1: List of ingredients used in the present study

Material	Function	Source
Ledipasvir (LDV)	Active Pharmaceuticals Ingredient (API)	Xiamen Halosyntech Co., LTD, China
Daclatasvir (DLV)	Active Pharmaceuticals Ingredient (API)	Xiamen Halosyntech Co., LTD, China
Velpatasvir (VLV)	Active Pharmaceuticals Ingredient (API)	Optimus Drugs (P) Limited, China
Poloxamer 188	Hydrophilic Carrier	BASF, Germany
Poloxamer 407	Hydrophilic Carrier	BASF, Germany
Hydroxypropylcellulose (Klucel™ EF)	Hydrophilic Carrier	Ashland, USA
Hydroxypropylcellulose (Klucel™ EXF)	Hydrophilic Carrier	Ashland, USA
Hydroprylmethylcellulsoe 5 cps	Hydrophilic Carrier	Dow Chemicals Co., USA
Povidone K17	Hydrophilic Carrier	BASF, Germany
Povidone K30	Hydrophilic Carrier	BASF, Germany
Carboxymethylcellulose Sodium 7MF (Aqualon® CMC 7MF)	Hydrophilic Carrier	Ashland Specialty Ingredients, USA
Ethanol	Solvent for solid dispersion	Merck, Germany
Methanol	Solvent for the solid dispersion	Sabic, Saudi Arabia
Methylene Chloride	Solvent for the solid dispersion	Ineor Chlor Ltd, UK

Material	Function	Source
Acetone	Solvent for solubility study	Merck, Germany
Potassium dihydrogen phosphate	For dissolution study	BASF, Germany
Tween 80	For dissolution study	BASF, Germany
Butylated Hydroxy Toluene (BHT)	For dissolution study	Scarlab S.L, Spain
Phosphoric Acid	For HPLC assay	Merck, Germany
Potassium Hydroxide Pellets	For HPLC assay	Merck, Germany
Acetonitrile (HPLC grade)	For HPLC assay	Active Fine Chemicals

2.1.1 Drug Profile

2.1.1.1 Ledipasvir

Ledipasvir is effective in the treatment of genotypes 1a, 1b, 2a, 3a, 4a, and 5a of HCV as part co-treatment with Sofosbuvir (Drugbank, 2014). It provides a strong barrier against the growth resistance (Bagaglio et al., 2017).

- Type:** Small molecule (Drugbank, 2014)
- Stereochemistry:** Ledipasvir is chiral and has 6 stereocenters (Hughes, 2016).
- Polymorphism:** There are three polymorphic forms available for Ledipasvir. Ledipasvir Acetone solvate is the commercially available form (Hughes, 2016).

2.1.1.2 Daclatasvir

Daclatasvir is used for the treatment of genotype 1 and 3 of HCV as part co-treatment with Sofosbuvir or Ribavirin (Drugbank, 2015). It provides a high barrier against the growth of resistance (Bagaglio et al., 2017).

- Type:** Small molecule (Drugbank, 2015)
- Stereochemistry:** Daclatasvir is chiral and has 4 stereocenters (European Medicines Agency, 2015).

Polymorphism:

There are two polymorphs available for Daclatasvir, N1 and N2. N2 is the thermodynamically most stable polymorph and only this form produced commercially (European Medicines Agency, 2015).

2.1.1.3 Velpatasvir

Velpatasvir is effective for the treatment of all 6 genotypes of HCV as part co-treatment with Sofosbuvir. It provides a prominently higher barrier to growth of resistance than as Ledipasvir and Daclatasvir. Therefore, it is a strong and dependable substitute for treatment of chronic HCV (Drugbank, 2016).

Type: Small molecule (Drugbank, 2016)

Stereochemistry: Velpatasvir is chiral and has 6 chiral centers (Gilead Sciences, 2016).

2.1.2 Excipients Profile**2.1.2.1 Poloxamer 188 and Poloxamer 407**

It is a nonionic hydrophilic copolymer applied as emulsifying or solubilizing agents. Different grades of Poloxamers are available based on their melting point, physical state and molecular weight (Rowe et al., 2018). Two grades of Poloxamers was used in this study – Poloxamer 188 and Poloxamer 407.

Description: White, waxy, free flowing granules or cast solids. These are free of odor and taste (Rowe et al., 2018).

Copolymer type: Triblock copolymer (Walsh et al., 2006)

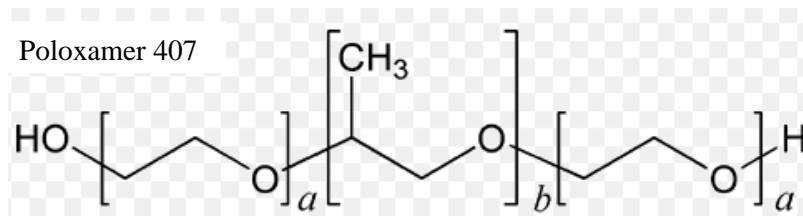
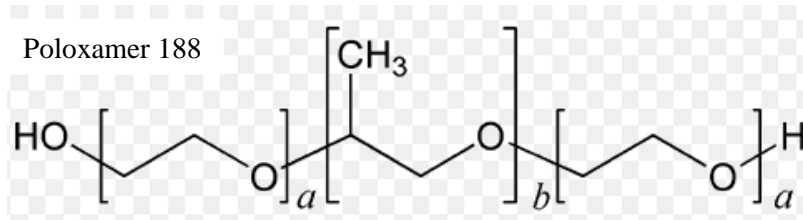
Molecular Weight: 7680–9510 g/mol (for 188) and 9840–14600 g/mol (for 407) (Rowe et al., 2018)

Length of 2 polyethylene glycol blocks: 80 repeat units (for 188) and 101 repeat units (for 407) (Walsh et al., 2006)

Length of propylene glycol blocks: 27 repeat units (for 188) and 56 repeat units (for 407) (Walsh et al., 2006)

Chemical Structure:

(Rowe et al., 2018)

**Melting Point:**

52–57°C (Rowe et al., 2018)

Solubility:

Freely soluble in water and ethanol (Rowe et al., 2018)

Flash Point:

260°C (Rowe et al., 2018)

Viscosity:

1000 mPas (for 188) (Rowe et al., 2018) and 3100 mPas (for 407) as a melt at 77°C (Walsh et al., 2006)

HLB value:

29 (for 188) (Rowe et al., 2018) and 18 – 23 (for 407) (Walsh et al., 2006)

2.1.2.2 Hydroxypropylcellulose (HPC)

HPC is a nonionic hydrophilic polymer which has been used for solubility enhancement of poorly water soluble drugs (Mohammed et al., 2012). Depending on viscosity of solution and molecular weight, different grades of HPC are existing (Rowe et al., 2018). In the present study, Klucel™ EF and EXF grades were used from Ashland.

Description:

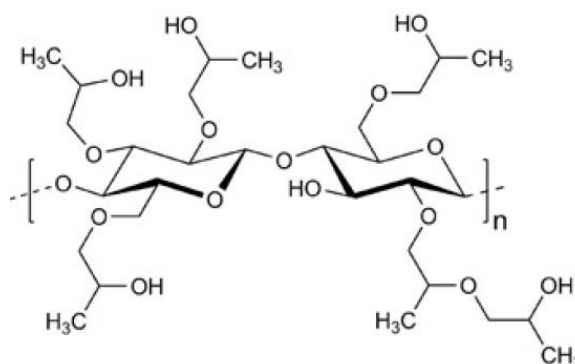
It is a white to slightly yellow, odor free and taste free powder (Rowe et al., 2018)

Molecular Weight:

Approx. 80000 g/mol (Rowe et al., 2018)

Chemical Structure:

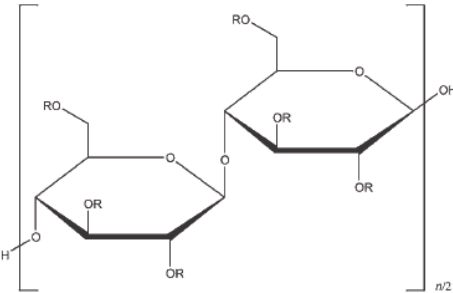
(Ashland, 2017)



Solubility:	Soluble in dichloromethane, water and ethanol (95%) (Rowe et al., 2018).
Specific Gravity:	1.22 for particles; 1.01 for a 2% w/v aqueous solution at 20°C (Rowe et al., 2018).
Viscosity:	200 – 600 mPas (10% w/v solution at 25°C) (Rowe et al., 2018).
Particle size:	595 micron (Klucel™ EF) and 250 micron (Klucel™ EXF) (Ashland, 2017)

2.1.2.3 Hydroxypropylmethylcellulose (HPMC) 5cps

It is a hydrophilic polymer which has been applied for solubility improvement of poorly water soluble drugs (Howlader et al., 2012). Depending on viscosity of solution and molecular weight, different grades of HPMC are existing (Rowe et al., 2018) (Rowe et al., 2018). HPMC 5cps was selected for the present study.

Description:	Hypromellose is a white to cream colored, odor free and taste free fibrous or granular powder (Rowe et al., 2018).
Molecular Weight:	Approx. 10000 g/mol (Rowe et al., 2018)
Chemical Structure: (Rowe et al., 2018)	 <p>where R is H, CH₃, or CH₃CH(OH)CH₂</p>

Solubility:	Soluble in cold water. Practically insoluble in ethanol (Rowe et al., 2018).
Specific Gravity:	1.26 (Rowe et al., 2018)
Viscosity:	4– 6 mPas (2% w/v solution at 20°C) (Rowe et al., 2018)

2.1.2.4 Povidone K 17 and Povidone K30

It is a hydrophilic polymer which has been proven to improve the dissolution of poorly soluble drugs from solid-dosage forms. Depending on the rate of polymerization, molecular weight, viscosity in aqueous solution (expressed as a K-value) different grades of Povidone

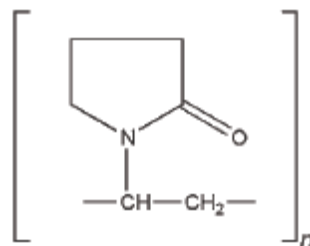
(polyvinylpyrrolidone) are available (Rowe et al., 2018). In the present study, Povidone K17 and K30 are used.

Description: Fine, white to creamy-white, almost odor free, hygroscopic powder (Rowe et al., 2018).

Molecular Weight: 10,000 g/mol (for K17) and 50,000 g/mol (for K30) (Rowe et al., 2018)

Chemical Structure:

(Rowe et al., 2018)



Solubility: Freely soluble ethanol (95%) and water (Rowe et al., 2018).

K value: 16 – 18 (for K17) and 28 – 32 (for K30) (Rowe et al., 2018)

Viscosity: 1.5 to 3.5 m Pas (for K17) and 5.5 to 8.5 m Pas (for K30) at 20°C of 10% w/v aqueous solution (Rowe et al., 2018)

2.1.2.5 Carboxymethylcellulose (CMC) Sodium

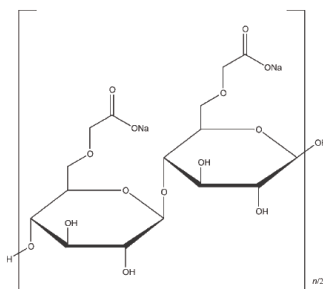
It is a hydrophilic polymer which has been applied for solubility improvement of poorly water-soluble drugs (Park et al., 2009; Rane et al., 2007). Aqualon[®] CMC Sodium (7MF) was used in the present study. It is most widely used CMC sodium with a medium viscosity which made it suitable for immediate release dosage forms (Hercules, 1999).

Description: White to almost white, granular powder free of odor and taste (Rowe et al., 2018).

Molecular Weight: Approx. 250000 g/mol (Hercules, 1999)

Chemical Structure:

(Rowe et al., 2018)



Solubility: Practically insoluble in acetone and ethanol (95%). Readily dispersed in water leading to formation of forming colloidal solutions (Rowe et al., 2018).

Viscosity: 200– 400 mPas (2% w/v solution at 25°C) (Hercules, 1999)

2.1.3 Equipment

Table 2.2: List of instruments used for the current study

Equipment	Model	Origin
Ultrasonic batch	Ultrachem M2	Sonoswiss, Switzerland
Magnetic Stirrer	LMS-1003	Labtech, Korea
UV-VIS Spectrophotometer	UV-1800	Shimadzu, Japan
HPLC	Prominace	Shimadzu, Japan
Zeta Sizer	ZS90	Malvern, Switzerland
DSC	DSC 4000	PerkinElmer, USA
FTIR	Prestige-21 / IR Tracer-100	Shimadzu, Japan
Particle Size Analyzer	Mastersizer 2000/3000	Malvern. England
Dissolution Apparatus with auto sampling system	TDT-14L	Electrolab, India
GC	2010-Plus	Shimadzu, Japan
Orbital Shaker	JSOS-500	(JSR, Australia)
Centrifuge Machine	PrimoTM	Thermo Scientific, Germany
Vortex Mixer	VM 2000	Digisystem laboratory Instruments Inc., Taiwan
Eppendorf Vacuum Concentrator	Concentrator Plus	Fisher Scientific, UK
Vacuum Oven	UFP 400	Memmert, Germany
Moisture Analyzer	MA 160-1	Sartorius, Germany

2.2 Methods

2.2.1 Suspension with non-micronized and micronized Ledipasvir

Suspensions were prepared using non-micronized and micronized Ledipasvir and they were evaluated for assay content and dissolution rate.

The following suspension vehicle was used where the non-micronized (particle size, $D_{90} = 61.478$ micron) and micronized (particle size, $D_{90} = 6.586$ micron) were incorporated in the following conventional suspension vehicle described in chapter 3.3.8.5 and mixed for 30 minutes to ensure uniformity.

Table 2.3: Composition of suspensions with non-micronized and micronized API

Materials	%w/w	
	Suspension with non-micronized API	Suspension with micronized API
Ledipasvir (Non-micronized)	1.800	-
Ledipasvir (micronized)	-	1.800
Sucrose	40.000	40.000
Xanthan Gum	0.500	0.500
Sorbitol Solution 70%	5.000	5.000
Glycerin	5.000	5.000
Citric Acid Monohydrate	0.366	0.366
Sodium Citrate*	0.477	0.477
MC and CMC Sodium (Avicel RC® 591)	0.6500	0.6500
Colloidal Silicon Dioxide (Aerosil® 200)	0.4000	0.4000
Methylparaben	0.180	0.180
Propylparaben	0.020	0.020
Sucralose	0.1000	0.1000
Mango flavor (liquid)	0.1000	0.1000
Purified Water	q.s to 100 ml	q.s to 100 ml

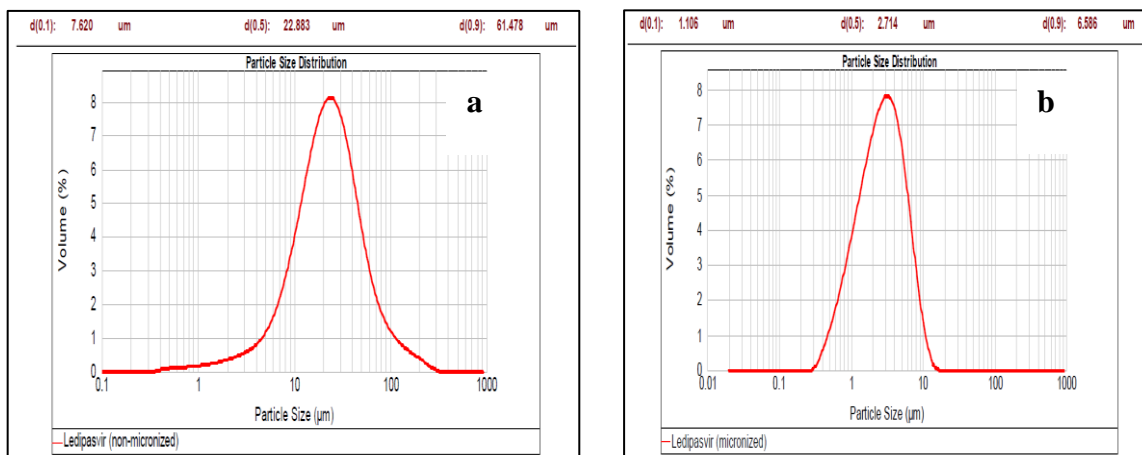


Figure 2.1: (a) Particle size distribution of non-micronized Ledipasvir; (b) Particle size distribution of micronized Ledipasvir

2.2.2 Characterization of suspensions with non-micronized and micronized Ledipasvir

Prepared suspensions were checked for assay content and dissolution profiles.

2.2.3 Solubility study of Ledipasvir

The information of solubility characteristics is important for selecting appropriate ingredient, carrier substances and drug formulation. Solubility study of Ledipasvir was done by the following procedure.

2.2.3.1 Study Procedure: The solubility of Ledipasvir (LDV) was determined in methanol, ethanol, dichloromethane and acetone using saturated shake flask method (Prakash et al., 2008). An excess amount of LDV was placed in four separate 25 mL volumetric flasks and 10 mL of methanol, ethanol, dichloromethane and acetone were placed in the flasks respectively. These flasks were sealed with stoppers and then mixed for 10 minutes using a Vortex Mixer to ensure adequate mixing of drug with the solvents. Mixtures were shaken for 24 hours in an Orbital Shaker maintained at room temperature. Afterwards, the mixtures were centrifuged at 3000 rpm for 5 minutes using a Centrifuge Machine and then filtration was through a 0.45-micron mSupor[®] membrane filter to remove undissolved drug. Filtrates were suitably diluted with methanol, ethanol, dichloromethane and acetone respectively to reduce the amount of solvent used. Three samples were prepared for each of the LDV in solvent solution. Then absorbance of these solutions was taken by a UV-VIS spectrophotometer.

2.2.3.2 Preparation of Standard Curve: Standard calibration curves were prepared for each of four LDV solutions. Solubility of LDV in each of the solvent was calculated with the help of the equation given below:

$$y = mx + c$$

Where, y = absorbance

m = concentration ($\mu\text{g/mL}$)

c = Y-intercept

Solubility ($\mu\text{g/mL}$) = Concentration / Dilution Factor.

Table 2.4 Solubility study design of Ledipasvir in methanol, ethanol, dichloromethane and acetone

Sample	Dilution	wavelength (nm) (λ_{max})	Dilution Factor	Diluent and Blank
LDV in Methanol	1 mL to 500 mL, then 1 mL to 200 mL	333	0.000001	Methanol
LDV in Ethanol	1 mL to 500 mL, then 1 mL to 200 mL	334	0.000001	Ethanol
LDV in Dichloromethane	1 mL to 500 mL, then 1 mL to 200 mL	335	0.000001	Dichloromethane
LDV in Acetone	1 mL to 100 mL, then 5 mL to 25 mL	335	0.002	Acetone

2.2.4 Solution stability study of Ledipasvir in different solvents

The stability of a drug solution in different solvent is very important to determine how long the standard/ sample solution can be hold for analytical testing. At the same time, this information also plays a prominent role in formulation and process design of a drug product. 10.0 mg, 10.4mg, 10.4mg and 10.6mg of Ledipasvir (LDV) were taken into four 100 mL clear volumetric flasks separately. Then 60 mL of methanol, ethanol, dichloromethane and acetone were placed in these flasks respectively to dissolve LDV. Volumes were then adjusted up to 100 mL with methanol, ethanol, dichloromethane and acetone respectively and then mixed well. 5 mL of each of the four solutions were taken in four separate 50mL clear volumetric flasks and diluted up to 50 mL by methanol, ethanol, dichloromethane and

acetone respectively and mixed well. The final concentration of LDV in the solutions were 10.0 µg/mL, 10.4 µg/mL, 10.4 µg/mL and 10.6 µg/mL respectively.

2.2.4.1 Solution stability determination procedure

The stability of solutions of Ledipasvir in methanol, ethanol, dichloromethane and acetone were determined for up to 24 hours at ambient temperature. Then the absorbance of these samples was taken by a UV-VIS spectrophotometer in triplicates. Study design was as per the table below-

Table 2.5: Solution stability study design of Ledipasvir in methanol, ethanol, dichloromethane and acetone

Ledipasvir concentration (µg/mL)	Solvent	wavelength (nm) (λ_{\max})	Time points (hour)	Replication	Blank
10.0	Methanol	333	0, 6, 12, 24	Triplicate	Methanol
10.4	Ethanol	334			Ethanol
10.4	Dichloromethane	335			Dichloromethane
10.6	Acetone	335			Acetone

Calculation: Calculation of recovery was done using the formula below:

$$\text{Recovery} = \{(\text{Absorbance of stability solution} \div \text{Absorbance of initially prepared solution}) \times \text{Weight of LDV in initially prepared solution}\}$$

$$\% \text{ Recovery} = \{(\text{Recovery} \div \text{Weight of LDV in initially prepared solution}) \times 100\}$$

Acceptance criteria: All of the % recovery results during this period of time should be within 98–102% of the initial value.

2.2.5 Drug-excipients compatibility study

2.2.5.1 Fourier Transform Infrared Spectroscopy (FTIR) analysis

FTIR spectrums are used to identify drug-excipients interaction (Purna Chandra Reddy Guntaka, 2018). It can notice the difference in the energy distribution of interactions between drug and matrix (Bugay, 2001).

The drugs and polymer were mixed physically in 1:1 ratio as binary mixture (Kumar Sarangi et al., 2018). The pure API, excipients and binary mixtures were scanned by FTIR over a

range of 2000 cm^{-1} to 400 cm^{-1} . The powder samples were mixed with potassium bromide powder which is in the dried form. The mixture was then compressed into disc with approx. five tons of pressure with the help of special dies in a hydraulic press (Islam et al., 2013). The disc was positioned in sample holder and the spectrum was recorded.

2.2.5.2 Differential Scanning Calorimetric (DSC) analysis

The drugs and polymer were mixed physically in 1:1 ratio as binary mixture. The physical nature of the drugs, polymers and binary mixtures was studied by DSC (Tomassetti et al., 2005). About 5 mg samples were positioned in a closed sample pans with pin hole. To obtain the thermograms, the heating of the samples were done at a constant rate of 10°C /min from 30°C to 300°C for Ledipasvir (Purna Chandra Reddy Guntaka, 2018) and Velpatasvir (Mehmood et al., 2020) whereas heating was continued up to 400°C for Daclatasvir owing to its high melting point (around 290°C) found from the experimental data. A dry nitrogen gas (40 ml/min) was purged during the sample runs (PerkinElmer®, 2018). The melting point and disappearance of the crystalline sharp peak of the samples were recorded.

2.2.6 Preparation of solid dispersions

To prepare the nanosuspension, initially the solid dispersions (SDs) were fabricated using solvent evaporation technique. Based on various previous works on SD for poorly soluble drugs, Poloxamer 188 (Park et al., 2009; Patil et al., 2011; Tran et al., 2019) Poloxamer 407 (Park et al., 2009), Povidone K 17 (Urbanetz, 2006), Povidone K 30 (Park et al., 2009), HPMC 5 cps (Tran et al., 2019), HPC (Klucel™ EF and EXF) (Mohammed et al., 2012), Carboxymethylcellulose (CMC) Sodium (Park et al., 2009; Rane et al., 2007) were primarily selected to prepared the SDs as these polymers have been used to produce SDs previously. Solid dispersions of LDV were prepared with Poloxamer 188, Poloxamer 407, Klucel™ EF, Klucel™ EXF, HPMC 5cps, Povidone K17, Povidone K30, Carboxymethylcellulose (CMC) Sodium at a drug:Polymer ratio of 1:1. Respective amount of carrier (except CMC Sodium and HPMC) was dissolved in a glass beaker containing ethanol and the drug was added in parts with continuous stirring. Because of the insolubility of HPMC and CMC Sodium in ethanol, a 50:50 ratio of ethanol: dichloromethane was used as solvent. In all cases, the concentration of the solution was 10% w/w in the solvent. Then the solvent was removed by evaporation at 40°C under vacuum using Eppendorf Vacuum Concentrator. The SD preparations were crushed with a mortar and pestle. Then the crushed preparations were sieved through a 0.60 mm (#30 mesh) screen to get uniform particles for convenience in the

next processing steps. The SD preparations were then dried at 60°C in a vacuum oven overnight to achieve the desired level of residual solvent. The prepared SDs were characterized by DSC to check for their crystallinity and amorphousity. The formulations are presented in the table below:

Table 2.6: Formulation for solid dispersions of Ledipasvir

Formula	API	Polymer	Ratio
F1SD	Ledipasvir	Poloxamer 188	1:1
F2SD		Poloxamer 407	
F3SD		HPC (Klucel EF)	
F4SD		HPC (Klucel EXF)	
F5SD		HPMC 5cps	
F6SD		PVP K 17	
F7SD		PVP K 30	
F8SD		CMC Na	

The best results were found with Poloxamer 188 in the Ledipasvir study in terms of *in-vivo* simulation. Therefore, Solid dispersions of Daclatasvir and Velpatasvir were prepared using same manner using Poloxamer 188 at 1:1 drug:polymer ratio. Ethanol was used as solvent as Daclatasvir is soluble in ethanol and Velpatasvir is freely soluble in ethanol. The prepared SDs were characterized by DSC to check for their crystallinity and amorphousity. The formulations for solid dispersions of Daclatasvir and Velpatasvir are presented below-

Table 2.7: Formulation for solid dispersions of Daclatasvir and Velpatasvir

Formula	API	Polymer	Ratio
DF1SD	Daclatasvir	Poloxamer 188	1:1
VF1SD	Velpatasvir	Poloxamer 188	1:1

2.2.7 Preparation of nanosuspensions

2.2.7.1 Nanosuspension of Ledipasvir

From the DSC curves of all solid dispersion formulations (see chapter 3.3.4), it could be understood that Ledipasvir transformed from the crystalline to amorphous form in solid dispersions manufactured with Poloxamer 188 (F1SD), Poloxamer 407 (F2SD), Klucel™ EF (F3SD), Klucel™ EXF (F4SD) and HPMC 5cps (F5SD). Ledipasvir remained in the

crystalline form in the solid dispersions prepared with Povidone K17 (F6SD), Povidone K 30 (F7SD), and CMC Na (F8SD).

Therefore, Poloxamer 188 (F1SD), Poloxamer 407 (F2SD), Klucel™ EF (F3SD), Klucel™ EXF (F4SD) and HPMC 5cps (F5SD) were primarily selected for the work of nanosuspension preparation in the current study. Polymer list were further shortened. For the preparaion of nanosuspension, Poloxamer 188 and Poloxamer 407 were selected. From Klucel™ EF and EXF, Klucel™ EXF was selected. Both are HPC with same chemistry but they differ only in particle size (Hercules, 2001). Klucel™ EXF was the choice of polymer as it is finer in size. HPMC 5 cps was selcted it has lower moelulcar weight and viscosity which makes it more suitable for immediate release formualtion (DOW, 2002).

Experimental design for formulation was fabricated using the D-Optimal design. The design and the results were statistically evaluated with the help of Design Expert® software (version 13). The proposed formulations were developed using mixtures of API and polymer. Examples of designs used for mixtures may incorporate simplex-lattice design, simplex-centroid design, D-optimal design etc. The advantages of D-optimal design are least number of runs and hence, economic. Moreover, combined mixture and process variables can be applied in the same design (Mohamad Zen et al., 2015).

D-optimal design is used in order to optimize the variables where responses of experiments depend on the ratio of the components of mixture only. It is a kind of response surface method where independent factors are the components of a mixture and responses are function of the proportions of each ingredient. The sum of the ingredients of mixture must be equal to 100% (Chouhan and Saini, 2016).

The API and the polymer in the mixture were selected as independent variables (categorical factors) whereas the particle size and polydispersity index (PDI) were selected as the dependent variables (response factors). Therefore, as a first step of the preparation of nanosuspensions, solid dispesions were prepared in three drug : polymer ratios for each of the polymers as per the tables below:

Table 2.8: Ratios of API and polymers for the D-Optimal mixture design

Particulars	API	Polymer	Total
Actually used (g)	0.7	1.3	2
	1	1	2
	1.3	0.7	2
Interpretation for D-optimal (%)	35	65	100
	50	50	100
	65	35	100

Table 2.9: Solid dispersion (SD) formulation with different ratios of Ledipasvir and polymers

Formula	API		Ratio	SD suspension in water
F1aSD	Ledipasvir	Poloxamer 188	0.7:1.3	NSF1a
F1bSD			1:1	NSF1b
F1cSD			1.3:0.7	NSF1c
F2aSD		Poloxamer 407	0.7:1.3	NSF2a
F2bSD			1:1	NSF2b
F2cSD			1.3:0.7	NSF2c
F4aSD		HPC (Klucel™ EXF)	0.7:1.3	NSF4a
F4bSD			1:1	NSF4b
F4cSD			1.3:0.7	NSF4c
F5aSD		HPMC 5 cps	0.7:1.3	NSF5a
F5bSD			1:1	NSF5b
F5cSD			1.3:0.7	NSF5c

All the solid dispersion preparations were dispersed in water separately at a concentration of 1g / 5 ml. Then ultrasonicated for 5, 10 and 15 minutes with occasional stirring to find out the optimum time to prepare lump free smooth dispersion. Then the suspensions were evaluated for viscosity, zeta potential, particle size distribution and polydispersity index.

F1aSD, F1bSD, F1cSD, F2aSD, F2bSD and F2cSD suspensions were ultrasonicated for 5 minutes with occasional stirring with spatula. It was found that smooth, lump free dispersions were obtained for all six samples.

F4aSD, F4bSD, F4cSD, F5aSD, F5bSD and F5cSD suspensions were ultrasonicated for 5, 10 and 15 minutes with occasional stirring with spatula. In both cases smooth, It was found that smooth, lump free dispersions were obtained for all six samples.

2.2.7.2 Nanosuspension of Daclatasvir

From the solid dispersion of Daclatasvir with Poloxamer 188, it was found that Daclatasvir was not converted into amorphous form and therefore, it was not further evaluated for nanosuspension.

2.2.7.3 Nanosuspension of Velpatasvir

Nanosuspensions of Velpatasvir were prepared in the same way as those of Ledipasvir but only using Poloxamer 188 in 0.7:1.3 ratio for drug:polymer because the formulated suspension of Ledipasvir (FNSF1a) using the same ratio produced best results in terms of *in-vivo* simulation.

Table 2.10: Solid dispersion (SD) formulation with different ratios of Velpatasvir and polymer

Formula	API	Polymer	Ratio	SD suspension in water
VF1aSD	Velpatasvir	Poloxamer 188	0.7:1.3	VNSF1a

2.2.8 Characterization of nanosuspensions

2.2.8.1 Measurement of viscosity

Viscosity plays an important role pharmaceutical suspension for stability and uniformity of dosing. If the viscosity is too low, there is a chance of rapid sedimentation and hard cake formation. On the contrary, if the viscosity is too high, then it becomes difficult for the patients to pour the suspension from the bottles. In both cases, dosing uniformity will be hampered. Therefore, the viscosity of suspension should be kept between 200 – 1500 cps to obtain stable and easily pourable suspension (R. Santosh and T. Naga Satya, 2016). However, as the current suspension is formulated also considering the pediatric and geriatric population, a viscosity ranging from 1090 cps to 1240 cps can be considered optimum in

terms of dosing accuracy to avoid side effects of overdose or low efficacy of under dose based on the study of some pediatric market preparations (Elliott et al., 2014).

To measure viscosity of the formulations, 0.5mL of each suspension was taken in a Brookfield viscometer using spindle no. 40 using 0.1 rpm.

2.2.8.2 Determination of zeta potential

Zeta potential of each of the SD suspensions were measured using a Zeta Sizer ZS90. Samples were suitably diluted using water and redispersed by gentle shaking. Then the zeta potential of the samples were measured after 10 runs in triplicates (Gumustas et al., 2017) using clear disposable zeta cell.

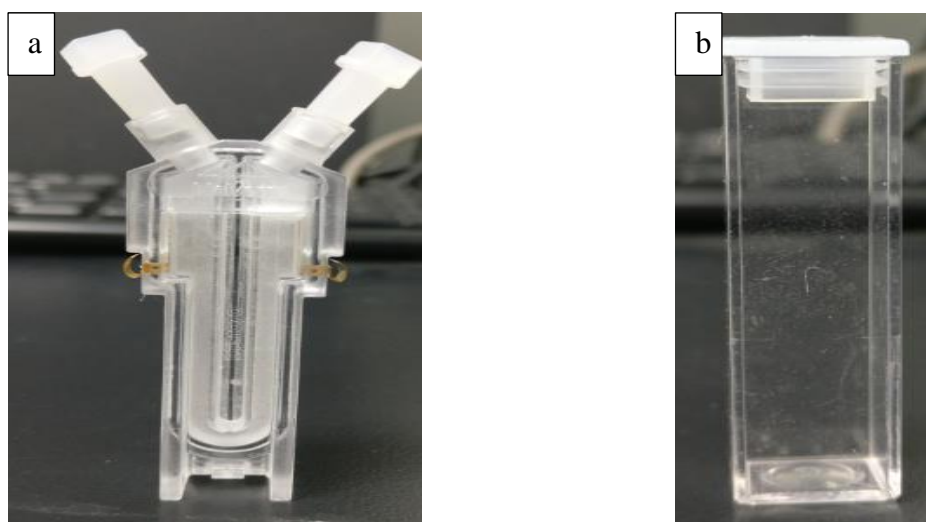


Figure 2.2: a) Disposable Zeta; b) Cell Disposable Sizing Cuvette

2.2.8.3 Particle size distribution (PSD) and polydispersity index determination

PSD and PDI were obtained with help of a Zetasizer ZS90. Samples were suitably diluted using water and redispersed by gentle shaking. The mean particle size diameter and PDI of the samples were measured after 25 runs using a disposable sizing cuvette in triplicates (Nawal, 2018).

2.2.8.4 Physical stability of the nanosuspensions

The physical stability of all the nanosuspensions of Ledipasvir were checked. All the suspensions were kept in test tubes in untouched conditions at room temperature. Visual observations were made after 1, 2, 3 and 4 weeks along with the redispersibility of the suspensions.

2.2.9 Stabilization of nanosuspensions

One of the major stability problems of the nanosuspension is aggregation of particles resulting in hard cake formation. Yield stress can be introduced in the suspension by incorporating a network structure in the continuous phase. Such suspensions remain immobile unless the applied shear crosses a specific value. The suspensions, therefore, show kinetic stability where particles remain immobile and dispersed within the network. By gelling the continuous phase, with the help of appropriate excipients, this kind of structure can be achieved (Newey-Keane and Carrington, 2016). Examples of such agents are Alginates, HPMC, Xanthan gum, CMC Sodium etc. are examples of excipients suitable for this purpose. These excipients prevent the particles of nanosuspension to contact by introducing stereospecific blockade between them. nanosuspensions particles and inhibited the particles contacting. The increase in stability can be confirmed by measuring the zeta potential (Larsson et al., 2012; Wang et al., 2013). However, zeta potential can also be modified by adding Citric Acid, Sodium citrate in the preparations to increase the suspension stability (Shinohara et al., 2018).

2.2.9.1 QbD approach for stabilization of prepared nanosuspensions

Conventionally, formulation development involves change of one variable at a time approach in pharma industry. This method involves loads of efforts and longer time period. It can also be troublesome to develop an ideal formulation with help of the traditional approach as the collective effects of all independent variables are not considered (El-Say et al., 2011). Therefore, it is very important to design a formulation with optimized quality in a short time period and minimum number of trials.

The response surface methodology (RSM) is applied for design and development of various pharmaceutical formulations. Because it involves least number of experiments. Therefore, it is fast and economic than the traditional approach of formulation development of dosage forms (Malakar, J., and Nayak, 2012). Box-Behnken designs (BBD) and central composite design (CCD) are two major experimental designs used in RSM.

BBD is fast (less experimental runs), more economic and more efficient than the CCD and full factorial designs (especially for 3 or more factors (Ferreira et al., 2007). 3 factors and 3 levels BBD was applied in the current study as BBD is most effective in case of such designs (M Manohar, Jomy Joseph, 2013).

2.2.9.2 Selection of excipients for the vehicle:

2.2.9.2.1 Sucrose: Sucrose is applied as vehicles in oral liquid preparations. It increases viscosity and taste of the preparations (Rowe et al., 2018). The recommended concentration of sugar is between 40-100gm/100 mL of the suspension (R. Santosh and T. Naga Satya, 2016).

2.2.9.2.2 Xanthan gum: Xanthan gum is commonly used in oral pharmaceutical formulations as a suspending and stabilizing agent. It exerts thickening properties too. It has no toxicity and does not interact with majority of other pharmaceutical materials (Rowe et al., 2018). Usually, it is applied form 0.05 to 0.5% w/w in pharmaceutical suspensions (R. Santosh and T. Naga Satya, 2016).

2.2.9.2.3 Sorbitol: In liquid preparations intended for oral use, sorbitol is used as a stabilizing and recrystallization inhibiting agent. Sorbitol has about 50-60% sweetening ability compared to sucrose. It increases palatability of suspensions by exerting sweet taste along with coolness. Usually, 70% sorbitol solution is applied in suspension (Rowe et al., 2018).

2.2.9.2.4 Glycerin: In liquid preparations intended for oral use, glycerin is applied as a sweetening agent, antimicrobial preservative, and viscosity imparting agent. As a preservative, its recommended concentration is less than 20% (Rowe et al., 2018).

2.2.9.2.5 Citric Acid: Citric acid is commonly applied in pharmaceutical formulations as pH adjusting agent, flavor enhancer, sequestering agent and antioxidant synergist (Rowe et al., 2018). Its recommended concentration is 1- 2% is buffer solution. (R. Santosh and T. Naga Satya, 2016). It is also applied to adjust the zeta potential of a suspension (Dheyab et al., 2020).

2.2.9.2.6 Sodium Citrate: Sodium citrate is commonly used in pharmaceutical formulations as pH adjusting agent, sequestering agent and also combinedly with citric acid as buffering agent and antioxidant synergist (Rowe et al., 2018); (R. Santosh and T. Naga Satya, 2016). Its recommended concentration is 0.3 – 2% (Rowe et al., 2018). The concentration of sodium citrate was selected in the current formulation in such a way that the pH of the suspension remains between 4 to 5. In general, majority of the liquid systems are stable from pH 4-10 (R. Santosh and T. Naga Satya, 2016).

2.2.9.2.7 Avicel[®] RC 591 (Mixture of Microcrystalline Cellulose and CMC Sodium): It contains 8.3 - 13.8% of CMC Sodium. Usually, It is used as stabilizing agents and suspending agents in pharmaceutical formulations (FMC, 2003). The microcrystalline cellulose in avicel[®] RC 591 forms a 3D network structure in the hydrogel system (Zhao et al., 2011). Its recommended concentration is 0.1 – 5% as suspending agent (R. Santosh and T. Naga Satya, 2016).

2.2.9.2.8 Colloidal Silicon Dioxide (Aerosil[®] 200): It is applied to prevent hard cake formation in pharmaceutical suspension at a concentration of 0.5% to 2.0% (Rowe et al., 2018).

2.2.9.2.9 Methylparaben: Methylparaben is commonly applied as an antimicrobial preservative in liquid preparations intended for oral use at a concentration of 0.015% - 0.2%. Optimum pH for its preservative action is from 4 to 8 (Rowe et al., 2018).

2.2.9.2.10 Propylparaben: Propylparaben is commonly applied as an antimicrobial preservative in liquid preparations intended for oral use at a concentration of 0.01% - 0.02%. Optimum pH for its preservative action is from 4 to 8. Generally, propylparaben (1 part) is combinedly with methylparaben (9 part) (Rowe et al., 2018).

2.2.9.2.11 Sucralose: Sucralose is utilized as a sweetening agent at a concentration of 0.03% to 2.4%. It is about three to five thousand fold sweeter than sucrose without any aftertaste (Rowe et al., 2018).

2.2.9.2.12 Mango flavor liquid: It is a generally regarded as safe (GRAS) flavoring agent applied in oral solution and suspension (The Product Makers (Australia) Pty Ltd, 2019).

2.2.9.2.13 Purified water: Purified water is applied as a carrier in suspension vehicle. The suggested amount of water contained in the suspension is 30 – 55% w/v (R. Santosh and T. Naga Satya, 2016).

The manufacturing processes of the suspension vehicle and the stabilized nanosuspension are described in chapter 3.3.8.4 and 3.3.8.5 respectively.

2.2.10 Dissolution Method

2.2.10.1 Dissolution method of Ledipasvir

Ledipasvir is an INN molecule and so, analytical method for Ledipasvir is not available in any official pharmacopoeia. To determine the extent of dissolution of Ledipasvir from its finished pharmaceutical product, an in-house UV-Vis spectrophotometric method was developed. The method was validated following ICH Q2 (R1) guideline.

2.2.10.1.1 Determination of λ_{\max} : The sample solution was scanned over a range of 250 – 400 nm in triplicates to find out the maximum absorbance.

2.2.10.1.2 Preparation of standard stock solution: About 10.0 mg of Ledipasvir working standard was placed into a 100 mL volumetric flask and then 60 mL of methanol was placed in the same flask to dissolve Ledipasvir. Afterwards, the volume was made up to 100 mL with methanol and mixed well.

2.2.10.1.3 Preparation of standard solution: 5 mL of the standard stock solution was taken in a 50 mL volumetric flask and the volume was made up to 50mL with diluent. The sample were collected following filtration through a 0.45-micron membrane filter.

2.2.10.1.4 Preparation of Blank, Diluent and Placebo: Methanol was used as both blank ad diluent. Placebo was prepared by excluding the API and mixing the excipients at the same ratio as that of the Ledipasvir 90mg/5mL suspension.

2.2.10.1.5 Dissolution Condition:

Apparatus:	Apparatus 2, Paddle
Dissolution medium:	1.5% Polysorbate 80 in 10 mM Potassium Phosphate Buffer with 0.0075 mg/mL Butylated Hydroxytoluene (BHT), pH 6.0
Volume:	900 ml
Rotation speed:	75rpm
Dissolution period:	60 minutes
Sampling points:	5, 10, 15, 20, 30, 45, 60 minutes
Temperature:	37 °C ± 0.5 °C

The dissolution method was selected as it is the discriminating dissolution method (CDER/FDA, 2014) and the conditions were selected as per USP <711> (USP, 2016).

2.2.10.1.6 Preparation of dissolution medium:

1.36 g of Potassium dihydrogen phosphate (KH_2PO_4) was dissolved in 1000 mL of water in a suitable volumetric flask. In case of need for pH adjustment, diluted phosphoric acid and potassium hydroxide solution was used to keep the pH 6.0 ± 0.05 (USP, 2012). Then 15.0 g Tween 80 and 7.5mg of BHT were added and stirred to dissolve clearly.

2.2.10.1.7 Dissolution procedure and sample preparation: Each of the test samples were placed individually in separate vessels and the test was carried out and sampling was done as per chapter 2.2.12.1.5. 20 mL of sample was taken after the specified period using a pipette and filtered through a Whatman filter paper#1. This solution was diluted 10 times by taking 5 mL in a 50 volumetric flask and making the final volume up to 50 mL with dissolution medium.

2.2.10.1.8 Calculation:

Calculation of % dissolution was done by using the following equation:

$$\frac{A_s}{A_{std}} \times \frac{W_{std} \times 5 \text{ mL}}{100 \text{ mL} \times 50 \text{ mL}} \times \frac{900 \text{ mL} \times 50}{L \times 5} \times P(\%) \times 100$$

Where, A_s and A_{std} are the absorbances of standard and sample solutions respectively, W_{std} is the weight of standard (mg), L is the label claim and P is the potency of the standard (%).

2.2.10.1.9 Validation of dissolution method

2.2.10.1.9.1 Specificity

In order to obtain specificity, the absorbances of blank, placebo, standard and sample solutions were taken.

Acceptance Criteria: Analyte spectrum must be resolved from that of the blank, placebo, standard and sample solution.

2.2.10.1.9.2 Linearity and Range

2.5 mL, 3.0 mL, 3.5 mL, 4.0 mL, 4.5 mL, 5.0 mL, 5.5 mL, 6.0 mL, 6.5 mL, 7.0 mL and 7.5 mL of the standard stock solution were taken in eleven 50 mL volumetric flasks separately and the volumes were adjusted with methanol up to 50 mL to achieve the concentration of 50% (5 $\mu\text{g/mL}$), 60% (6 $\mu\text{g/mL}$), 70% (7 $\mu\text{g/mL}$), 80% (8 $\mu\text{g/mL}$), 90% (9 $\mu\text{g/mL}$), 100%

(10 µg/mL), 110% (11 µg/mL), 120% (12 µg/mL), 130% (13 µg/mL), 140% (14 µg/mL) and 150% (15 µg/mL) of nominal concentration (10 µg/mL). The concentrations of these samples were plotted at X-axis and the relevant absorbances were plotted at Y-axis to prepare the linearity curve and the regression coefficient, R^2 was determined.

Range was determined by considering minimum concentration (5.0 µg/mL) and maximum concentration (15.0 µg/mL) of the linear range.

Acceptance criteria: R^2 should not be less than 0.985.

2.2.10.1.9.3 Precision

Repeatability: Six test samples of nominal concentration were prepared and the absorbances of samples were measured in order to obtain repeatability.

Acceptance Criteria: RSD should be $\leq 10\%$.

Intermediate precision: Six test samples of nominal concentration were prepared by a 2nd analyst on a different day and the absorbances of samples were measured. Relative standard deviation (RSD) was obtained combining 12 results from both analysts to get the intermediate precision.

Acceptance Criteria: RSD for 12 samples should be $\leq 10\%$.

2.2.10.1.9.4 Accuracy

Nine different test samples were prepared in nine different 100 mL volumetric flasks as per the table below-

Table 2.11: Preparation of sample solution for accuracy (UV)

% of Nominal Concentration	Weight (mg)	
	API	Placebo
80%	9.10	112.5
	9.05	113.1
	9.13	112.8
100%	11.39	140.6

% of Nominal Concentration	Weight (mg)	
	API	Placebo
120%	11.20	141.0
	11.14	141.1
	13.71	169.2
120%	13.66	168.4
	13.87	168.7

In each volumetric flask, 60 mL methanol was placed and sonicated for 5 minutes. The volume was made 100 mL using Methanol, mixed well and filtered through a Whatman filter paper no.#1. Then 5.0 mL of each of these filtrates was diluted to 50 mL using Methanol in 50 mL volumetric flasks and mixed well.

Concentrations were calculated from the respective absorbance values. % recoveries were obtained with the formula below:

$$\% \text{ Recovery} = \{(\text{Experimental Conc.} / \text{Theoretical Conc.}) \times 100\}$$

Acceptance criteria: % Recovery should be between 95.0% and 105.0%.

2.2.10.1.9.5 Robustness

The robustness of this method was conducted by changing one parameter (maximum wavelength) of the method by using test sample of same concentration of repeatability sample. Concentration value was calculated from the corresponding absorbance for the concentration. The spectrophotometric condition was changed by shifting the maximum wavelength ± 2 nm from the required wavelength of analysis to measure the absorbance of test sample.

Acceptance Criteria: $\geq 75\%$ dissolution within 30 minutes.

2.2.10.1.9.6 Solution stability study

The solution stability study was conducted by analyzing each standard and sample kept at two conditions, room/ambient conditions ($25^{\circ}\text{C} \pm 5^{\circ}\text{C}$, $55\% \text{ RH} \pm 5\% \text{RH}$, exposed and

unexposed to light) and refrigerator for 24 hours. Absorbance of each sample was taken in triplicates.

Solution stability study was established as follows:

- a) Absorbances of freshly prepared solutions (both standard and sample) were taken.
- b) Absorbances of both standard and sample solutions prepared in both clear and amber volumetric flasks at all conditions (ambient and refrigerator) after 12 hours were taken.
- c) Absorbances of both standard and sample solutions prepared in both clear and amber volumetric flasks at all conditions (ambient and refrigerator) after 24 hours were taken.
- d) Recovery was calculated by the following formula:

Recovery of standard = {(Absorbance of stability standard solution ÷ Absorbance of initially prepared Standard) x Weight of initially prepared standard}

% Recovery of standard = {(Recovery ÷ Weight of stability standard solution) x 100}

% Recovery of sample = {(% dissolution of stability sample solution ÷ % dissolution of initially prepared sample solution) x 100}

Acceptance criteria:

- The recovery between initially prepared standard and each standard solution kept at every condition at given period should be between 99.0 – 101.0%.
- Assay value at each condition and given time should be between 98.5 – 101.5% of the initial sample dissolution.

2.2.10.2 Dissolution method of Velpatasvir

2.2.10.2.1 Dissolution conditions:

Apparatus	:	Apparatus 2, Paddle
Dissolution medium	:	pH 6.8 phosphate buffer
Medium volume	:	900 mL
Rotation speed	:	75 rpm
Sampling points	:	5, 10, 15, 20, 30, 45, 60 minutes
Temperature	:	37 °C ± 0.5 °C

The volume of the dissolution medium and the rpm were selected as per EMA guideline on investigation of bioequivalence (EMA, 2014).

2.2.10.2.2 Preparation of dissolution medium: About 6.805 g of KH_2PO_4 was dissolved in sufficient amount of water. 111 mL of 0.2N Sodium hydroxide solution (0.84% solution) was added into it and finally water was added to make the volume 1000 mL (USP, 2016). This medium was selected because Velpatasvir is practically insoluble above pH 5.0 and hence, this medium would be the choice for establishing a discriminatory dissolution method (Mehmood et al., 2020).

2.2.10.2.3 Dissolution procedure and sample preparation:

Each of the test samples were placed individually in separate vessels and the test was carried out and sampling was done as per chapter 2.2.10.2.1.

Preparation of Sample: 20 mL of sample was taken after the specified period using a pipette and filtered through a Whatman filter paper#1. This solution was diluted 10 times by taking 5 mL in a 50 volumetric flask and making the final volume up to 50 mL with dissolution medium.

Preparation of Standard: Approximately 20.0 mg of Velpatasvir standard was dissolved with sufficient amount of diluent and the volume was made up to 100 mL using diluent. This solution was diluted 10 times by taking 5 mL in a 50 volumetric flask and making the final volume up to 50 mL with diluent.

Preparation of Diluent: Acetonitrile and water in 1:1 ratio was used as diluent (Somia Gul et al., 2018).

Preparation of Blank: Diluent was used as blank.

UV spectrophotometric system (Somia Gul et al., 2018):

Cell : Special Quartz Macro Cuvette 10 mm (3.5ml)

Wavelength (λ) : 303 nm

2.2.10.2.4 Calculation:

Calculation of % dissolution was done by using the following equation:

$$\frac{A_s}{A_{std}} \times \frac{W_{std} \times 5 \text{ mL}}{100 \text{ mL} \times 50 \text{ mL}} \times \frac{900 \text{ mL} \times 50}{L \times 5} \times P(\%) \times 100$$

Where, A_s and A_{std} are the absorbances of standard and sample solutions respectively, W_{std} is the weight of standard (mg), L is the label claim and P is the potency of the standard (%).

2.2.11 Dissolution profile comparison

The dissolution profiles were compared for similarity factor (f_2), difference factor (f_1) and dissolution efficiency (%DE) using DDSolver[®] software program (Zhang, Huo, Zhou, Zou, et al., 2010).

Two dissolution profiles are considered similar if f_1 is between 0 to 15 and f_2 is between 50 to 100 (EMEA/CHMP/VWP/164653/2005, 2010; Naeem Aamir et al., 2011). Moreover, two dissolution profiles can be considered equivalent if the difference between their %DE is within $\pm 10\%$ (Anderson et al., 1998; Karmoker et al., 2017).

2.2.12 Drug Release Kinetics

There are various drug release kinetic mathematical models which can be followed by IR dosage like Zero-order, First order, Hixson-Crowell, Korsmeyer–Peppas and the Higuchi kinetic models (Baishya, 2017; “Mathematical Models of Drug Release,” 2015).

2.2.13 *In-vivo* simulation study:

2.2.13.1 *In-vivo* simulation of Ledipasvir

The *in-vivo* simulation was made with the help of convolution process to obtain the blood concentration of Ledipasvir from the dissolution profiles of the formulated suspensions FNSF1(a), FNSF2(a) and market product 1. The aim was to simulate and compare the pharmacokinetic parameters (peak plasma concentration, C_{max} and area under the curve, $AUC_{(0\text{ to }t)}$).

Convolution is the process of combined effect of dissolution and elimination of drug in the body to represent blood drug concentration vs time profile (figure 2.3 right to left) whereas obtaining dissolution profiles from blood drug concentration vs time profile is referred as deconvolution (figure 2.3 left to right) (Qureshi, 2010).

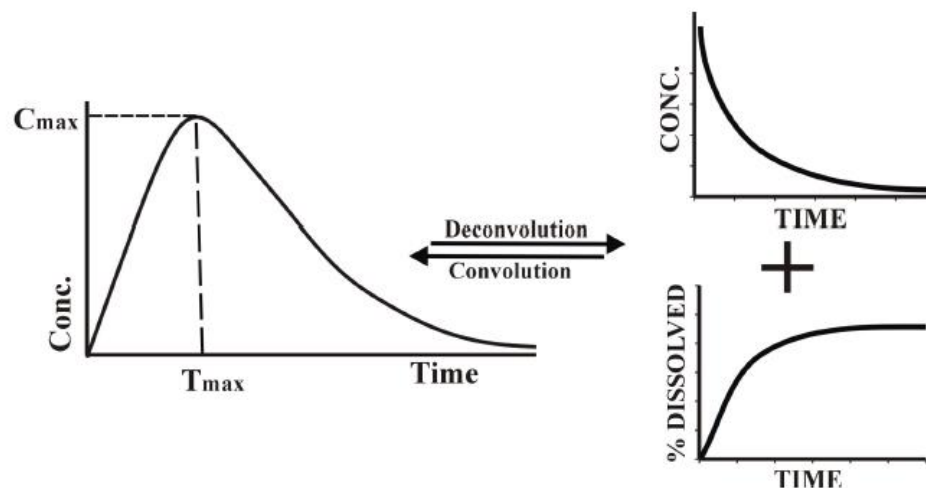


Figure 2.3: Deconvolution and convolution (Qureshi, 2010)

Following equations were used during the simulation process:

$$1) K_e = 0.693/t_{1/2}$$

where, K_e = Elimination rate constant

$$t_{1/2} = \text{Half life}$$

$$2) C_t = C_0 \cdot e^{-K_e t}$$

Where, C_t is amount of drug in blood after ingestion (ng/mL)

C_0 is the initial amount ($t=0$) (mg)

$$3) \text{Blood concentration} = C_t \times F \times 1000 / V_d \times \text{Body weight (Kg)}$$

Where, F = Bioavailability factor

V_d = Apparent volume of distribution (L/kg)

C_{\max} and $AUC_{(0 \text{ to } t)}$ were predicted using PKSolver[®] which works on the principle of convolution and deconvolution (Zhang, Huo, Zhou, and Xie, 2010).

At first, the predicted values of C_{\max} and AUC were obtained for the market product 1 (using 1 tablet of a dose of 90mg of Ledipasvir). These predicted values were compared with the experimental C_{\max} and AUC obtained from the studied literature. Then, the predictability of the model was evaluated.

Following equation was applied to calculate the percent prediction error (% PE) for C_{\max} and AUC:

$$\% \text{ PE} = [(\text{Observed value} - \text{Predicted value}) / \text{Observed value}] \times 100$$

A %PE value $\leq 10\%$ ensures the predictability of the model. A %PE value between 10% and 20% indicates inconclusive predictability and needs further data. A %PE value $>20\%$ indicates insufficient or lack of predictability (Malinowski et al., 1997; Rastogi et al., 2018).

The Pharmacokinetic parameters of Ledipasvir were collected from published literatures and the values are presented below:

Volume of distribution, $V_d = 299\text{L}/60\text{kg}$ body weight (Cada et al., 2015)

Relative bioavailability, $F = 1$ (CDER/FDA, 2014)

Peak plasma concentration, $C_{\max} = 323.26 \text{ ng/mL}$ (CDER/FDA, 2014)

Area under the curve at time t, $AUC_{(0 \text{ to } t)} = 10628.88 \text{ ng.h/mL}$ (CDER/FDA, 2014)

Time to reach the C_{\max} , $T_{\max} = 4$ hours (EMA, 2014)

Elimination half-life, $t_{1/2} = 47$ hours (CDER/FDA, 2014)

Elimination rate constant, $k_e = 0.0147 \text{ hour}^{-1}$

After completion of model predictability study, at first, a single dose study with 90mg dose of Ledipasvir was selected in this simulation study. For this purpose, 1 tablet of market product 1 (MP1), 5mL of FNSF1a and FNSF2a were used. The results of pharmacokinetic parameters of FNSF1a and FNSF2a were compared with the those of the market product 1 with the help of paired t-test (Singh et al., 2019). Later on, a triple dose i.e. 270mg dose of Ledipasvir was used in the simulation study to find out the extent of absorption of the drug by determining the saturation point of the drug absorption. The aim of this triple dose study was to support any future study where more than current daily dose may be required for a new application of the drug. For this purpose, 3 tablets of the market product 1 (MP1), 15 mL of FNSF1(a) and FNSF2(a) suspensions were used. From the dissolution data, plasma concentrations were determined up to 48 hours using convolution method (Gillespie, 1997; Qureshi, 2010).

2.2.13.2 In-vivo simulation of Velpatasvir

The daily dose of Velpatasvir is 100mg which was selected for this simulation study. For this purpose, 1 tablet of market product 3 (MP3) and 5mL of VFNSF1a were used and the simulation was done by the same method used for the simulation of Ledipasvir above.

The Pharmacokinetic parameters of Velpatasvir were collected from published literatures and the values are presented below:

Volume of distribution, $V_d = 392/60\text{kg}$ body weight (European Medicines Agency, 2016)

Relative bioavailability, $F = 0.25$ to 0.3 (European Medicines Agency, 2016)

Peak plasma concentration, $C_{\max} = 372.8 \text{ ng/mL}$ (TGA, 2017)

Area under the curve at time t, $AUC_{(0 \text{ to } t)} = 2727.3 \text{ ng.h/mL}$ (TGA, 2017)

Time to reach the C_{\max} , $T_{\max} = 3$ hours (TGA, 2017)

Elimination half-life, $t_{1/2} = 18.8$ hours (European Medicines Agency, 2016)

Elimination rate constant, $k_e = 0.037 \text{ hour}^{-1}$

2.2.14 Stability study of the formulated suspensions

Physical and chemical studies of the final formulations of Ledipasvir, FNSF1a and FNSF2a were evaluated at accelerated stability conditions ($40^\circ\text{C} \pm 2^\circ\text{C}$ and $75\% \pm 5\%\text{RH}$) (ICH guideline Q1A(R2), 2003; WHO, 2009) after three and six months. For physical stability, zeta potential values, sedimentation volume (Patel et al., 2019) and redispersibility were checked. For chemical stability, assay and dissolution profiles were checked. After 6 months of stability studies, assay results were compared with the initial assay results by one-way analysis of variance (ANOVA) (Zou et al., 2017) using Minitab[®], version 17 (Jena et al., 2020). ANOVA is used to compare the stability results of the drug product (Raphael, 1999; Zou et al., 2017). The dissolution results were compared with the initial dissolution results for similarity factor (f_2), difference factor (f_1) and dissolution efficiency (%DE) using DDSolver[®] software.

2.2.15 Analytical method for analysis of Ledipasvir content in pharmaceutical dosage forms

2.2.15.1. Development and validation of RP-HPLC based method for Ledipasvir

The content of Ledipasvir was determined in pharmaceutical finished product by In-house developed reverse phase HPLC method. Later, the method was validated as per ICH guideline Q2 (R1) guideline.

2.2.15.1.1 QbD based approach for method development: Quality by Design (QbD) based approach for the development of analytical methods is becoming popular as the conventional approach involved high degree of variability. QbD is a science-based approach where quality is designed to establish a detailed understanding of the response of the system quality to system parameters. Factorial design is one of the response surface methods (RSM) which aids in development of analytical methods systematically (Das et al., 2017).

Advantages of Factorials:

- More efficient than traditional approach.
- Needed where interactions may be possible.
- Possible to estimate the impact of a factor at different levels of other factor resulting in producing a design space (Reda, 2017).

In this study, a two factor three level (3^2) factorial design was implemented to construct the experimental runs. Independent variables of the study were flow rate and buffer percentage of the mobile phase whereas the response factors were retention time, tailing factor and theoretical plate count.

2.2.15.1.2 Selection of column: Supelcosil™ Diphenyl column (250 mm X 4.6 mm, 5 μ m) was selected to get optimum separation of the peaks. This column contains a diphenyl bonded phase, which gives better specificity for aromatic groups compared to alkyl-type bonded phases (Sigma-Aldrich, 2017). Since Ledipasvir is an aromatic heterocyclic compound, biphenyl column is the preferred choice of column for the current study. Use of Phenyl column is also found in previous works of Ledipasvir (Mastanamma et al., 2018).

2.2.15.1.3 Selection of detector: PDA (photo diode array) detector was selected owing to its capability to scan over a range of multiple wavelength quickly with precision (Rote et al., 2017). This detector was also found in the previous work on Ledipasvir (Mastanamma et al., 2018).

2.2.15.1.4 Selection of column oven temperature: Column oven temperature was initially selected 30°C based on the previous work for Ledipasvir (Mastanamma et al., 2018). However, this parameter was further evaluated during robustness checking of the method with other selected chromatographic conditions.

2.2.15.1.5 Selection of wavelength: Wavelength was selected 330nm based on the maximum absorption peak for Ledipasvir found during the experiment. This finding matches the findings in the previous work on Ledipasvir (Eguchi et al., 2017). However, this parameter was further evaluated during robustness checking of the method with other selected chromatographic conditions.

2.2.15.1.6 Selection of components of the mobile phase: Acetonitrile can improve the separation of the studied drug with a sufficient run time. The buffer pH from pH 5 to 7 specifically pH around 6.0 phosphate buffer provides the optimal resolution with balanced peaks for Ledipasvir (Eguchi et al., 2017). Therefore, Acetonitrile and phosphate buffer (pH 6) combination was selected initially as mobile phase. Nevertheless, for the mobile phase, the buffer concentration was finalized by QBD.

2.2.15.1.7 Optimized Chromatographic Conditions:

Column	:	Diphenyl (250 mm X 4.6 mm, 5 μ m)
Flow Rate	:	1.7 mL/min
Wavelength	:	330 nm
Injection Volume	:	20 μ L
Temperature	:	30°C
Run Time	:	20 minutes

2.2.15.1.8 Preparation of buffer: 1.36 g of KH_2PO_4 was dissolved in 1000 mL of water. In case of pH adjustment to 6.0 ± 0.05 , diluted phosphoric acid or potassium hydroxide solution was applied (USP, 2012).

2.2.15.1.9 Preparation of Mobile Phase: Buffer and Acetonitrile was mixed at a volume ratio of 48:52 and filtered a 0.45- μ m millipore[®] membrane filter.

2.2.15.1.10 Preparation of Analytical Stock Standard Solution: Approximately 10.0 mg of Ledipasvir working standard was dissolved in 100 mL diluent in a volumetric flask.

2.2.15.1.11 Preparation of analytical standard solution: 5 mL of standard stock solution was diluted in a 50 mL volumetric flask with Methanol to obtain a concentration of 10 μ g/mL. Afterwards, the solution was collected in a vial after filtration through a 0.45- μ m membrane filter.

2.2.15.1.12 Preparation of Diluent, blank and placebo: Methanol was applied as both blank ad diluent. The placebo used in dissolution method validation was used here too.

2.2.15.1.13 Preparation of test sample: Approximately 0.5 mL of formulated suspension equivalent to 9.0 mg of Ledipasvir was placed in sufficient amount of diluent in a 100 mL volumetric flask, sonicated for 10 minutes and diluted to the mark. The solution was then filtered through Whatman Filter paper#1. The solution was diluted in a 50 mL volumetric flask with diluent to get the final concentration of 9 μ g/mL. Afterwards, the solution was collected in a vial after filtration through a 0.45 μ m membrane filter.

2.2.15.1.14 Calculation of Assay:

Ledipasvir per 0.5 mL

$$= \frac{A_s}{A_{std}} \times \frac{W_{std} \times 5 \text{ mL}}{100 \text{ mL} \times 50 \text{ mL}} \times \frac{100 \text{ mL} \times 50 \text{ mL}}{W_s \times 5 \text{ mL}} \times (P\%) \times W_a$$

Where, A_s is the peak area of sample solution, A_{std} is the peak area of standard solution, W_{std} is the weight of standard (mg), W_s is the volume of sample (mL), P is the potency of the standard (%) and W_a is the wt/mL of sample (mg/mL).

2.2.15.2 Validation of developed RP-HPLC method

The developed method was validated per ICH Q2 (R1) guideline for linearity, precision, accuracy, specificity, robustness, system suitability, solution stability study and filter compatibility study.

2.2.15.2.1 Linearity and Range

The standard stock solution was diluted to achieve 50%, 60%, 80%, 100%, 120%, 140% and 150% of nominal concentration of 10.0 $\mu\text{g/mL}$ for Ledipasvir with the help of diluent. Single injection was made for each concentration level. The concentrations of these samples were plotted at X-axis and the relevant peak area (of the main peak) were plotted at Y-axis to prepare the linearity curve and the regression coefficient, R^2 was determined. Range was determined by considering minimum concentration (5.0 $\mu\text{g/mL}$) and maximum concentration (15.0 $\mu\text{g/mL}$) of the linear range.

Acceptance criteria: $R^2 \geq 0.995$ and the % Y-intercept compared to 100% area will not be more than 5%.

2.2.15.2.2 Precision

Repeatability

To determine repeatability, 6 test samples of nominal concentration were injected maintaining optimized chromatographic conditions.

Acceptance Criteria: RSD should be $\leq 2\%$.

Intermediate precision

Repeatability study was repeated by a 2nd analyst on another day. RSD was obtained combining 12 results from both analysts to obtain intermediate precision.

Acceptance Criteria: RSD of 12 samples should be $\leq 2\%$.

2.2.15.2.3 Accuracy

Nine different weight of Ledipasvir working standard were taken as per the table 2.12 below and placebo solution was added at a concentration of about 500.0 $\mu\text{g/mL}$ to all the samples, 50 mL of diluent was added. The volumes were made up to 50 mL using diluent after 15

minutes of sonication. Filtering was done through a Whatman Filter paper#1, discarding the first 10 mL of filtrate.

Table 2.12: Standard and placebo for accuracy study (HPLC)

% of Nominal Value	Ledipasvir WS for spiking	
	Weight (mg)	Placebo solution
80%	8.0	500.0 µg/mL
	8.2	
	8.1	
100%	10.3	
	10.2	
	10.0	
120%	12.0	
	12.0	
	12.1	

Then 5.0 mL of each of these filtrates was diluted to 50 mL using diluent in 50 mL volumetric flasks and mixed well. Then filtered through 0.45-µm filter and collected in vials. % Recoveries were obtained with the formula below:

$$\% \text{ Recovery} = \{(\text{Experimental Conc.} / \text{Theoretical Conc.}) \times 100\}$$

Acceptance criteria: % Recovery should be 98.0% - 102.0%.

2.2.15.2.4 Specificity

In order to obtain specificity, the injections of blank, placebo, standard and sample solutions were made.

Acceptance Criteria:

Analyte peak must be resolved from that of blank, placebo, sample solution and standard solution.

2.2.15.2.5 Robustness

Recovery was obtained by injecting one sample and standard by altering the pH of the buffer of the mobile phase from pH 6 to 5.8 and 6.2.

Acceptance Criteria:

The tailing factor should be ≤ 1.5 . The % RSD of the system suitability should be $\leq 2.0\%$ and the theoretical plates count should be ≥ 1000 .

2.2.15.2.6 System Suitability Test

Analytical standard solution was used as system suitability solution. Before starting validation, System Suitability was established by injecting six replicates of system suitability solution and %RSD was calculated from six peak areas.

Acceptance Criteria: %RSD of six replicates should be $\leq 2.0\%$, the tailing should be ≤ 1.5 and the theoretical plates count should be ≥ 1000 .

2.2.15.2.7 Solution Stability Study

The solution stability study was conducted by analyzing each standard and sample kept at two conditions, room/ambient condition ($25^{\circ}\text{C}\pm 5^{\circ}\text{C}$, $55\% \text{RH}\pm 5\% \text{RH}$, exposed and unexposed to light) and refrigerator for 48 hours. Solution stability study must be established as follows:

- a) Single injection of standard and sample solutions prepared at zero time (freshly prepared).
- b) Single injection of standard and sample solutions prepared in both clear and amber HPLC vials at all conditions (ambient and refrigerator) after 24 hours.
- c) Single injection of standard and sample solutions prepared in both clear and amber HPLC vials at all conditions (ambient and refrigerator) after 48 hours.

- d) Percent recoveries of each of solutions was calculated using freshly prepared standard as comparison. Recovery will be calculated by the following formulation:

Recovery = {(Peak area stability standard solution \div Peak area of freshly prepared standard) x Weight of freshly prepared standard}

% Recovery = {(Recovery \div Weight of stability standard solution) x 100}

Acceptance criteria:

- The recovery between freshly prepared Standard and each Standard solution kept in every condition at given period should be between 99.0 – 101.0%.
- Assay value in each condition and given time should be between 98.5 – 101.5%.

2.2.15.2.8 Filter Compatibility Study

To check filter compatibility, blank, sample and standard solutions are analyzed with and without filtration in triplicates. %Recovery of filtered and unfiltered solutions were compared.

Acceptance Criteria: The difference between the % recovery of the filtered and unfiltered samples should be $\leq \pm 1.5\%$.

2.2.15.3 Equivalency between UV and HPLC assay method of Ledipasvir in pharmaceutical dosage forms

It was aimed to establish equivalency between UV and HPLC method to determine Ledipasvir content in dosage forms so that UV method can be applied for day to day analysis.

2.2.15.3.1 Comparison between HPLC and UV methods: Standard calibration curves were prepared for both HPLC and UV methods and comparative regression analysis was done. Regression coefficient (R^2) was determined for both methods. Reproducibility, intermediate precision, accuracy and solution stability were done for both methods. % RSD of all these parameters was determined for both methods.

2.2.15.3.2 Equivalency between HPLC and UV methods: To establish equivalency between HPLC and UV methods, same standard and same 6 sample solutions were run in both HPLC and UV machines. Assay was calculated using the calculation as per the respective method validation protocol. Finally, the % RSD was calculated between assay results of the two methods.

2.2.15.3.3 Statistical analysis: The equivalency between HPLC and UV methods were statistically evaluated at 95 % confidence interval applying ANOVA, paired t-test and paired equivalence test (Mara and Cribbie, 2012) using Minitab[®], version 17.

2.2.16 Method of analysis for Velpatasvir content in pharmaceutical dosage forms

A UV spectrophotometric method was applied for the determination of Velpatasvir content in dosage forms (Somia Gul et al., 2018) which. The detailed method is described below-

2.2.16.1 Preparation of Sample

Approximately 0.5 mL of formulated suspension equivalent to 10.0 mg of Velpatasvir was placed in sufficient amount of diluent in a 100 mL volumetric flask, sonicated for 15 minutes and diluted up to 100 mL. After filtration through a Whatman Filter paper#1, the solution was diluted 10 times to get the final concentration of 20 $\mu\text{g/mL}$.

2.1.16.2 Preparation of Standard

Approximately 20.0 mg of Velpatasvir standard was taken dissolved in 100 mL of diluent. This solution was diluted to get the final concentration of 20 $\mu\text{g/mL}$.

2.1.16.3 Preparation of Blank and Diluent

Acetonitrile and demineralized water in 1:1 ratio were used as diluent and blank.

2.1.16.4 UV spectrophotometric system

Cell : Special Quartz Macro Cuvette 10 mm (3.5ml)
Wavelength (λ) : 303 nm

2.1.16.5 Calculation

Velpatasvir per 0.5 mL

$$= \frac{A_s}{A_{std}} \times \frac{W_{std} \times 5 \text{ mL}}{100 \text{ mL} \times 50 \text{ mL}} \times \frac{100 \text{ mL} \times 50 \text{ mL}}{W_s \times 5 \text{ mL}} \times (P\%) \times W_a$$

Where, A_s and A_{std} are the peak areas of sample and standard solutions respectively, W_{std} is the weight of standard (mg), W_s is the volume of sample (mL), P is the potency of the standard (%) and W_a is the wt/mL of sample (mg/mL).

2.2.17 Development and validation of GC headspace method for Ledipasvir**2.2.17.1 QbD based approach for development of GC method**

Development of GC method was also done using 3^2 full factorial design where split flow and increment of temperature of column oven were regarded as independent variables, retention time, tailing factor and theoretical plate count were regarded as dependent variables.

2.2.17.2 Selection of detector

Flame ionization detector (FID) was selected because it meets or exceeds meeting or exceeds all requisites of USP method (Thermoscientific, 2018). It also has excellent sensitivity (Sojitra et al., 2019).

2.2.17.3 Selection of carrier gas (mobile phase)

Commonly used carrier gases include Helium, nitrogen etc. (Raja, P. M. V., and Barron, 2021). Nitrogen was used as carrier gas as it is non-reactive and cheaper than helium (Raja, P. M. V., and Barron, 2021; Sojitra et al., 2019).

2.2.17.4 Selection of column (stationary phase)

Fused Silica DB-624 (30-m x 0.32-mm x 1.8- μ m) capillary GC column was selected as it is highly inert, can operate 260 °C temperature and has good sensitivity (Gras et al., 2014). It is very rapid and precisely designed residual solvent determination (Agilent, 2018)

2.2.17.5 Optimized chromatographic condition

Column	: Fused Silica DB-624 (30-m x 0.32-mm x 1.8- μ m)
Detector	: FID
Injection port temperature	: 150°C (Dubey et al., 2020)
Detector temperature	: 250°C (Pandey et al., 2011)
Carrier gas	: Nitrogen, 14.0 psi through Head space (Chasteen, 2000)
Split flow	: 50.0 mL/min (Pandey et al., 2011)
Injection mode	: split mode/head space (Dubey et al., 2020)
Column temperature program	:

Temperature, °C	Hold time, min	Rate, °C/min
60	1.0	0.0
90	2.0	5.0
120	1.0	15.0

Headspace:

Oven temperature	: 80°C
Needle temperature	: 110°C
Transfer line temperature	: 130°C
Injection time	: 0.1 min
GC cycle time	: 15.0 min

2.2.17.6 Preparation of sample and standard solutions

Stock Standard Solution: About 100mg of dichloromethane (DCM) was taken in a 100 mL volumetric flask and diluted up to 100 mL with the help of organic free water.

Analytical Standard Solution: 10.0 mL of stock solution was placed in a 100 mL volumetric flask and diluted up to 100 mL with the help of organic free water. Then 5 mL of this solution was taken to a GC vial and sealed properly.

Preparation of Test Sample: 2000 mg of SD powder was taken into a GC vial and 5 mL of organic free water was added. Then it was mixed well and sealed properly.

Preparation of Blank and Diluent: Organic free water was used as blank and diluent.

Specification Limit: Dichloromethane content should be not more than 600 ppm.

2.2.17.7 Calculation

The content of residual DCM of the samples was calculated in ppm by using the following equation:

$$= \frac{A_s}{A_{std}} \times \frac{W_{std} \times 10\text{mL} \times 5\text{mL}}{100\text{mL} \times 100\text{mL} \times W_s} \times \frac{100 \times 1000 \times Wa}{100 \times}$$

Where, A_s and A_{std} are the peak areas of impurity in sample and standard solution respectively, W_{std} is the weight of impurity in standard solution (mg), W_s is the weight of sample (mg), D is the content of of Ledipasvir and W_a is the average weight of sample (mg).

2.2.17.8 Validation of developed GC method

The developed method was validated as per ICH Q2 (R1) guidelines. The parameters evaluated were linearity and range, precision, repeatability, accuracy, specificity, robustness and system suitability.

2.2.17.8.1 Linearity and Range

The standard stock solution was diluted to achieve 50%, 60%, 80%, 100%, 120%, 140% and 150% of nominal concentration of 100.0 $\mu\text{g/mL}$ for Ledipasvir with the help of diluent. Single injection was made for each concentration level. The concentrations of these samples were plotted at X-axis and the relevant peak area (of the main peak) were plotted at Y-axis to prepare the linearity curve and the regression coefficient, R^2 was determined.

Range was determined by considering minimum concentration (50.0 $\mu\text{g/mL}$) and maximum concentration (150.0 $\mu\text{g/mL}$) of the linear range.

Acceptance criteria: R^2 should be ≥ 0.990 .

2.2.17.8.2 Precision

Repeatability: To determine repeatability, 6 test samples of nominal concentration were injected maintaining optimized chromatographic conditions.

Acceptance Criteria: RSD should be $\leq 10\%$.

Intermediate precision: Repeatability study was repeated by a 2nd analyst on another day. RSD was obtained combining 12 results from both analysts to obtain intermediate precision.

Acceptance Criteria: RSD of 12 samples should be $\leq 10.0\%$.

2.2.17.8.3 Accuracy

2000 mg of placebo powder was transferred into 3 GC vials separately; 5.0 mL of 80%, 100% and 120% linearity solutions were taken in those 3 vials respectively. Then mixed well and sealed properly.

The Recovery of Dichloromethane content of the sample was calculated using the following equation:

$$\frac{A_s}{A_{std}} \times \frac{W_{std}}{W_s} \times 100$$

Where, A_s is the peak area of impurity in sample solution, A_{std} is the peak area of impurity in standard solution, W_{std} is the weight of impurity in standard solution (mg) and W_s is the weight of impurity for spiking (mg).

% Recovery = {(Recovery ÷ Weight of dichloromethane in initially prepared solution) x 100}

Acceptance Criteria: The % Recovery should be between 80.0% and 120.0%.

2.2.17.8.4 Robustness

The check the robustness of the method, two different parameters (detector temperature and column temperature program) was changed by applying the system suitability solution. The chromatographic condition was changed by changing the detector temperature from 250°C to 245°C and 255°C. The chromatographic condition was also changed by changing the column temperature program as below:

Temperature, °C	Hold time, min	Changed Temperature, °C	Changed Hold time, min	Rate, °C /min
60	1.0	65	0.5	0.0
90	2.0	90	3.0	5.0
120	1.0	125	5.0	15.0

Each time the chromatographic condition was changed, the equilibrium condition of the column was checked by injecting the system suitability solution repeatedly until the %RSD of the peak area is ≤10.0% for 6 consecutive injections.

Acceptance Criteria:

- The RSD form 6 injections should be ≤ 10.0%.
- Tailing factor should be ≤ 1.5.

- Theoretical plate count should be ≥ 5000 .

2.2.17.8.5 System Suitability Test

The analytical standard solution was used as system suitability solution. System Suitability was checked by injecting the solution for 6 times from 6 different GC vials.

Acceptance Criteria:

- The RSD from 6 injections should be $\leq 10.0\%$.
- Tailing factor should be ≤ 1.5 .
- Theoretical plate count should be ≥ 5000 .

2.2.18 Residual solvent determination

2.2.18.1 Residual solvent determination for Ledipasvir SDs

In the present study, eight solid dispersion formulations of Ledipasvir were prepared using same concentration of solute in the solvent using same process. Among the eight formulations, F1SD, F2SD, F3SD, F4SD, F6SD and F7SD were prepared using ethanol whereas F5SD and F8SD were prepared using 50:50 ratio of ethanol and dichloromethane as solvent. In all cases, the solvents were removed by evaporation at 40°C under vacuum using Eppendorf Vacuum Concentrator. For F1SD, F2SD, F3SD, F4SD, F5SD, F6SD, F7SD and F8SD, residual ethanol was determined using Loss on drying (LOD) method using the method of Ph. Eur. 2.2.32. As ethanol is a class 3 solvent, LOD method was used to determine the residual ethanol and the limit of LOD was $\leq 0.5\%$ (ICH, 2019). 5g sample was used and drying was done at 105°C to determine the LOD for ethanol in all SD samples (Grodowska and Parczewski, 2010; Nogueira et al., 2012; Singh and Sinha, 2013) using a Sartorius MA 160-1 moisture balance.

First, the LODs of those 6 SDs (F1SD, F2SD, F3SD, F4SD, F6SD and F7SD) were determined. Then a secondary drying was done in a vacuum oven at 60°C done for 24 hours (samples were taken at 1, 3, 6, 12 and 24 hours) to bring down the LOD within limit.

Along with the residual ethanol, residual dichloromethane of F5SD and F8SD was also determined as per as per Ph. Eur. 2.4.24 using GC with head space method (ICH, 2019; Singh and Sinha, 2013). The residual dichloromethane content was determined Initially. Then a secondary drying was done in a vacuum oven at 60°C for 24 hours (samples were taken at 1, 3, 6, 12 and 24 hours) to bring down the residual dichloromethane content.

2.2.18.2 Residual solvent determination for Velpatasvir SDs

The LOD of Velpatasvir solid dispersions were determined at the same procedure to determine the LOD of Ledipasvir solid dispersions above with an exception that the samples were taken only after 24 hours of drying.

*Chapter 3: Preparation and Characterization of
Nanosuspensions*

3.1 Challenges with delivery of Ledipasvir, Daclatasvir and Velpatasvir

3.1.1 Absorption and dissolution: As Ledipasvir and Daclatasvir belong to BCS class 2 drugs, they have high absorption but low dissolution rates. BCS identifies dissolution rate as rate limiting step for oral absorption of these drugs. Velpatasvir is a BCS class 4 drug i.e. it has a low dissolution and low absorption rate. Velpatasvir shows poor dissolution with gradual increment in pH of dissolution media which could limit its bioavailability after oral administration (Mehmood et al., 2020). These drugs exhibit variable bioavailability and need the enhancement in dissolution for increasing the bioavailability.

3.1.2 Difficulty for paediatric and geriatric patients: Currently two dosage forms of Ledipasvir, tablet and pellets, are available in the market. The tablets can be taken with or without food. Pellets can be taken in pediatric patients who cannot swallow the tablet formulation. But the administration of the pellets is complicated. It is indicated that if pellets are administered with food, it is needed to sprinkle the pellets on one or more spoonful of non-acidic soft food at or below room temperature. Examples of non-acidic foods include pudding, chocolate syrup, mashed potato, and ice cream. And then it is advised to take pellets within 30 minutes of gently mixing with food and swallow the entire contents without chewing to avoid a bitter aftertaste (Gilead Sciences, 2014). So, this process is really complicated for those who are unable to swallow tablets.

Currently, Daclatasvir is present as tablet dosage forms in the market (McEwan et al., 2016). On the other hand, Velpatasvir is available as tablets and pellets (Hughes et al., 2017). However, the administration of the pellets is complicated in case of difficulty to swallow. Suitable dosage forms for children and elderly population or patients having difficulty with swallowing are not available at this moment for these drugs.

3.2 Objectives of the study

The main objective of the study was to develop an oral suspension dosage form of Ledipasvir, Daclatasvir and Velpatasvir with improved dissolution and bioavailability for children and elderly patients. To accomplish the main objective, the following secondary objectives were set-

- ❖ Development of solid dispersion based nanosuspensions of Ledipasvir, Daclatasvir and Velpatasvir for overcoming the challenge associated with dissolution of the drug.

- ❖ Development of a stable suspension as suitable dosage form for paediatric and geriatric patients and patient with difficulty to swallow.
- ❖ *In-vivo* simulation of the formulated suspensions against the market product.
- ❖ Development of a QbD based RP-HPLC method for analysis of Ledipasvir.
- ❖ Establishment of equivalency between RP-HPLC and UV method for analysis of Ledipasvir.
- ❖ Development of a QbD based GC method for determination of residual solvent in Ledipasvir dosage form.

3.3 Results and discussion

3.3.1 Characterization of suspensions prepared with non-micronized and micronized Ledipasvir

3.3.1.1 Assay content: Assay content of Ledipasvir in per 5 ml of each of the suspensions prepared with non-micronized and micronized API, were measured in triplicates using the validated UV method described in chapter 2.2.15.2. Dissolution profiles of the suspensions were checked following the method described in chapter 2.2.11.3. Dissolutions were checked for six samples. Sampling points for the dissolution profiles were 5, 10, 15, 20, 30 minutes. Label claim for both cases was ‘each 5ml suspension contains 90 mg Ledipasvir.

Table 3.1: Assay of Ledipasvir in suspensions prepared with non-micronized and micronized API

Stabilized Ledipasvir nanosuspensions	Assay of Ledipasvir (% of label claim)				SD	%RSD
	Sample 1	Sample 2	Sample 3	Average		
Suspension with non-micronized API	99.54	99.26	99.79	99.5	0.3	0.27
Suspension with micronized API	100.42	101.33	101.00	100.9	0.5	0.46

In all cases, content of Ledipasvir was within 99.26% to 101.33% and the RSD values of less than 1 indicating good uniformity of the formulation.

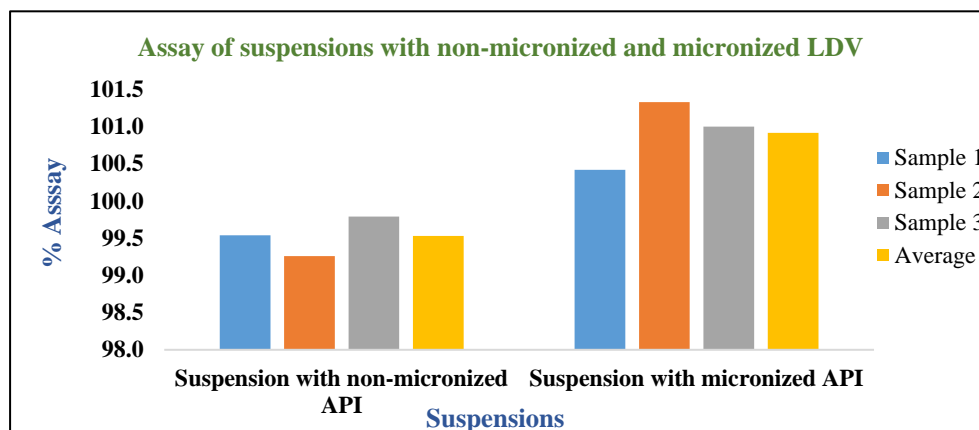


Figure 3.1: Assay of Ledipasvir in the suspensions prepared with non-micronized and micronized API

3.3.1.2 Dissolution profiles: Dissolution profiles of the suspensions prepared with non-micronized and micronized API are presented below:

Table 3.2: Dissolution profiles of suspensions prepared with non-micronized and micronized API

Time Points (min)	Suspension with non-micronized API	Suspension with micronized API
0	0	0
5	8.27	13.72
10	14.54	20.4
15	21.77	28.05
20	31.92	37.66
30	41.63	48.01
45	44.21	50.48
60	45.13	50.91

The dissolution of the suspension prepared with the non-micronized API was found 45.13% and for the suspension with micronized API, the dissolution was 50.91% after 60 minutes.

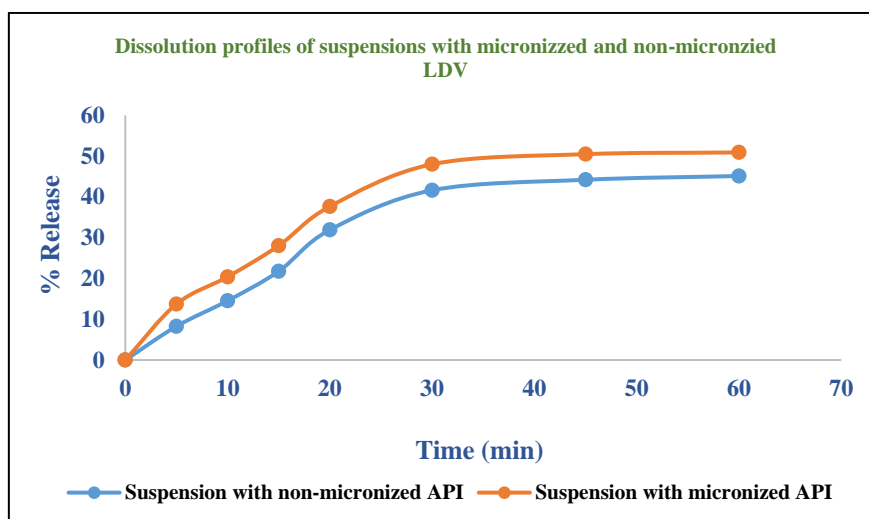


Figure 3.2: Dissolution profiles of suspensions prepared with non-micronized and micronized LDV

In both cases, complete dissolution of LDV was not found. Therefore, it was needed to apply suitable solubility improvement technique to obtain complete dissolution of LDV in the drug product.

3.3.2 Solubility Study

Results of the solubility study of Ledipasvir is presented in the table below:

Table 3.3: Solubility data of Ledipasvir in methanol, ethanol, dichloromethane and acetone

Sample	Equation for standard curve	Regression Coefficient (R^2)	Solubility ($\mu\text{g/mL}$)	Average solubility ($\mu\text{g/mL}$)	% RSD
LDV in methanol	$y = 0.0544x + 0.003$	0.9996	846.0	842.0	0.5
			838.0		
			842.0		
LDV in ethanol	$y = 0.0517x + 0.0004$	0.9998	721.0	727.0	0.9
			726.0		
			734.0		
LDV in dichloromethane	$y = 0.0455x - 0.0019$	0.9998	879.0	868.7	1.3
			870.0		
			857.0		
LDV in acetone	$y = 0.0564x - 0.001$	0.9996	4.8	4.9	1.1
			4.9		
			4.9		

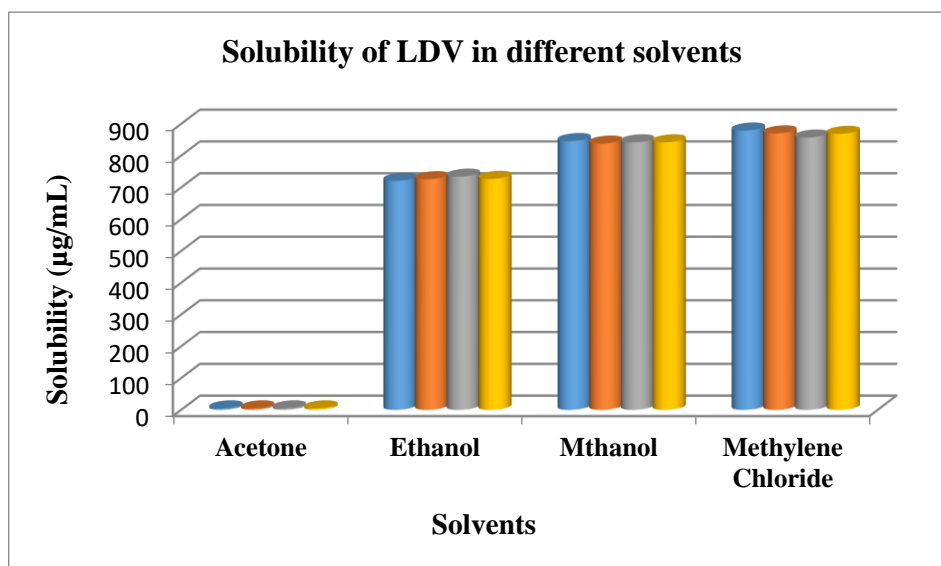
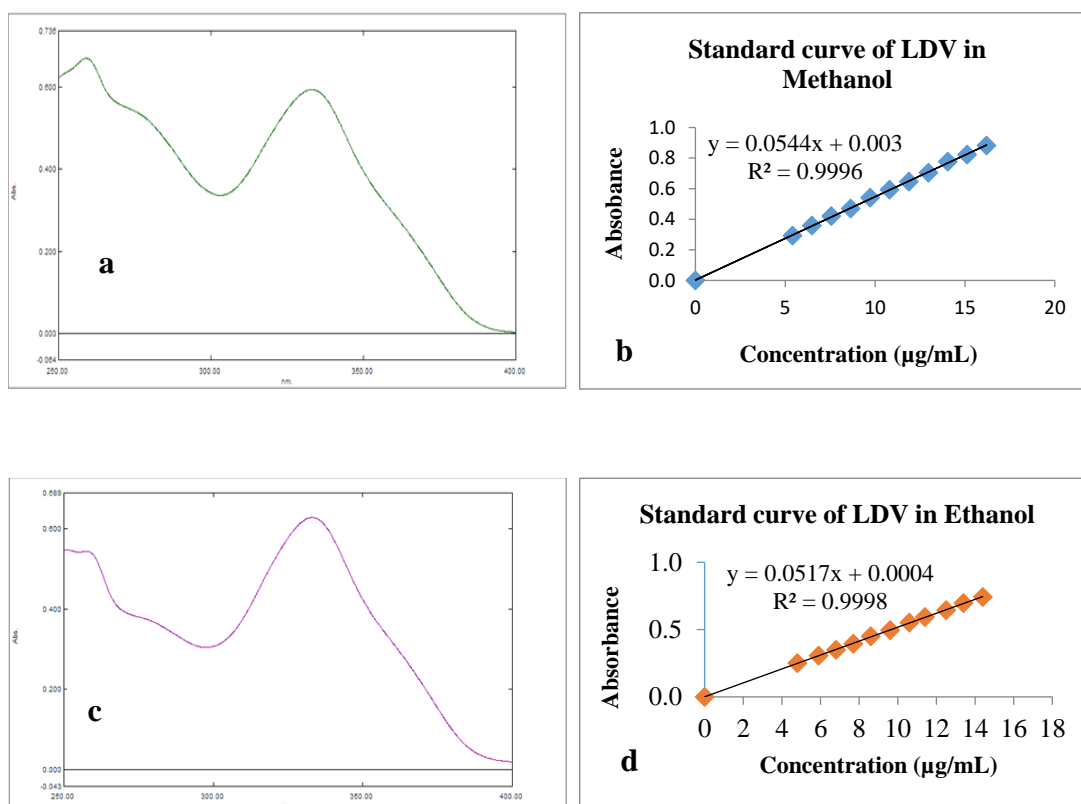


Figure 3.3: Solubility data of Ledipasvir in methanol, ethanol, dichloromethane and acetone



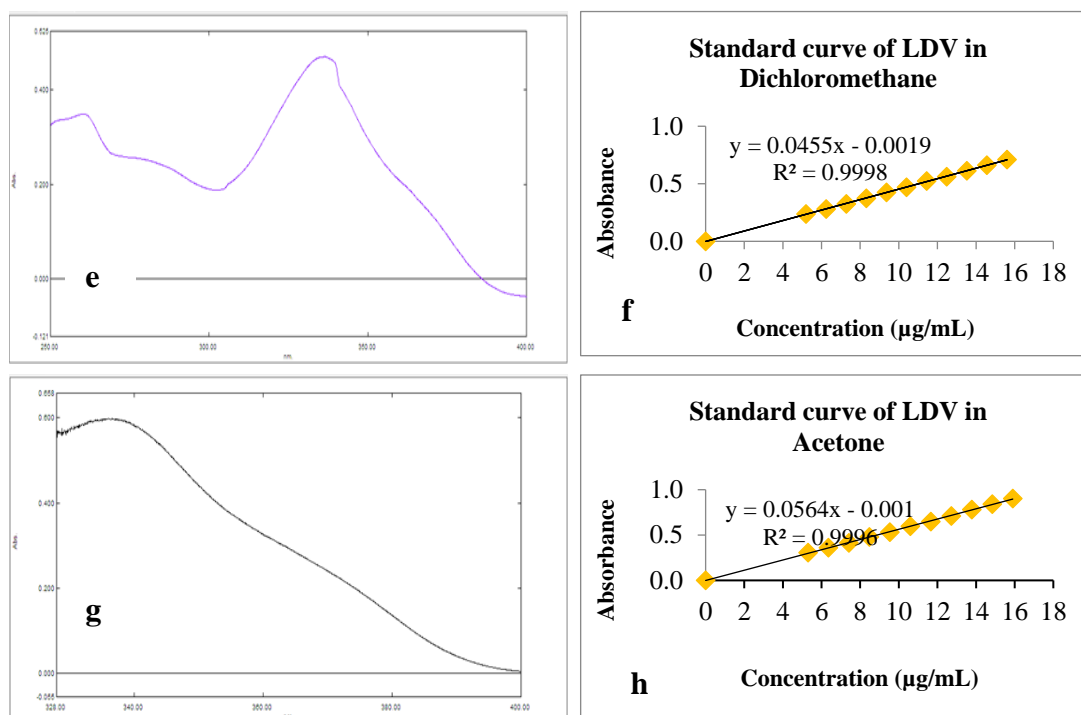


Figure 3.4: (a) Detection of λ_{\max} of Ledipasvir in methanol; (b) Standard curve of Ledipasvir in methanol; (c) Detection of λ_{\max} of Ledipasvir in ethanol; (d) Standard curve of Ledipasvir in ethanol; (e) Detection of λ_{\max} of Ledipasvir in dichloromethane; (f) Standard curve of Ledipasvir in dichloromethane; (g) Detection of λ_{\max} of Ledipasvir in acetone; (h) Standard curve of Ledipasvir in acetone

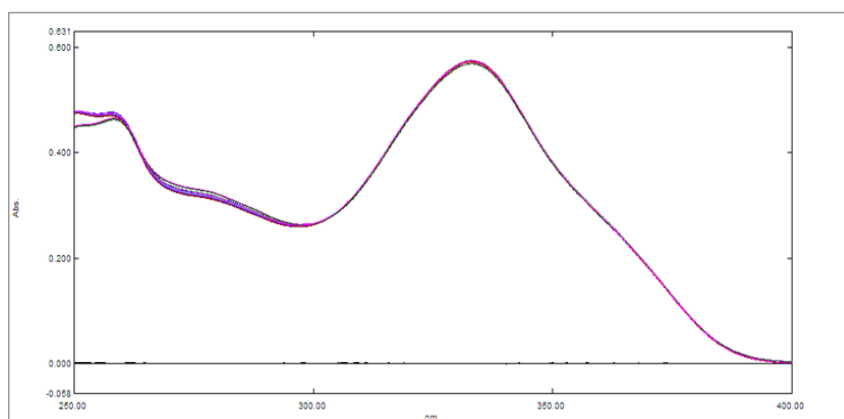
Standard curves of Ledipasvir in acetone, ethanol, methanol and dichloromethane produced acceptable values of regression coefficient (R^2).

3.3.3 Solution stability

3.3.3.1 Solution stability of LDV in methanol: The data of the stability study of the solution of LDV in methanol are presented in Table 3.4 with acceptance criteria. Solution stability was determined by measuring the absorbance of the solution under at room temperature for up to 24 hours. All of the % recovery results during this period of time were within 98–102% of the initial value. From the results it can be said that the solution exhibits stability for 24 hours at room temperature and no significant changes were observed with the exposure of light.

Table 3.4: Solution stability study of the solution of Ledipasvir in methanol

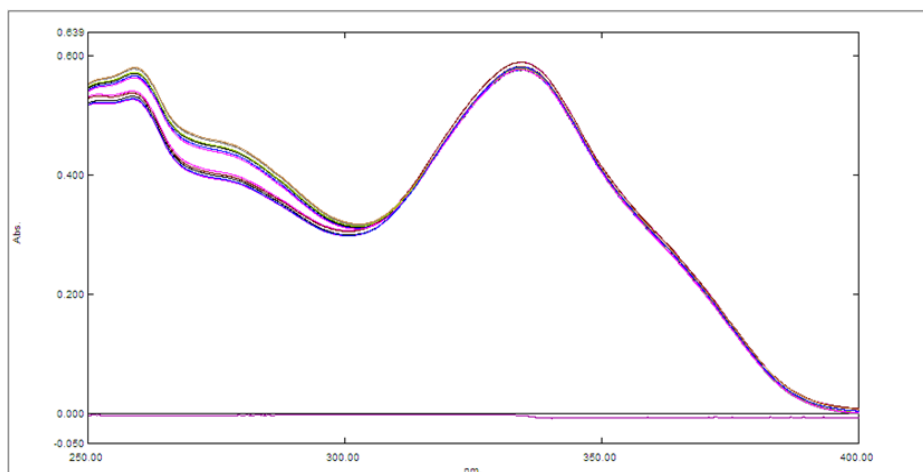
Time (hour)	Weight of Initial sample (mg)	Recovery (mg)	% Recovery	Limit
0	10.00			98.0% - 102%
6		10.03	100.29	
12		10.03	100.35	
24		9.98	99.77	

**Figure 3.5:** UV spectra of the solution of Ledipasvir in methanol. at 0, 6, 12 and 24 hour and blank (methanol)

3.3.3.2 Solution stability of Ledipasvir in ethanol: The data is of the stability study of the solution of Ledipasvir in ethanol are presented in Table 3.5 with acceptance criteria. Solution stability was determined by measuring absorbance of the solution of Ledipasvir at room temperature for up to 24 hours. All of the % recovery results during this period of time were within 98–102% of the initial value. From the results it can be said that the solution exhibits stability for 24 hours at room temperature and no significant changes were observed with the exposure of light.

Table 3.5: Solution stability study of the solution of Ledipasvir in ethanol

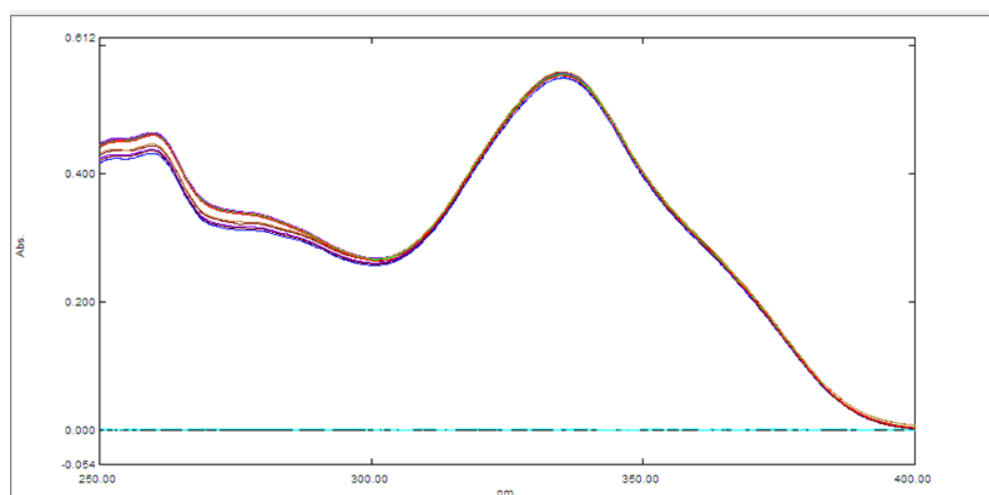
Time (hour)	Weight of Initial sample (mg)	Recovery (mg)	% Recovery	Limit
0	10.40			98.0% - 102%
6		10.45	100.46	
12		10.48	100.46	
24		10.53	101.22	

**Figure 3.6:** UV spectra of the solution of Ledipasvir in ethanol. at 0, 6, 12 and 24 hour and blank (ethanol)

3.3.3.3 Solution stability of Ledipasvir in dichloromethane: The data is of the stability study of the solution of Ledipasvir in dichloromethane are presented in Table 3.6 with acceptance criteria. Solution stability was determined by measuring absorbance of the solution of Ledipasvir at room temperature for up to 24 hours. All of the % recovery results during this period of time were within 98–102% of the initial value. From the results it can be said that the solution exhibits stability for 24 hours at room temperature and no significant changes were observed with the exposure of light.

Table 3.6: Solution stability study of the solution of Ledipasvir in dichloromethane

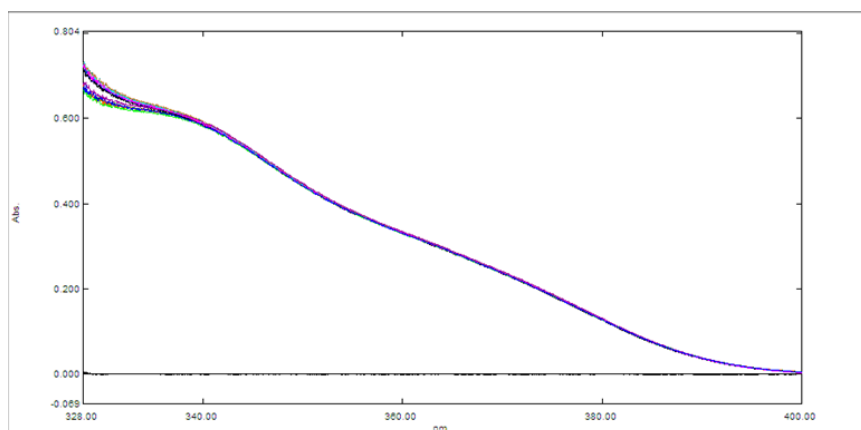
Time (hour)	Weight of Initial sample (mg)	Recovery (mg)	% Recovery	Limit
0	10.40			98.0% - 102%
6		10.40	100.00	
12		10.42	100.24	
24		10.36	99.58	

**Figure 3.7:** UV spectra of the solution of Ledipasvir in dichloromethane at 0, 6, 12 and 24 hour and blank (dichloromethane)

3.3.3.4 Solution stability of Ledipasvir in acetone: The data is of the stability study of the solution of Ledipasvir in acetone are presented in Table 3.7 with acceptance criteria. Solution stability was determined by measuring absorbance of the solution of Ledipasvir at room temperature for up to 24 hours. All of the % recovery results during this period of time were within 98–102% of the initial value. From the results it can be said that the solution exhibits stability for 24 hours at room temperature and no significant changes were observed with the exposure of light.

Table 3.7: Solution stability study of the solution of Ledipasvir in acetone

Time (hour)	Weight of Initial sample (mg)	Recovery (mg)	% Recovery	Limit
0	10.60			98.0% - 102%
6		10.52	99.25	
12		10.67	100.65	
24		10.66	100.54	

**Figure 3.8:** UV spectra of the solution of Ledipasvir in acetone at 0, 6, 12 and 24 hour and blank (acetone)

The results of the stability study of the solutions of Ledipasvir in methanol, ethanol, dichloromethane and acetone were found to be within the acceptable limit. Hence, the solutions of LDV in methanol, ethanol, dichloromethane and acetone are stable up to 24 hours at room condition with exposure to light. Although solubility of Ledipasvir was highest in methanol and dichloromethane, they were avoided as they are class 2 solvents. Both acetone and ethanol are class 3 solvents with low toxic potential. Ledipasvir had higher solubility in ethanol compared to acetone. Therefore, ethanol was selected as the solvent of choice for the preparation of Ledipasvir solid dispersions. Moreover, all the excipients selected for the solid dispersions are highly soluble in ethanol except HPMC and CMC Sodium. Because of the insolubility of HPMC and CMC Sodium in ethanol, a 50:50 ratio of ethanol:dichloromethane was used as solvent.

3.3.4 Drug-exipients compatibility study

3.3.4.1 Fourier Transform Infrared Spectroscopy (FTIR) analysis

3.3.4.1.1 FTIR study for Ledipasvir

Pure drug (Ledipasvir): The prominent peaks of Ledipasvir was observed in the region 1660 cm^{-1} due to $>\text{N-H}$ (Secondary amine NH bend), 1288 cm^{-1} due to $-\text{C-N}$ (primary amine, CN stretch), 1240 cm^{-1} due to $-\text{C-C}$ (vibration), 1098 cm^{-1} due to $-\text{C-N}$ (primary amine, CN stretch), 1040 cm^{-1} due to cyclohexane ring vibrations.

Ledipasvir and Poloxamer 188: The IR spectrum of Poloxamer 188 is characterized by principal absorption peaks at 1340 cm^{-1} (in-plane O-H bend) and 1097 cm^{-1} (C-O stretch) (Sharma et al., 2013). The FTIR spectra of physical mixtures were similar to those of Ledipasvir and Poloxamer 188 individual spectra. Overall there was no alteration in the characteristic peaks of the physical mixture suggesting that there was no chemical interaction between Ledipasvir and Poloxamer 188 in physical mixtures (figure 3.10 a) (Purna Chandra Reddy Guntaka, 2018).

Ledipasvir and Poloxamer 407: The FTIR spectrum of Poloxamer 407 is characterized by principal absorption peaks at 1379 cm^{-1} (in-plane O-H bending) and 1110 cm^{-1} (C-O stretching) (Islam et al., 2013). The FTIR spectra of physical mixtures were similar to those of Ledipasvir and Poloxamer 407 individual spectra. Overall there was no alteration in the characteristic peaks of the physical mixture suggesting that there was no chemical interaction between Ledipasvir and Poloxamer 407 in physical mixtures (figure 3.10 b).

Ledipasvir and Klucel™ EF: FTIR absorption spectra for HPC, the monomer (Klucel™ EF), is characterized by an absorption band at 1535 cm^{-1} is due to C=C stretching vibration and absorption band at 1080 cm^{-1} is due to C-O-C stretching vibration (Eguchi et al., 2017). The FTIR spectra of physical mixtures were similar to those of Ledipasvir and Klucel™ EF individual spectra. Overall there was no alteration in the characteristic peaks of the physical mixture suggesting that there was no chemical interaction between Ledipasvir and Klucel™ EF in physical mixtures (figure 3.10 c).

Ledipasvir and Klucel™ EXF: FTIR absorption spectra for HPC, the monomer (Klucel™ EXF), is characterized by an absorption band at 1535 cm^{-1} is due to C=C stretching vibration and absorption band at 1080 cm^{-1} is due to C-O-C stretching vibration (Eguchi et

al., 2017). The FTIR spectra of physical mixtures were similar to those of Ledipasvir and Klucel™ EXF individual spectra. Overall there was no alteration in the characteristic peaks of the physical mixture suggesting that there was no chemical interaction between Ledipasvir and Klucel™ EXF in physical mixtures (figure 3.10 d).

Ledipasvir and HPMC 5cps: In the FTIR spectrum of HPMC 5cps, bands at 1070 cm^{-1} represent the stretching vibration C-O bonds. The bending vibration of -OH groups on the HPMC is appeared at 1380 cm^{-1} (Mahdavinia et al., 2015). Bands caused by ether COC stretch are seen in the region $1151\text{--}1059\text{ cm}^{-1}$, while secondary alcohols absorb strongly at 1075 cm^{-1} . Methoxy groups give rise to a band around $1201\text{--}1174\text{ cm}^{-1}$ and Carbonyl is seen at 1630 cm^{-1} (Gustafsson et al., 2003). Overall there was no alteration in the characteristic peaks of the physical mixture suggesting that there was no chemical interaction between Ledipasvir and HPMC 5cps in physical mixtures (figure 3.10 e).

Ledipasvir, Povidone K17: FTIR spectrum of Povidone K17 is characterized by the peaks of PVP K17 at 1650 cm^{-1} (C=O stretching), 1460 cm^{-1} (C-H beading of CH_2) and 1286 cm^{-1} (C-N stretching) (Asawahame et al., 2015; Shams et al., 2011). The FTIR spectra of physical mixtures were similar to those of Ledipasvir and Povidone K17 individual spectra. Overall there was no alteration in the characteristic peaks of the physical mixture suggesting that there was no chemical interaction between Ledipasvir and Povidone K17 in physical mixtures (figure 3.10 f).

Ledipasvir and Povidone K30: The characteristic peaks of PVP K30 at 1650 cm^{-1} (C=O stretching), 1460 cm^{-1} (C-H beading of CH_2) and 1286 cm^{-1} (C-N stretching) (Asawahame et al., 2015; Shams et al., 2011). The FTIR spectra of physical mixtures (figure 3.14) were similar to those of Ledipasvir and Povidone K30 individual spectra. Overall there was no alteration in the characteristic peaks of the physical mixture suggesting that there was no chemical interaction between Ledipasvir and Povidone K30 in physical mixtures (figure 3.10 g).

Ledipasvir and CMC Sodium: The FTIR spectrum of Carboxymethyl Cellulose (CMC) Sodium is characterized by the band due to ring stretching of glucose at 1610 cm^{-1} . In addition, the bands in the region $1351\text{--}1449\text{ cm}^{-1}$ are due to symmetrical deformations of - CH_2 and -COH groups. The bands due to primary alcoholic - CH_2OH stretching mode and CH_2 twisting vibrations appear at 1080 and 1020 cm^{-1} , respectively. The weak bands at

around 771 cm^{-1} are due to ring stretching and ring deformation of $\alpha\text{-D-(1-4)}$ and $\alpha\text{-D-(1-6)}$ linkages (Wang and Somasundaran, 2005). The FTIR spectra of physical mixtures were similar to those of Ledipasvir and CMC Sodium individual spectra. Overall there was no alteration in the characteristic peaks of the physical mixture suggesting that there was no chemical interaction between Ledipasvir and CMC Sodium in physical mixtures (figure 3.10 h).

In the FTIR spectrum of drug, excipients and physical mixture of drug and excipients, all the principal peaks of drug and excipients are visible in the spectrums. From the above observations, it has been concluded that there is no significant shifting of the peaks of the mixtures compared to their individual data. Hence the result of the study reveals good compatibility between drug and polymers (Kumar Sarangi et al., 2018).

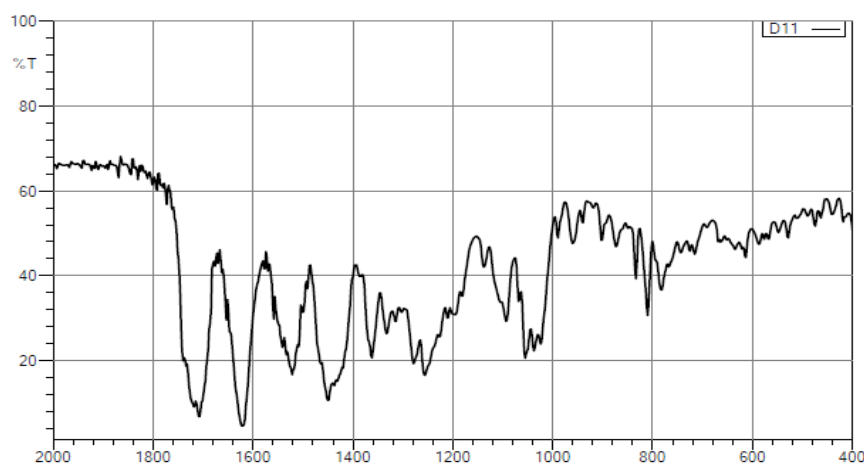
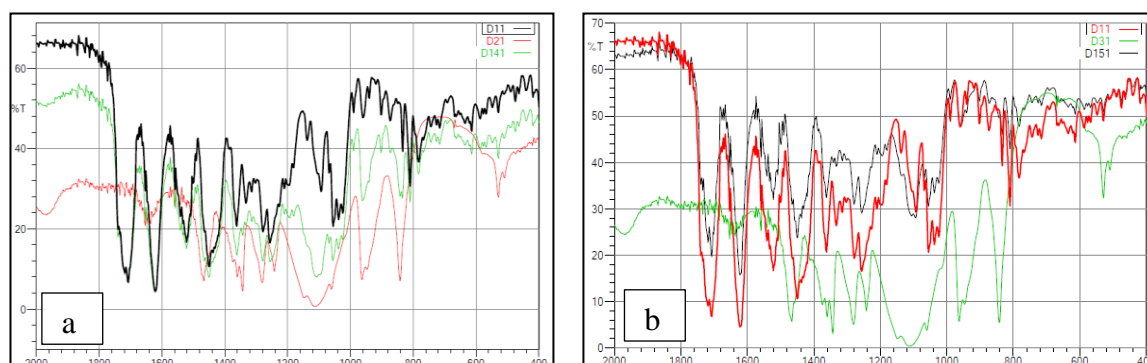


Figure 3.9: FTIR spectrum of Ledipasvir



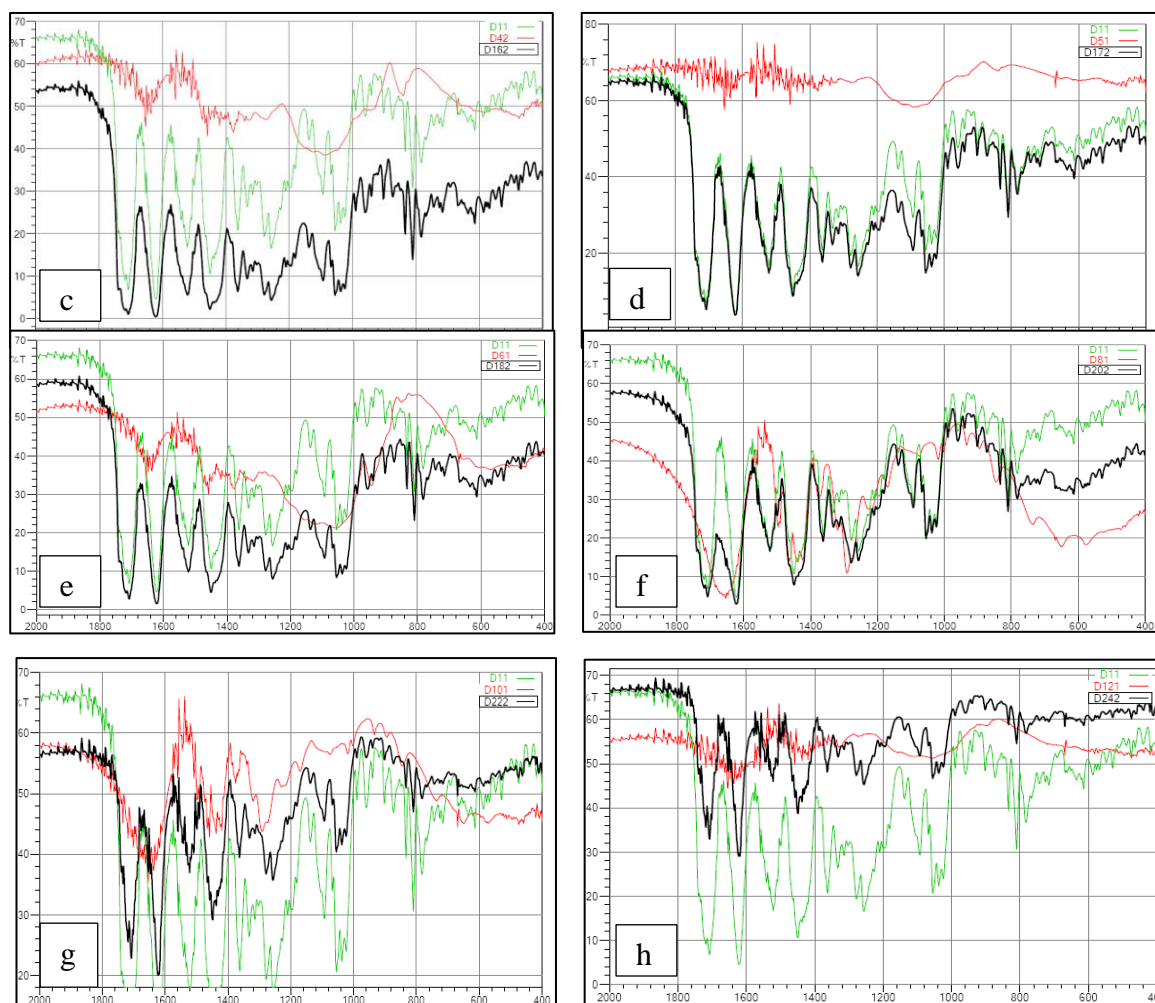


Figure 3.10: a) FTIR spectrum of Ledipasvir, Poloxamer 188 and binary mixture of Ledipasvir and Poloxamer 188 (D11=LDV, D21=Poloxamer 188, D141=LDV+Poloxamer 188 mixture); b) FTIR spectrum of Ledipasvir, Poloxamer 407 and binary mixture of Ledipasvir and Poloxamer 407 (D11=LDV, D31=Poloxamer 407, D151=LDV+Poloxamer 407 mixture); c) FTIR spectrum of Ledipasvir, Klucel™ EF and binary mixture of Ledipasvir and Klucel™ EF (D11=LDV, D42=Klucel™ EF, D162=LDV+Klucel™ EF mixture); d) FTIR spectrum of Ledipasvir, Klucel™ EXF and binary mixture of Ledipasvir and Klucel™ EXF (D11=LDV, D51=Klucel™ EXF, D172=LDV+Klucel™ EXF mixture); e) FTIR spectrum of Ledipasvir, HPMC 5cps and binary mixture of Ledipasvir and HPMC 5cps (D11=LDV, D61=HPMC 5cps, D182=LDV+ HPMC 5cps mixture); f) FTIR spectrum of Ledipasvir, Povidone K17 and binary mixture of Ledipasvir and Povidone K17 (D11=LDV, D81=Povidone K17, D202=LDV+ Povidone K17 mixture); g) FTIR spectrum of Ledipasvir, Povidone K30 and binary mixture of Ledipasvir and

Povidone K30 (D11=LDV, D101=Povidone K30, D222=LDV+ Povidone K30 mixture);
h) FTIR spectrum of Ledipasvir, CMC Sodium and binary mixture of Ledipasvir and CMC Sodium (D11=LDV, D121= CMC Sodium , D232=LDV+ CMC Sodium mixture)

3.3.4.1.2 FTIR study for Daclatasvir (DLV)

Pure drug (Daclatasvir): The prominent peaks of Daclatasvir were observed in the region of 1730 cm^{-1} , 1641 cm^{-1} , 1430 cm^{-1} , 1240 cm^{-1} , 1098 cm^{-1} and 1011 cm^{-1} . The peak at 1641 cm^{-1} was observed due to $>\text{N-H}$ (Secondary amine NH bend), 1430 cm^{-1} and 1730 cm^{-1} due to the C–H asymmetric stretching and C=C stretching respectively, 1240 cm^{-1} due to –C–C (vibration), 1098 cm^{-1} due to –C–N (primary amine, CN stretch) (Mehmood et al., 2020; Purna Chandra Reddy Guntaka, 2018) (figure 3.11).

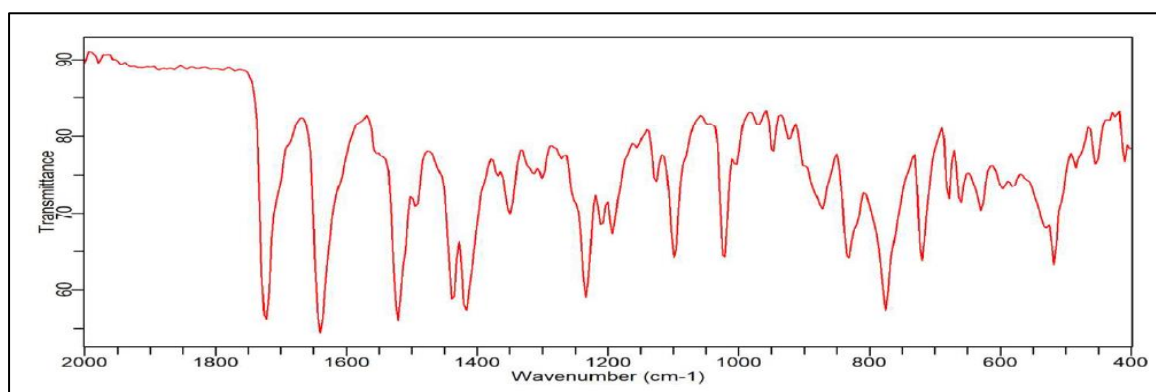


Figure 3.11: FTIR spectrum of Daclatasvir

Daclatasvir and Poloxamer 188: The IR spectrum of Poloxamer 188 is characterized by principal absorption peaks at 1340 cm^{-1} (in-plane O–H bend) and 1098 cm^{-1} (C–O stretch). The FTIR spectra of physical mixtures (figure 3.12) were similar to those of Daclatasvir and Poloxamer 188 individual spectra. Overall there was no alteration in the characteristic peaks of the physical mixture suggesting that there was no chemical interaction between Ledipasvir and Poloxamer 188 in physical mixtures (Kumar Sarangi et al., 2018).

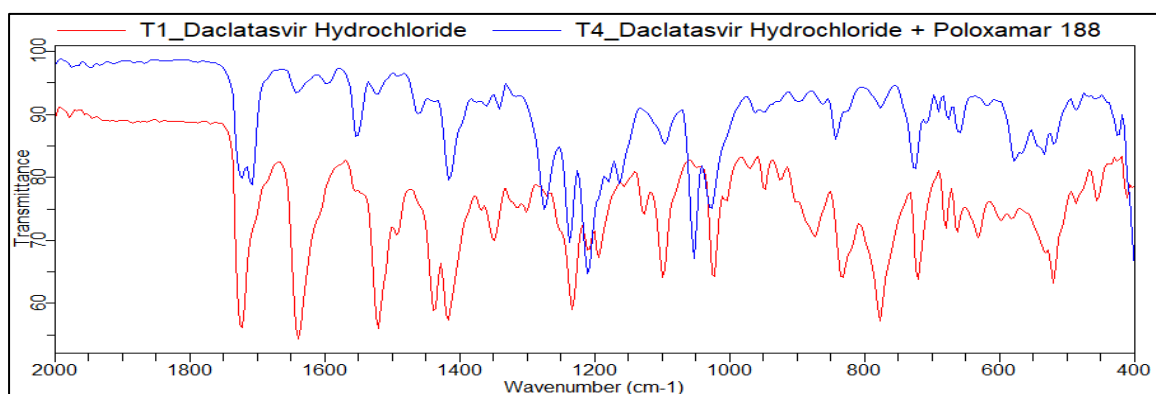


Figure 3.12: FTIR spectrum of Daclatasvir and binary mixture of Daclatasvir and Poloxamer 188

3.3.4.1.3 FTIR study for Velpatasvir (VLV)

VLV showed main peaks at 1236, 1424, 1508, 1636 and 1696. Peaks at 1508 cm^{-1} indicated stretching vibration due to C=C aromatic ring stretching. Similarly, characteristic peak at 1636 cm^{-1} depicted N-H bending vibration. Furthermore, peaks at 1424 and 1696 cm^{-1} correspond to the C-H asymmetric stretching and C=C stretching, respectively (Mehmood et al., 2020) (figure 3.13).

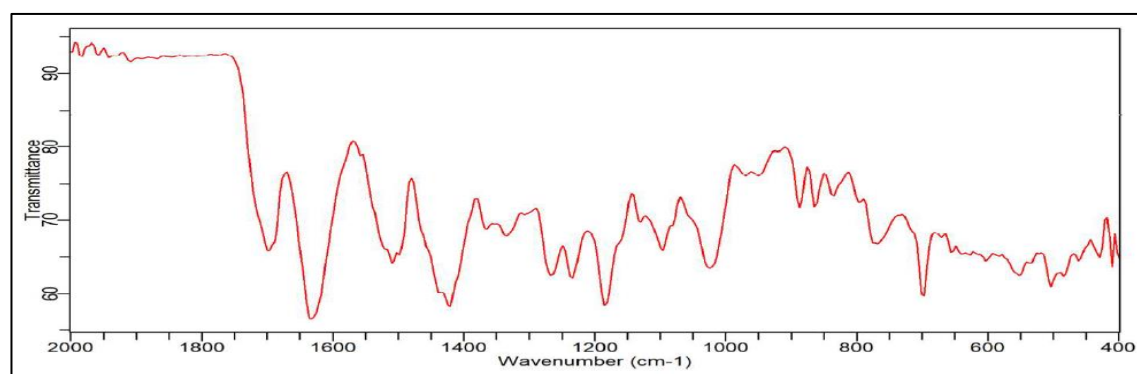


Figure 3.13: FTIR spectrum of Velpatasvir

Velpatasvir and Poloxamer 188: The IR spectrum of Poloxamer 188 is characterized by principal absorption peaks at 1340 cm^{-1} (in-plane O-H bend) and 1098 cm^{-1} (C-O stretch). The FTIR spectra of physical mixtures (figure 3.14) were similar to those of Velpatasvir and Poloxamer 188 individual spectra. Overall there was no alteration in the characteristic peaks of the physical mixture suggesting that there was no chemical interaction between Ledipasvir and Poloxamer 188 in physical mixtures (Kumar Sarangi et al., 2018).

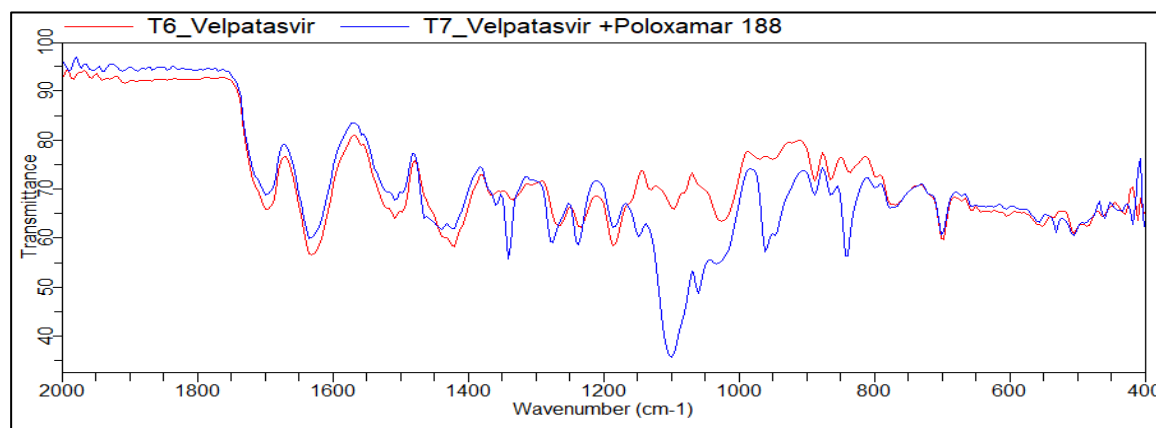


Figure 3.14: FTIR spectrum of Velpatasvir and binary mixture of Velpatasvir and Poloxamer 188

3.3.4.2 DSC analysis:

3.3.4.2.1 DSC analysis for Ledipasvir

Pure drug (Ledipasvir): From the DSC curve of Ledipasvir a sharp endothermic peak was found at 172.91°C due to the melting of the API which indicated the drug is in crystalline state (Purna Chandra Reddy Guntaka, 2018) (figure 3.15a).

Ledipasvir and Poloxamer 188: The thermogram of Poloxamer 188 showed a sharp endothermic peak at 65.82°C (figure 3.15b). The thermogram of physical mixture of Ledipasvir and Poloxamer 188 showed endothermic peaks at 65.31°C and 172.79°C. Overall, no significant shift of endothermic peaks or absence of endothermic peaks or appearance of new endothermic peaks were observed for the DSC curve of physical mixture of Ledipasvir and Poloxamer 188 suggesting that there was no chemical interaction between Ledipasvir and poloxamer 188 in physical mixtures (Tomassetti et al., 2005) (figure 3.15c).

Ledipasvir and Poloxamer 407: The thermogram of Poloxamer 407 showed a sharp endothermic peak at 67.25°C (figure 3.15d). The thermogram of physical mixture of Ledipasvir and Poloxamer 407 showed endothermic peaks at 67.13°C and 172.60°C (figure 3.15e). Overall, no significant shift of endothermic peaks or absence of endothermic peaks or appearance of new endothermic peaks were observed for the DSC curve of physical mixture of Ledipasvir and Poloxamer 407 suggesting that there was no chemical interaction between Ledipasvir and poloxamer 407 in physical mixtures (Tomassetti et al., 2005).

Ledipasvir and Klucel™ EF: The thermogram of Klucel™ EF did not show an endothermic peak which indicates that the polymer is in amorphous form (Leuner and Dressman, 2000) (figure 3.15f). The thermogram of physical mixture of Ledipasvir and Klucel™ EF showed endothermic peaks at 172.99°C (figure 3.15g). Overall, no significant shift of endothermic peaks or absence of endothermic peaks or appearance of new endothermic peaks were observed for the DSC curve of physical mixture of Ledipasvir and Klucel™ EF suggesting that there was no chemical interaction between Ledipasvir and Klucel™ EF in physical mixtures (Tomassetti et al., 2005).

Ledipasvir and Klucel™ EXF: The thermogram of Klucel™ EXF did not show an endothermic peak which indicates that the polymer is in amorphous form (Leuner and Dressman, 2000) (figure 3.15h). The thermogram of physical mixture of Ledipasvir and Klucel™ EXF showed endothermic peaks at 172.33°C (figure 3.15i). Overall, no significant shift of endothermic peaks or absence of endothermic peaks or appearance of new endothermic peaks were observed for the DSC curve of physical mixture of Ledipasvir and Klucel™ EXF suggesting that there was no chemical interaction between Ledipasvir and Klucel™ EXF in physical mixtures (Tomassetti et al., 2005).

Ledipasvir and HPMC 5cps: The thermogram of HPMC 5 cps did not show an endothermic peak which indicates that the polymer is in amorphous form (Leuner and Dressman, 2000) (figure 3.15j). The thermogram of physical mixture of Ledipasvir and HPMC 5 cps showed endothermic peaks at 172.42°C (figure 3.15k). Overall, no significant shift of endothermic peaks or absence of endothermic peaks or appearance of new endothermic peaks were observed for the DSC curve of physical mixture of Ledipasvir and HPMC 5cps suggesting that there was no chemical interaction between Ledipasvir and HPMC 5cps in physical mixtures (Tomassetti et al., 2005).

Ledipasvir and Povidone K17: The thermogram of Povidone K17 did not show an endothermic peak (figure 3.15l) which indicates that the polymer is in amorphous form (Leuner and Dressman, 2000). The thermogram of physical mixture of Ledipasvir and Povidone K17 showed endothermic peaks at 172.85°C (figure 3.15m). Overall, no significant shift of endothermic peaks or absence of endothermic peaks or appearance of new endothermic peaks were observed for the DSC curve of physical mixture of Ledipasvir

and Povidone K17 suggesting that there was no chemical interaction between Ledipasvir and Povidone K17 in physical mixtures (Tomassetti et al., 2005).

Ledipasvir and Povidone K30: The thermogram of Povidone K30 did not show an endothermic peak (figure 3.15n) which indicates that the polymer is in amorphous form (Leuner and Dressman, 2000). The thermogram of physical mixture of Ledipasvir and Povidone K30 showed endothermic peaks at 172.45°C (figure 3.15o). Overall, no significant shift of endothermic peaks or absence of endothermic peaks or appearance of new endothermic peaks were observed for the DSC curve of physical mixture of Ledipasvir and Povidone K30 compared to DSC curves of Ledipasvir and Povidone K30 suggesting that there was no chemical interaction between Ledipasvir and Povidone K30 in physical mixtures (Tomassetti et al., 2005).

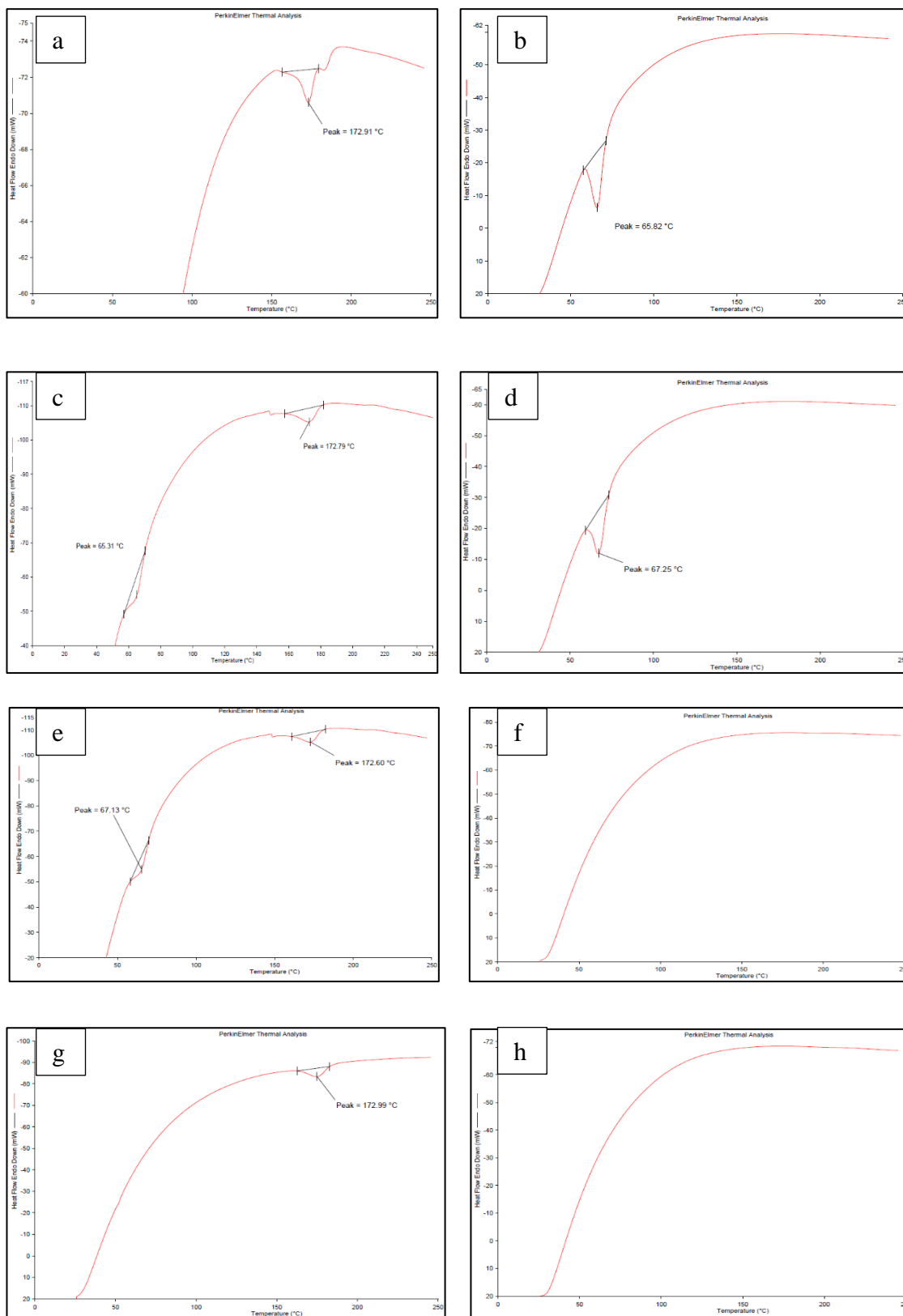
Ledipasvir and CMC Sodium : The thermogram of CMC Sodium did not show an endothermic peak (figure 3.15p) which indicates that the polymer is in amorphous form (Leuner and Dressman, 2000). The thermogram of physical mixture of Ledipasvir and CMC Sodium showed endothermic peaks at 172.39°C (figure 3.15q). Overall, no significant shift of endothermic peaks or absence of endothermic peaks or appearance of new endothermic peaks were observed for the DSC curve of physical mixture of Ledipasvir and CMC Sodium suggesting that there was no chemical interaction between Ledipasvir and CMC Sodium in physical mixtures (Tomassetti et al., 2005).

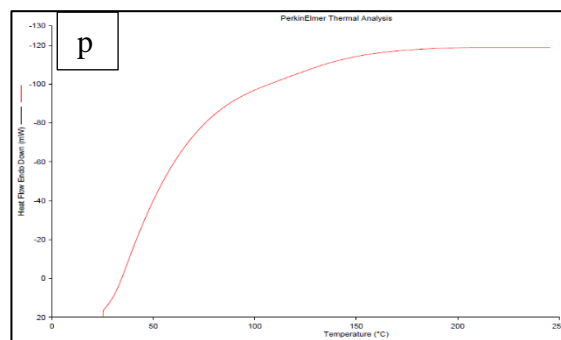
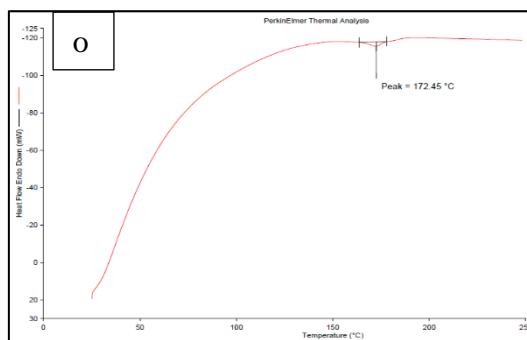
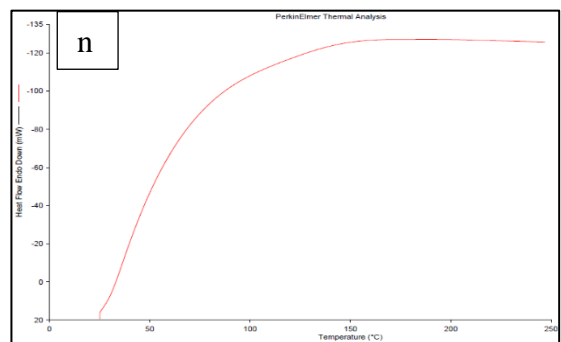
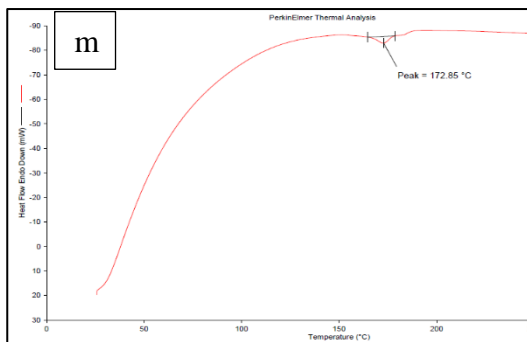
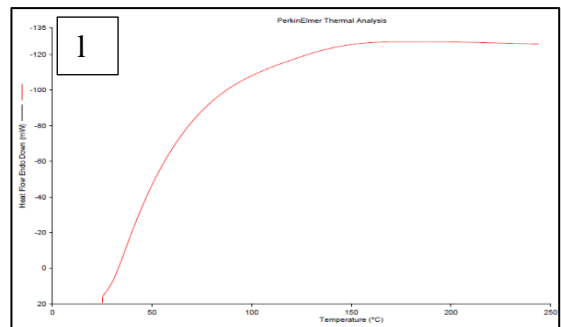
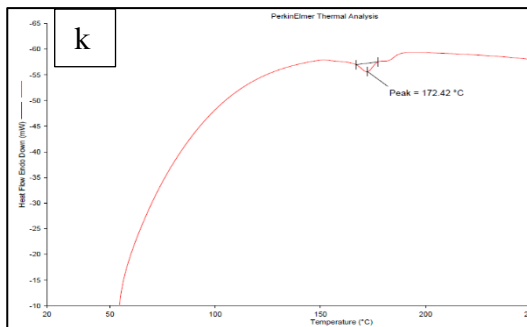
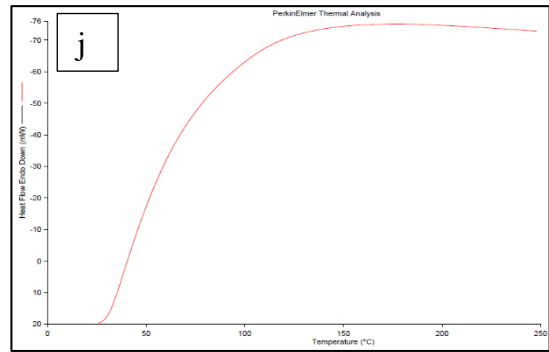
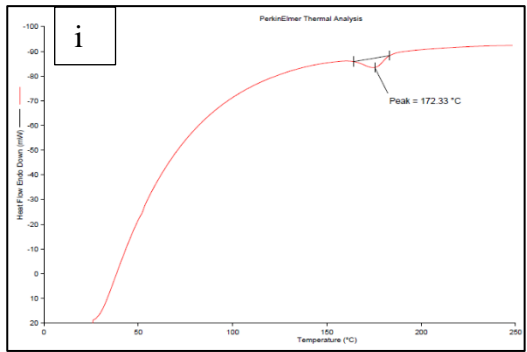
From the DSC curves of Ledipasvir and all the LDV-polymer binary mixtures, it could be understood that Ledipasvir there is no interaction between the API and the excipients.

Table 3.8: DSC characteristics of Ledipasvir, polymers and the physical mixtures

Drug or polymer or physical mixtures	Endothermic peak (°C)
Ledipasvir	172.91
Poloxamer 188	65.82
Poloxamer 407	67.25
Klucel EF	Absent
Klucel EXF	Absent
HPMC 5cps	Absent

Drug or polymer or physical mixtures	Endothermic peak (°C)
Povidone K17	Absent
Povidone K30	Absent
CMC Sodium	Absent
Ledipasvir-Poloxamer 188 physical mixture	65.31 and 172.79
Ledipasvir-Poloxamer 407 physical mixture	67.13 and 172.60
Ledipasvir-Klucel™ EF physical mixture	172.99
Ledipasvir-Klucel™ EXF physical mixture	172.33
Ledipasvir-HPMC 5 cps physical mixture	172.42
Ledipasvir-Povidone K17 physical mixture	172.85
Ledipasvir-Povidone K30 physical mixture	172.45
Ledipasvir- CMC Sodium physical mixture	172.39





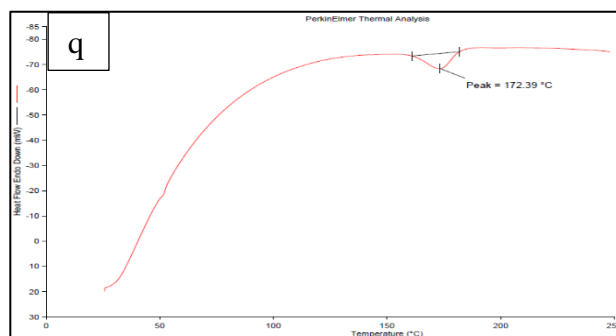


Figure 3.15: a) DSC thermogram of Ledipasvir; b) DSC thermogram of Poloxamer 188; c) DSC thermogram of physical mixture of Ledipasvir and Poloxamer 188; d) DSC thermogram of Poloxamer 407; e) DSC thermogram of physical mixture of Ledipasvir and Poloxamer 407; f) DSC thermogram of Klucel™ EF; g) DSC thermogram of physical mixture of Ledipasvir and Klucel™ EF; h) DSC thermogram of Klucel™ EXF ; i) DSC curve of physical mixture of Ledipasvir and Klucel™ EXF; j) DSC thermogram of HPMC 5 cps; k) DSC thermogram of physical mixture of Ledipasvir and HPMC 5cps; l) DSC thermogram of Povidone K17; m) DSC thermogram of physical mixture of Ledipasvir and Povidone K17; n) DSC thermogram of Povidone K30; o) DSC thermogram of physical mixture of Ledipasvir and Povidone K30; p) DSC thermogram of CMC Sodium (7MF); q) DSC thermogram of physical mixture of Ledipasvir and CMC Sodium

3.3.4.2.2 DSC analysis for Daclatasvir

Pure drug (Daclatasvir): From the DSC curve of Daclatasvir (figure 3.16) a sharp endothermic peak was found at 293.91°C due to the melting of the API which indicated the drug is in crystalline state (Purna Chandra Reddy Guntaka, 2018).

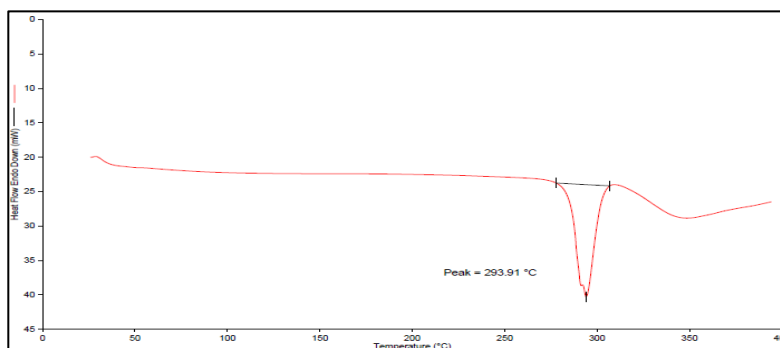


Figure 3.16: DSC thermogram of Daclatasvir

Daclatasvir and Poloxamer 188: The thermogram of Poloxamer 188 showed a sharp endothermic peak at 63.20°C (figure 3.17a). The thermogram of physical mixture of Daclatasvir and Poloxamer 188 showed endothermic peaks at 63.21°C and 293.75°C (figure 3.17b). Overall, no significant shift of endothermic peaks or absence of endothermic peaks or appearance of new endothermic peaks were observed for the DSC curve of physical mixture of Daclatasvir and Poloxamer 188 suggesting that there was no chemical interaction between Daclatasvir and Poloxamer 188 in physical mixtures (Tomassetti et al., 2005).

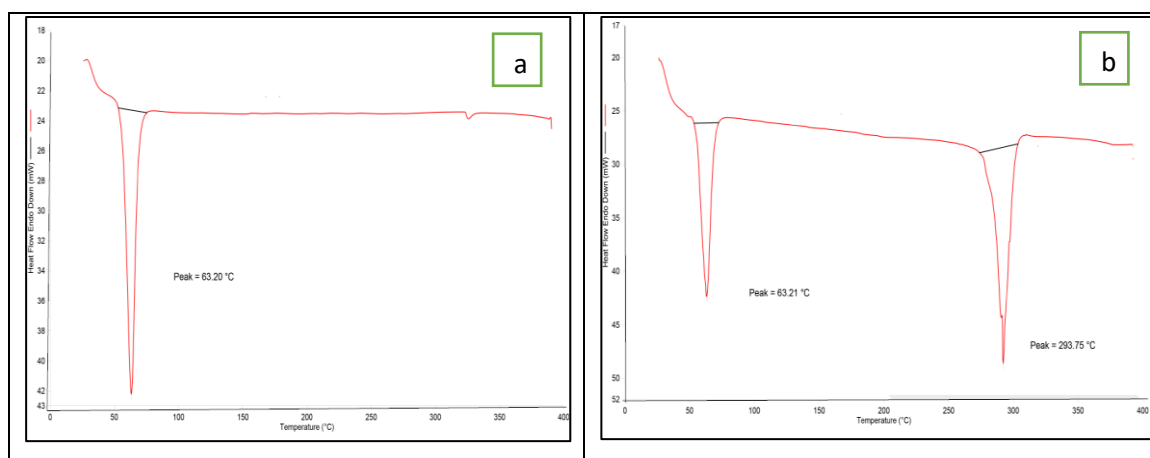


Figure 3.17: a) DSC thermogram of Poloxamer 188; b) DSC thermogram of physical mixture of Daclatasvir and Poloxamer 188

3.3.4.2.3 DSC analysis for Velpatasvir

Pure drug (Velpatasvir): From the DSC curve of Velpatasvir (figure 3.18) a sharp endothermic peak was found at 204.62°C due to the melting of the API which indicated the drug is in crystalline state (Purna Chandra Reddy Guntaka, 2018).

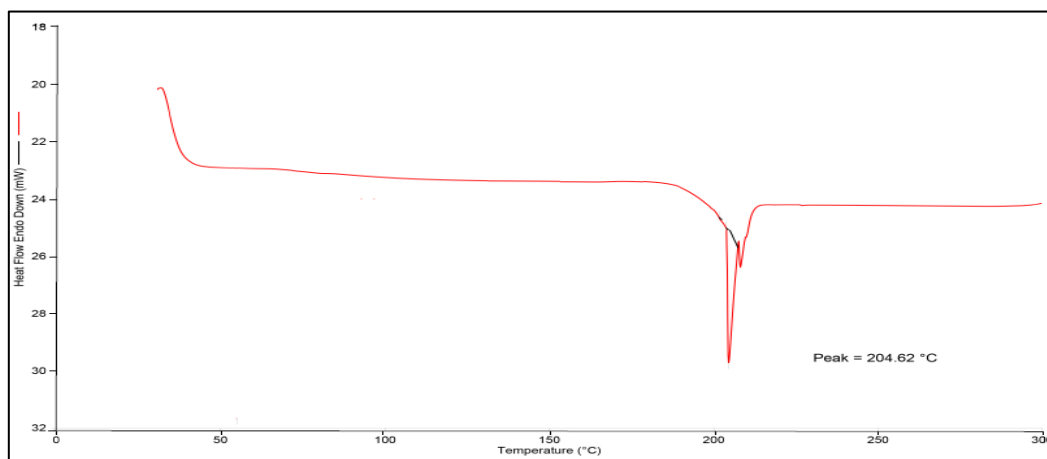


Figure 3.18: DSC thermogram of Velpatasvir

Velpatasvir and Poloxamer 188: The thermogram of Poloxamer 188 showed a sharp endothermic peak at 63.20°C (figure 3.17a). The thermogram of physical mixture of Velpatasvir and Poloxamer 188 showed endothermic peaks at 63.03°C and 206.73°C (figure 3.19). Overall, no significant shift of endothermic peaks or absence of endothermic peaks or appearance of new endothermic peaks were observed for the DSC curve of physical mixture of Ledipasvir and Poloxamer 188 suggesting that there was no chemical interaction between Ledipasvir and poloxamer 188 in physical mixtures (Tomassetti et al., 2005).

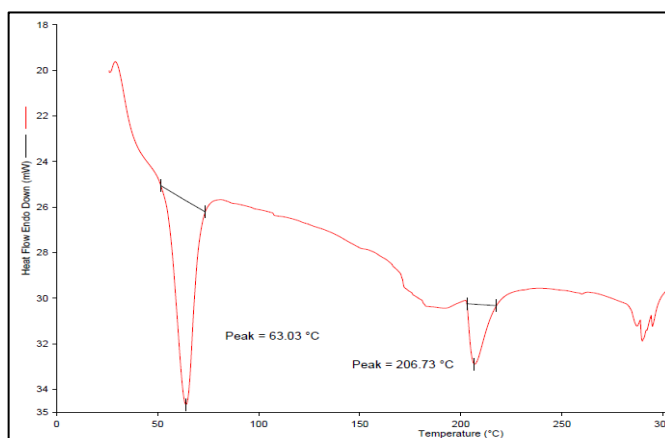


Figure 3.19: DSC thermogram of physical mixture of Velpatasvir and Poloxamer 188

3.3.5 Characterization of prepared solid dispersions

3.3.5.1 Characterization of Ledipasvir SDs

The prepared solid dispersions (SDs) were characterized by DSC to check for their crystallinity and amorphousity.

Figure 3.20a shows the DSC curve of F1SD. The characteristic endothermic peak of Poloxamer 188 is retained at 64.68°C but the characteristic peak of Ledipasvir is absent in the solid dispersion which indicates the conversion of the drug into amorphous form (Kerč & Srčič, 1995; Leuner & Dressman, 2000).

Figure 3.20b shows the DSC curve of F2SD. The characteristic endothermic peak of Poloxamer 407 is retained at 67.53°C but the characteristic peak of Ledipasvir is absent in the solid dispersion which indicates the conversion of the drug into amorphous form (Kerč & Srčič, 1995; Leuner & Dressman, 2000).

Figure 3.20c shows the DSC curve of F3SD. The characteristic peak of Ledipasvir is absent in the solid dispersion which indicates the conversion of the drug into amorphous form (Kerč & Srčič, 1995; Leuner & Dressman, 2000).

Figure 3.20d shows the DSC curve of F4SD. The characteristic peak of Ledipasvir is absent in the solid dispersion which indicates the conversion of the drug into amorphous form (Kerč & Srčič, 1995; Leuner & Dressman, 2000).

Figure 3.20e shows the DSC curve of F5SD. The characteristic peak of Ledipasvir is absent in the solid dispersion which indicates the conversion of the drug into amorphous form (Kerč & Srčič, 1995; Leuner & Dressman, 2000).

Figure 3.20f shows the DSC curve of F6 SD. The characteristic peak of Ledipasvir is retained at 171.91°C in the solid dispersion which indicates the drug is present in the crystalline form and there is no conversion of the drug into amorphous form (Kerč and Srčič, 1995; Leuner and Dressman, 2000).

Figure 3.20g shows the DSC curve of F7SD. The characteristic peak of Ledipasvir is retained at 173.01°C in the solid dispersion which indicates the drug is present in the crystalline form and there is no conversion of the drug into amorphous form (Kerč & Srčič, 1995; Leuner & Dressman, 2000).

Figure 3.20h shows the DSC curve of F8SD. The characteristic peak of Ledipasvir is retained at 171.75°C in the solid dispersion which indicates the drug is present in the crystalline form and there is no conversion of the drug into amorphous form (Kerč & Srčić, 1995; Leuner & Dressman, 2000).

From the DSC curves of all solid dispersion formulations, it could be understood that Ledipasvir has been converted from the crystalline form to the amorphous form in solid dispersions prepared with Poloxamer 188 (F1SD), Poloxamer 407 (F2SD), Klucel™ EF (F3SD), Klucel™ EXF (F4SD) and HPMC 5cps (F5SD). Ledipasvir remained in the crystalline form in the solid dispersions prepared with Povidone K17 (F6SD), Povidone K30 (F7SD), and CMC Na (F8SD).

The amorphous form has higher solubility and dissolution rate compared to the crystalline form because amorphous state is a high-energy state than the crystalline state (Savolainen et al., 2009). In other words, The atoms or molecules of an amorphous solid do not possess a distinguishable crystal lattice and are arranged in a non-ordered, random system, such as in the liquid state (Dey & Chowdhury, 2020). In general, as no energy is needed to break up the crystal lattice, the amorphous forms dissolve faster than crystalline form (Vale & Cox, 1978).

Therefore, Poloxamer 188 (F1SD), Poloxamer 407 (F2SD), Klucel™ EF (F3SD), Klucel™ EXF (F4SD) and HPMC 5cps (F5SD) were primarily selected for the work of nanosuspension preparation in the current study. Polymer list were further shortened. For the preparation of nanosuspension, Poloxamer 188 and Poloxamer 407 were selected. From Klucel™ EF and EXF, Klucel™ EXF was selected. Both are HPC with same chemistry but they differ only in particle size. Klucel™ EXF was the choice of polymer as it is finer in size. HPMC 5 cps was selected it has lower molecular weight and viscosity which makes it more suitable for immediate release formulation.

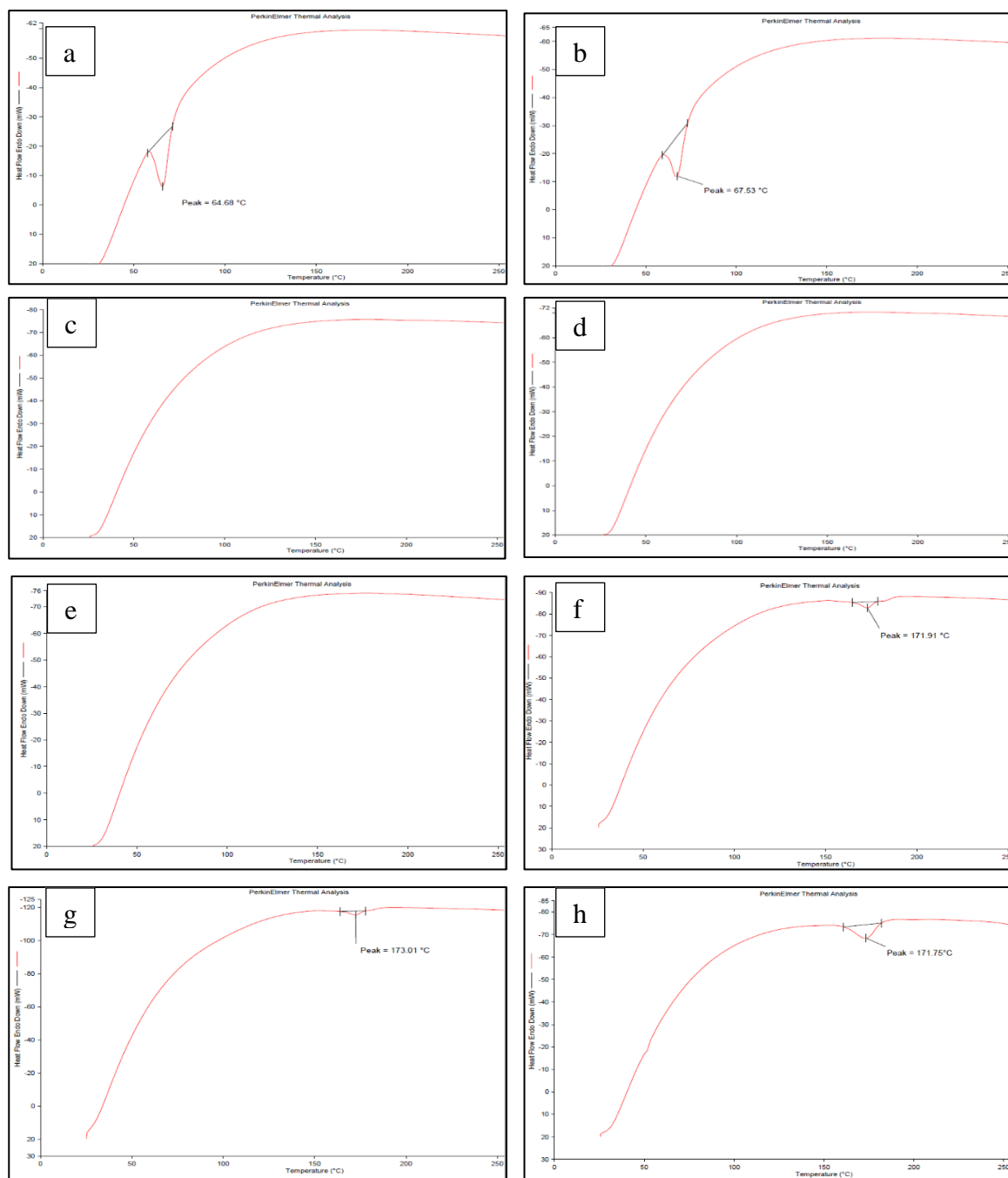


Figure 3.20: a) DSC curve of F1 SD (Ledipasvir-Poloxamer 188 solid dispersion); b) DSC curve of F2 SD (Ledipasvir-Poloxamer 407 solid dispersion); c) DSC curve of F3 SD (Ledipasvir-Klucel™ EF solid dispersion); d) DSC curve of F4 SD (Ledipasvir-Klucel™ EXF solid dispersion); e) DSC curve of F5 SD (Ledipasvir-HPMC 5cps solid dispersion); f) DSC curve of F6 SD (Ledipasvir-PVP K17 solid dispersion); g) DSC curve of F7 SD (Ledipasvir-PVP K30 solid dispersion); h) DSC curve of F8 SD (Ledipasvir-CMC Sodium solid dispersion)

3.3.5.2 Characterization of Daclatasvir SD

Figure 3.21 shows the DSC curve of DF1SD. The characteristic endothermic peak of Poloxamer 188 was retained at 62.86°C and that of Daclatasvir was retained at 291.73°C in the solid dispersion which indicates that the drug has retained its crystalline form and is not converted into amorphous form (Kerč & Srčić, 1995; Leuner & Dressman, 2000). The amorphous form has higher solubility and dissolution rate compared to the crystalline form because amorphous state is a high-energy state than the crystalline state (Savolainen et al., 2009). In other words, The atoms or molecules of an amorphous solid do not possess a distinguishable crystal lattice and are arranged in a non-ordered, random system, such as in the liquid state (Dey & Chowdhury, 2020). In general, as no energy is needed to break up the crystal lattice, the amorphous forms dissolve faster than crystalline form (Vale & Cox, 1978) Therefore, Daclatasvir was not further evaluated for preparing the nanosuspensions.

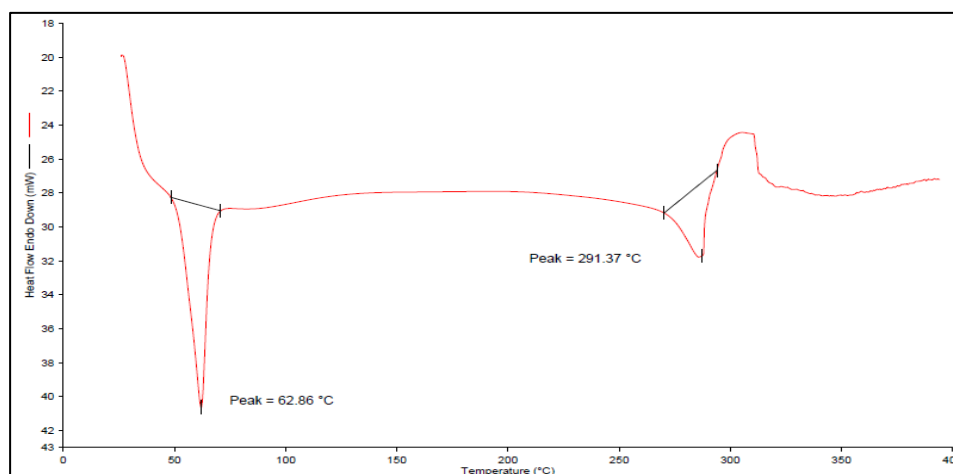


Figure 3.21: DSC curve of DF1SD (Daclatasvir-Poloxamer 188 solid dispersion)

3.3.5.3 Characterization of Velpatasvir SD

Figure 3.21 shows the DSC curve of VF1SD. The characteristic endothermic peak of Poloxamer 188 was retained at 62.53°C in the solid dispersion but the characteristic peak of Velpatasvir was absent indicating that the drug has been converted amorphous form (Kerč & Srčić, 1995; Leuner & Dressman, 2000). Therefore, Velpatasvir was further evaluated for preparing the nanosuspensions.

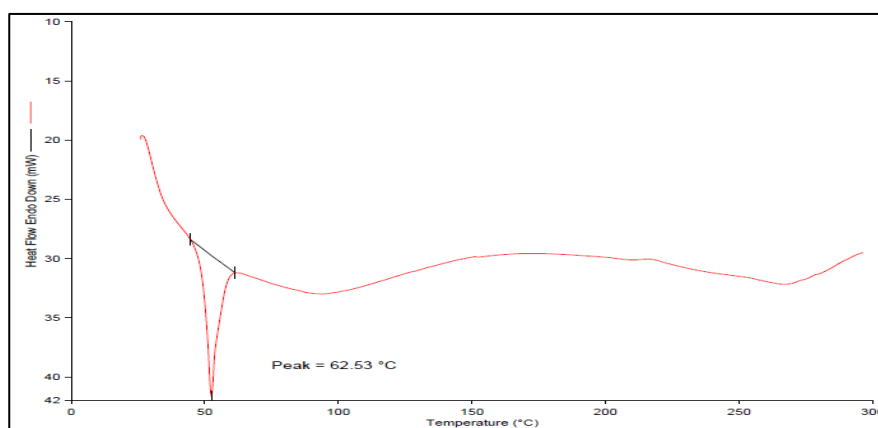


Figure 3.22: DSC curve of VF1SD (Velpatasvir-Poloxamer 188 solid dispersion)

3.3.6 Characterization of prepared nanosuspensions

3.3.6.1 Characterization of *Ledipasvir* nanosuspension

3.3.6.1.1 Particle size distribution (PSD)

Particle size distribution for all the SD suspensions are presented in the table below-

Table 3.9: PSD of different SD suspensions

SD suspension Formulation	PSD (nm)		
	Record 1	Record 2	Record 3
NS F1a	302.2	295.7	299.4
NS F1b	331.3	339.2	334.9
NS F1c	372.4	377.2	389.6
NS F2a	394.6	401.6	403.7
NS F2b	441.8	446.9	440.1
NS F2c	480.0	491.8	488.5
NS F4a	637.5	622.0	629.8
NS F4b	692.4	675.7	688.7
NS F4c	803.3	838.4	833.3
NS F5a	2071.0	2236.0	2371.0
NS F5b	2460.0	2494.0	2497.0
NS F5c	2713.0	2736.0	2958.0

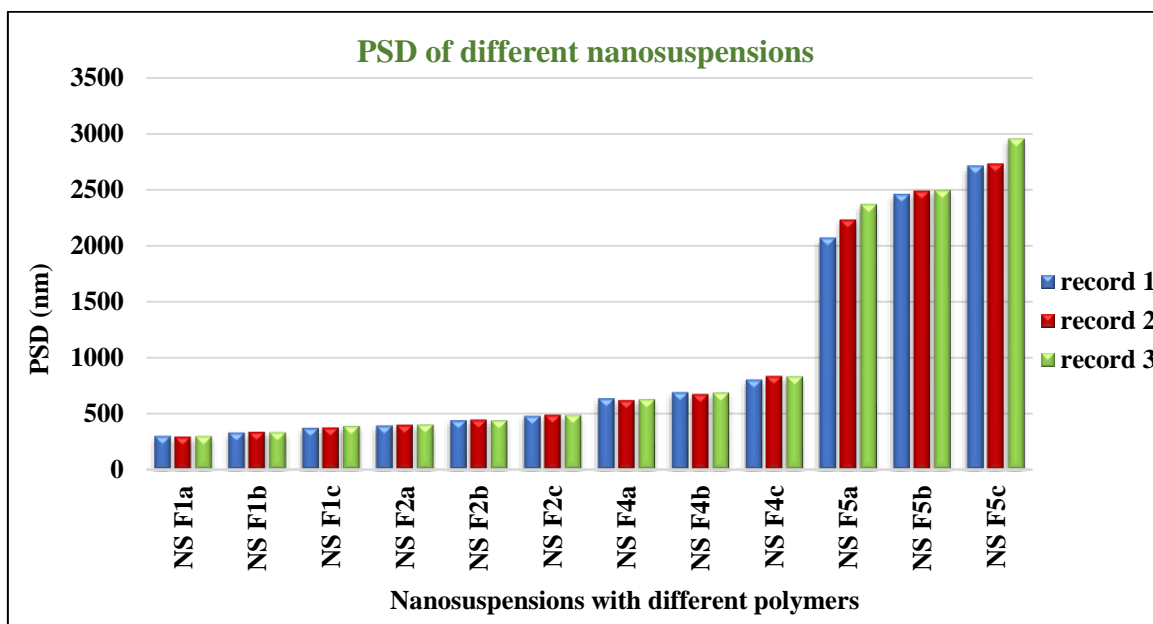


Figure 3.23: Particle size distribution of formulated different nanosuspensions

From the above results (Table 3.9, figure 3.23) it can be said that solid dispersion suspensions NSF1(a), NSF1(b), NSF1(c), NsF2(a), NSF2(b) and NSF2(c), NSF4(a), NSF4(b) and NsF4(c) are nanosuspensions as their particle size ranges within 1000 nm. However, a further investigation of NSF4(a), NSF4(b) and NsF4(c) revealed that these formulations contain significant number of particles outside the nanosuspension range which makes them unacceptable. Moreover, NSF5(a), NSF5(b) and NSF5(c) did not produce nanosuspension as all of them have particle size over 1000 nm (Müller, R. H., Peters, K., Becker, R., & Kruss, 1995) (figure 3.24).

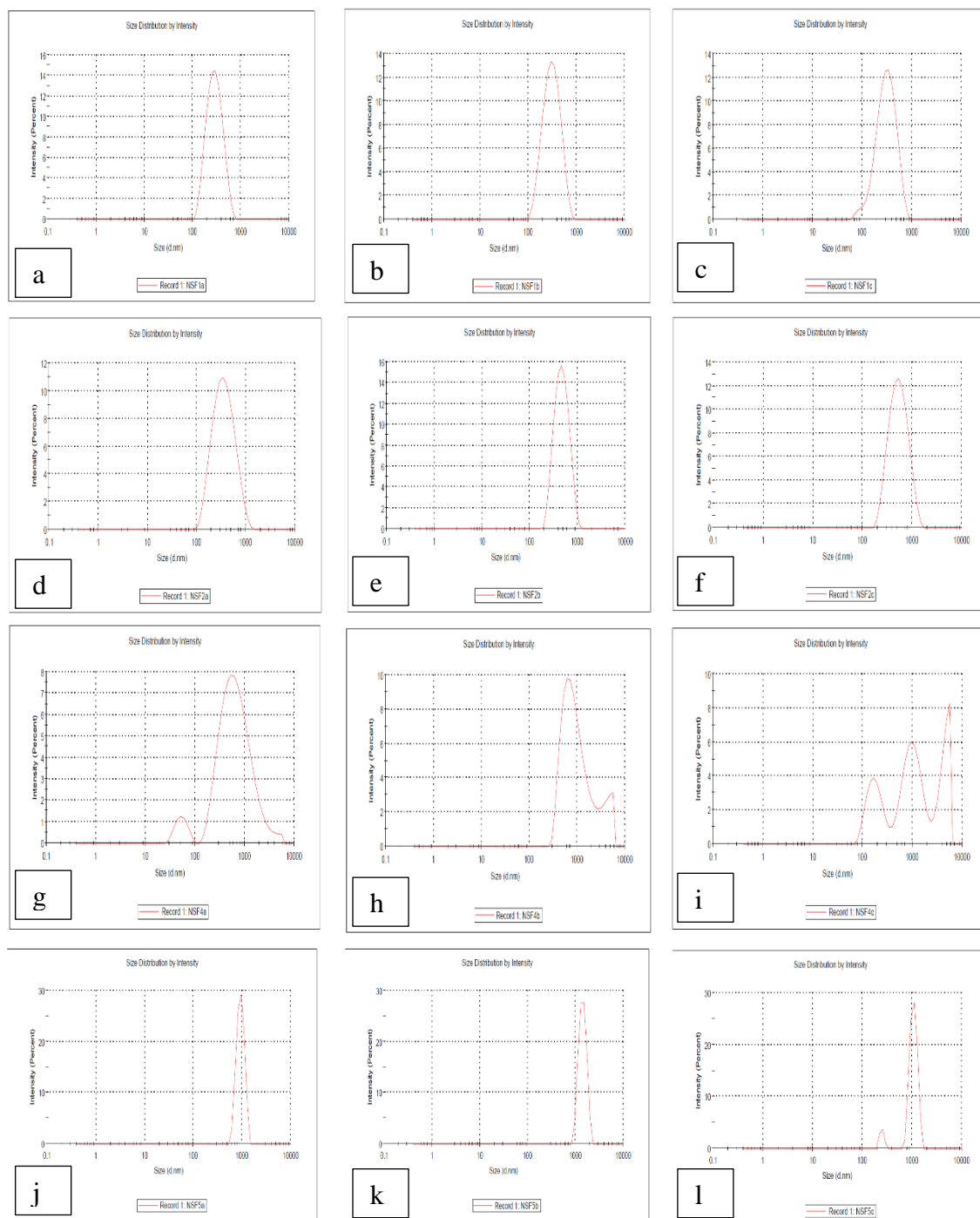


Figure 3.24: a) Particle size distribution of NSF1; b) Particle size distribution of NSF1b; c) Particle size distribution of NSF1c; d) Particle size distribution of NSF2a; e) Particle size distribution of NSF2b; f) Particle size distribution of NSF2c; g) Particle size distribution of NSF4a; h) Particle size distribution of NSF4b; i) Particle size distribution of NSF4c; j) Particle size distribution of NSF5a; k) Particle size distribution of NSF5b; l) Particle size distribution of NSF5c

3.3.6.1.2 Polydispersity Index (PDI)

Polydispersity index (PDI) for all the nanosuspensions are presented in the table below-

Table 3.10: PDI of different nanosuspensions

SD suspension Formulation	PDI		
	Record 1	Record 2	Record 3
NS F1a	0.163	0.184	0.146
NS F1b	0.241	0.294	0.217
NS F1c	0.305	0.321	0.331
NS F2a	0.328	0.297	0.301
NS F2b	0.350	0.360	0.354
NS F2c	0.426	0.407	0.399
NS F4a	0.838	0.857	0.962
NS F4b	0.725	0.783	0.766
NS F4c	1.000	1.000	1.000
NS F5a	1.000	0.588	0.657
NS F5b	0.472	1.000	0.872
NS F5c	0.679	0.588	0.680

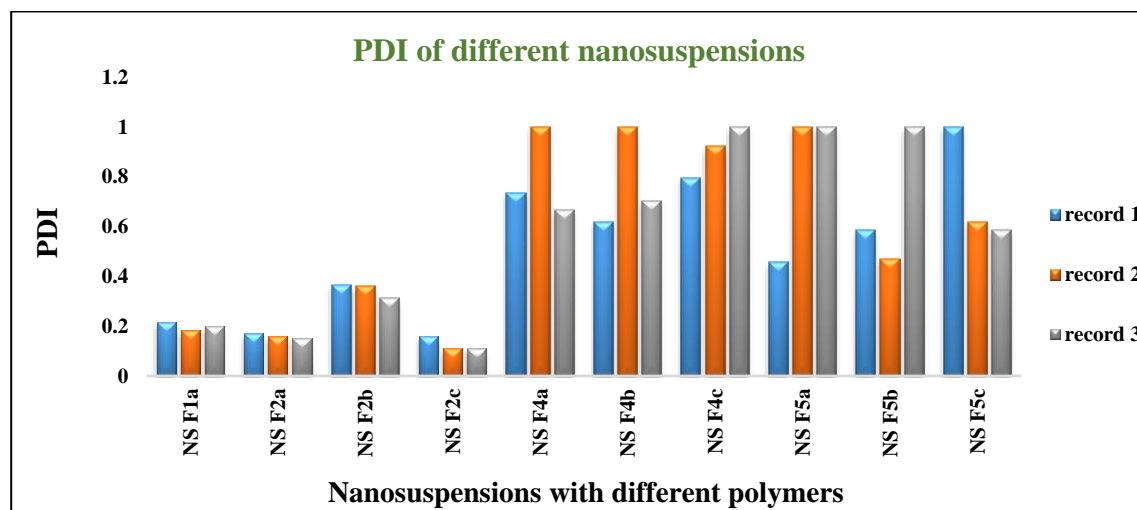


Figure 3.25: PDI of different nanosuspensions

From the above results (Table 3.10, figure 3.25) it can be said that SD suspensions, NSF1(a), NSF1(b), NSF1(c), NSF2(a), NSF2(b), NSF2(c), NSF4(a), NSF4(b) and NSF4(c) are nanosuspensions in terms of the definition of nanosuspension. Nevertheless, NSF4(a),

NSF4(b) and NsF4(c) have PDI over 0.7 which indicates a very wide range of particle size distribution and are not suitable to be measured by a Zetasizer (photon correlation spectroscopy) (Gumustas et al., 2017). PDI values of nanosuspensions NSF1(a), NSF1(b), NSF1(c), NsF2(a), NSF2(b) and NSF2(c) are well below 0.7 and therefore, the PSD results can be considered acceptable. Poloxamers have better wettability than HPC and HPMC (Howlader et al., 2012). Because of this higher wettability, Poloxamers have produced nanosuspensions whereas HPC and HPMC failed to do so due to their relatively lower wettability compared to Poloxamers. Moreover, as the concentration of the Poloxamers have been increased, the particle size has decreased and the PDI value has also decreased indicating more uniform distribution of the particle in presence of higher concentration of Poloxamers.

From the results of PSD and PDI, it was also found that nanosuspensions, NSF1(a) and NSF2(a) produced best results as they had lowest particle size with acceptable PDI values.

3.3.6.1.3 Viscosity

Table 3.11: Viscosity of all SD suspensions

SD suspension Formulation	Viscosity (cps)
NSF1a	36
NSF1b	61
NSF1c	35
NSF2a	40
NSF2b	68
NSF2c	47
NSF4a	195
NSF4b	181
NSF4c	169
NSF5a	262
NSF5b	237
NSF5c	216

From the above table it can be said that viscosity of the suspensions decreased gradually with gradual decrease of polymer concentrations for HPC (Klucel™ EXF) and HPMC 5cps. In

case of all three polymers, viscosity was maximum at 50% polymer concentration whilst the viscosity was lower for both 65% and 35% polymer concentration (Figure 3.26).

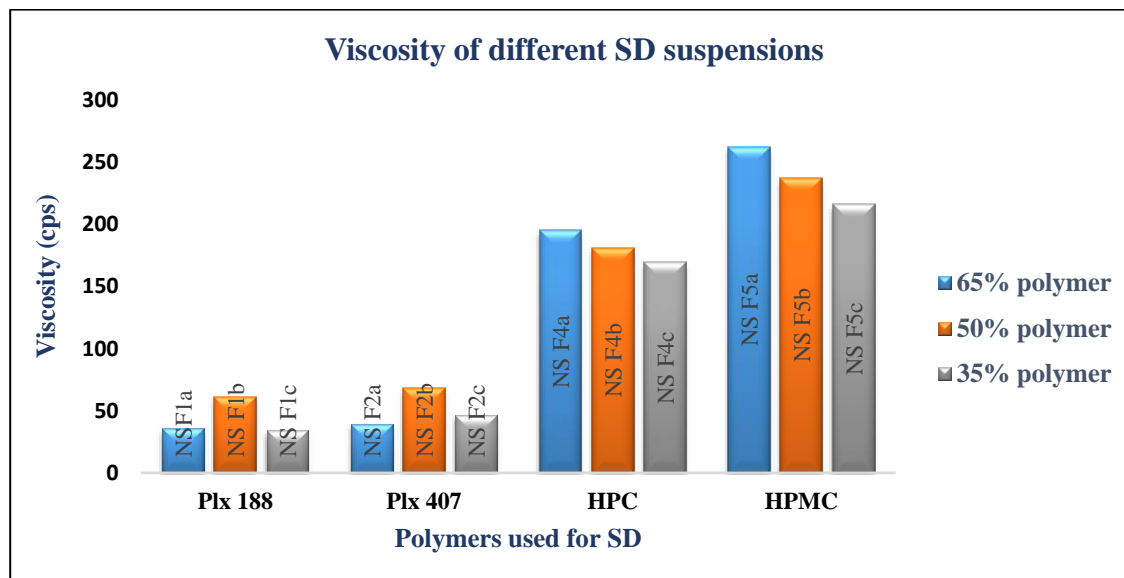


Figure 3.26: Viscosity of all SD suspensions

Most of the suspensions had viscosity lower than 200 cps which is not ideal for an oral suspension. Only NSF5a, 5b and 5c had viscosity above 200 cps. Although the suspensions were easily pourable, the lower viscosity may cause too fast sedimentation to ensure dose uniformity. Furthermore, there are chances of hard cake formation upon storage for longer period which may cause dose uniformity and bioavailability problem (Abood, 2016).

3.3.6.1.4 Zeta Potential

Zeta potential of all the SD suspensions was measured using a Zeta Sizer and the values of zeta Potential of all the SD suspensions are included in the table 3.11. Furthermore, a deep insight was developed by analyzing zeta potential of each individual formulation (figure 3.67 to figure 3.79).

Table 3.12: Zeta Potential of different SD suspensions

SD suspension Formulation	Zeta Potential (mV)		
	Record 1	Record 2	Record 3
NSF1a	-1.4460	-1.4100	-1.6000
NS F1b	-1.2100	-1.2710	-1.1900
NS F1c	-1.1120	-1.0340	-1.0600

NS F2a	-0.9850	-1.0030	-1.0200
NS F2b	-0.9520	-0.9580	-0.9450
NS F2c	-0.8300	-0.8600	-0.7040
NS F4a	-0.5390	-0.4916	-0.4860
NS F4b	-0.3770	-0.4010	-0.3970
NS F4c	-0.3250	-0.3120	-0.3640
NS F5a	-0.5030	-0.4910	-0.4220
NS F5b	-0.1410	-0.1992	-0.1710

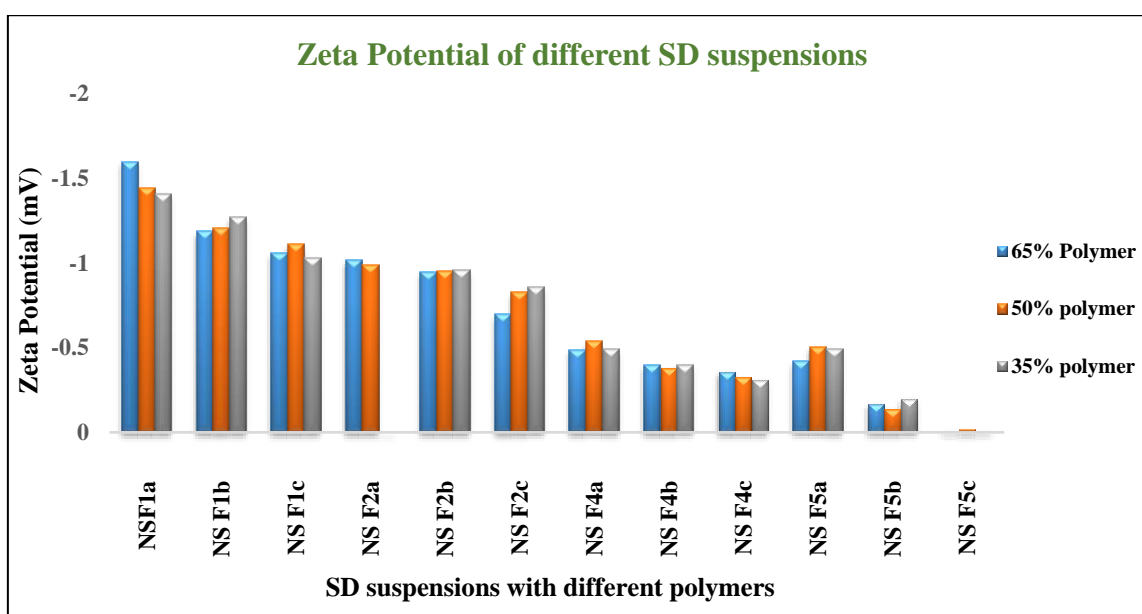


Figure 3.27: Zeta potential of different SD suspensions

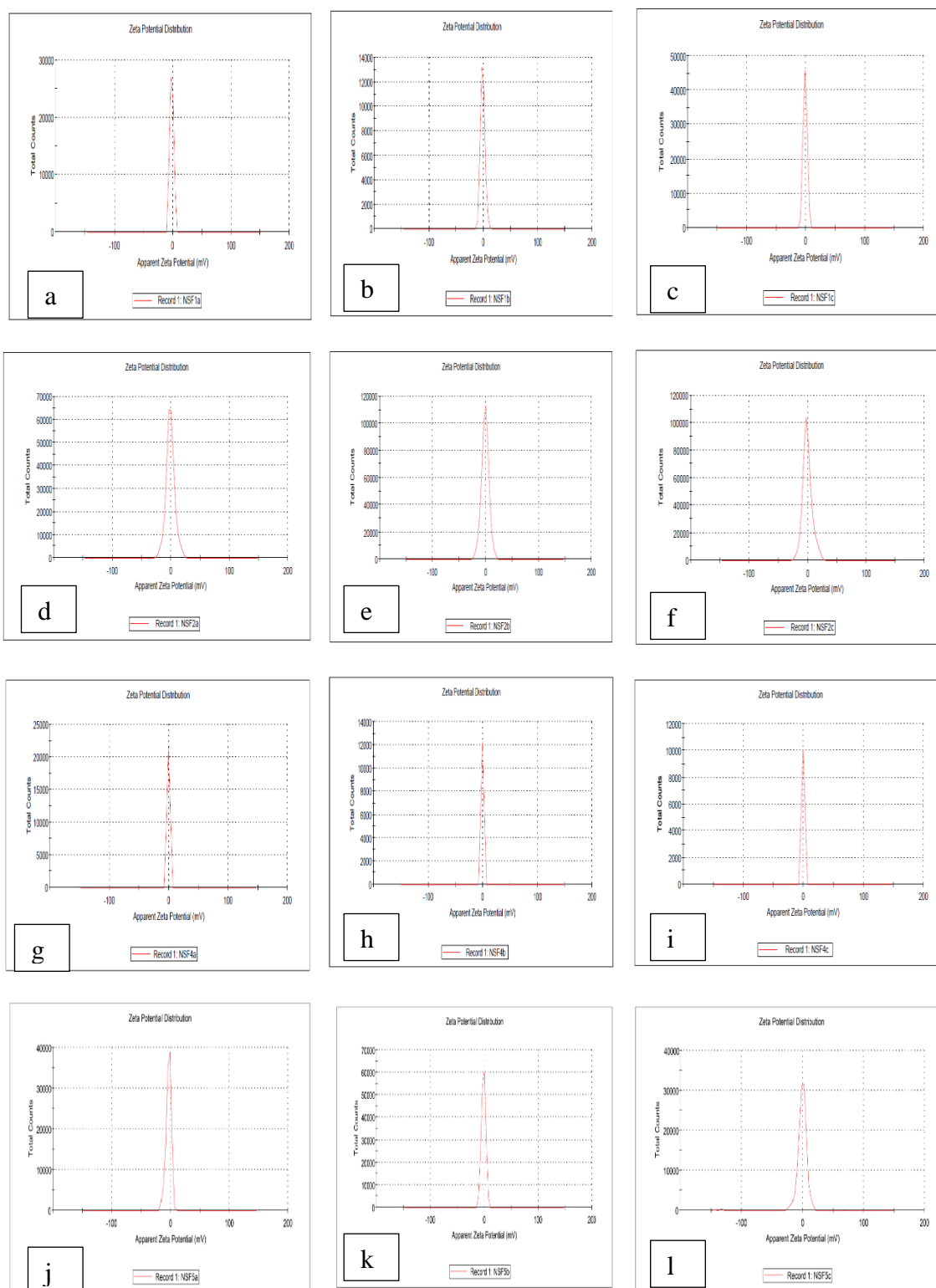


Figure 3.28: a) Zeta potential distribution of NSF1a SD suspension; b) NSF1b SD suspension; c) NSF1c SD suspension; d) NSF2a SD suspension; e) NSF2b SD suspension; f) NSF2c SD suspension; g) NSF4a SD suspension; h) NSF4b SD suspension; i) NSF4c SD suspension; j) NSF5a SD suspension; k) NSF5b SD suspension; l) NSF5c SD suspension.

From the above data it can be viewed that all the SD suspensions had very low Zeta Potentials. It indicates that all the suspensions were unstable (Müller et al., 2001). There were possibilities of rapid settling, agglomeration and hard cake formation upon storage. Hence, the formulations needed to be stabilized using some appropriate techniques.

3.3.6.2 Characterization of Velpatasvir nanosuspension:

3.3.6.2.1 Particle size distribution (PSD):

Particle size distribution for the Velpatasvir SD suspensions are presented in the table below-

Table 3.13: PSD of different SD suspensions of Velpatasvir

SD suspension Formulation	PSD (nm)		
	Record 1	Record 2	Record 3
VNS F1a	348.3	352.7	342.6

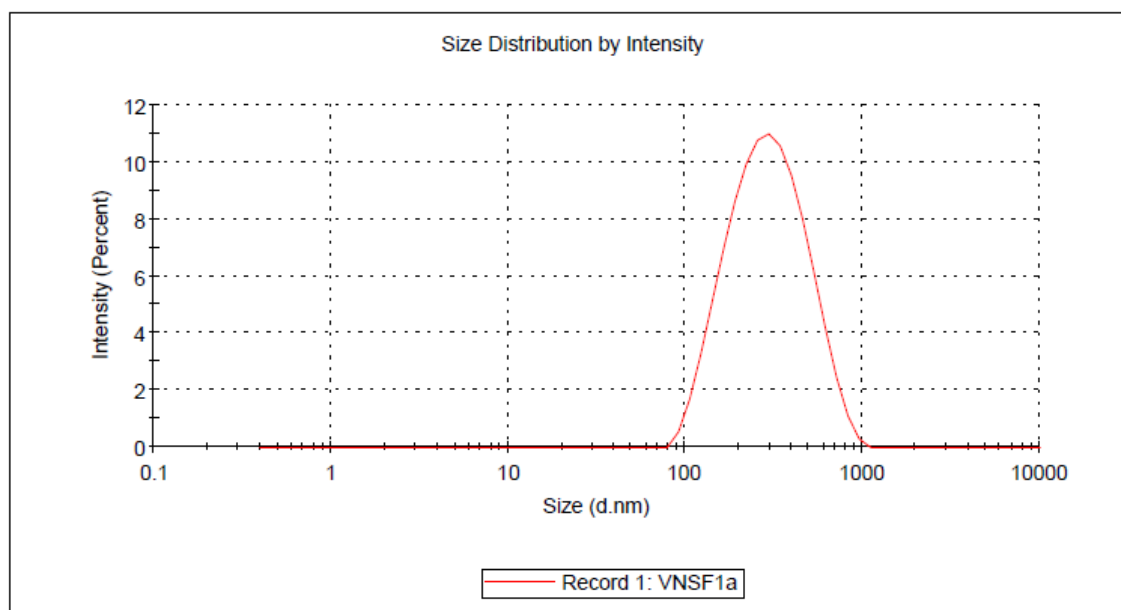


Figure 3.29: Particle size distribution of VNSF1a

From the above results of PSD (table 3.13, figure 3.29), it can be said that SD suspension of Velpatasvir, VNSF1a is a nanosuspension as the particle size is below 1000 nm (Müller, R. H., Peters, K., Becker, R., & Kruss, 1995).

3.3.6.2.2 Polydispersity Index (PDI):

Polydispersity index (PDI) for the Velpatasvir nanosuspensions are presented in the table below-

Table 3.14: PDI of different nanosuspensions of Velpatasvir

SD suspension Formulation	PDI		
	Record 1	Record 2	Record 3
VNS F1a	0.260	0.315	0.299

From the above results (Table 3.14), it can be said that the PDI values of the SD suspension VNSF1 are well below 0.7 and the VNSF1a suspension has narrow range of particle size distribution. Hence, PSD results can be considered acceptable and VNSF1a can be claimed as a nanosuspension (Howlader et al., 2012).

3.3.6.2.3 Viscosity

The viscosity for VNS1a SD suspension was found 114 cps. The suspensions had viscosity lower than 200 cps which is not ideal for an oral suspension. Although the suspensions were easily pourable, the lower viscosity may cause too fast sedimentation to ensure dose uniformity. Furthermore, there are chances of hard cake formation upon storage for longer period which may cause dose uniformity and bioavailability problem (Abood, 2016).

3.3.6.2.4 Zeta Potential

Zeta potential of all the SD suspensions was measured using a Zeta Sizer and the values of zeta Potential of all the SD suspensions are included in the table 3.15. Furthermore, a deep insight was developed by analyzing zeta potential of the formulation (figure 3.30).

Table 3.15: Zeta Potential of SD suspensions of Velpatasvir

SD suspension Formulation	Zeta Potential (mV)		
	Record 1	Record 2	Record 3
VNSF1a	-1.8011	-1.9130	-1.892

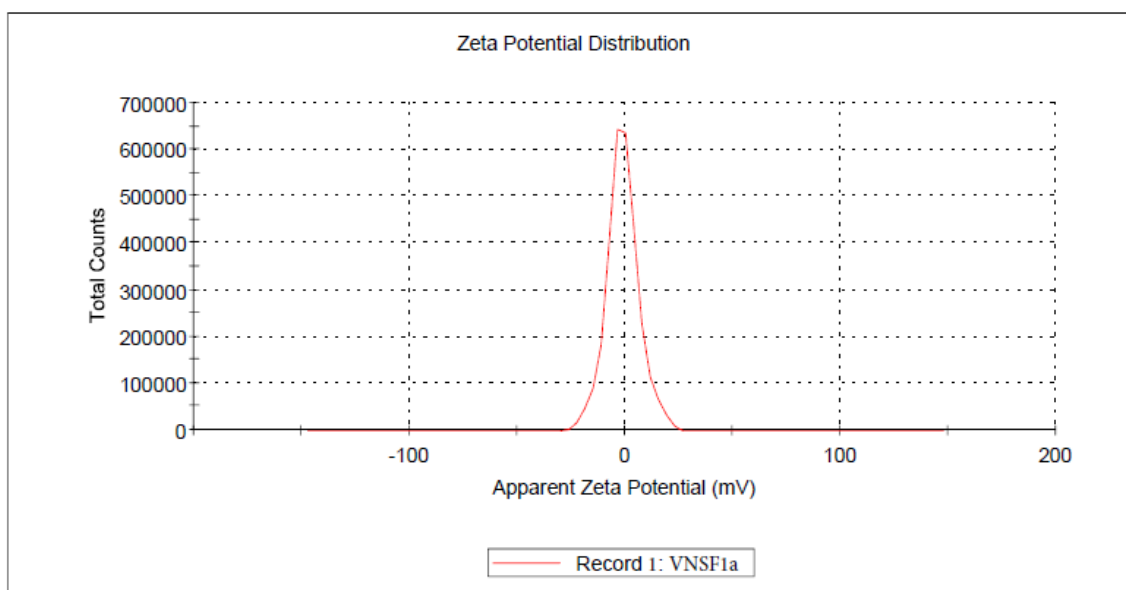


Figure 3.30: Zeta potential distribution of VNSF1a SD suspension

From the above data it can be viewed that the SD suspensions of Velpatasvir had very low Zeta Potentials (Jacobs and Müller, 2002). It indicates that all the suspensions were unstable. There were possibilities of rapid settling, agglomeration and hard cake formation upon storage. Hence, the formulations needed to be stabilized using some appropriate techniques.

3.3.6.9 Visual Observation:

3.3.6.9.1 Observation for Ledipasvir SD suspensions

The results of visual observations of all the suspensions of Ledipasvir are presented in the table below-

Table 3.16: Results of visual observation of prepared LDV SD suspensions at week 1, 2, 3 and 4

SD suspension Formulation	Visual observations				
	Day 0	Week 1	Week 2	Week 3	Week 4
NS F1a	No sediment	Small volume of sediment	Sediment volume increased from week 1	Sediment volume increased from week 2	Sediment volume remained constant, hard cake formed. The suspension was

SD suspension Formulation	Visual observations				
	Day 0	Week 1	Week 2	Week 3	Week 4
					not redispersible upon shaking.
NS F1b	No sediment	Small volume of sediment	Sediment volume increased from week 1	Sediment volume increased from week 2	Sediment volume remained constant, hard cake formed. The suspension was not redispersible upon shaking.
NS F1c	No sediment	Small volume of sediment	Sediment volume increased from week 1	Sediment volume increased from week 2	Sediment volume remained constant, hard cake formed. The suspension was not redispersible upon shaking.
NS F2a	No sediment	Small volume of sediment	Sediment volume increased from week 1	Sediment volume increased from week 2	Sediment volume remained constant, hard cake formed. The suspension was not redispersible upon shaking.
NS F2b	No sediment	Small volume of sediment	Sediment volume increased from week 1	Sediment volume increased from week 2	Sediment volume remained constant, hard cake formed. The suspension was not redispersible upon shaking.
NS F2c	No sediment	Small volume of sediment	Sediment volume increased	Sediment volume	Sediment volume remained constant, hard cake formed.

SD suspension Formulation	Visual observations				
	Day 0	Week 1	Week 2	Week 3	Week 4
			from week 1	increased from week 2	The suspension was not redispersible upon shaking.
NS F4a	No sediment	Small volume of sediment	Sediment volume increased from week 1	Sediment volume increased from week 2	Sediment volume remained constant, hard cake formed. The suspension was not redispersible upon shaking.
NS F4b	No sediment	Small volume of sediment	Sediment volume increased from week 1	Sediment volume increased from week 2	Sediment volume remained constant, hard cake formed. The suspension was not redispersible upon shaking.
NS F4c	No sediment	Small volume of sediment	Sediment volume increased from week 1	Sediment volume increased from week 2	Sediment volume remained constant, hard cake formed. The suspension was not redispersible upon shaking.
NS F5a	No sediment	Small volume of sediment	Sediment volume increased from week 1	Sediment volume increased from week 2	Sediment volume remained constant, hard cake formed. The suspension was not redispersible upon shaking.

SD suspension Formulation	Visual observations				
	Day 0	Week 1	Week 2	Week 3	Week 4
NS F5b	No sediment	Small volume of sediment	Sediment volume increased from week 1	Sediment volume increased from week 2	Sediment volume remained constant, hard cake formed. The suspension was not redispersible upon shaking.
NS F5c	No sediment	Small volume of sediment	Sediment volume increased from week 1	Sediment volume increased from week 2	Sediment volume remained constant, hard cake formed. The suspension was not redispersible upon shaking.

So, from the observation it can be found that none of the prepared SD suspensions were physically stable upon storage.

3.3.7 QbD for preparation of Ledipasvir nanosuspension

3.3.7.1 Results for formulated NSF1

Three experimental runs were designed and experimented based on different composition. Results obtained for responses of the study response 1 (PSD) and response 2 (PDI) are mentioned below.

Run	Component 1 A:Ledipasvir	Component 2 B:Poloxamer 188	Response 1 PSD nm	Response 2 PDI
1	35	65	299.1	0.164
2	50	50	335.1	0.251
3	65	35	379.7	0.319

Analysis of response 1 (PSD) for NSF1:

Table 3.17: Fit summary for response 1 (PSD) of NSF1

Source	Sequential p-value	Adjusted R ²	Predicted R ²	
Linear	0.0392	0.9924	0.9490	Suggested
Cubic				Aliased

Table 3.18: ANOVA for linear model of response 1 (PSD) of NSF1

Source	Sum of Squares	df	Mean Square	F-value	p-value	Remarks
Model	3248.18	1	3248.18	263.51	0.0392	Significant
Linear Mixture	3248.18	1	3248.18	263.51	0.0392	
Residual	12.33	1	12.33			
Cor Total	3260.51	2				

The Model F-value of 263.51 implies the model is significant. There is only a 3.92% chance that an F-value this large could occur due to noise. P-values less than 0.05 indicate model terms are significant. Values greater than 0.1 indicate the model terms are not significant.

*Analysis of response 2 (PDI) of NSF1:***Table 3.19:** Fit summary for response 2 (PDI) of NSF1

Source	Sequential p-value	Adjusted R ²	Predicted R ²	
Linear	0.0450	0.9900	0.9327	Suggested
Cubic				Aliased

Table 3.20: ANOVA for linear model of response 2 (PDI) of NSF1

Source	Sum of Squares	df	Mean Square	F-value	p-value	Remarks
Model	0.0120	1	0.0120	199.65	0.0450	Significant
Linear Mixture	0.0120	1	0.0120	199.65	0.0450	
Residual	0.0001	1	0.0001			
Cor Total	0.0121	2				

The Model F-value of 199.65 implies the model is significant. There is only a 4.50% chance that an F-value this large could occur due to noise. P-values less than 0.0500 indicate model terms are significant.

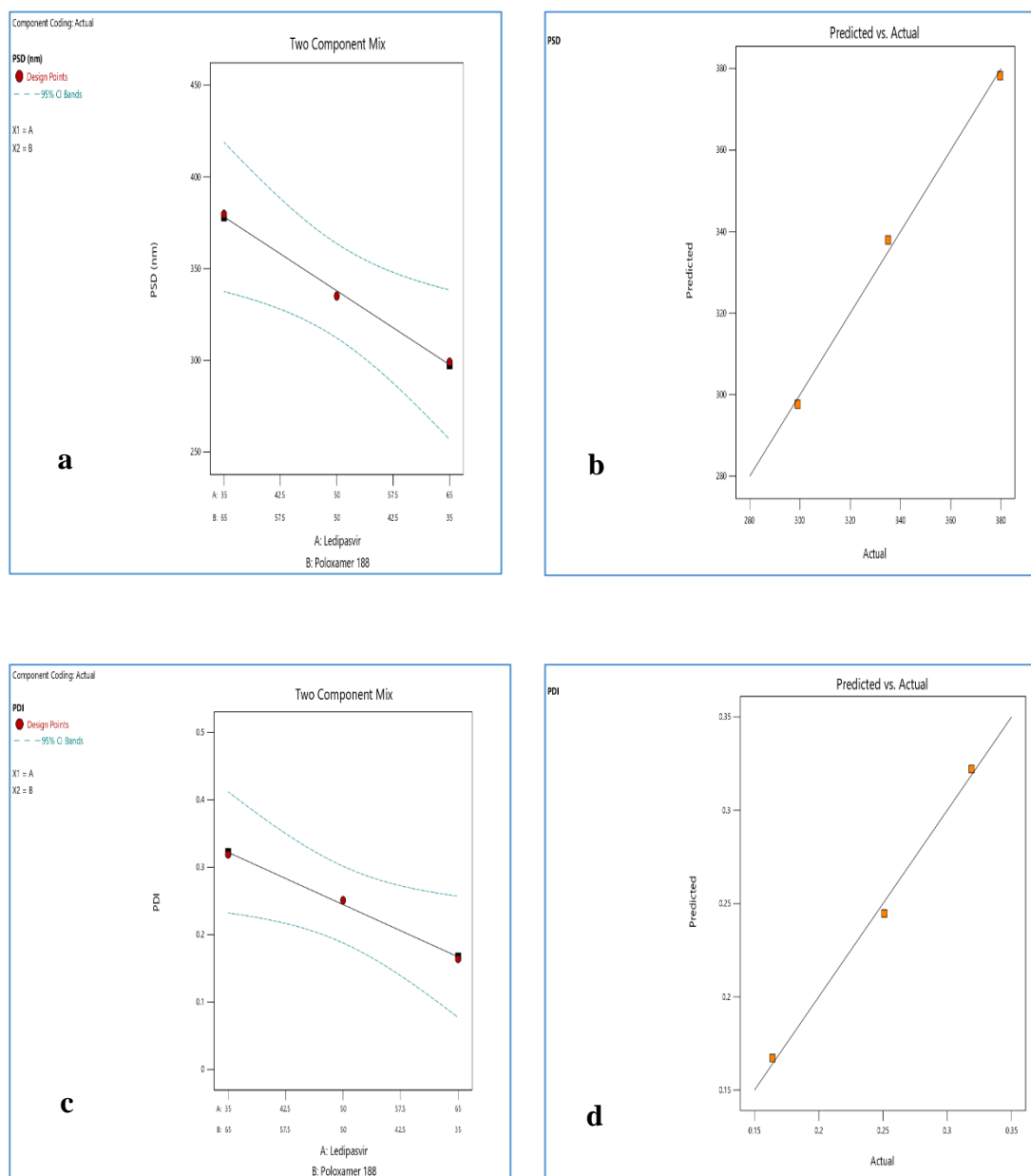


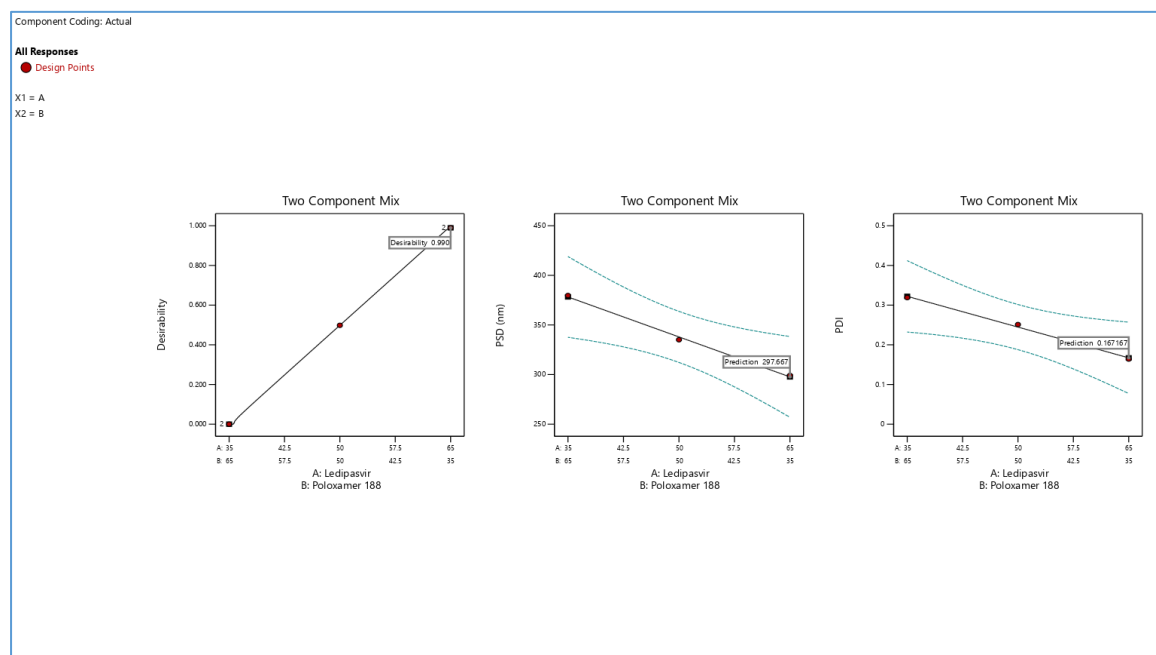
Figure 3.31: (a) Two component mix plot, (b) Predicted vs Actual plot for response 1 (PSD); (c) Two component mix plot, (d) Predicted vs Actual plot for response 2 (PDI) of formulation NSF1

Optimization of formulation NSF1:**Table 3.21:** Constraints for optimization of NSF1

Name	Goal	Lower Limit	Upper Limit	Lower Weight	Upper Weight	Importance
A:Ledipasvir	is in range	35	65	1	1	3
B:Poloxamer 188	is in range	35	65	1	1	3
PSD	Minimize	299.1	379.7	1	1	3
PDI	Minimize	0.164	0.319	1	1	3

Table 3.22: Solution for optimized formulation

Number	Ledipasvir	Poloxamer 188	PSD	PDI	Desirability	
1	35.000	65.000	297.667	0.167	0.990	Selected

**Figure 3.32:** Optimization plot for NSF1 formulation

3.3.7.2 Results of formulation NSF2

Three experimental runs were designed and experimented based on different composition. Results obtained for response 1 (PSD) and response 2 (PDI) are mentioned below.

Run	Component 1 A:Ledipasvir	Component 2 B:Poloxamer 407	Response 1 PSD nm	Response 2 PDI
1	35	65	400	0.309
2	50	50	442.9	0.355
3	65	35	486.8	0.411

Table 3. 23: Fit summary for response 1 (PSD) of NSF2

Source	Sequential p-value	Adjusted R ²	Predicted R ²	
Linear	0.0042	0.9999	0.9994	Suggested
Cubic				Aliased

Analysis of response 1 (PSD) of NSF2:

Table 3.24: ANOVA for linear model of response 1 (PSD) of NSF2

Source	Sum of Squares	df	Mean Square	F-value	p-value	Remarks
Model	3767.12	1	3767.12	22602.72	0.0042	significant
Linear Mixture	3767.12	1	3767.12	22602.72	0.0042	
Residual	0.1667	1	0.1667			
Cor Total	3767.29	2				

The Model F-value of 22602.72 implies the model is significant. There is only a 0.42% chance that an F-value this large could occur due to noise. P-values less than 0.0500 indicate model terms are significant.

*Analysis of response 2 (PDI) of NSF2:***Table 3.25:** Fit summary for response 2 (PDI) of NSF2

Source	Sequential p-value	Adjusted R ²	Predicted R ²	
Linear	0.0360	0.9936	0.9569	Suggested
Cubic				Aliased

Table 3.26: ANOVA for linear model of response 2 (PDI) of NSF2

Source	Sum of Squares	df	Mean Square	F-value	p-value	
Model	0.0052	1	0.0052	312.12	0.0360	Significant
Linear Mixture	0.0052	1	0.0052	312.12	0.0360	
Residual	0.0000	1	0.0000			
Cor Total	0.0052	2				

The Model F-value of 312.12 implies the model is significant. There is only a 3.60% chance that an F-value this large could occur due to noise. P-values less than 0.0500 indicate model terms are significant.

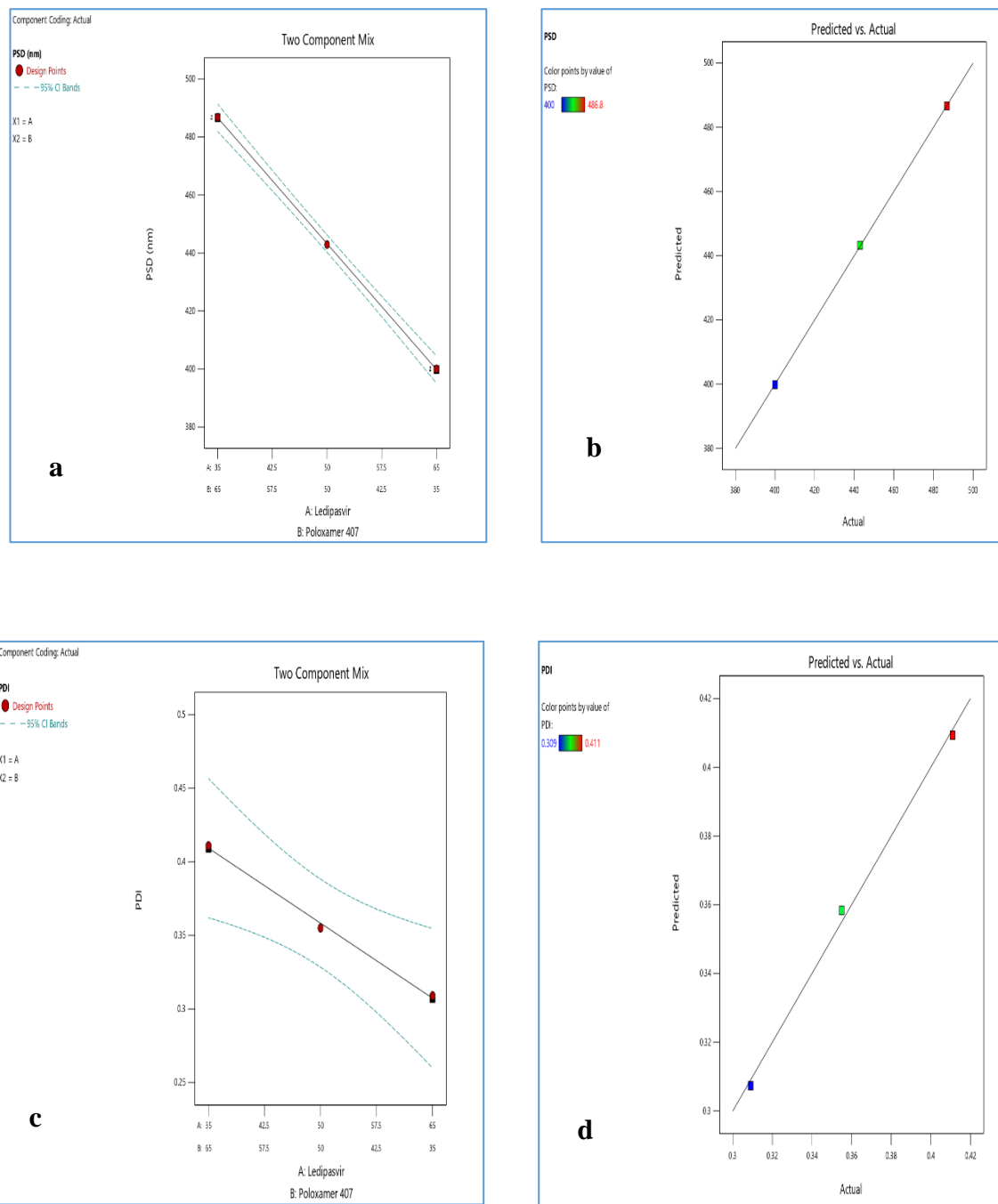


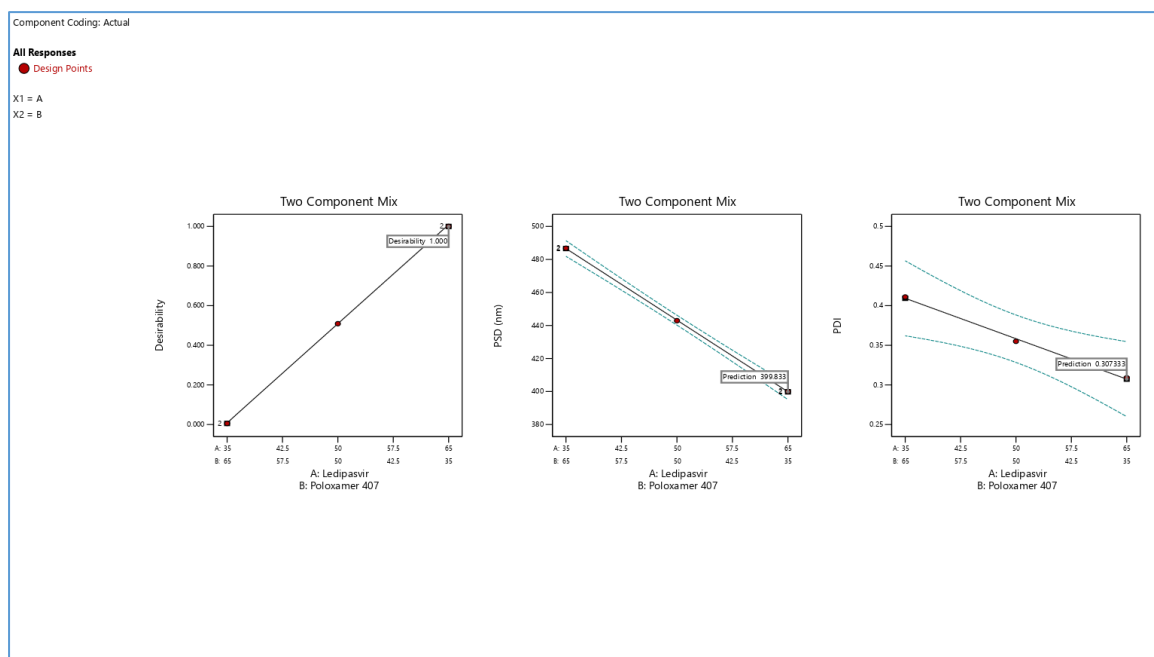
Figure 3.33: (a) Two component mix plot, (b) Predicted vs Actual plot for response 1; (c) Two component mix plot, (d) Predicted vs Actual plot for response 2 of formulation NSF2

*Optimization of NSF2:***Table 3.27:** Constraints for optimization of NSF2

Name	Goal	Lower Limit	Upper Limit	Lower Weight	Upper Weight	Importance
A:Ledipasvir	is in range	35	65	1	1	3
B:Poloxamer 407	is in range	35	65	1	1	3
PSD	minimize	400	486.8	1	1	3
PDI	minimize	0.309	0.411	1	1	3

Table 3.28: Optimized solution for NSF2

Number	Ledipasvir	Poloxamer 407	PSD	PDI	Desirability	
1	35.000	65.000	399.833	0.307	1.000	Selected

**Figure 3.34:** Optimization plot for NSF2 formulation

3.3.7.3 Results for formulated NSF4

Three experimental runs were designed and experimented based on different composition. Results obtained for responses of the study response 1 (PSD) and response 2 (PDI) are mentioned below.

Run	Component 1 A:Ledipasvir	Component 2 B:HPC	Response 1 PSD nm	Response 2 PDI
1	35	65	629.8	0.886
2	50	50	685.6	0.758
3	65	35	825	1

Analysis of response 1 (PSD) of NSF4:

Table 3.29: Fit Summary for response 1 (PSD) of NSF4

Source	Sequential p-value	Adjusted R ²	Predicted R ²	
Linear	0.1543	0.8848	0.2222	Suggested
Cubic				Aliased

Table 3.30: ANOVA for linear model of response 1 (PSD) of NSF4

Source	Sum of Squares	df	Mean Square	F-value	p-value	Remarks
Model	19051.52	1	19051.52	16.36	0.1543	not significant
Linear Mixture	19051.52	1	19051.52	16.36	0.1543	
Residual	1164.83	1	1164.83			
Cor Total	20216.35	2				

The Model F-value of 16.36 implies the model is not significant relative to the noise. There is a 15.43% chance that an F-value this large could occur due to noise. P-values less than 0.0500 indicate model terms are significant.

Analysis of response 2 (PDI) of NSF4:

Table 3.31: Fit summary for response 2 (PDI) of NSF4

Source	Sequential p-value	Adjusted R ²	Predicted R ²	
Mean	0.0062			Suggested
Linear	0.6879	-0.5567	-9.5075	
Cubic				Aliased

Table 3.32: ANOVA for mean model of response 2 (PDI) of NSF4

Source	Sum of Squares	df	Mean Square	F-value	p-value
Model	0.0000	0		N/A	N/A
Residual	0.0293	2	0.0147		
Cor Total	0.0293	2			

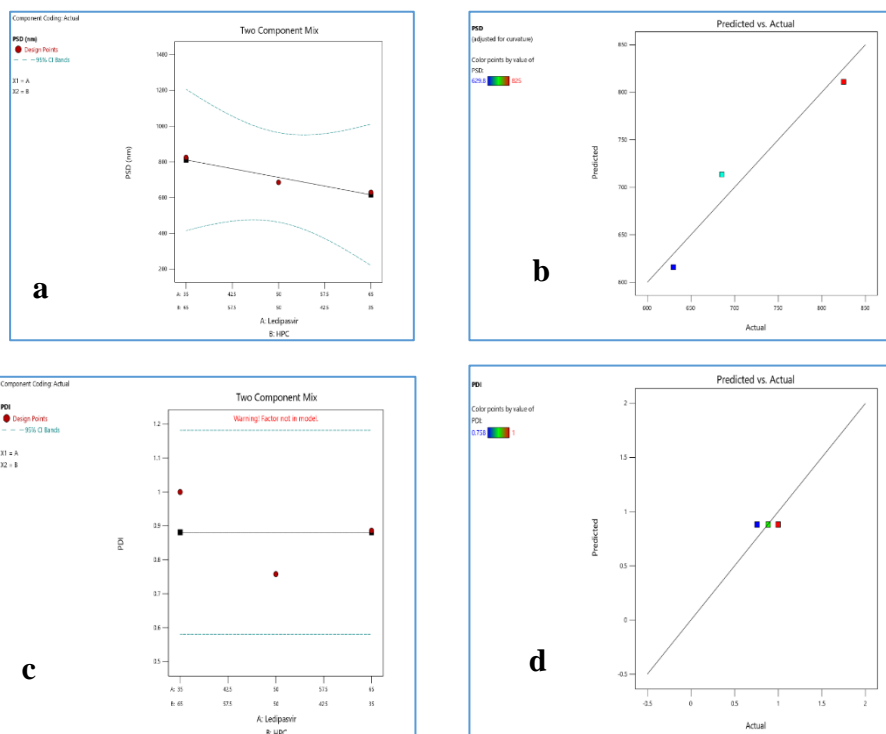


Figure 3.35: (a) Two component mix plot, (b) Predicted vs Actual plot for response 1 (PSD); (c) Two component mix plot, (d) Predicted vs Actual plot for response 2 (PDI) of formulation NSF4

3.3.7.4 Results for formulated NSF5

Three experimental runs were designed and experimented based on different composition. Results obtained for responses of the study response 1 (PSD) and response 2 (PDI) are mentioned below.

Run	Component 1 A:Ledipasvir	Component 2 B:HPMC	Response 1 PSD nm	Response 2 PDI
1	35	65	2268	0.748
2	50	50	2483.7	0.781
3	65	35	2802.3	0.649

Analysis of response 1 (PSD) of NSF5:

Table 3.33: Fit summary for response 1 (PSD) of NSF5

Source	Sequential p-value	Adjusted R ²	Predicted R ²	
Linear	0.0705	0.9756	0.8351	Suggested
Cubic				Aliased

Table 3.34: ANOVA for linear model of response 1 (PSD) of NSF5

Source	Sum of Squares	Df	Mean Square	F-value	p-value	Remarks
Model	1.427E+05	1	1.427E+05	80.88	0.0705	not significant
Linear Mixture	1.427E+05	1	1.427E+05	80.88	0.0705	
Residual	1764.74	1	1764.74			
Cor Total	1.445E+05	2				

The Model F-value of 80.88 implies that the model is not significant relative to the noise. There is a 7.05% chance that an F-value this large could occur due to noise. P-values less than 0.0500 indicate model terms are significant.

*Analysis of response 2 (PDI) of NSF5:***Table 3.35:** Fit summary for response 2 (PDI) of NSF5

Source	Sequential p-value	Adjusted R ²	Predicted R ²	
Linear	0.4878	0.0385	-5.4904	Suggested
Cubic				Aliased

Table 3.36: ANOVA for linear model of response 2 (PDI) of NSF5

Source	Sum of Squares	Df	Mean Square	F-value	p-value	Remarks
Model	0.0049	1	0.0049	1.08	0.4878	not significant
Linear Mixture	0.0049	1	0.0049	1.08	0.4878	
Residual	0.0045	1	0.0045			
Cor Total	0.0094	2				

The Model F-value of 1.08 implies the model is not significant relative to the noise. There is a 48.78% chance that an F-value this large could occur due to noise. P-values less than 0.0500 indicate model terms are significant.

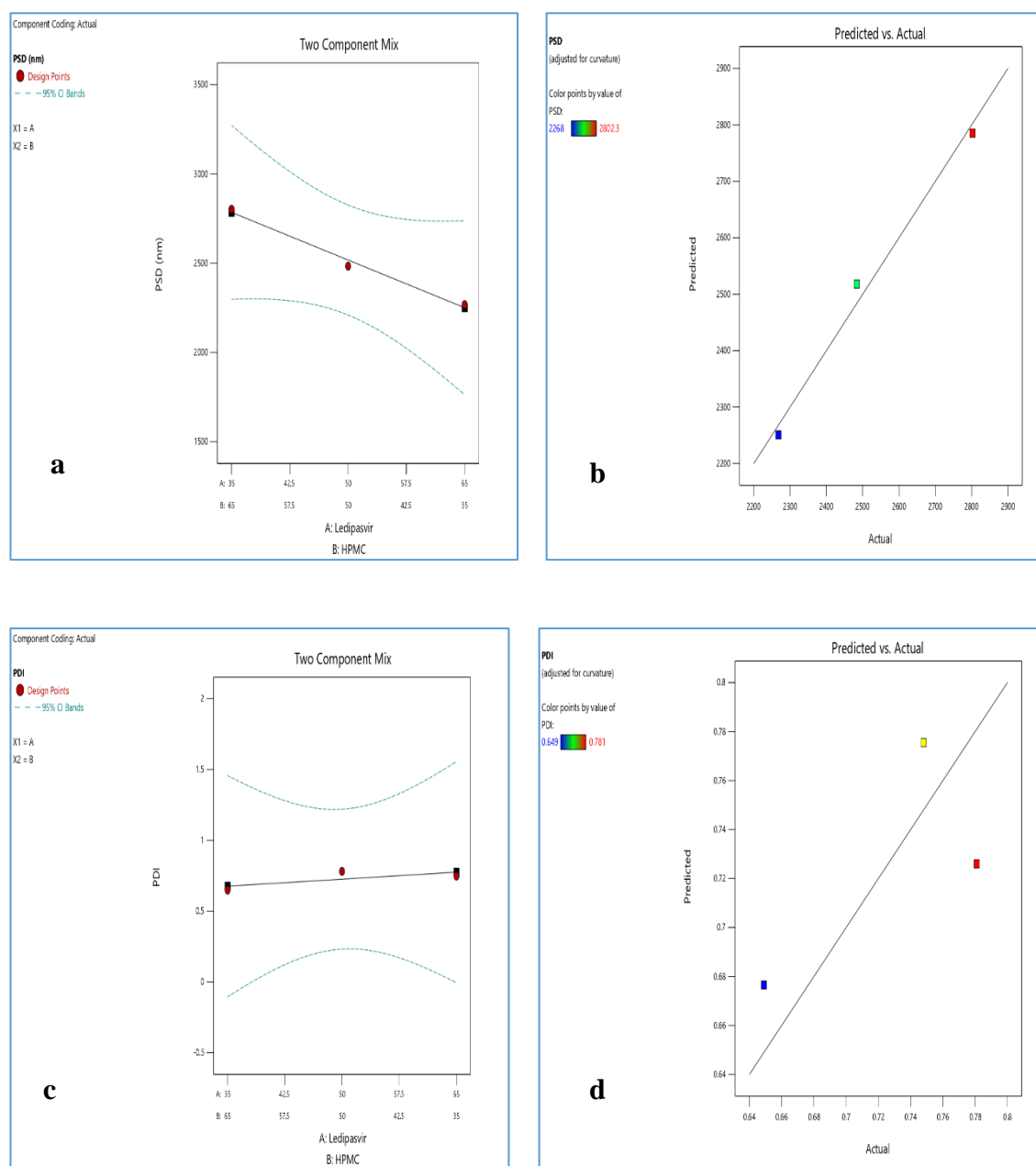


Figure 3.37: (a) Two component mix plot, (b) Predicted vs Actual plot for response 1 (PSD); (c) Two component mix plot, (d) Predicted vs Actual plot for response 2 (PDI) of formulation NSF5

Responses analyzed using ANOVA were found significant for NSF1 and NSF2. But models suggested that the responses for NSF4 and NSF5 were insignificant. Therefore, these two formulations were then removed from the study. Later on, optimization of NSF1 and NSF2 were done to have the best responses. After that, NSF1a and NSF2a were found as optimized batches of the experiments based on the desirability of the model which were

then taken for further study. It is to be noted that the formulation having higher concentration of the polymer exhibited the most desirable results as they had the lowest PSD and PDI. The results of the nanosuspensions can be chronologically classified as below in terms of PSD and PDI-

Drug: Polymer (35:65) < Drug: Polymer (50:50) < Drug: Polymer (65:35).

3.3.8 Stabilization of prepared nanosuspension

3.3.8.1 Experimental design for optimizing suspension vehicle

Table 3.37: Independent variables for designing of suspension vehicle

Independent variables	Level		
	-1	0	+1
Xanthan gum	0.1	0.3	0.5
Avicel [®] RC-591	0.25	0.5	0.75
Citric acid monohydrate	0.3	0.5	0.7

Table 3.38: Designed runs using Box-Behnken design and experimental observation of responses for stabilization of prepared nanosuspensions

Run	Factor 1	Factor 2	Factor 3	Response 1	Response 2
	A:Xanthan gum (g)	B:Avicel RC 591 (g)	C:Citric Acid (g)	Viscosity (cp)	Zeta potential (mv)
1	0.500	0.250	0.6	926.0	-30.0
2	0.100	0.250	0.6	792.0	-29.0
3	0.500	0.750	0.6	1226.0	-32.0
4	0.300	0.500	0.6	1016.0	-30.0
5	0.100	0.500	0.9	856.0	-18.0

Run	Factor 1	Factor 2	Factor 3	Response 1	Response 2
	A:Xanthan gum (g)	B:Avicel RC 591 (g)	C:Citric Acid (g)	Viscosity (cp)	Zeta potential (mv)
6	0.300	0.250	0.3	934.0	-36.0
7	0.300	0.750	0.3	1097.0	-37.0
8	0.300	0.750	0.9	1088.0	-19.0
9	0.100	0.500	0.3	839.0	-36.0
10	0.100	0.750	0.6	907.0	-31.0
11	0.500	0.500	0.3	1124.0	-37.0
12	0.300	0.250	0.9	965.0	-18.0
13	0.500	0.500	0.9	1141.0	-20.0

3.3.8.2 Analysis of responses

Analysis of response 1 (Viscosity, cp):

Table 3.39: Fit summary for response 1 for optimization of suspension vehicle

Source	Sequential p-value	Adjusted R ²	Predicted R ²	Remarks
Linear	< 0.0001	0.8739	0.7937	Suggested
2FI	0.2846	0.8950	0.7175	
Quadratic	0.3010	0.9284		
Cubic				Aliased

Table 3.40: ANOVA for linear model for response 1 for optimization of suspension vehicle

Source	Sum of Squares	df	Mean Square	F-value	p-value	Remarks
Model	1.926E+05	3	64211.08	28.71	< 0.0001	Significant
A-Xanthan gum	1.308E+05	1	1.308E+05	58.50	< 0.0001	
B-Avicel RC 591	61425.12	1	61425.12	27.47	0.0005	
C-Citric Acid	392.00	1	392.00	0.1753	0.6853	
Residual	20126.44	9	2236.27			
Cor Total	2.128E+05	12				

The Model F-value of 28.71 implies the model is significant. There is only a 0.01% chance that an F-value this large could occur due to noise. P-values less than 0.0500 indicate model terms are significant. In this case A, B are significant model terms.

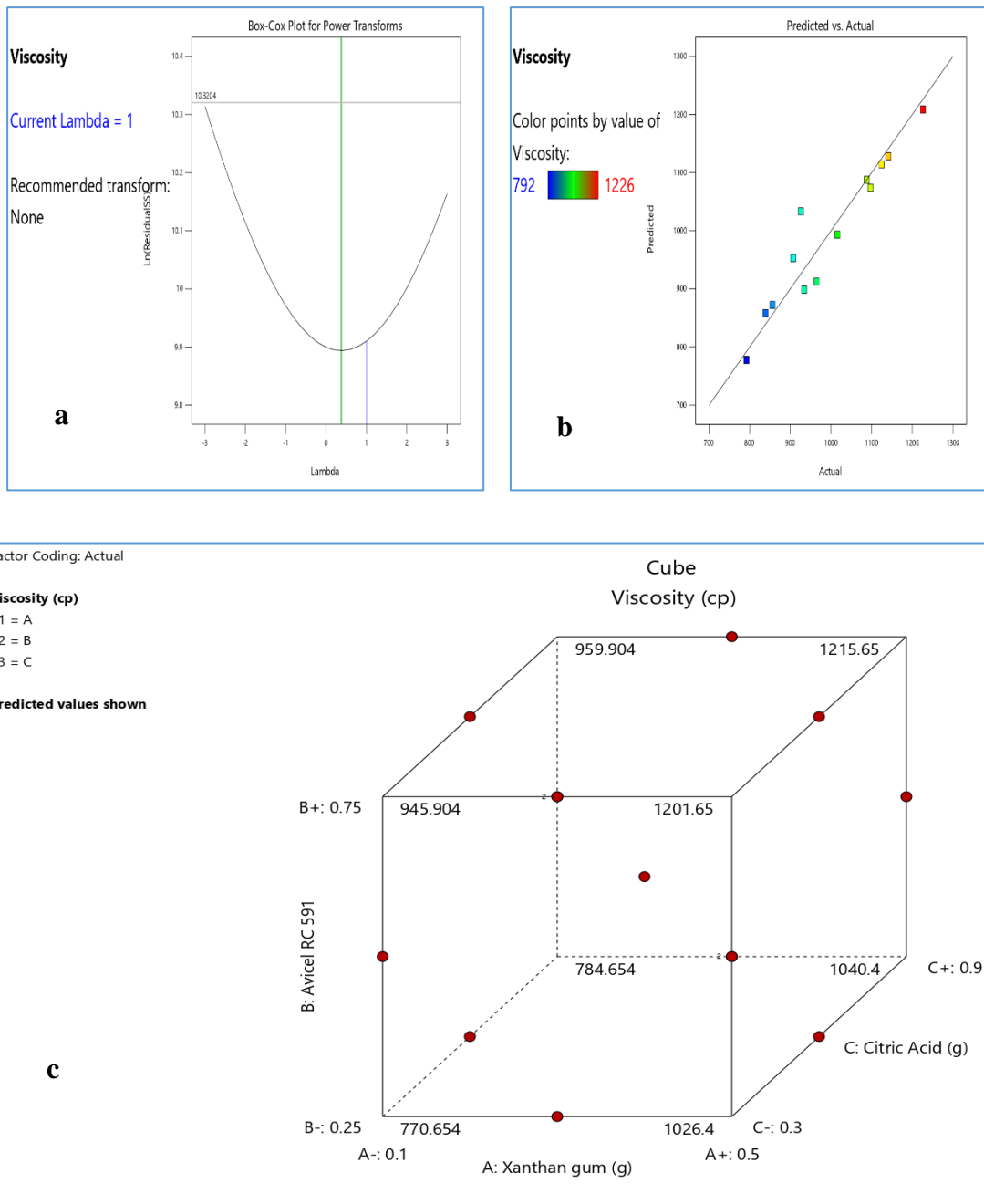


Figure 3.37: (a) Box-Cox plot; (b) Predicted vs Actual plot and; (c) Cubic plot for response 1 for optimization of suspension vehicle

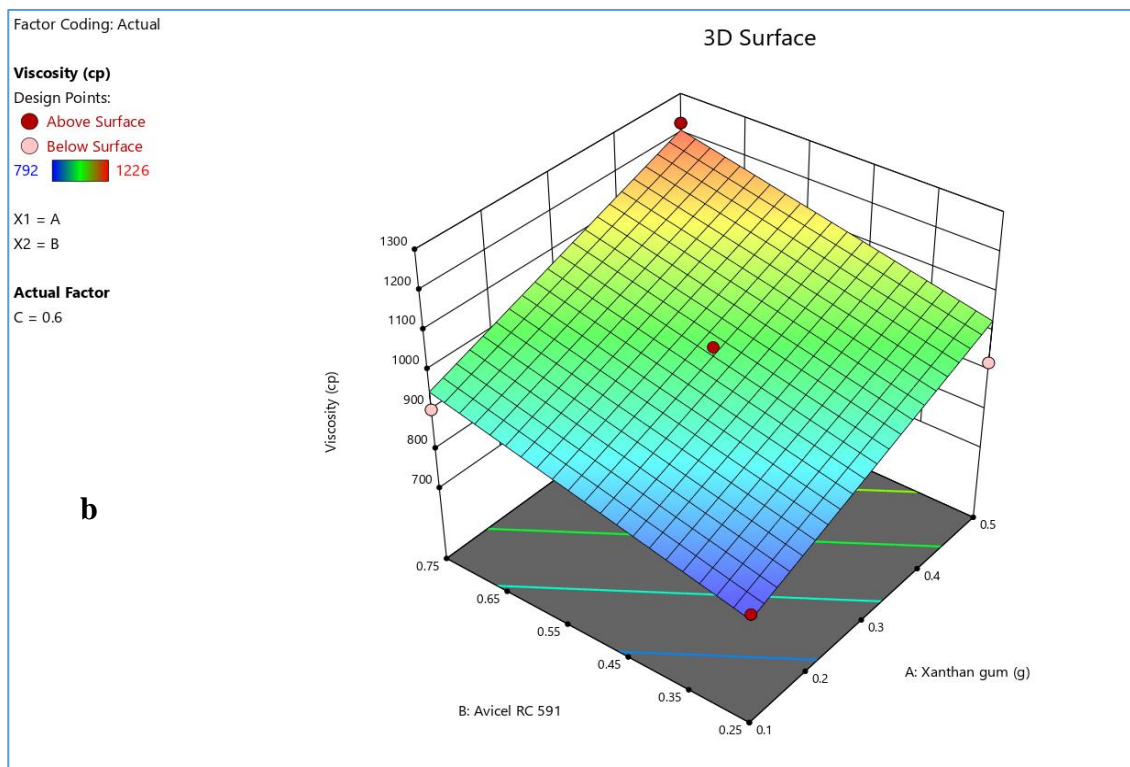
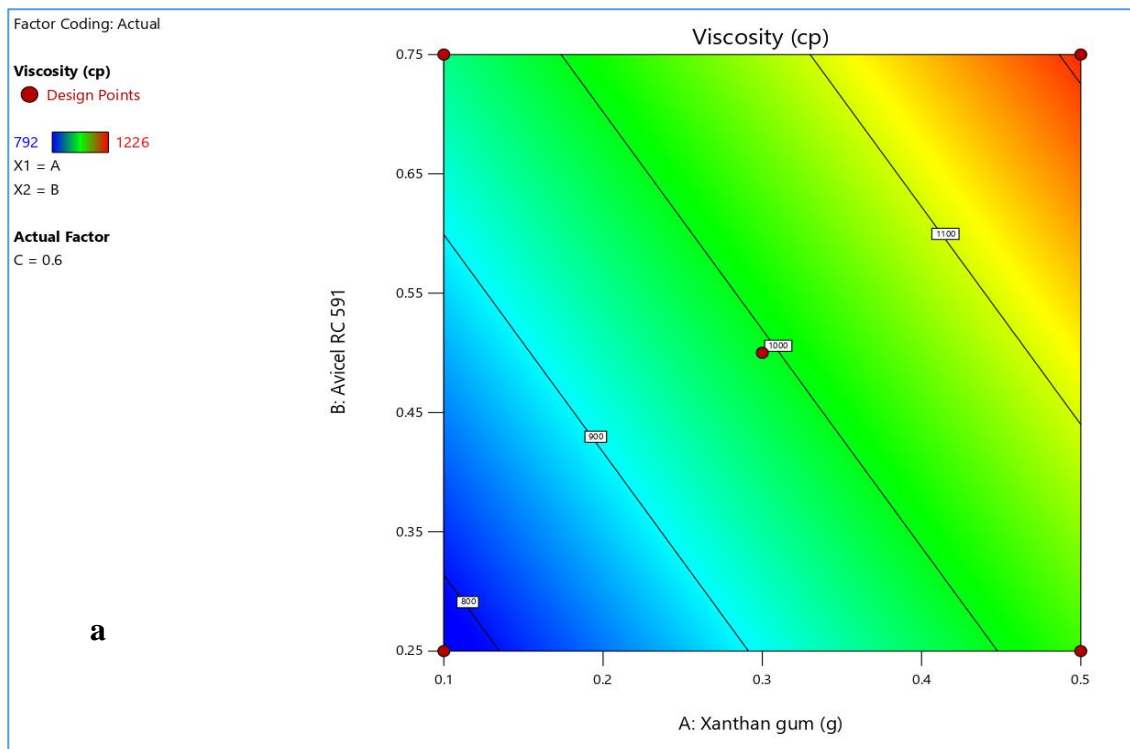


Figure 3.38: (a) Contour plot; (b) 3D response surface plot for response 1 (Viscosity) for optimization of suspension vehicle

Analysis of response 2 (Zeta potential, mv):**Table 3.41:** Fit summary for response 2 for optimization of suspension vehicle

Source	Sequential p-value	Adjusted R ²	Predicted R ²	Remarks
Linear	< 0.0001	0.9497	0.9193	Suggested
2FI	0.9957	0.9253	0.8026	
Quadratic	0.0089	0.9955		Suggested
Cubic				Aliased

Table 3.42: ANOVA for quadratic model for response 2 for optimization of suspension vehicle

Source	Sum of Squares	df	Mean Square	F-value	p-value	Remarks
Model	662.02	9	73.56	294.23	0.0003	significant
A-Xanthan gum	3.13	1	3.13	12.50	0.0385	
B-Avicel RC 591	4.50	1	4.50	18.00	0.0240	
C-Citric Acid	630.12	1	630.12	2520.50	< 0.0001	
AB	0.0000	1	0.0000	0.0000	1.0000	
AC	0.2500	1	0.2500	1.00	0.3910	
BC	0.0000	1	0.0000	0.0000	1.0000	
A ²	0.3214	1	0.3214	1.29	0.3393	
B ²	0.0357	1	0.0357	0.1429	0.7306	
C ²	15.75	1	15.75	63.00	0.0042	
Residual	0.7500	3	0.2500			
Cor Total	662.77	12				

The Model F-value of 294.23 implies the model is significant. There is only a 0.03% chance that an F-value this large could occur due to noise. P-values less than 0.0500 indicate model terms are significant. In this case A, B, C, C² are significant model terms.

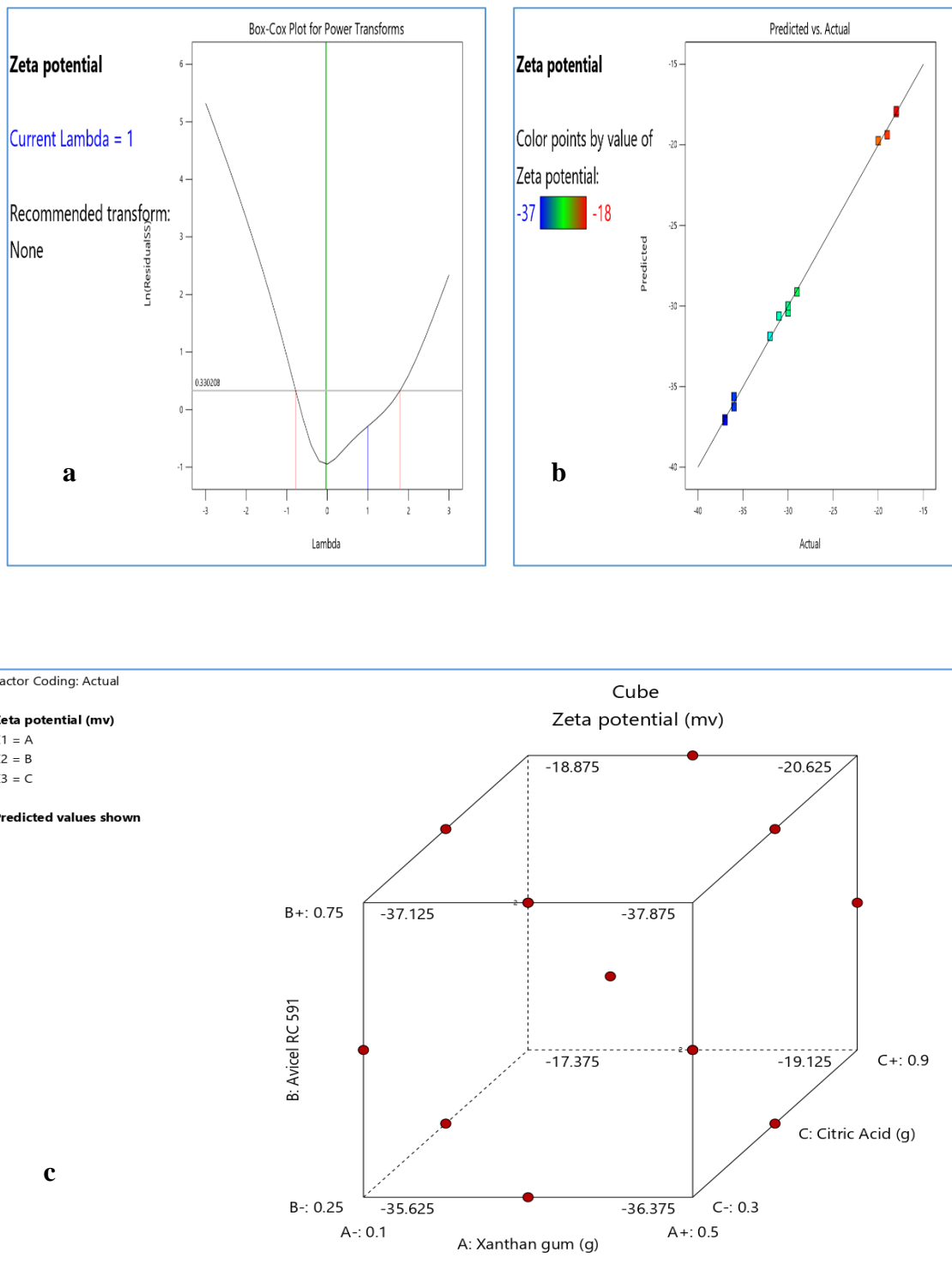


Figure 3.39: (a) Box-Cox plot; (b) Predicted vs Actual plot and; (c) Cubic plot for response 2 (Zeta potential) for optimization of suspension vehicle

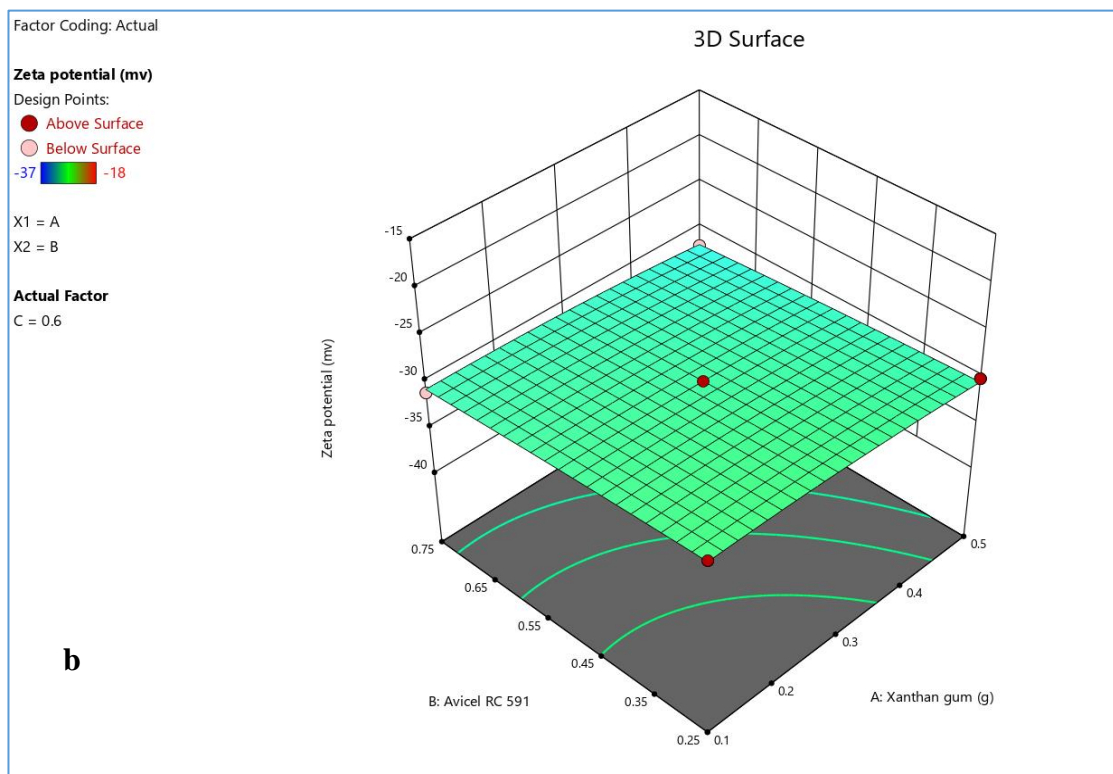
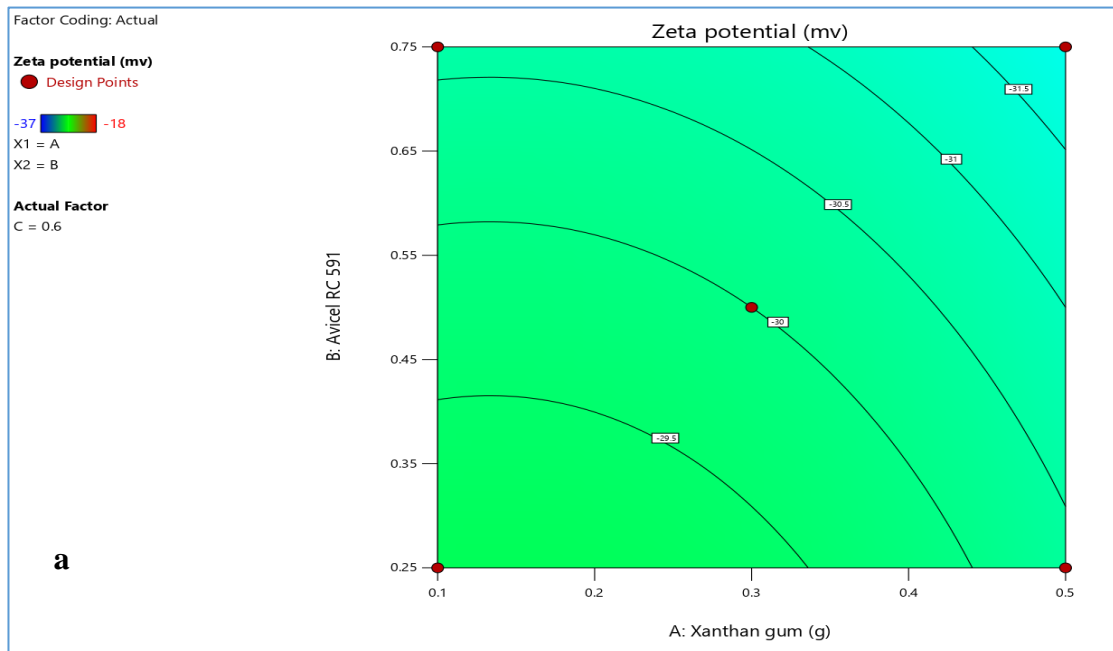


Figure 3.40: (a) Contour plot; (b) 3D response surface plot for response 2 (Zeta potential) for optimization of suspension vehicle

3.3.8.3 Optimization of design

Table 3.43: Optimization criteria for optimization of responses

Components	Criteria
Xanthan gum	In range
Avicel RC 591	In range
Citric Acid	In range
Viscosity	Maximize
Zeta potential	Minimize

Table 3.44: Constraints for optimization of design

Name	Goal	Lower Limit	Upper Limit	Lower Weight	Upper Weight	Importance
A:Xanthan gum	is in range	0.1	0.5	1	1	3
B:Avicel RC 591	is in range	0.25	0.75	1	1	3
C:Citric Acid	is in range	0.3	0.9	1	1	3
Viscosity	Maximize	792	1226	1	1	3
Zeta potential	Minimize	-37	-18	1	1	3

Solutions: Among 54 solutions found from the software, the one with maximum desirability was selected as the optimized solution.

Number	Xanthan gum	Avicel RC 591	Citric Acid	Viscosity	Zeta potential	Desirability
1	0.500	0.750	0.366	1203.201	-37.000	0.973

Final formulation for the suspension vehicle:

The following formulation was selected for using as final formulation for the suspension vehicle. The nanosuspension were incorporated in the following suspension vehicle for stabilization of formulations-

Table 3.45: Final formulation for the suspension vehicle for stabilization of prepared nanosuspension

Excipients	%w/w
Sucrose	40.000
Xanthan Gum	0.500
Sorbitol Solution 70%	5.000
Avicel RC 591	0.750
Glycerin	5.000
Citric Acid Monohydrate	0.366
Sodium Citrate*	0.477
MC and CMC Sodium (Avicel RC [®] 591)	0.6500
Colloidal Silicon Dioxide (Aerosil [®] 200)	0.4000
Methylparaben	0.180
Propylparaben	0.020
Sucralose	0.1000
Mango Flavor (liquid)	0.1000
Purified Water	q.s to 100 ml

*Sodium Citrate was calculated to prepare citrate buffer in order to achieve pH 4.5 (AAT Bioquest, 2020).

3.3.8.4 Manufacturing process of suspension vehicle

Purified water, methylparaben, propylparaben and Sucrose were taken in a S.S vessel and heated 85°C-90°C with continuous stirring to dissolve clearly. Sorbitol solution 70% was added then under continuous stirring and cooled down to room temperature. Later, xanthan gum was dispersed in glycerin and added under continuous stirring. avicel® RC 591 and aerosil® 200 were dispersed in purified water and added to above mixture under continuous stirring. After that, Citric acid monohydrate, sodium citrate and sucralose were dissolved clearly in purified water and added under continuous stirring. The final volume was adjusted with purified water and stirred for 15 minutes. The pH of final preparation was found 4.5.

3.3.8.5 Preparation of stabilized suspensions

3.3.8.5.1 Preparation of stabilized suspensions of Ledipasvir

NSF1a and NsF2a nanosuspensions were selected for the stabilization experiment as they produced best results in terms of PSD and PDI. NSF1a and NsF2a nanosuspensions of Ledipasvir were added with the above suspension vehicle in the following manner and mixed for 30 minutes to mix uniformly –

Table 3.46: Composition of stabilized suspensions of Ledipasvir

Formulation Code	Composition	Ratio (ml) in 100 ml	Label claim
FNSF1a	NSF1a nanosuspension + suspension vehicle	25.71 + 74.29	Each 5ml suspension contains 90mg Ledipasvir
FNSF2a	NSF2a nanosuspension + suspension vehicle	25.71 + 74.29	

3.3.8.5.2 Preparation of stabilized suspensions of Ledipasvir:

Table 3.47: Composition of stabilized suspensions of Velpatasvir

Formulation Code	Composition	Ratio (ml) in 100 ml	Label claim
VFNSF1a	NSF1a nanosuspension + suspension vehicle	28.57 + 71.43	Each 5ml suspension contains 100mg Velpatasvir

3.3.8.6 Evaluation of stabilized suspension:

3.3.8.6.1 Determination of Zeta potential of the suspension vehicle

When zeta potential value of the suspension vehicle becomes more than -30, it indicates physical stability of the vehicle. Zeta potential of the stabilized suspensions was measured and mentioned below:

Table 3.48: Zeta Potential of the suspension vehicle

Formulation	Zeta potential (mv)			
	Run 1	Run 2	Run 3	Average
Suspension Vehicle	-36.6	-36.7	-36.4	36.6

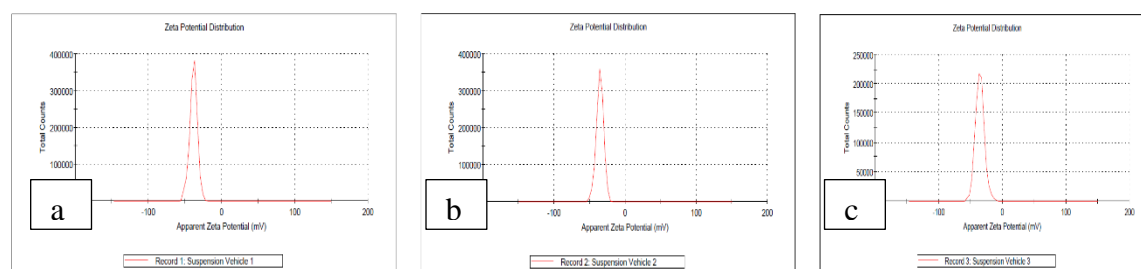


Figure 3.41: Zeta potential distribution of the optimized suspension vehicle a) run 1 b) run 2 c) run 3

3.3.8.6.2 Particle size distribution (PSD) of the suspension vehicle

Table 3.49: PSD of the suspension vehicle

Formulation	PSD (nm)			
	Run 1	Run 2	Run 3	Average
Suspension Vehicle	6678	6322	6145	6381.66

Above table indicates that the particle size of the suspension vehicle is more than 1 micron and this was due to gelling of components used in developing the formulation for suspension vehicle.

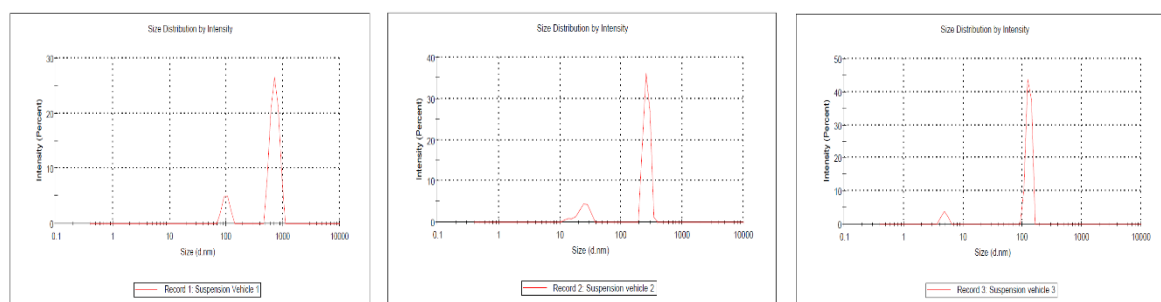


Figure 3.42: PSD of the optimized suspension vehicle a) run 1 b) run 2 c) run 3

3.3.8.6.3 Zeta Potential of the stabilized suspensions

3.2.8.6.3.1 Zeta potential for stabilized suspensions of Ledipasvir

Table 3.50: Zeta potential of the stabilized Ledipasvir suspensions

Formulation	Zeta potential (mv)			
	Run 1	Run 2	Run 3	Average
FNSF1a	-34.3	-34.2	-33.8	-34.1
FNSF2a	-33.9	-34.1	-33.5	-33.8

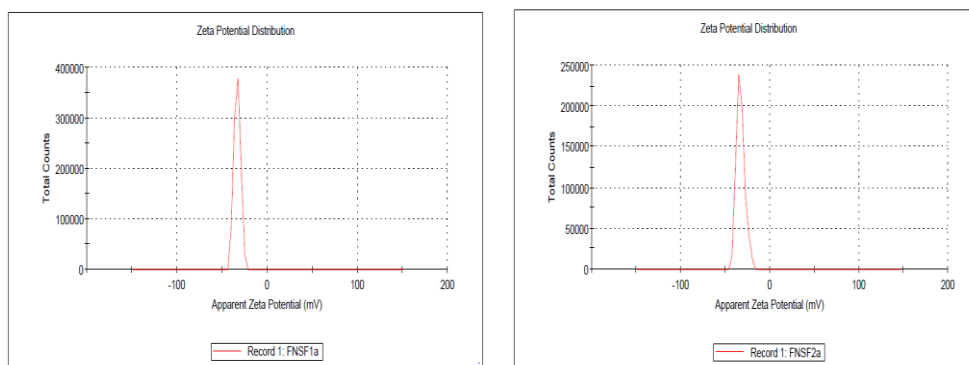


Figure 3.43: Zeta potential of the stabilized suspensions a) FNSF1a b) FNSF2a

From the above data it can be said that the zeta potential of all formulated suspensions of Ledipasvir were more than or equal to -30 which denoted that the suspension had become stable after adding to suspension vehicle (Jacobs and Müller, 2002).

3.2.8.6.3.2 Zeta potential for stabilized suspensions of Velpatasvir

Table 3.51: Zeta potential of the stabilized Velpatasvir suspension

Formulation	Zeta potential (mv)			
	Run 1	Run 2	Run 3	Average
VFNSF1a	-35.1	-36.0	-36.4	-35.8

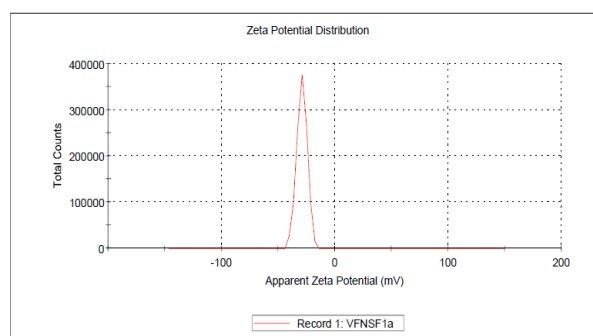


Figure 3.44: Zeta potential of the stabilized suspension VFNSF1a

From the above data it can be said that the zeta potential of Velpatasvir suspension was more than -30 which indicated that the suspension had become stable after adding to suspension vehicle (Jacobs and Müller, 2002).

3.2.8.6.4 Sedimentation volume of stabilized suspension

The sedimentation volumes (F) of the formulated Ledipasvir suspensions FNSF1a and FNSF2a at different time points (day 0, 30, 60, 90, 120, 150 and 180) are presented below (Table 3.52, Figures 3.45 and 3.46):

Table 3.52: Sedimentation volumes of FNSF1a and FNSF2a at different time points

Formulation	Volume (ml)							Sedimentation volume (F)					
	Initial (Day 0)	Day 30	Day 60	Day 90	Day 120	Day 150	Day 180	Day 30	Day 60	Day 90	Day 120	Day 150	Day 180
FNSF1a	6.30	6.10	6.00	5.60	5.50	5.20	5.20	1.00	0.97	0.95	0.89	0.87	0.83
FNSF2a	6.20	6.00	5.90	5.60	5.40	5.20	5.20	1.00	0.97	0.95	0.90	0.87	0.84

From the above table 3.52, it can be observed that both formulations have F value near to 1 after 6 months of study which indicates that these are flocculated suspensions with excellent physical stability.

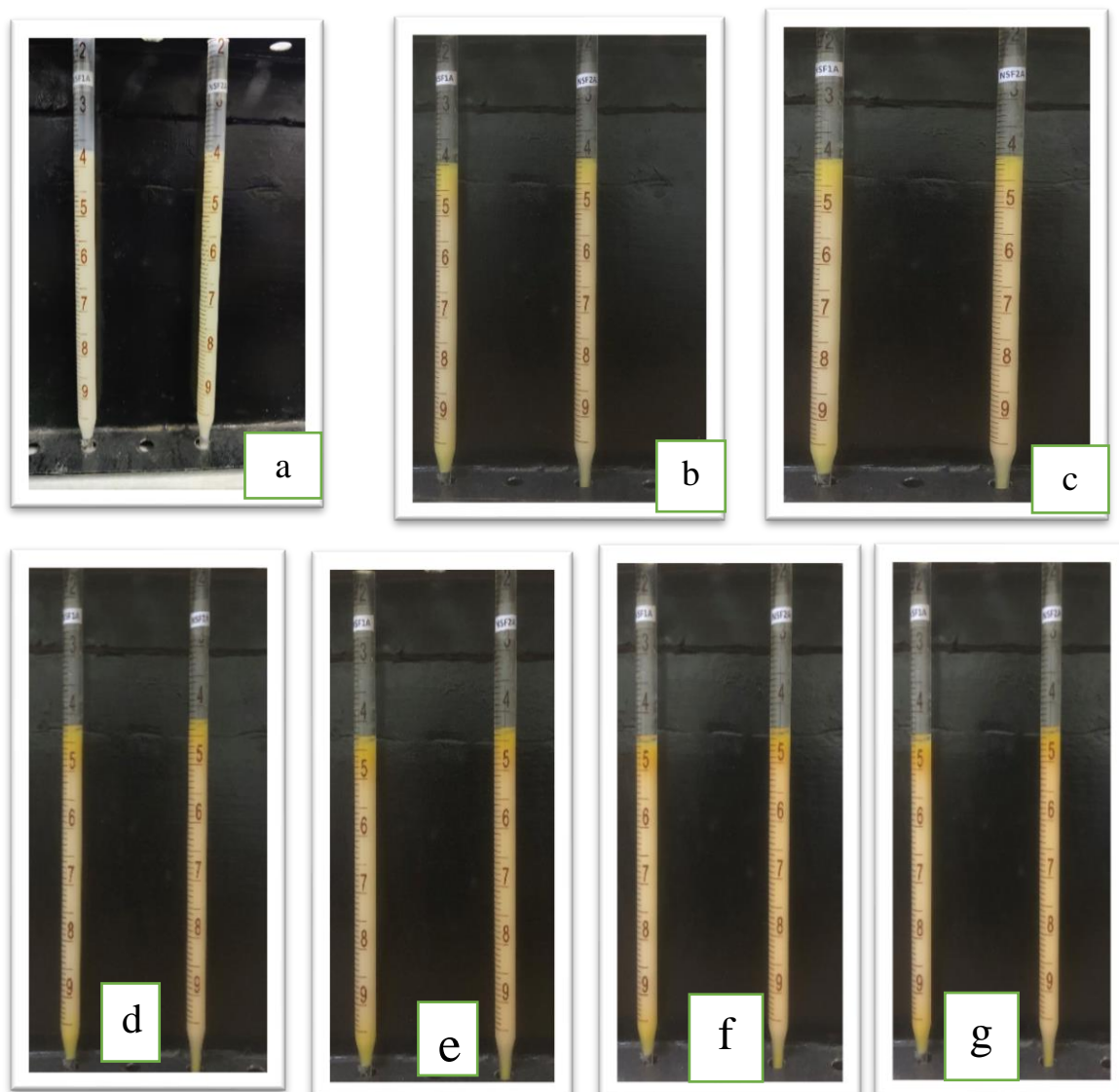


Figure 3.45: Sedimentation volume FNSF1a and FNSF2a at a) day 0 b) at day 30 c) day 60 d) day 90 e) day 120 f) day 150 and g) day 180

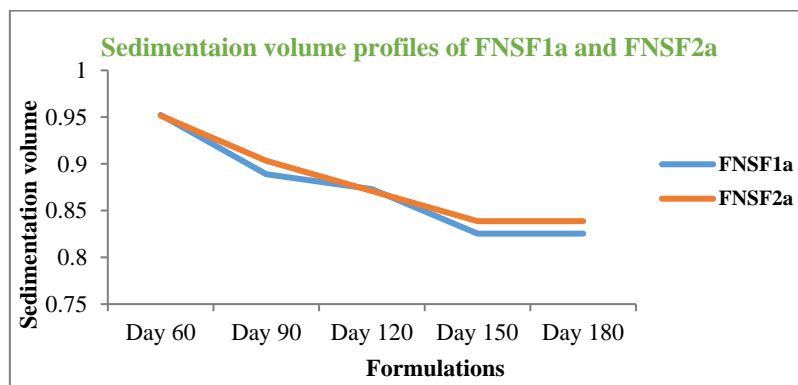


Figure 3.46: Sedimentation volume profiles of FNSF1a and FNSF2a suspensions at day 0, 30, 60, 90, 120, 150 and 180

From the above results of sedimentation volume, it was found that formulated suspensions of Ledipasvir FNSF1a and FNSF2a have F values of 0.83 and 0.84 respectively. This indicates that the prepared suspensions are stable, flocculated, the chance of cake formation is less and should be easily redispersible. Therefore, it can be said that dose uniformity can be ensured (Mahato and Narang, 2011).

3.3.8.7 Assay of the stabilized suspensions

3.3.8.7.1 Assay for Ledipasvir stabilized suspensions

Table 3. 53: Assay of Ledipasvir in the stabilized suspensions

Stabilized suspensions	Assay of Ledipasvir (% of label claim)				Standard Deviation	%RSD
	Sample 1	Sample 2	Sample 3	Average		
FNSF1(a)	99.4	98.9	99.5	99.3	0.30	0.30
FNSF2(a)	98.5	99.8	99.1	99.1	0.64	0.65

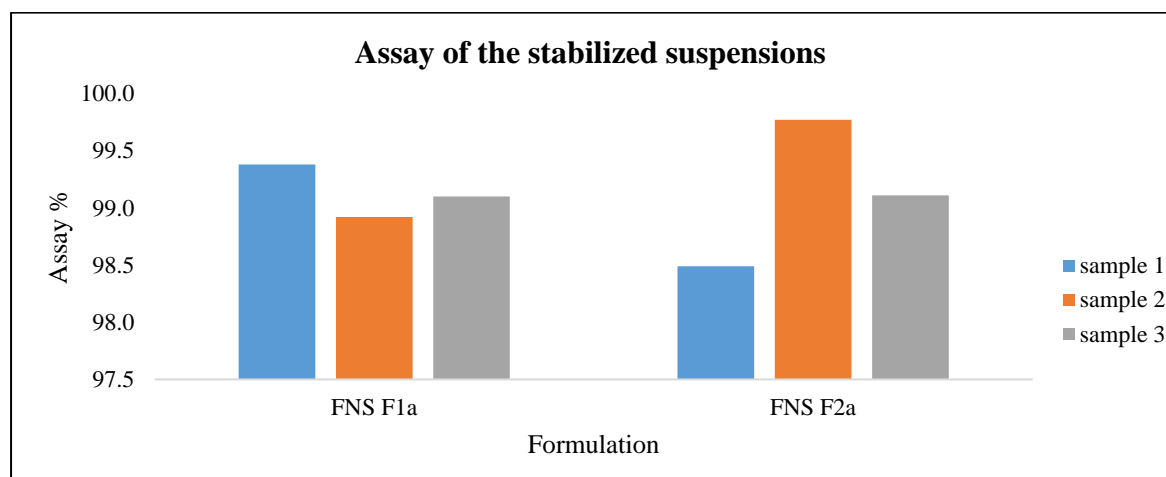


Figure 3.47: Assay of Ledipasvir in the stabilized suspensions

In all cases, content of Ledipasvir was within 98.5% to 99.5% whereas the %RSD values were less than 1 indicating good uniformity of the formulation.

3.3.8.7.2 Assay for Velpatasvir stabilized suspensions

Table 3.54: Assay of Velpatasvir in the stabilized suspension

Stabilized suspension	Assay of Velpatasvir (% of label claim)				Standard Deviation	%RSD
	Sample 1	Sample 2	Sample 3	Average		
VFNSF1(a)	100.4	100.5	99.9	100.3	0.29	0.29

In all cases, content of Velpatasvir was within 99.9% to 100.5% whereas the %RSD values were less than 1 indicating good uniformity of the formulation.

3.3.8.8 Dissolution profiles of the stabilized suspensions

3.3.8.8.1 Dissolution profiles for Ledipasvir stabilized suspensions

Dissolution profiles of the stabilized suspensions FNSF1a and FNSF2a were checked. Label claim for both cases were 'each 5 ml suspension contains 90mg Ledipasvir.

Table 3.55: Dissolution profiles of the stabilized suspension, FNSF1a (Individual samples)

Time Points	% Drug release											
	Sample 1	Sample 2	Sample 3	Sample 4	Sample 5	Sample 6	Sample 7	Sample 8	Sample 9	Sample 10	Sample 11	Sample 12
0	0	0	0	0	0	0	0	0	0	0	0	0
5	80.57	82.48	81.62	83.59	84.82	80.93	79.62	79.59	80.77	81.08	82.85	83.53
10	96.54	95.81	96.28	97.85	99.69	98.75	97.08	96.56	98.15	99.35	98.31	95.83
15	100.35	99.68	97.82	100.2	98.63	98.57	98.32	97.26	99.27	101.07	100.25	98.18
20	99.24	98.59	100.32	101.52	98.05	100.89	100.33	98.58	99.03	98.52	97.87	100.32
30	99.96	98.8	100.65	100.36	101.72	100.88	99.35	100.76	101.6	98.88	99.67	99.75
45	100.83	100.59	99.65	101.46	101.49	100.59	99.37	100.16	98.73	97.94	100.13	98.17
60	99.86	101.73	102.42	100.39	101.92	101.69	99.57	99.59	100.91	101.33	100.17	101.37

Table 3.56: Dissolution profiles of the stabilized suspension, FNSF2a (Individual samples)

Time Points (min)	% Drug release											
	Sample 1	Sample 2	Sample 3	Sample 4	Sample 5	Sample 6	Sample 7	Sample 8	Sample 9	Sample 10	Sample 11	Sample 12
0	0	0	0	0	0	0	0	0	0	0	0	0
5	76.21	77.26	78.24	79.05	80.21	79.63	78.72	77.92	79.2	81.74	80.67	80.55
10	95.52	94.12	96.32	97.23	95.08	98.26	96.12	98.14	97.21	96.18	96.07	98.29
15	97.27	97.43	97.37	99.06	100.13	97.65	100.23	101.52	98.67	99.11	98.75	97.95
20	96.88	98.55	100.08	99.49	100.15	97.28	101.63	100.55	97.82	99.5	100.27	98.95
30	99.04	97.85	100.17	101.49	100.15	98.35	99.68	101.25	100.37	102.09	99.45	99.93
45	101.14	98.44	100.29	99.71	100.85	99.63	100.72	101.79	101.38	102.23	98.45	99.93
60	101.17	99.96	99.67	99.64	100.85	99.14	101.26	102.26	101.28	100.18	102.31	99.55

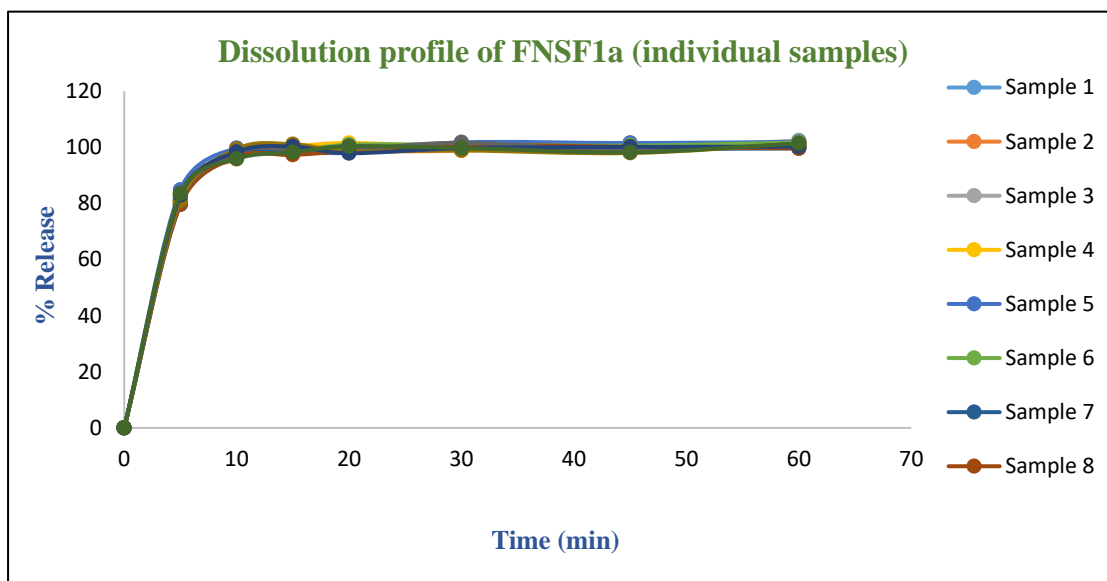


Figure 3.48: Dissolution profiles of the stabilized suspension, FNSF1a (Individual samples)

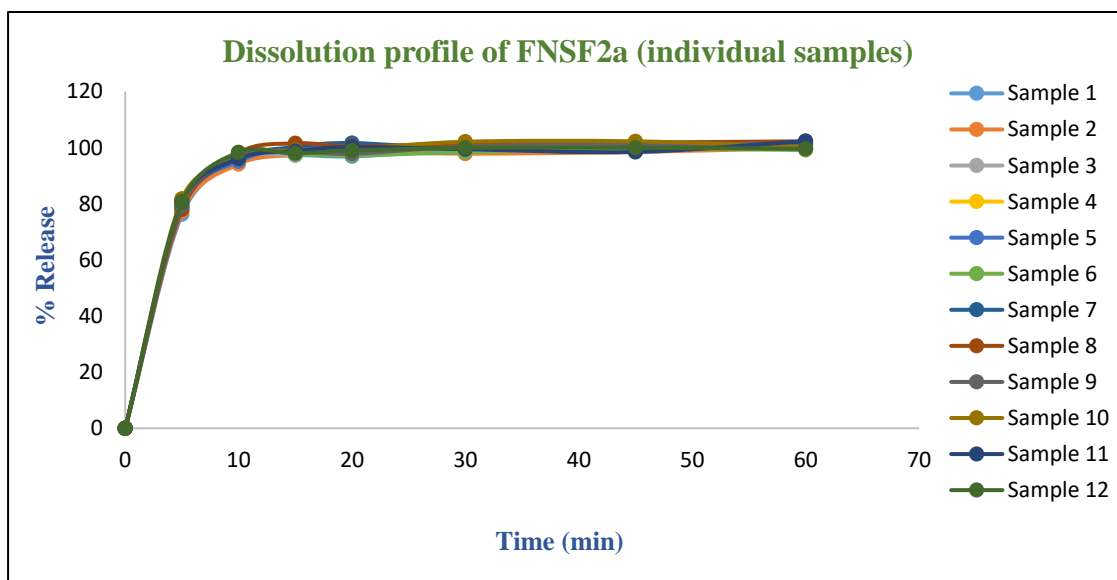


Figure 3.49: Dissolution profiles of the stabilized suspension, FNSF2a (Individual samples)

Table 3.57: Dissolution profiles of the stabilized suspension, FNSF1a and FNSF2a (average)

Time Points (min)	% Drug release (average)	
	FNSF1a	FNSF2a
0	0	0
5	81.79	79.12
10	97.52	96.55
15	99.21	98.76
20	99.44	99.26
30	100.20	99.99
45	99.93	100.38
60	100.91	100.61

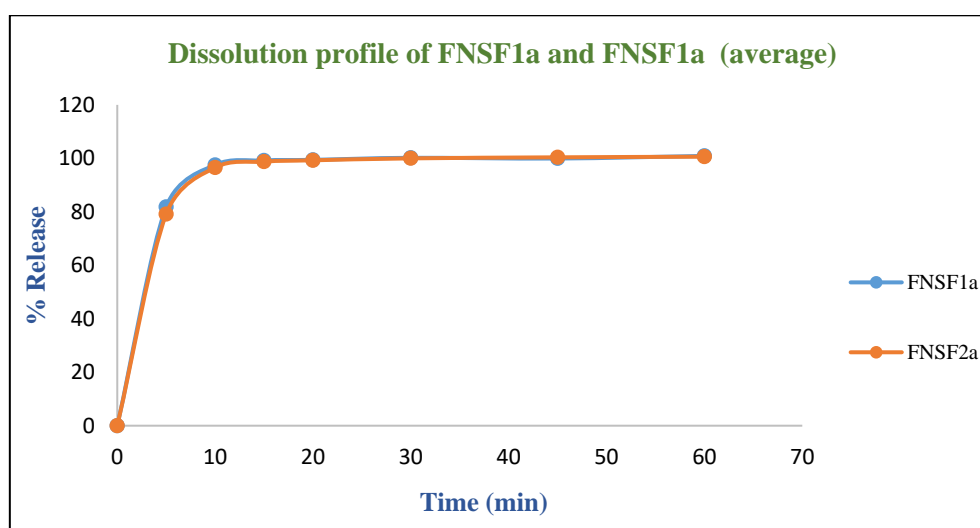


Figure 3.50: Dissolution profiles of the stabilized suspension, FNSF1a and FNSF2a (average)

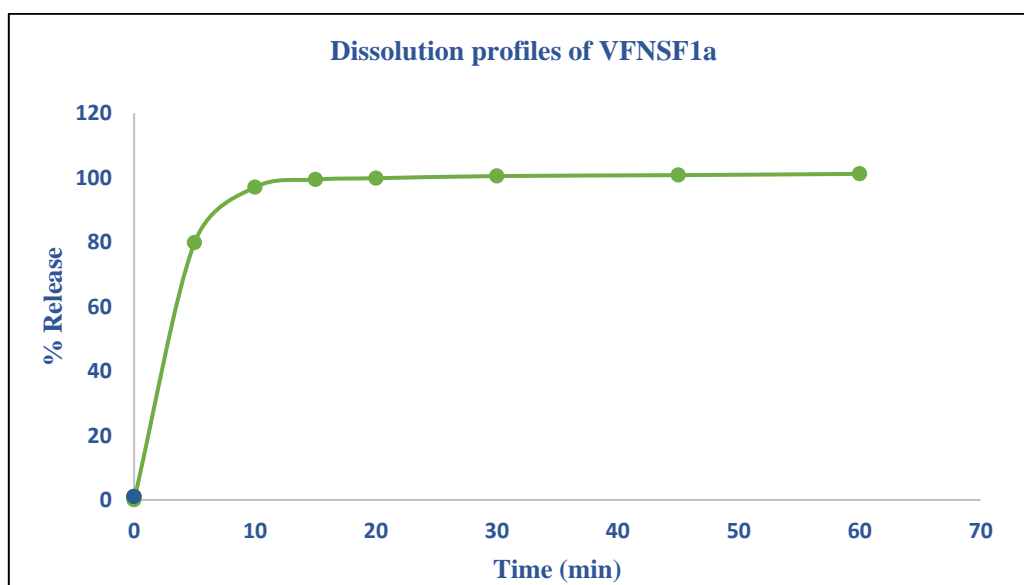
From the above results, it can be said that the stabilized suspensions of Ledipasvir had very fast dissolution where almost complete release of the drug was achieved within 10 minutes for all the formulations. This is achieved due to significant reduction in particle size and hence, increase in surface area.

3.3.8.8.2 Dissolution profiles for Velpatasvir stabilized suspension

Dissolution profiles of the nanosuspensions of Velpatasvir, VFNSF1a were checked. Label claim for both cases were 'each 5 ml suspension contains 100mg Velpatasvir.

Table 3.58: Dissolution profiles of the stabilized suspension, VFNSF1a

Time Points (min)	% Drug release (average)
	VFNSF1a
0	0.00
5	79.80
10	97.00
15	99.37
20	99.79
30	100.46
45	100.75
60	101.14

**Figure 3.51:** Dissolution profiles of the stabilized suspension, VFNSF1a

From the above results, it can be said that the stabilized suspension of Velpatasvir had very fast dissolution where almost complete release of the drug was achieved within 10 minutes. This is achieved due to significant reduction in particle size and hence, increase in surface area.

3.3.9 Comparative dissolution profiles and kinetics study

3.3.9.1 Comparative dissolution profiles

3.3.9.1.1 Comparative dissolution profiles of Ledipasvir

Dissolution profiles for market product 1 (origin – Ireland) and 2 (origin – Bangladesh), pure API, suspensions with micronized API and non-micronized API, formulated suspensions FNSF1a and FNSF2a were compared to find the dissolution characteristics of these preparations (Table 3.59).

Table 3.59: Dissolution profiles of different preparations of Ledipasvir

Time (min)	% Release						
	Market product 1	Market product 2	Pure API	Suspension with non-micronized API	Suspension with micronized API	FNS-F1a	FNS-F2a
0	0.00	0.00	0.00	0.00	0.00	0.00	0.00
5	36.11	22.47	3.19	8.27	13.72	81.79	79.12
10	69.23	30.94	10.3	14.54	20.4	97.52	96.55
15	80.09	43.05	14.79	21.77	28.05	99.21	98.76
20	92.35	57.72	17.22	31.92	37.66	99.44	99.26
30	99.83	74.97	20.11	41.63	48.01	100.20	99.99
45	100.07	81.31	26.46	44.21	50.48	99.93	100.38
60	100.00	83.72	27.85	45.13	50.91	100.91	100.61

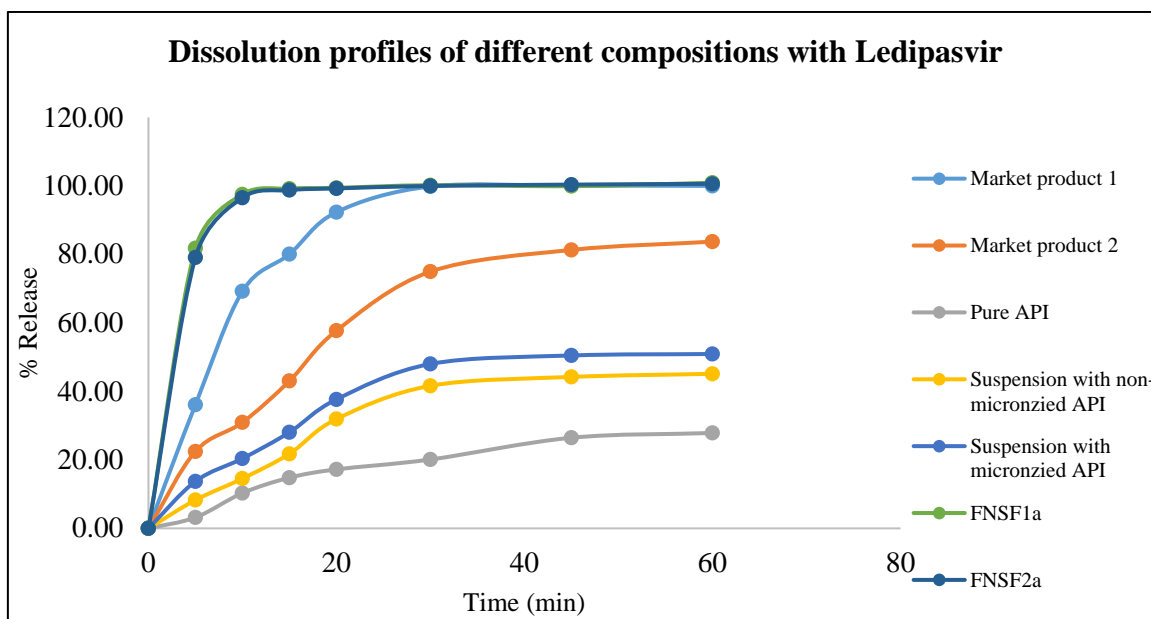


Figure 3.52: Dissolution profiles of different preparations of Ledipasvir

Table 3.60: Dissolution profile comparison with similarity factor (f_2), difference factor (f_1) and dissolution efficiency (%DE)

Products	Difference factor (f_1)	Similarity factor (f_2)	Dissolution efficiency (%DE)
Market product 1	-	-	48.46
Market product 2	31.76	29.13	24.98
Pure API	79.24	10.13	6.96
Suspension with non-micronized API	64.09	14.87	11.23
Suspension with micronized API	56.86	17.38	16.05
FNS F1a	17.59	34.58	76.30
FNS F2a	16.79	35.65	75.01

From the above table it can be said that the market product 2, suspension with micronized API and non-micronized API, formulated suspensions FNSF1a and FNSF2a had non-similar dissolution profiles than the market product 1, because the f_1 value was above 15, f_2 value was below 50 for all formulation when compared to the market product 1 and at the same time, the difference in %DE value was more than 10% different for all formulation compared with the market product 1. Formulated nanosuspensions FNSF1a and FNSF2a had significantly faster dissolution rate whereas market product 2, suspension with micronized API and non-micronized API had substantially slower dissolution rate compared to the market product 1.

3.3.9.1.1 Comparative dissolution profiles of Velpatasvir

Dissolution profiles for market product 3 (origin – Bangladesh) and VNSF1a were to find the dissolution characteristics of these preparations (Table 3.61).

Table 3.61: Dissolution profiles of different preparations of Velpatasvir

Time (min)	% Release	
	Market product 3 (MP3)	VFNSF1a
0	0.00	0.00
5	17.53	79.80
10	25.90	97.00
15	26.98	99.37
20	27.79	99.79
30	33.73	100.46
45	44.19	100.75
60	51.72	101.14

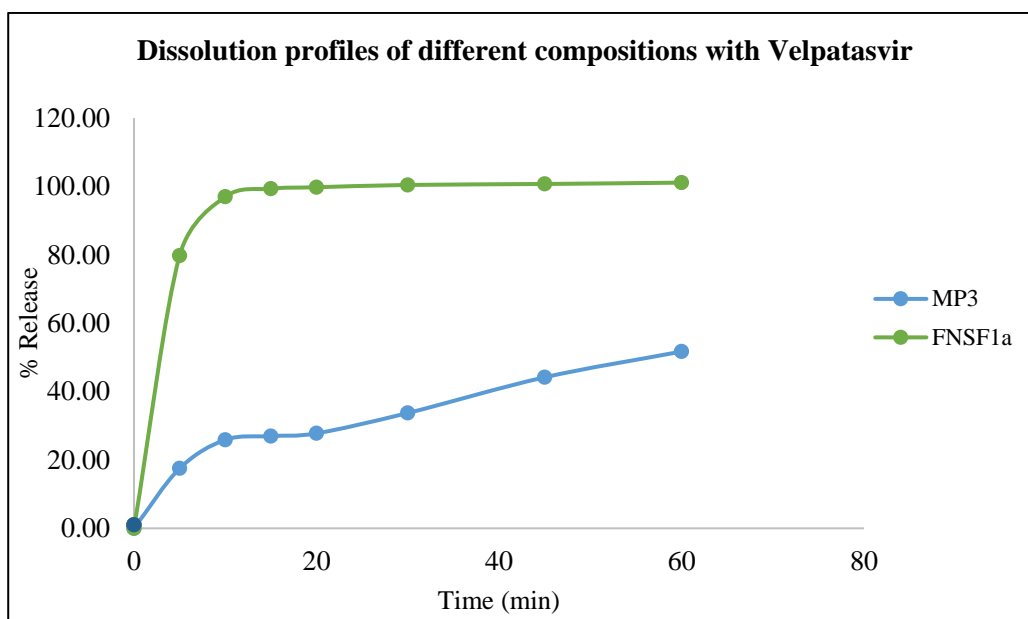


Figure 3.53: Dissolution profiles of different preparations of Velpatasvir

Table 3.62: Dissolution profile comparison with similarity factor (f_2), difference factor (f_1) and dissolution efficiency (%DE)

Products	Difference factor (f_1)	Similarity factor (f_2)	Dissolution efficiency (%DE)
Market product 3 (MP3)	-	-	18.97
VFNS F1a	66.41	10.85	75.50

From the above table it can be said that none of the market product 3 and formulated suspension VFNSF1a had non-similar dissolution profiles, because the f_1 value is above 15, f_2 value is below 50 for the formulated suspension when compared to the market product 3 and at the same time, the difference in %DE value is more than 10% between VFNSF1a and the market product 2. Formulated nanosuspension VFNSF1a had significantly faster dissolution rate whereas market product 3 had substantially slower dissolution rate.

3.3.9.2 Study of drug release kinetics

3.3.9.2.1 Release kinetics for Ledipasvir

Drug release kinetics were evaluated and described below for the market product 1 and 2, formulated suspensions of Ledipasvir, FNSF1a and FNSF2a.

Zero order plot:

Table 3.63: Data for zero order plot

Time (Hr)	Cumulative % drug released			
	MP 1	MP 2	FNSF1a	FNSF2a
0	0	0	0	0
0.08	36.11	22.47	81.79	79.12
0.16	69.23	30.94	97.52	96.55
0.25	80.09	43.05	99.21	98.76
0.33	92.35	57.72	99.44	99.26
0.5	99.83	74.97	100.2	99.99
0.75	100.07	81.31	99.93	100.38
1	100	83.72	100.91	100.61

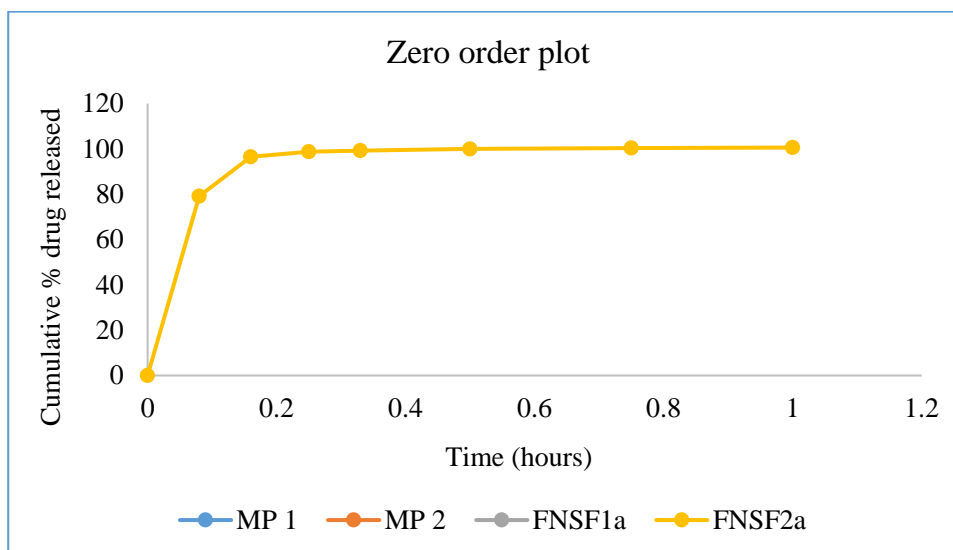
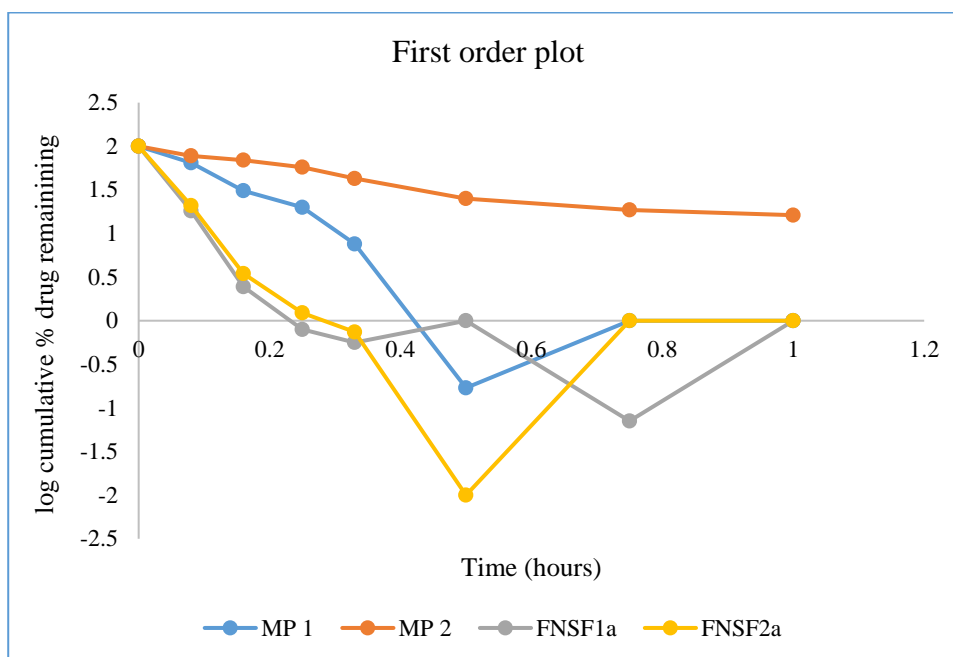


Figure 3.54: Zero order plot of market product 1 and 2 and formulated suspensions, FNSF1a and FNSF2a

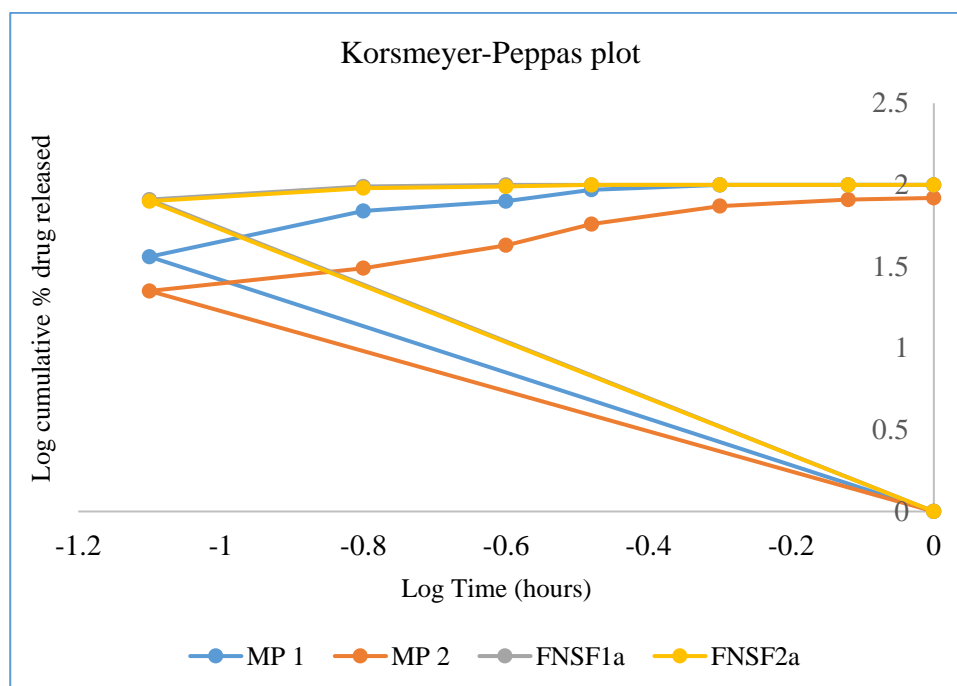
First Order Plot:**Table 3.64:** Data for first order plot

Time (Hrs)	Log cumulative % drug remaining			
	MP 1	MP 2	FNSF1a	FNSF2a
0	2	2	2	2
0.08	1.81	1.89	1.26	1.32
0.16	1.49	1.84	0.39	0.54
0.25	1.30	1.76	-0.10	0.09
0.33	0.88	1.63	-0.25	-0.13
0.5	-0.77	1.40	-	-2
0.75	-	1.27	-1.15	-
1	-	1.21	-	-

**Figure 3.55:** First order plot of market product 1 and 2 and formulated suspensions, FNSF1a and FNSF2a

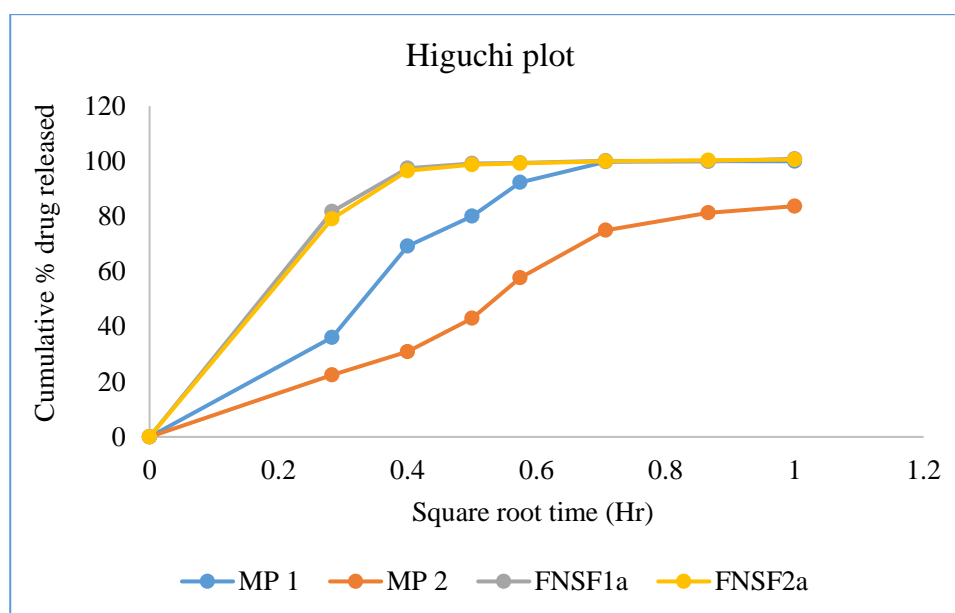
Korsmeyer-Peppas Plot:**Table 3.65:** Data for Korsmeyer-Peppas plot

log time (Hr)	Log cumulative % drug released			
	MP 1	MP 2	FNSF1a	FNSF2a
0.00	0.00	0.00	0.00	0.00
-1.10	1.56	1.35	1.91	1.90
-0.80	1.84	1.49	1.99	1.98
-0.60	1.90	1.63	2.00	1.99
-0.48	1.97	1.76	2.00	2.00
-0.30	2.00	1.87	2.00	2.00
-0.12	2.00	1.91	2.00	2.00
0.00	2.00	1.92	2.00	2.00

**Figure 3.56:** Korsmeyer-Peppas plot of market product 1 and 2 and formulated suspensions, FNSF1a and FNSF2a

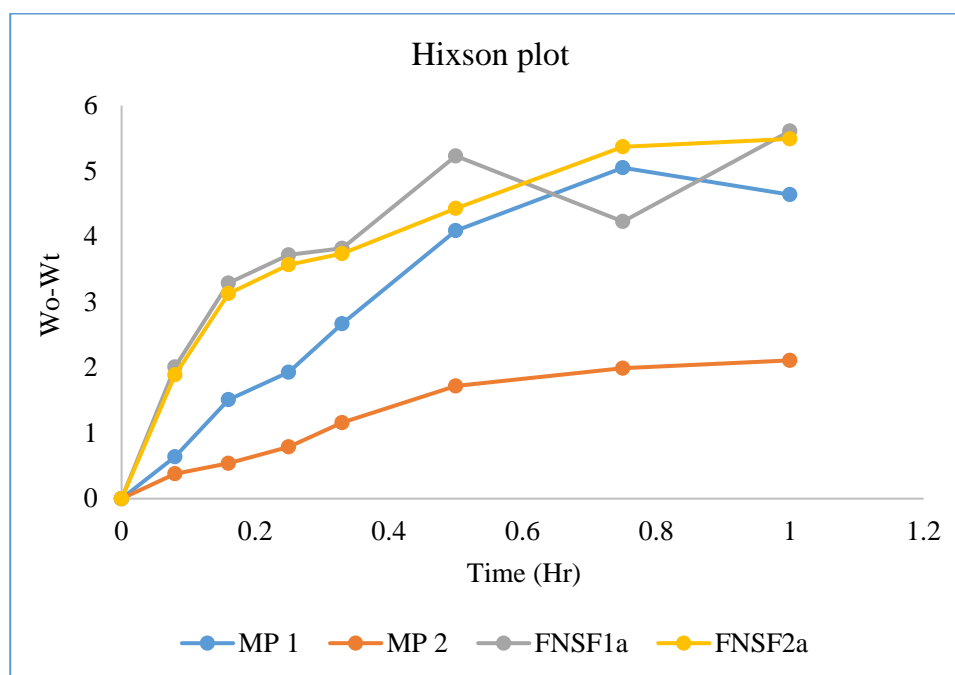
Higuchi Plot:**Table 3.66:** Data for Higuchi plot

Square root time (Hr)	Cumulative % drug released			
	MP 1	MP 2	FNSF1a	FNSF2a
0	0	0	0	0
0.282843	36.11	22.47	81.79	79.12
0.4	69.23	30.94	97.52	96.55
0.5	80.09	43.05	99.21	98.76
0.574456	92.35	57.72	99.44	99.26
0.707107	99.83	74.97	100.2	99.99
0.866025	100.07	81.31	99.93	100.38
1	100	83.72	100.91	100.61

**Figure 3.57:** Higuchi plot of market product 1 and 2 and formulated suspensions, FNSF1a and FNSF2a

Hixson Plot:**Table 3.67:** Data for Hixson plot

Time (Hr)	Wo-Wt			
	MP 1	MP 2	FNSF1 a	FNSF2 a
0	0	0	0	0
0.08	0.64	0.38	2.01	1.89
0.16	1.51	0.54	3.29	3.13
0.25	1.93	0.79	3.72	3.57
0.33	2.67	1.16	3.82	3.74
0.5	4.09	1.72	5.23	4.43
0.75	5.05	1.99	4.23	5.37
1	4.64	2.11	5.61	5.49

**Figure 3.58:** Hixson plot of market product 1 and 2 and formulated suspensions, FNSF1a and FNSF2a **R^2 values:**

R^2 values obtained from several mathematical models are displayed below (Table 3.68). From the values it can be seen that market product 1 best followed Hixson plot whereas

market product 2 best followed Higuchi plot. On the other hand, both formulated suspensions FNSF1a and FNSF2a followed Hixson.

Table 3.68: R² values of different mathematical models obtained for studied preparations

Mathematical Model	MP1	MP2	FNSF1a	FNSF2a
Zero order plot	0.5887	0.8406	0.2860	0.3003
First order plot	0.6630	0.9444	0.4848	0.2885
Korsmeyer-Peppas plot	0.0619	0.0155	0.1623	0.1579
Higuchi plot	0.8451	0.9619	0.5756	0.5930
Hixson plot	0.8760	0.9165	0.6699	0.7825

3.3.9.2.2 Release kinetics for Velpatasvir

Drug release kinetics were evaluated and described below for the market product 3 and formulated suspensions of Velpatasvir, VNSF1a.

Zero order plot:

Table 3.69: Data for zero order plot

Time (Hr)	Cumulative % drug released	
	MP 3	VFNSF1a
0	0	0.00
0.08	17.53	79.8
0.16	25.9	97
0.25	26.98	99.37
0.33	27.79	99.79
0.5	33.73	100.46
0.75	44.19	100.75
1	51.72	101.14

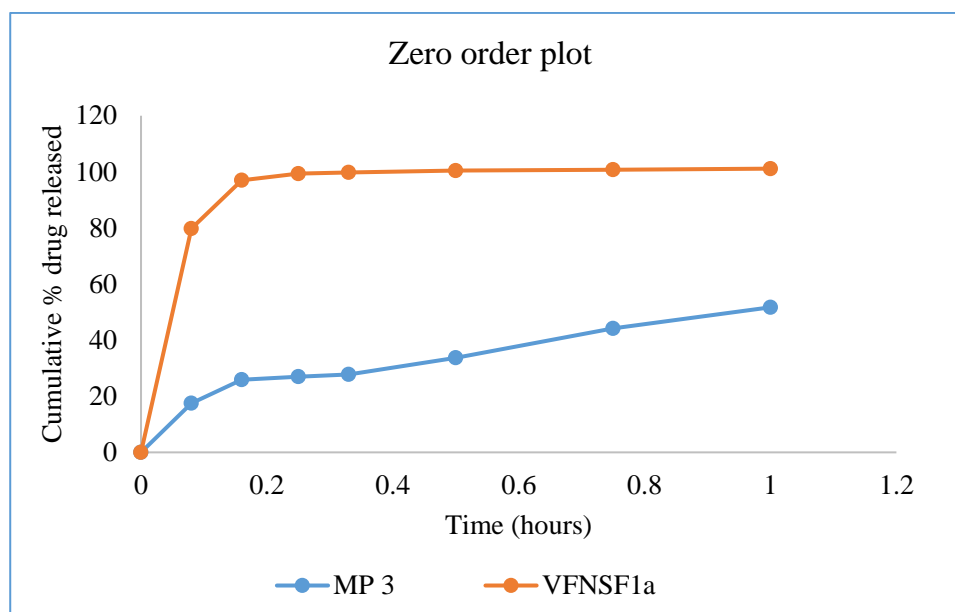


Figure 3.59: Zero order plot of market product 3 and formulated suspension, VNSF1a

First Order Plot:

Table 3.70: Data for first order plot

Time (Hrs)	Log cumulative % drug remaining	
	MP 3	VFNSF1a
0		
0.08	2	2
0.16	1.92	1.31
0.25	1.87	0.48
0.33	1.86	-0.20
0.5	1.86	-0.68
0.75	1.82	-
1	1.75	-

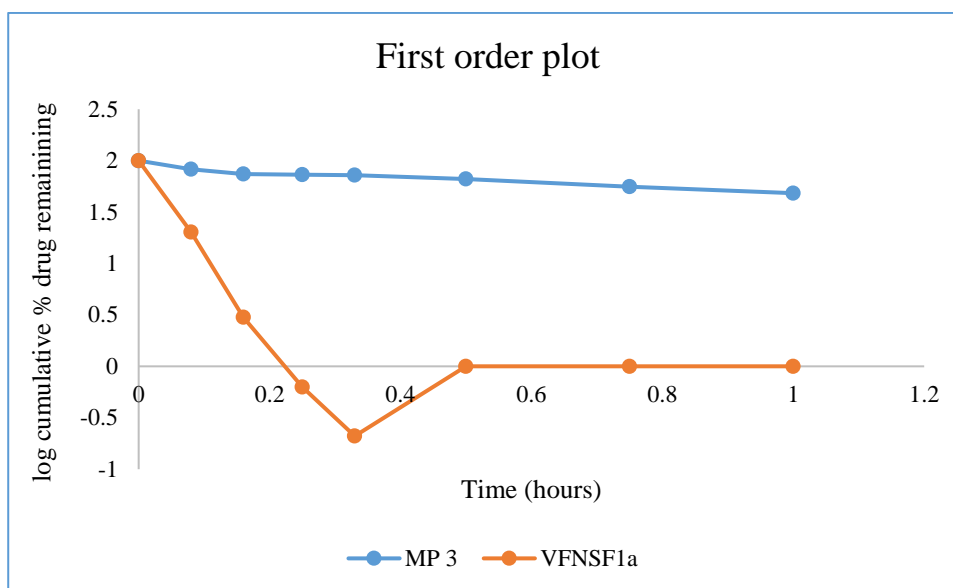


Figure 3.60: First order plot of market product 3 and formulated suspension, VNSF1a

Korsmeyer-Peppas Plot:

Table 3.71: Data for Korsmeyer-Peppas plot

Log time (Hr)	Log cumulative % drug released	
	MP 1	MP 2
0.00	0	0
-1.10	1.24	1.90
-0.80	1.41	1.99
-0.60	1.43	2.00
-0.48	1.44	2.00
-0.30	1.53	2.00
-0.12	1.65	2.00
0.00	1.71	2.00

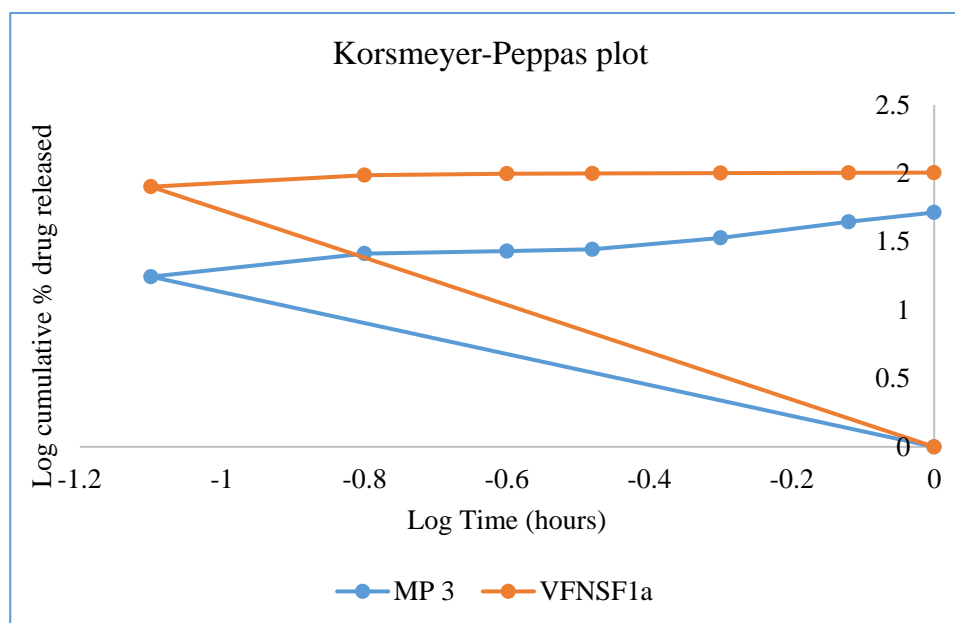


Figure 3.61: Korsmeyer-Peppas plot of market product 3 and formulated suspension VNSF1a

Higuchi Plot:

Table 3.72: Data for Higuchi plot

Square root time (Hr)	Cumulative % drug released	
	MP 3	VNSF1a
0	0	0.00
0.282843	17.53	79.8
0.4	25.9	97
0.5	26.98	99.37
0.574456	27.79	99.79
0.707107	33.73	100.46
0.866025	44.19	100.75
1	51.72	101.14

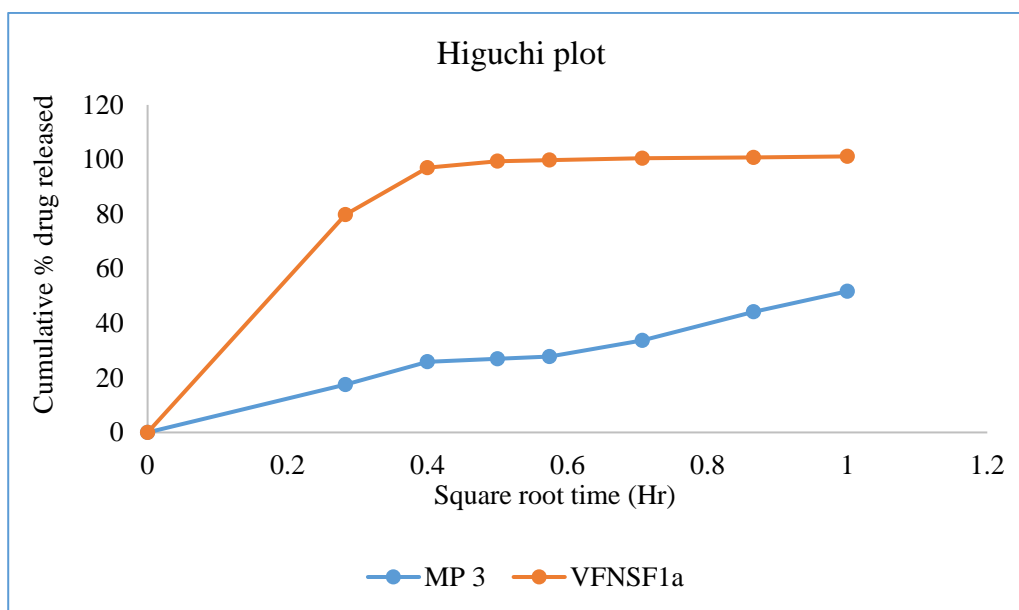


Figure 3.62: Higuchi plot of market product 3 and formulated suspension VFNSF1a

Hixson Plot:

Table 3.73: Data for Hixson plot

Time (Hr)	Wo-Wt	
	MP 3	VFNSF1a
0	0.00	0.00
0.08	0.29	1.92
0.16	0.44	3.20
0.25	0.46	3.78
0.33	0.48	4.05
0.5	0.60	5.41
0.75	0.82	5.55
1	1.00	5.69

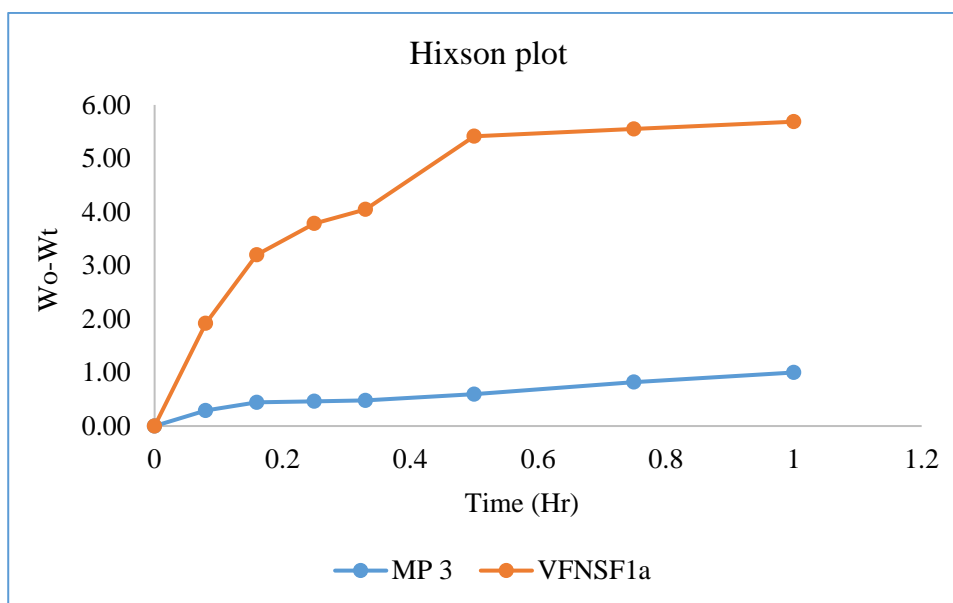


Figure 3.63: Hixson plot of market product 3 and formulated suspension, VNSF1a

R² values:

R^2 values obtained from several mathematical models are displayed below (Table 3.73). From the values it can be seen that market product 3 best Higuchi plot. On the other hand, formulated VFNSF1a followed Hixson plot (Baishya, 2017; “Mathematical Models of Drug Release,” 2015).

Table 3.74: R^2 values of different mathematical models obtained for studied preparations

Mathematical Model	MP3	VFNSF1a
Zero order plot	0.8696	0.2987
First order plot	0.9335	0.3237
Korsmeyer-Peppas plot	0.0337	0.1580
Higuchi plot	0.9772	0.5911
Hixson plot	0.9155	0.7441

3.3.10 *In-vivo* simulation study

3.3.10.1 *In-vivo* simulation study for Ledipasvir

The dissolution profile (cumulative % release, % release within sampling interval and amount of drug released with sampling interval) of 90 mg dose of the market product 1 (MP1) is presented in the table 3.75 and figure 3.64.

Table 3.75: Amount of Ledipasvir released from market product 1 (MP1) (90mg dose)

Time (hr)	%Released (Cumulative)	%Released (within sampling interval)	Amount (mg) released (within sampling interval)
0.00	0.00	-	-
0.08	36.11	36.11	32.50
0.17	69.23	33.12	29.81
0.25	80.09	10.86	9.77
0.33	92.35	12.26	11.03
0.50	99.83	7.48	6.73
0.75	100.07	0.24	0.22
1.00	100.00	-0.07	-0.06

Drug concentration after different time intervals were calculated for MP1 from the dissolution profile by convolution method and presented in the table below-

Table 3.76: Predicted blood conc. of Ledipasvir from *in-vitro* dissolution data from MP1 (90mg dose) MP1

Time after absorption (hr)	Blood Amount after Absorption							Total Blood Amt. (mg) after Absorption Conc	Conc. (ng/mL) at Times
0.00								0.00	0.00
0.08	32.50							32.50	108.69
0.17	32.42	29.81						62.23	208.12
0.25	32.38	29.70	9.77					71.85	240.31
0.33	32.34	29.66	9.73	11.03				82.76	276.79
0.50	32.26	29.59	9.70	10.95	6.73			89.24	298.46
0.75	32.14	29.48	9.67	10.91	6.66	0.22		89.08	297.92
1.00	32.02	29.37	9.63	10.87	6.64	0.21	-0.06	88.69	296.61
8	28.89	26.50	8.69	9.81	5.99	0.19	-0.06	80.01	267.61
9	28.47	26.11	8.56	9.66	5.90	0.19	-0.06	78.85	263.70
10	28.06	25.73	8.44	9.52	5.81	0.14	-0.05	77.65	259.71
12	27.24	24.99	8.19	9.25	5.65	0.18	-0.05	75.45	252.33
24	22.84	20.95	6.87	7.75	4.73	0.15	-0.04	63.24	211.52
36	19.14	17.56	5.76	6.50	3.97	0.13	-0.04	53.02	177.31
48	16.05	14.72	4.83	5.45	3.33	0.11	-0.03	44.44	148.64

From the above table 3.76, the drug concentration data at different time points were used to determine the pharmacokinetic (PK) parameters, peak plasma concentration (C_{max}) and area under the curve (AUC) with the help of PKSolver[®]. The calculated (predicted) pharmacokinetic parameters are given below along with the %PE (Predicted Error).

Table 3.77: Predicted PK parameters for MP1 along with %PE

PK parameters	Predicted values	Observed values from literatures	%PE
C_{\max} (ng/ml)	300.37	323.26	7.08
$AUC_{(0 \text{ to } t)}$ (ng.h/ml)	10336.10	10628.88	2.75

From the above table 3.77, it can be observed that the %PE values for both C_{\max} and $AUC_{(0 \text{ to } t)}$ are below 10 which establishes the predictability of the convolution model and this approach to PK parameters simulation can be considered valid.

At next, the *in-vivo* simulation of the formulated suspensions of FNSF1a, FNSF2a were done with a dose of 90mg. Drug concentration after different time intervals were calculated for FNSF1a and FNSF2a from the dissolution profiles by convolution method and presented in the table below-

Table 3.78: Drug conc. calculated from dissolution profiles for FNSF1a and FNSF2a for a dose of 90mg

Time after absorption (hr)	Conc. (ng/mL)	
	FNSF1a	FNSF2a
0.00	0.0000	0.0000
0.08	246.1906	238.1538
0.17	292.936	290.036
0.25	297.5486	296.2048
0.33	297.858	297.3229
0.50	299.4134	298.7853
0.75	297.4857	298.8472
1.00	299.3532	298.4304
8	270.0427	269.2399
9	266.1021	265.311
10	262.6013	260.9016
12	254.622	253.8651
24	213.4452	212.8107
36	178.9274	178.3955
48	149.9917	149.5458

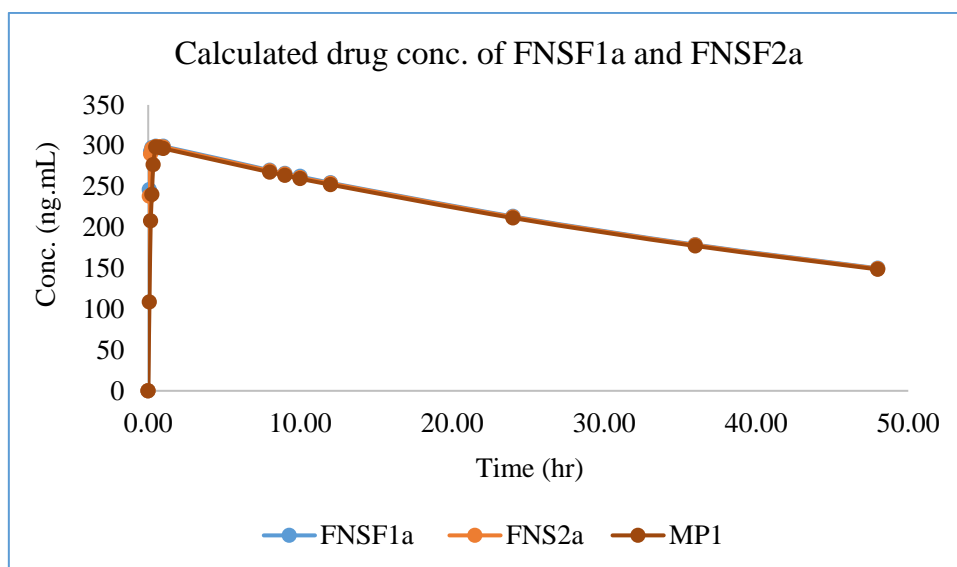


Figure 3.64: Drug conc. calculated from dissolution profiles for MP1, FNSF1a and FNSF2a for a dose of 90mg

From the above table 3.78, the drug concentration data at different time points were used to determine the pharmacokinetic (PK) parameters, peak plasma concentration (C_{max}) and area under the curve (AUC) with the help of PKSolver[®] and the following pharmacokinetic (PK) parameters were obtained (table 3.79). The PK results of FNSF1a and FNSF2a were compared with those of MP1 by paired t-test.

Table 3.79: Predicted PK parameters for FNSF1a and FNSF2a suspensions for 90mg dose

PK parameters	MP1	FNSF1a	FNSF2a	p value for paired T-test	
				FNSF1a	FNSF2a
C_{max} (ng/ml)	300.37 ± 4.19	300.26 ± 3.12	299.75 ± 4.81	0.875	0.225
$AUC_{(0 \text{ to } t)}$ (ng.h/ml)	10336.10 ± 144.19	10438.05 ± 51.87	10404.83 ± 67.01	0.196	0.263

From the above table 3.78, it can be said that the p values for t-test of both FNSF1a and FNSF2a with the market product 1 (MP1) are greater than 0.05 for both C_{max} and AUC. Therefore, it can be concluded that both formulated suspensions, FNSF1a and FNSF2a have similar *in-vivo* performance compared to the market product (MP1) (Singh et al., 2019) for a dose of 90mg. However, this prediction is based on a simulation study and more insights are needed on this topic based on actual *in-vivo* study.

Afterwards, dissolution profiles were carried out for 3 tablets of the market product 1, 15 ml of FNSF1(a) and FNSF2(a) suspensions respectively and the results are presented in the table 3.80 below:

Table 3.80: Dissolution profiles of MP1, FNSF1a, FNSF2a (270mg dose)

Time (hr)	% Release		
	MP1	FNSF1a	FNSF2a
0.00	0.00	0.00	0.00
0.50	25.69	96.07	71.61
1.00	42.76	98.71	72.14
1.50	50.85	99.29	74.96
2.00	58.07	99.59	77.60
2.50	58.24	100.30	78.65
3.00	58.42	99.77	79.89
4.00	61.76	100.47	85.34

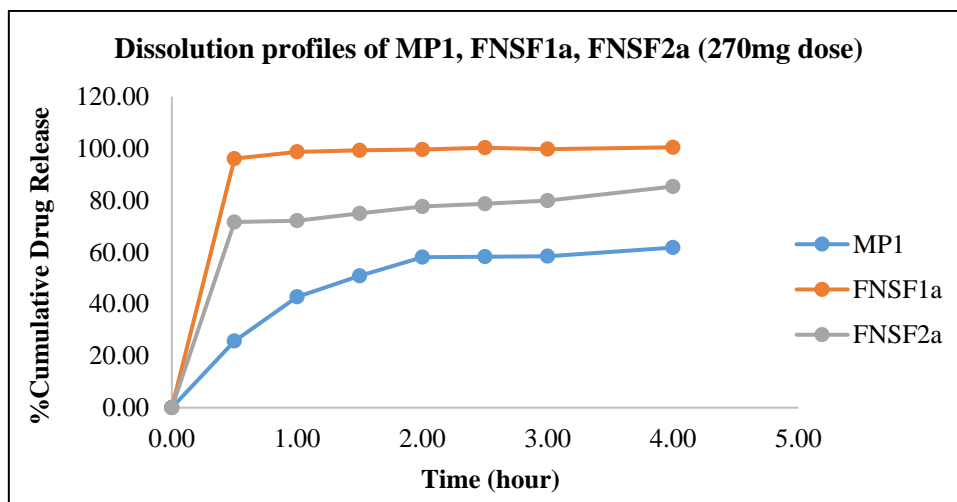


Figure 3.65: Dissolution profiles of MP1, FNSF1a, FNSF2a (270mg dose)

Drug concentration after different time intervals were calculated for MP1, FNSF1a, FNSF2a from the dissolution profiles by convolution method (Table 3.81 and Figure 3.62).

Table 3.81: Drug conc. calculated from dissolution profiles for MP1, FNSF1a and FNSF2a for a dose of 270mg

Time after absorption (hr)	Conc. (ng/mL)		
	MP1	FNSF1a	FNSF2a
0.00	0.00	0.00	0.00
0.08	77.33	289.183	215.5635
0.17	127.57	292.908	214.0068
0.25	150.26	292.386	220.8908
0.33	170.35	291.117	227.0344
0.50	169.00	291.078	228.3212
0.75	168.28	287.282	230.2428
1.00	175.86	285.276	243.1442
8	165.28	268.871	228.3755
9	162.87	264.947	225.0429
10	160.43	261.923	220.1946
12	155.84	253.517	215.3342
24	130.64	212.519	180.5109
36	109.51	178.151	151.3192
48	91.80	152.322	143.339

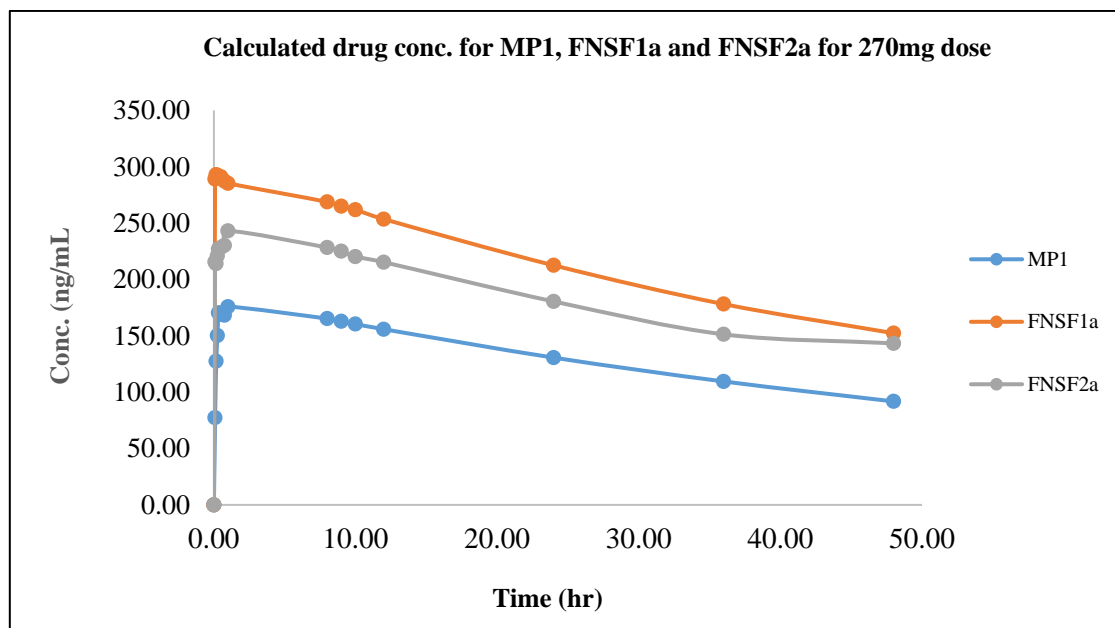


Figure 3.66: Drug conc. calculated from dissolution profiles for MP1, FNSF1a and FNSF2a for a dose of 270 mg

Predicted pharmacokinetic parameters were determined for MP1, FNSF1a and FNSF2a and a paired t-test was done for comparison. The results are listed in the table below (Table 3.82).

Table 3.82: Predicted pharmacokinetic parameters for MP1, FNSF1a and FNSF2a for a dose of 270mg

PK parameters	Predicted values			p value for the paired t-test	
	MP1	FNSF1a	FNSF2a	FNSF1a	FNSF2a
C_{max} (ng/ml)	177.38±2.89	293.23±1.77	233.13±2.18	0.000	0.000
$AUC_{(0\ to\ t)}$ (ng.h/ml)	6343.39±27.10	10399.61±34.53	8885.97±32.94	0.000	0.000

From the above table 3.82, it was found that the p values for t-test between FNSF1a and MP1 and FNSF2a and MP1 are smaller than 0.05 for both C_{max} and AUC. Therefore, it can be concluded that both formulated suspensions, FNSF1a and FNSF2a have significantly different *in-vivo* performance compared to the market product (MP1).

The absorption of Ledipasvir increased 1.65 fold for FNSF1a and 1.31 fold for FNSF2a compared to the market product, MP1 for a dose of 270mg.

3.3.10.2 *In-vivo simulation study for Velpatasvir:*

At next, the *in-vivo* simulation of the formulated suspension of Velpatasvir, VFNSF1a was done. Drug concentration after different time intervals were calculated for VFNSF1a from the dissolution profiles by convolution method and presented in the table below-

Table 3.83: Drug conc. calculated from dissolution profiles for VFNSF1a

Time after absorption (hr)	Conc. (ng/mL)	
	MP3	VFNSF1a
0.00	0.00	0.00
0.08	56.35	50.89
0.17	83.11	112.63
0.25	86.10	175.72
0.33	88.49	238.91
0.50	107.14	302.08
0.75	139.93	364.76
1.00	162.95	427.22
8	139.61	384.60
9	136.67	378.99
10	133.41	341.33
12	128.27	362.64
24	100.41	303.99
36	79.61	254.83
48	63.81	213.62

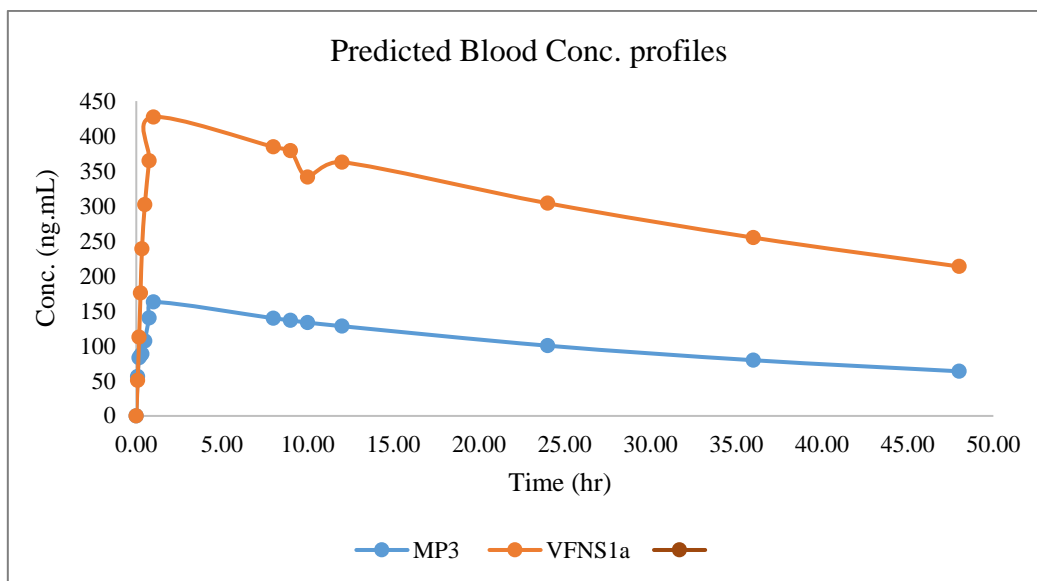


Figure 3.67: Drug conc. calculated from dissolution profiles for MP3 and VNSF1a

From the above table 3.83, the drug concentration data at different time points were used to determine the pharmacokinetic (PK) parameters, peak plasma concentration (C_{max}) and area under the curve (AUC) with the help of PKSolver[®] and the following pharmacokinetic (PK) parameters were obtained (table 3.84). The PK results of VFNSF1a were compared with those of MP3 by paired t-test.

Table 3.84: Predicted PK parameters for VFNSF1a suspension

PK parameters	Predicted value		p value for paired T-test
	MP3	VFNSF1a	
C_{max} (ng/ml)	158.98±2.39	485.23±3.25	0.000
AUC _(0 to t) (ng.h/ml)	5652.62±19.47	14788.31±24.84	0.000

From the above table 3.84, it can be said that the p value for t-test between MP3 and VFNSF1a is smaller than 0.05 for both C_{max} and AUC. Therefore, it can be concluded that both formulated suspensions, VFNSF1a have significantly difference *in-vivo* performance compared to the market product (MP3). The absorption of Velpatasvir increased around 3 fold for VFNSF1a compared to the market product, MP3 for a dose of 270mg.

3.3.11 Stability Study

3.3.11.1 Zeta Potential

Zeta potential of the formulated suspensions of Ledipasvir, FNSF1a and FNSF2a were checked after 3 and 6 months at accelerated stability conditions ($40^{\circ}\text{C} \pm 2^{\circ}\text{C}$ and $75\% \pm 5\% \text{RH}$). Values obtained from the study are mentioned below:

Table 3.85: Zeta potential of the formulated suspensions of Ledipasvir, FNSF1a and FNSF2a after 3 and 6 months at accelerated conditions

Formulation	Zeta potential (mv)					
	3 months			6 months		
	Run 1	Run 2	Run 3	Run 1	Run 2	Run 3
FNSF1a	-34.0	-34.3	-34.9	-34.7	-35.1	-34.9
FNSF2a	-32.9	-33.6	-33.5	-33.3	-32.7	-33.2

From the above table, it can be said that the zeta potential of formulated suspensions of Ledipasvir, FNSF1a and FNSF2a were more than or equal to -30 and hence, can be claimed stable physically.

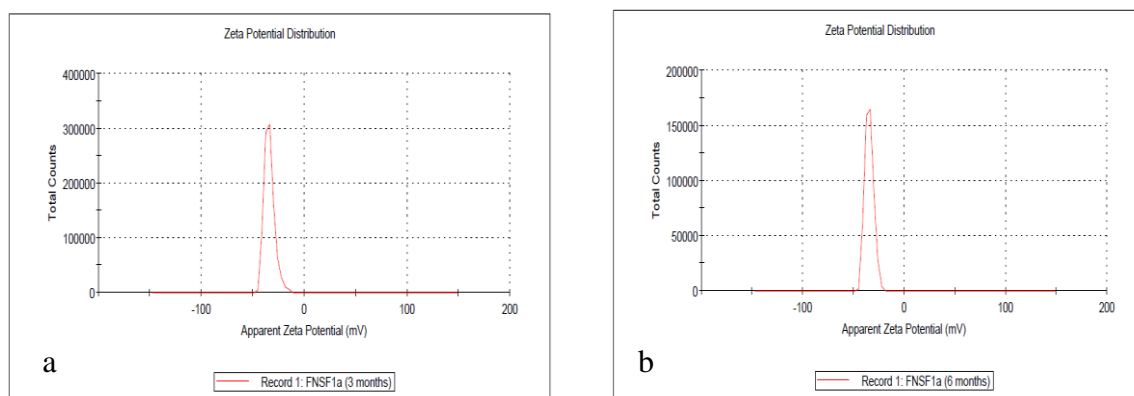


Figure 3.68: Zeta potential of the FNSF1a formulation after 3 months at accelerated conditions; (b) formulations after 6 months at accelerated conditions.

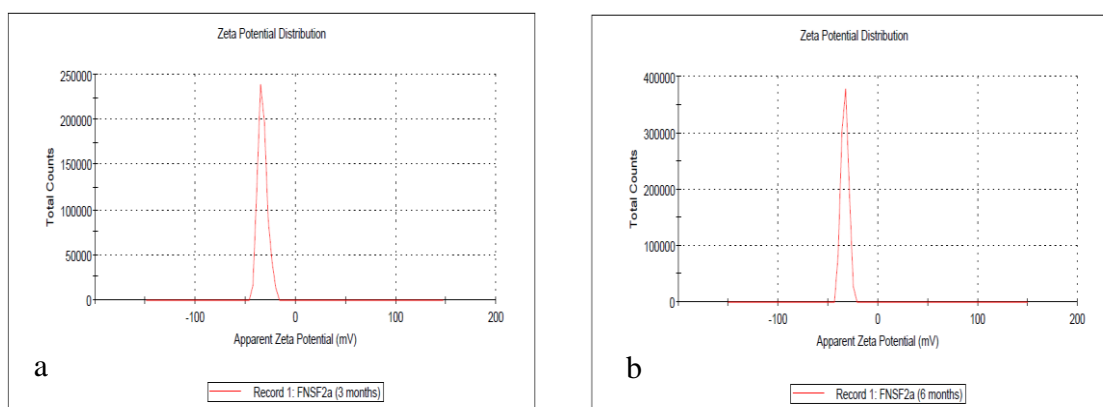


Figure 3.69: Zeta potential of the FNSF2a formulations after 3 months at accelerated conditions; (b) formulations after 6 months at accelerated conditions.

3.3.11.2 Assay content

Assay content of Ledipasvir of the formulated suspensions were checked after 3 and 6 months at accelerated conditions ($40^{\circ}\text{C} \pm 2^{\circ}\text{C}$ and $75\% \pm 5\%\text{RH}$) to study stability status of the formulations. Data has been presented in table 3.86 below.

Table 3.86: Assay content of the formulated suspensions of Ledipasvir, FNSF1a and FNSF2a after 3 and 6 months at accelerated conditions

Samples	FNSF1a			FNSF2a		
	Initial	3 months	6 months	Initial	3 months	6 months
Sample 1	99.38	100.70	98.62	98.49	98.51	99.29
Sample 2	98.92	100.13	98.38	99.77	100.07	98.58
Sample 3	99.49	100.44	100.29	99.11	100.23	98.36
Average	99.26	100.42	99.10	99.12	99.60	98.74
Standard Deviation	0.30	0.29	1.04	0.64	0.95	0.49
%RSD	0.30	0.28	1.05	0.65	0.95	0.49

From the above table it can be said that there was no significant change in the formulated suspensions of Ledipasvir, FNSF1a and FNSF2a in terms of assay compared to the initial results. Percentages of relative standard deviation were found within limits. One-way ANOVA was done using Minitab®, version 17 to compare the assay results for further evaluation (Table 3.87 and 3.88).

Table 3.87: ANOVA table for assay results of FNSF1a

Method		Description			
Null hypothesis		All means are equal			
Alternative hypothesis		At least one mean is different			
Significance level		$\alpha = 0.05$			
Analysis of Variance					
Source	DF	Adj SS	Adj MS	F-Value	P-Value
Factor	2	3.133	1.5667	3.74	0.088
Error	6	2.511	0.4184		
Total	8	5.644			
Means					
Factor	N	Mean	StDev	95% CI	
T0	3	99.263	0.302	(98.349, 100.177)	
T3	3	100.423	0.285	(99.509, 101.337)	
T6	3	99.097	1.040	(98.183, 100.011)	
Pooled StDev = 0.646864					

Table 3.88: ANOVA table for assay results of FNSF2a

Method		Description			
Null hypothesis		All means are equal			
Alternative hypothesis		At least one mean is different			
Significance level		$\alpha = 0.05$			
Analysis of Variance					
Source	DF	Adj SS	Adj MS	F-Value	P-Value
Factor	2	1.114	0.5572	1.08	0.398
Error	6	3.098	0.5163		
Total	8	4.212			
Means					
Factor	N	Mean	StDev	95% CI	
T0	3	99.123	0.640	(98.108, 100.138)	
T3	3	99.603	0.950	(98.588, 100.618)	
T6	3	98.743	0.486	(97.728, 99.758)	
Pooled StDev = 0.718540					

From the ANOVA table 3.87 and 3.88, it was found that the P values were higher than 0.05 which means the null hypothesis cannot be rejected i.e. all means are equal (Raphael, 1999; Zou et al., 2017). There was no significant change as per ICH Q1(R2) guideline in the formulated suspensions in terms of assay of Ledipasvir after six months of accelerated study compared to the initial results presented.

3.3.11.3 Redispersibility

Both FNSF1a and FNSF2a were easily redispersible upon shaking and there was no hard cake formation after 3 and 6 months of accelerated stability study.

3.3.11.4 Dissolution profiles

Dissolution profiles of the formulated suspensions were checked after 3 and 6 months at accelerated conditions ($40^{\circ}\text{C} \pm 2^{\circ}\text{C}$ and $75\% \pm 5\%\text{RH}$) to determine the consistency with initial preparations.

Table 3.89: Dissolution profiles of Ledipasvir formulated suspensions after 6 months at accelerated conditions

Time (min)	FNSF1a			FNSF2a		
	Initial	3 months	6 months	Initial	3 months	6 months
0	0	0	0	0	0	0
5	81.79	78.05	77.93	79.12	76.57	73.54
10	97.52	96.82	94.28	96.55	94.73	94.62
15	99.21	99.49	99.08	98.76	98.88	98.51
20	99.44	99.20	99.66	99.26	99.75	98.88
30	100.20	100.73	101.66	99.99	100.15	99.50
45	99.93	101.03	101.62	100.38	101.05	100.74
60	100.91	100.88	101.70	100.61	101.53	101.01

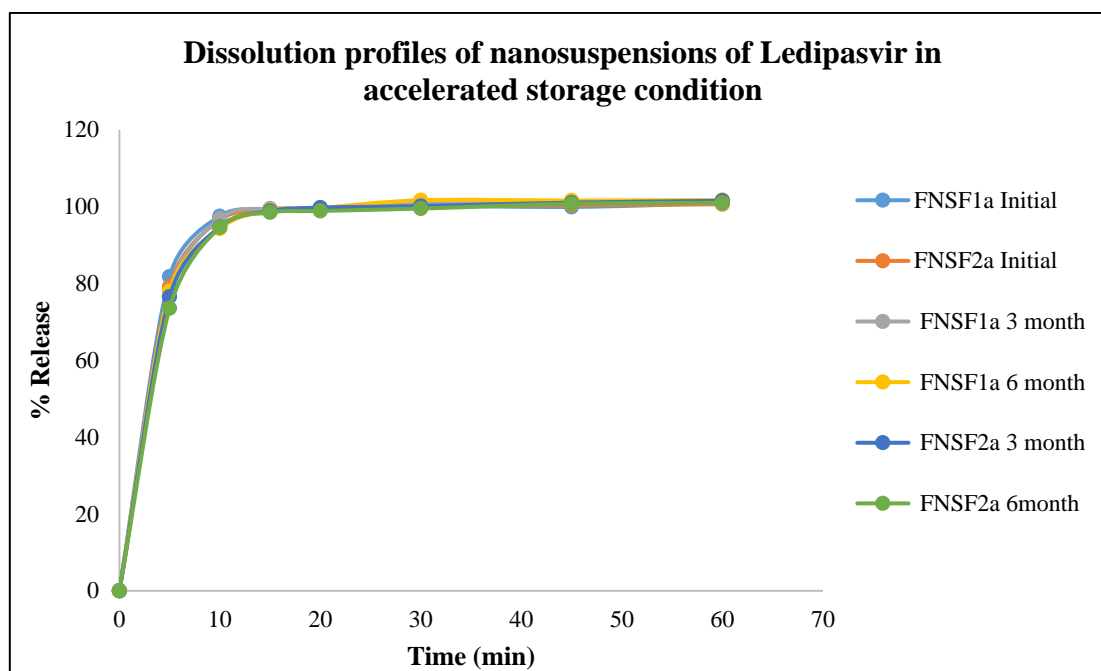


Figure 3.70: Dissolution profiles of Ledipasvir of the formulated suspensions after 3 and 6 months at accelerated conditions

From the above data it can be comprehended that there was no significant change in the final formulations, FNSF1a and FNSF2a, in terms of zeta potential, assay and dissolution of Ledipasvir compared to the initial status. The release of the drug from the suspensions were still the same even after 6 months of exposure at accelerated stability conditions which indicates that the formulations were stable throughout the period of storage at accelerated conditions.

3.3.11.5 Evaluation of similarity (f_2) and difference (f_1) factor after stability study

The dissolution results of preparations FNSF1a and FNSF2a after 3,6 months of stability period were then compared with the initial dissolution results for similarity factor (f_2), difference factor (f_1) and dissolution efficiency (%DE).

Table 3.90: Dissolution profile comparison with similarity factor (f2), difference factor (f1) and dissolution efficiency (%DE)

Time points	FNSF1a			FNSF2a		
	f1	f2	%DE	f1	f2	%DE
Initial	-	-	76.31	-	-	75.02
3 months	1.69	83.34	74.88	1.64	86.53	73.58
6 months	2.60	78.34	73.92	2.83	75.30	72.47

From the above table, it was found that for both FNSF1a and FNSF2a, similarity factors were well above 50 whereas the difference factors were well below 15 at 3 months and 6 months timepoints. Moreover, the %DE for both FNSF1a and FNSF2a were well within $\pm 10\%$ at 3 months and 6 months timepoints compared to their respective initial dissolution results. Therefore, the dissolution profiles can be considered similar.

From the above table it can be observed that there was no significant change in the formulated suspensions in terms of zeta potential, assay and dissolution of Ledipasvir compared to the initial results. The release of the drug from the suspensions were still very fast even after 6 months of exposure at accelerated stability conditions.

3.3.12 Development and validation of analytical methods for Ledipasvir

3.3.12.1 Development of RP-HPLC method

Based on 3^2 full factorial design nine experimental runs were generated. After experimentation, observed values for responses were plotted in the software (Design Expert®) for analysis.

Run	Factor 1 A:% of Buffer %	Factor 2 B:Flow Rate ml/min	Response 1 RT min	Response 2 TF	Response 3 TP
1	65	2	13.29	1.31	1533
2	35	2	11.97	1.56	1826
3	50	1	17.99	1.48	2227
4	65	1	22.39	1.85	1405
5	50	2	11.2	1.18	2280
6	50	1.5	14.61	1.07	2994
7	65	1.5	18.1	1.22	2242
8	35	1.5	16.41	1.27	2589
9	35	1	20.6	1.4	1904

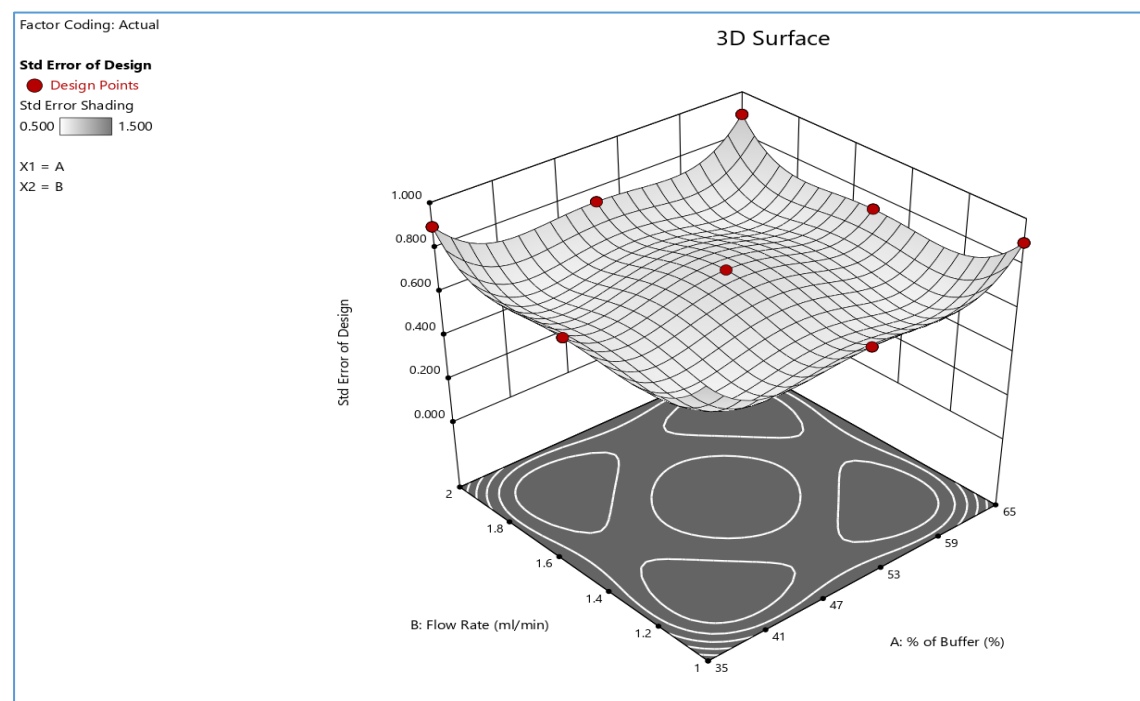


Figure 3.71: 3D response surface plot for standard error of design for development of RP-HPLC method

*Analysis of response 1 (Retention time, min):***Table 3.91:** Fit summary for response 1 (Retention time) for development of RP-HPLC method

Source	Sequential p-value	Adjusted R ²	Predicted R ²	Remarks
Linear	0.0018	0.8387	0.7505	
2FI	0.8948	0.8072	0.5689	
Quadratic	0.0326	0.9672	0.8507	Suggested
Cubic	0.0981	0.9991	0.9784	Aliased

Table 3.92: ANOVA for quadratic model for response 1 (Retention time) for development of RP-HPLC method

Source	Sum of Squares	df	Mean Square	F-value	p-value	
Model	116.90	5	23.38	48.20	0.0046	significant
A-% of Buffer	3.84	1	3.84	7.92	0.0671	
B-Flow Rate	100.21	1	100.21	206.57	0.0007	
AB	0.0552	1	0.0552	0.1138	0.7580	
A ²	12.77	1	12.77	26.32	0.0143	
B ²	0.0356	1	0.0356	0.0733	0.8042	
Residual	1.46	3	0.4851			
Cor Total	118.36	8				

The Model F-value of 48.20 implies the model is significant. There is only a 0.46% chance that an F-value this large could occur due to noise. P-values less than 0.0500 indicate model terms are significant. In this case B, A² are significant model terms.

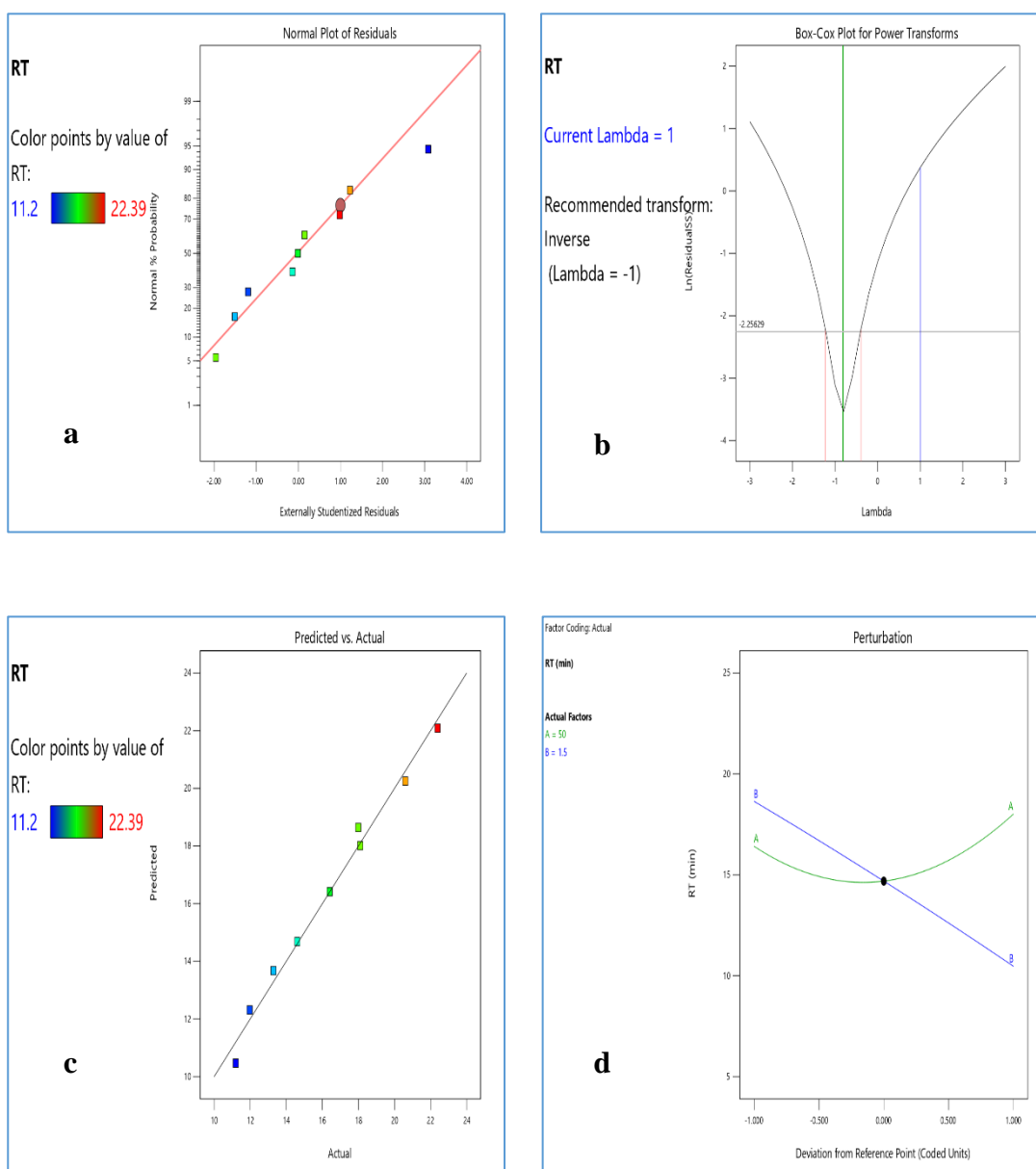


Figure 3.72: (a) Normal plot of residuals; (b) Box-Cox plot for power transform; (c) Predicted vs Actual plot; (d) Perturbation plot for response 1 (Retention time) for development of RP-HPLC method

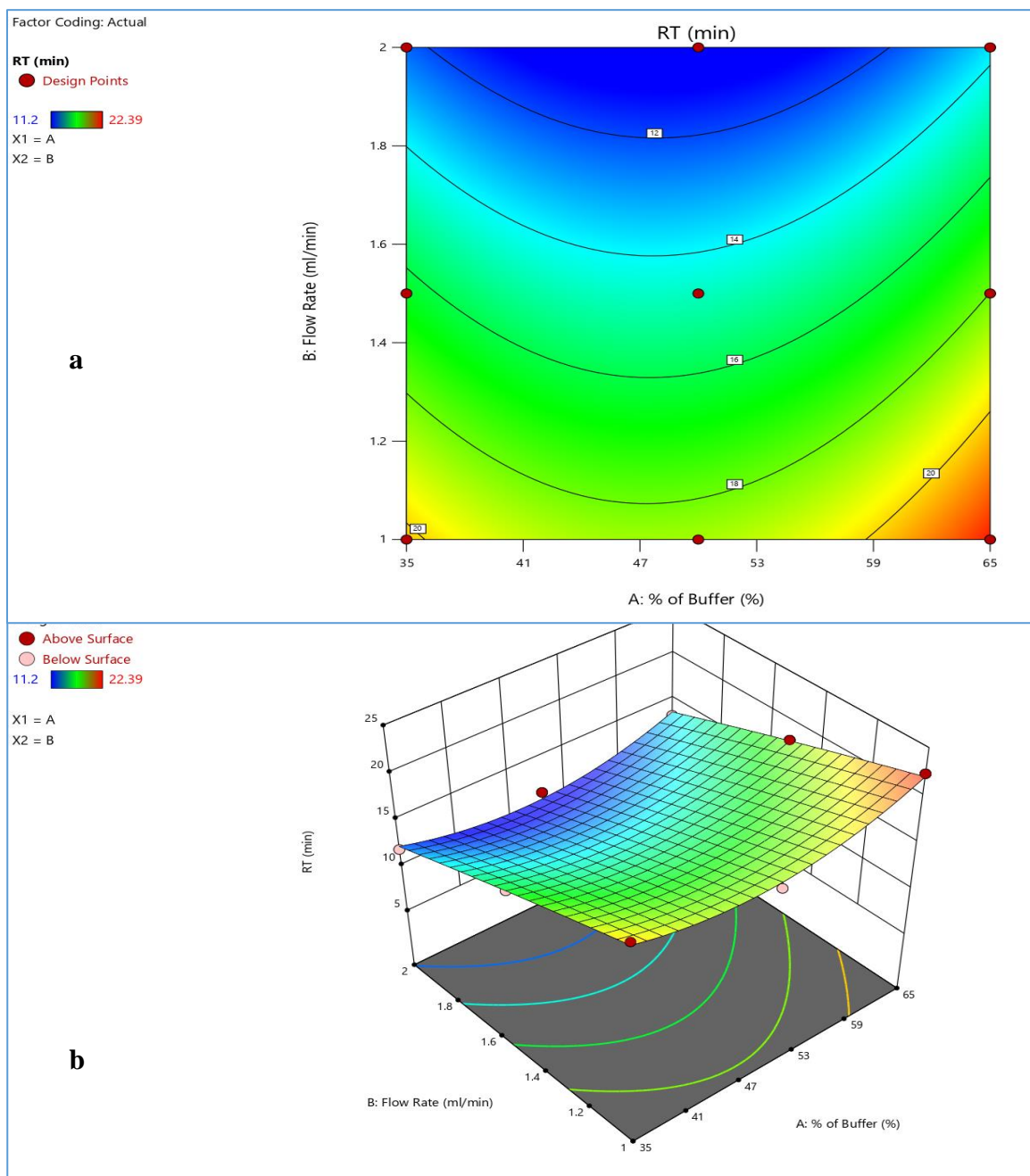


Figure 3.73: (a) Contour plot; (b) 3D response surface plot for response 1 (Retention time) for development of RP-HPLC method

*Analysis of response 2 (Tailing factor):***Table 3.93:** Fit summary for response 2 (Tailing factor) for development of RP-HPLC method

Source	Sequential p-value	Adjusted R ²	Predicted R ²	Remarks
Linear	0.5454	-0.0894	-1.1135	
2FI	0.1698	0.1365	-1.9879	
Quadratic	0.0110	0.9287	0.6770	Suggested
Cubic	0.1534	0.9950	0.8854	Aliased

Table 3.94: ANOVA for quadratic model for response 2 (Tailing factor) for development of RP-HPLC method

Source	Sum of Squares	df	Mean Square	F-value	p-value	Remarks
Model	0.4299	5	0.0860	21.84	0.0145	significant
A-% of Buffer	0.0038	1	0.0038	0.9525	0.4011	
B-Flow Rate	0.0771	1	0.0771	19.57	0.0214	
AB	0.1225	1	0.1225	31.11	0.0114	
A ²	0.0735	1	0.0735	18.66	0.0229	
B ²	0.1531	1	0.1531	38.88	0.0083	
Residual	0.0118	3	0.0039			
Cor Total	0.4417	8				

The Model F-value of 21.84 implies the model is significant. There is only a 1.45% chance that an F-value this large could occur due to noise. P-values less than 0.0500 indicate model terms are significant. In this case B, AB, A², B² are significant model terms.

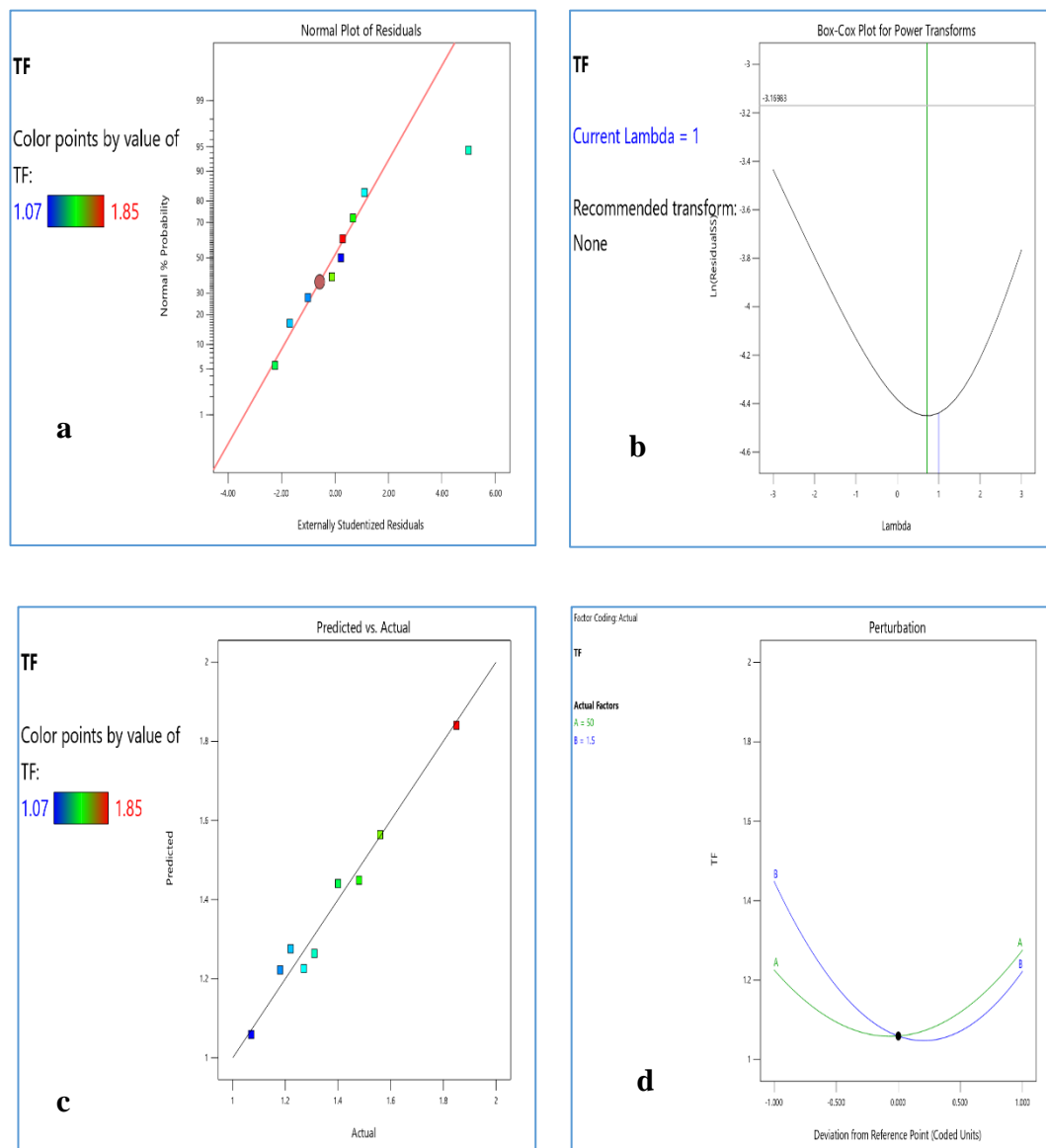


Figure 3.74: (a) Normal plot of residuals; (b) Box-Cox plot for power transform; (c) Predicted vs Actual plot; (d) Perturbation plot for response 2 (Tailing factor) for development of RP-HPLC method

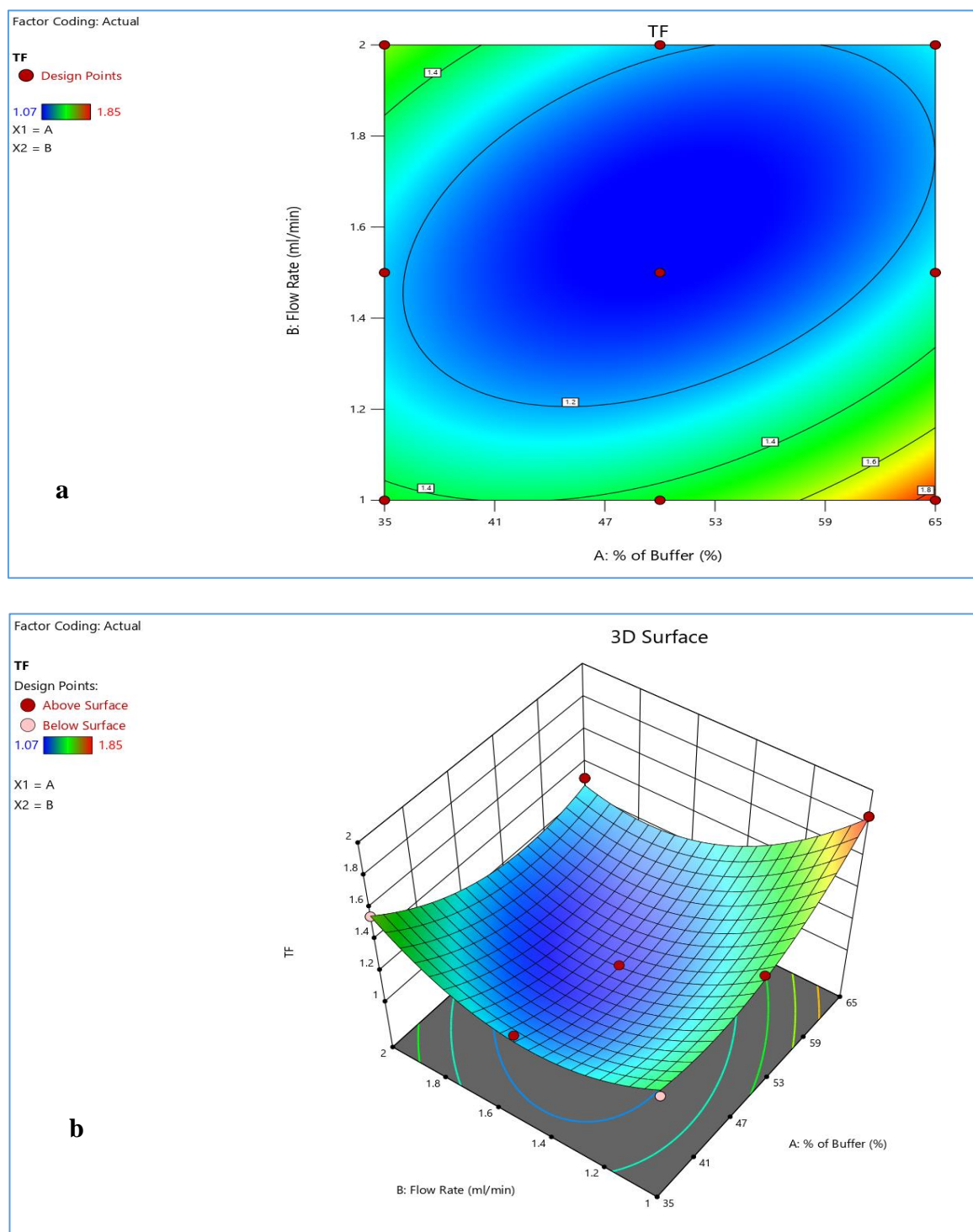


Figure 3.75: (a) Contour plot; (b) 3D response surface plot for response 2 (Tailing factor) for development of RP-HPLC method

*Analysis of response 3 (Theoretical plate count):***Table 3.95:** Fit summary for response 3 (Theoretical plate count) for development of RP-HPLC method

Source	Sequential p-value	Adjusted R ²	Predicted R ²	Remarks
Linear	0.7104	-0.1897	-0.9826	
2FI	0.8703	-0.4193	-3.8790	
Quadratic	< 0.0001	0.9986	0.9935	Suggested
Cubic	0.1615	0.9999	0.9974	Aliased

Table 3.96: ANOVA for quadratic model for response 3 (Theoretical plate count) for development of RP-HPLC method

Source	Sum of Squares	df	Mean Square	F-value	p-value	Remarks
Model	2.023E+06	5	4.046E+05	1113.38	< 0.0001	significant
A-% of Buffer	2.162E+05	1	2.162E+05	595.04	0.0002	
B-Flow Rate	1768.17	1	1768.17	4.87	0.1145	
AB	10609.00	1	10609.00	29.20	0.0124	
A ²	6.817E+05	1	6.817E+05	1876.11	< 0.0001	
B ²	1.113E+06	1	1.113E+06	3061.71	< 0.0001	
Residual	1090.11	3	363.37			
Cor Total	2.024E+06	8				

The Model F-value of 1113.38 implies the model is significant. There is only a 0.01% chance that an F-value this large could occur due to noise. P-values less than 0.0500 indicate model terms are significant. In this case A, AB, A², B² are significant model terms.

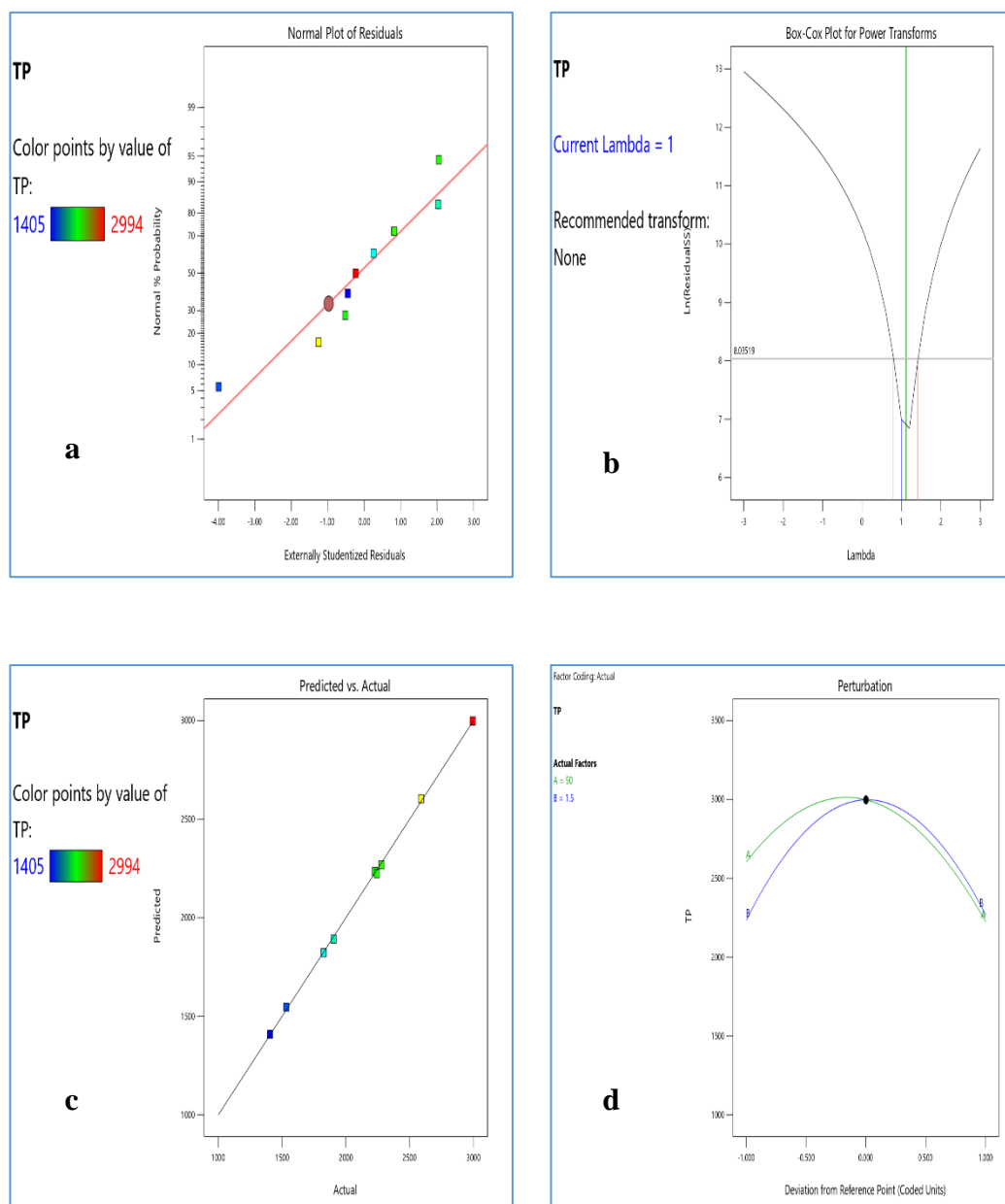


Figure 3.76: (a) Normal plot of residuals; (b) Box-Cox plot for power transform; (c) Predicted vs Actual plot; (d) Perturbation plot for response 3 (Theoretical plate count) for development of RP-HPLC method

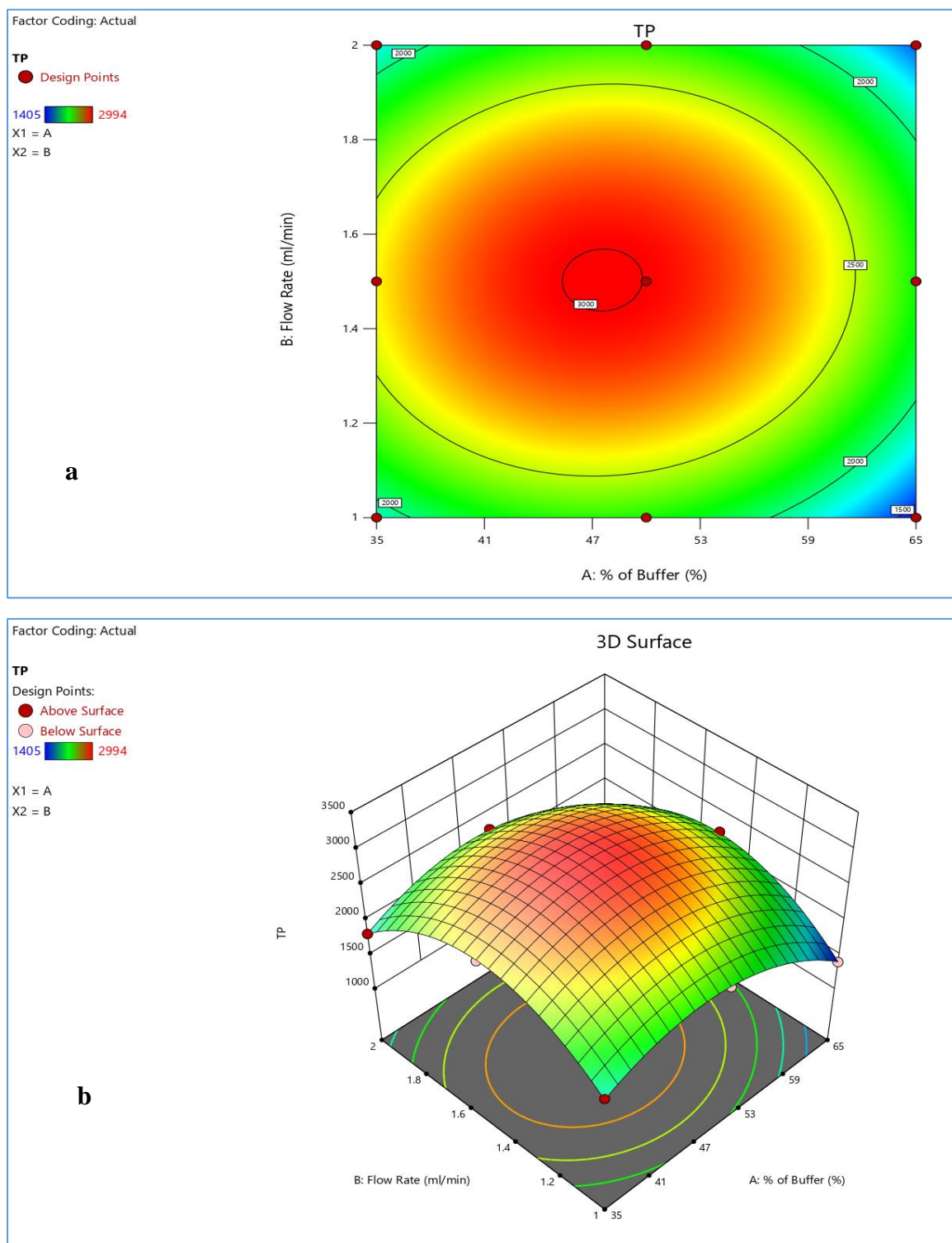


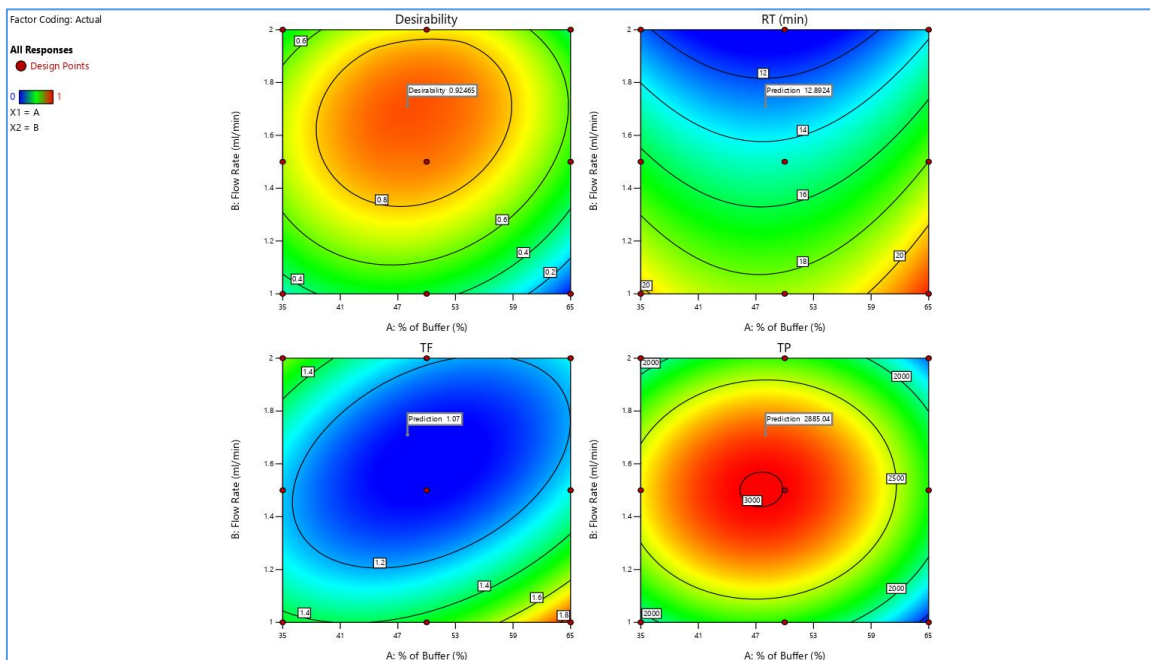
Figure 3.77: (a) Contour plot; (b) 3D response surface plot for response 3 (Theoretical plate count) for development of RP-HPLC method

*Optimization of design:***Table 3.97:** Constraints for optimization of developed RP-HPLC method

Name	Goal	Lower Limit	Upper Limit	Lower Weight	Upper Weight	Importance
A:% of Buffer	is in range	35	65	1	1	3
B:Flow Rate	is in range	1	2	1	1	3
RT	minimize	11.2	22.39	1	1	3
TF	minimize	1.07	1.85	1	1	3
TP	maximize	1405	2994	1	1	3

Table 3.98: Solution for optimized method

Number	% of Buffer	Flow Rate	RT	TF	TP	Desirability	
1	48.007	1.710	12.892	1.070	2884.902	0.925	Selected

**Figure 3.78:** Optimization of developed RP-HPLC method for analysis of Ledipasvir

3.3.13 Validation of developed RP-HPLC analytical method

3.3.13.1 Specificity: Specificity of the analyte peak was determined from the blank, standard, sample injections and all the peaks were well resolved. The chromatograms obtained during the experiment are presented below:

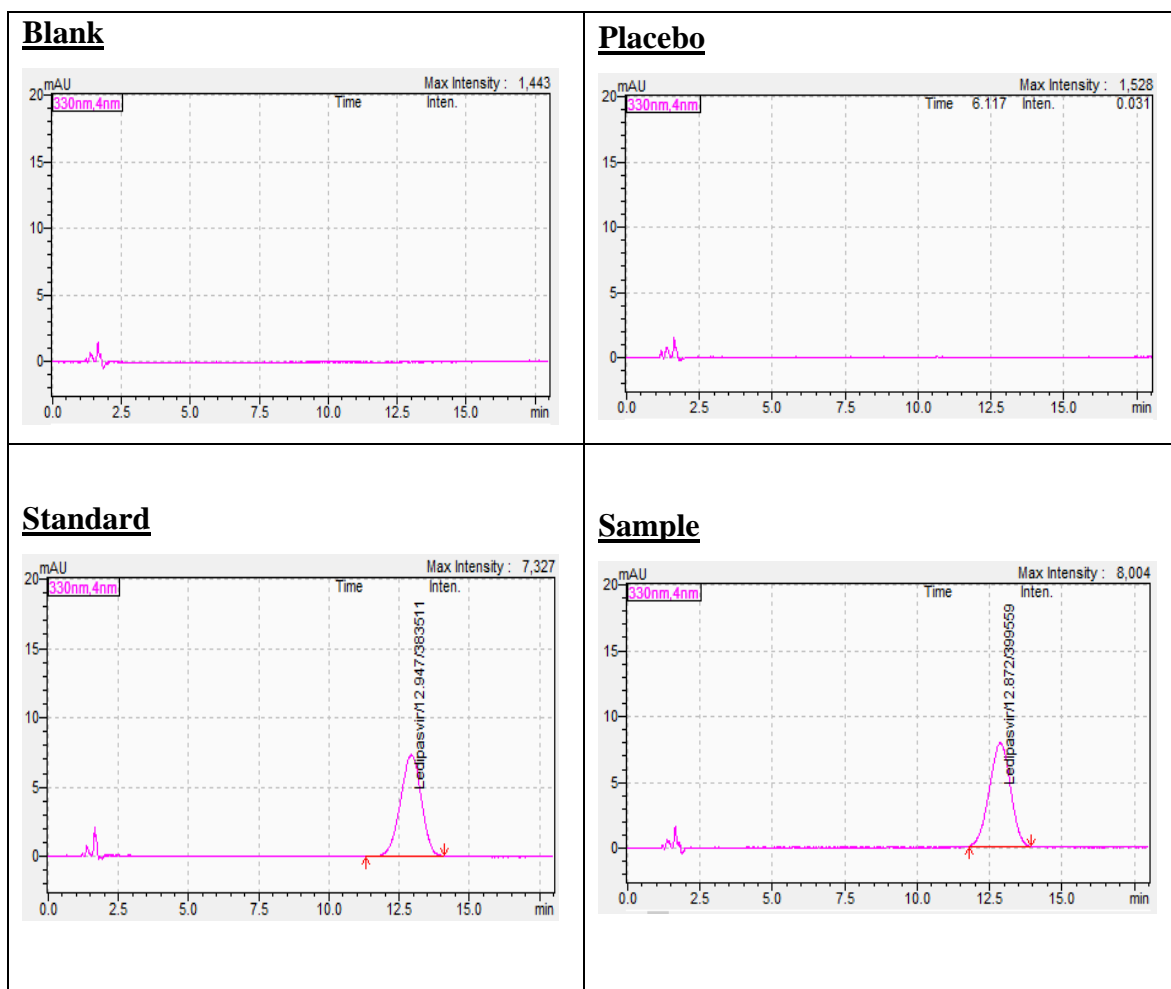
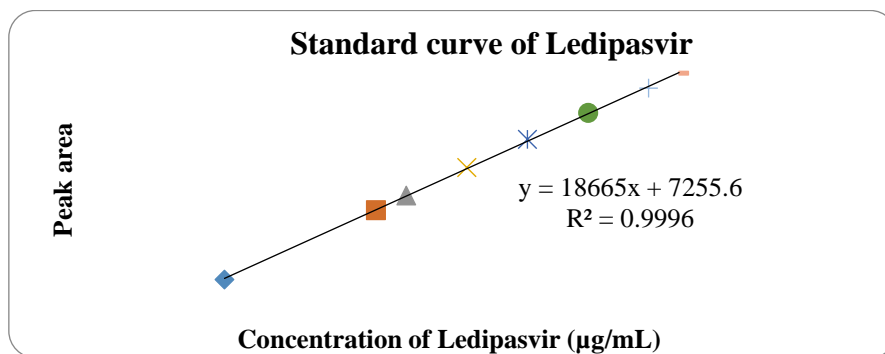


Figure 3.79: Chromatograms of specificity study for analysis of Ledipasvir

3.3.13.2 Linearity and range: The actual concentrations of the standards were computed against the respective absorbance. The linear regression curve was generated using Microsoft Office Excel[®]. The method was found linear with a correlation coefficient (R^2) of 0.9996 and a % of Y-intercept of 7255.6 which is 1.89% compared to total area standard at nominal concentration (20 $\mu\text{g}/\text{mL}$).

Table 3.99: Result of linearity and range for validation of RP-HPLC method

% of nominal value	Ledipasvir	
	Concentration ($\mu\text{g/mL}$)	Peak areas
50%	10.0	190634
60%	12.0	230846
80%	16.0	307571
100%	20.0	384798
120%	24.0	457738
140%	28.0	525720
150%	30.0	566617
R^2 (NLT 0.995)	0.9996	
Y-Intercept	7255.6	
Slope of regression line	18665	

**Figure 3.80:** Linearity and range study for RP-HPLC method of Ledipasvir

3.3.13.3 Accuracy: The data is presented in Table 3.1009 with acceptance criteria. The accuracy was found to be 100.08%.

Table 3.100: Result of accuracy study for validation of RP-HPLC method

% of Nominal Value	Ledipasvir WS for spiking			Contains about 500.0 µg/mL of placebo	Ledipasvir WS		Ry	% Ry	Limit		
	Wt (mg)	Cn (µg/mL)	Peak area		Wt (mg)	Peak area					
80%	8.0	8.0	304627	19.8	381723	7.90	99.38	98.0% to 102.0%			
	8.2	8.2	315619			8.19	99.82				
	8.1	8.1	310797			8.06	100.13				
100%	10.3	10.3	399505			10.36	101.08				
	10.2	10.2	392526			10.18	99.81				
	10.0	10.0	386155			10.01	100.15				
120%	12.0	12.0	463502			12.02	100.17				
	12.0	12.0	461029			11.96	100.06				
	12.1	12.1	467160			12.12	100.13				
Mean (%)							100.08				
RSD (%)							0.46				

*WS-Working Standard; Wt- Weight; Cn-Concentration; Ry-Recovery

3.3.13.4 Precision:

Repeatability (Intra-assay precision): The data is presented in table 3.101 with acceptance criteria. The % RSD of Repeatability of the method was found to be 0.05%.

Table 3.101: Result of repeatability study for validation of RP-HPLC method

Sample	Ledipasvir WS		Sample				%RSD	Limit
	Weight (mg)	Peak area	Weight (mg)	Peak area	Content (mg/tab)	% of assay		
1	9.9	381723	140.0	399317	90.21	100.23	0.05	RSD NMT 2.0%
2			140.2	399784	90.19	100.21		
3			140.2	399750	90.18	100.20		
4			140.3	400503	90.28	100.31		
5			139.8	398735	90.21	100.23		
6			139.7	398251	90.16	100.18		
Average of Assay (%)					90.20 mg/tab (100.23%)			

Intermediate precision: The data is presented in table 3.102 with acceptance criteria. The intermediate precision of the method was found to be 0.23%.

Table 3.102: Result of intermediate precision study for validation of RP-HPLC method

Sample		Ledipasvir WS		Sample				%RSD	% RSD of 12 samples	Limit	
		Weight (mg)	Peak area	Weight (mg)	Peak area	Content (mg/tab)	% of assay				
Analyst 1	1	9.9	381723	140.0	399317	90.21	100.23	0.05	0.23	Not more than 2.0%	
	2			140.2	399784	90.19	100.21				
	3			140.2	399750	90.18	100.20				
	4			140.3	400503	90.28	100.31				
	5			139.8	398735	90.21	100.23				
	6			139.7	398251	90.16	100.18				
Analyst 2	1	10.1	466068	141.2	492193	90.52	100.58	0.32	0.23		Not more than 2.0%
	2			140.0	485855	90.13	100.14				
	3			139.8	485397	90.17	100.19				
	4			140.4	486835	90.05	100.06				
	5			142.1	496847	90.80	100.89				
	6			139.7	485321	90.22	100.24				
		Average of Assay (%)				90.26 mg/tab (100.29%)					

3.3.13.5 Robustness: The robustness of this validation was conducted by changing the pH of the buffer from 6.0 to two different pH (5.8 and 6.2) by using system suitability solution (figure 3.81). The method was found to be robust. The data is presented in table 3.103 with acceptance criteria.

Table 3.103: Result of robustness study for validation of RP-HPLC method

Test	Limit	Result from system suitability	Changed condition of pH of buffer	
		Supelcosil, 35°C, Buffer pH 6.0	(5.8)	(6.2)
%RSD	Not more than 2%	0.269	0.275	0.094
Tailing factor	Not more than 2%	0.950	0.941	0.952
Theoretical plates	Not less than 1000	2611	2480	2487

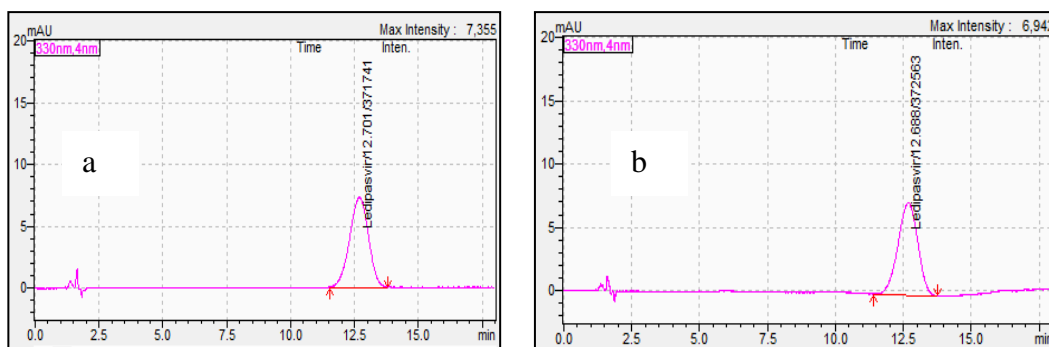


Figure 3.81: Chromatograms of robustness study of Ledipasvir (a) at pH 5.8; (b) at pH 6.2

3.3.13.6 System suitability: Chromatograms were automatically integrated and visually inspected for an acceptable integration. The data is presented in table 3.104. The % RSD was found 0.269, tailing factor was 0.950 and number of theoretical plates was 1411.

Table 3.104: Result of system suitability test for validation of RP-HPLC method

Replicates	Peak area
1	381959
2	381701
3	383511
4	380874
5	381713
6	380581
Average of area	381723
SD	1027.44
%RSD (Limit: Not more than 2.0%)	0.269
Tailing Factor (Limit: Not More than 2.0)	0.950
Number of theoretical plate (Limit: Not less than 1000)	1411

3.3.13.7 Solution stability study: The data is presented in table 3.105 for standard and in table 3.105 for sample (recovery). The results showed that the standard and sample solutions were stable for 24 hours at room temperature as well as at refrigerator and no significant changes are observed with the exposure to light.

Table 3.105: Result of solution stability study (Standard) for validation of RP-HPLC method

Time	Condition	Astd	Fresh standard		Recovery (mg)	%Recovery compared to initial	Limit
			Weight	Area			
0 hr	Initial		9.9	381723			99.0 – 101.0%
24 hr	Ambient amber	378502	10.1	387519	19.73	99.65	
	Ambient Exposed to light	379155			19.24	99.82	
	Refrigerator	381476			19.88	100.43	
48 hr	Ambient amber	379961	10.0	382916	19.75	99.73	
	Ambient Exposed to light	365916			19.02	96.04	
	Refrigerator	381245			19.81	100.07	

Table 3.106: Result of solution stability study (Sample) for validation of RP-HPLC method

Time	Condition	*Astd	**As	Recovery (mg)	%Recovery	Limit
0 hr	Initial	381723	399317	90.21		98.5 – 101.5%
24 hr	Ambient amber	378502	395436	90.09	99.87	
	Ambient Exposed to light	369155	393013	91.81	101.77	
	Refrigerator	381476	396855	89.71	99.45	
48 hr	Ambient amber	379961	398527	90.45	100.27	
	Ambient Exposed to light	365916	397174	93.60	103.76	
	Refrigerator	381245	396075	89.59	99.31	

*Astd- Area of standard; **As- Area of sample

3.3.13.8 Filter compatibility study: The data is presented in table 3.106 (figure 3.82). The result showed that the recovery difference between unfiltered and filtered solutions was outside the range. No significant change was observed in the peak shapes/areas. Thus, it is necessary to filter the solutions before chromatographic analysis.

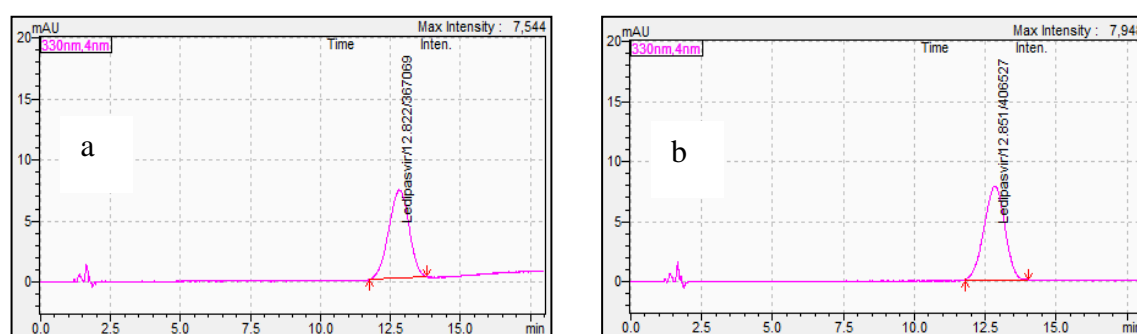


Figure 3.82: Chromatograms of filter compatibility study of Ledipasvir analysis (a) Unfiltered Standard; (b) Unfiltered Sample

Table 3.107: Result of filter compatibility study for validation of RP-HPLC method

Replicate	Unfiltered		Filtered		Recovery (%)	
	Standard	Sample	Standard	Sample	Unfiltered	Filtered
1	372715	409855	Table 3.101	400524	105.92	100.39
2	367069	398908		399559		
3	359585	406527		399731		
Average of area	366456	405097	381723	399938		
SD	6586.41	5611.92	1027.44	514.73		
%RSD (Limit: Not more than 1.5%)	1.80	1.39	0.27	0.13		
Recovery difference between unfiltered and filtered (Limit: Not more than 1.5% absolute)= 5.53%						

From the above test results, it can be observed that the specificity, linearity and range, accuracy, precision (repeatability, intermediate), robustness, system suitability, solution stability and filter compatibility studies were found within the specified ranges. Therefore, as per ICH Q2 (R1) guideline, the developed RP-HPLC method for analysis of Ledipasvir is validated and can be applicable for the analysis of Ledipasvir in its dosage form.

3.3.14 Development and validation of UV method for analysis of Ledipasvir

3.3.14.1 Development of UV method

The sample solution was prepared at nominal concentration (10 $\mu\text{g/mL}$) and scanned in triplicates. The maximum absorbance was found at 333 nm (λ_{max}) in an UV-Vis spectrophotometer (figure 3.83).

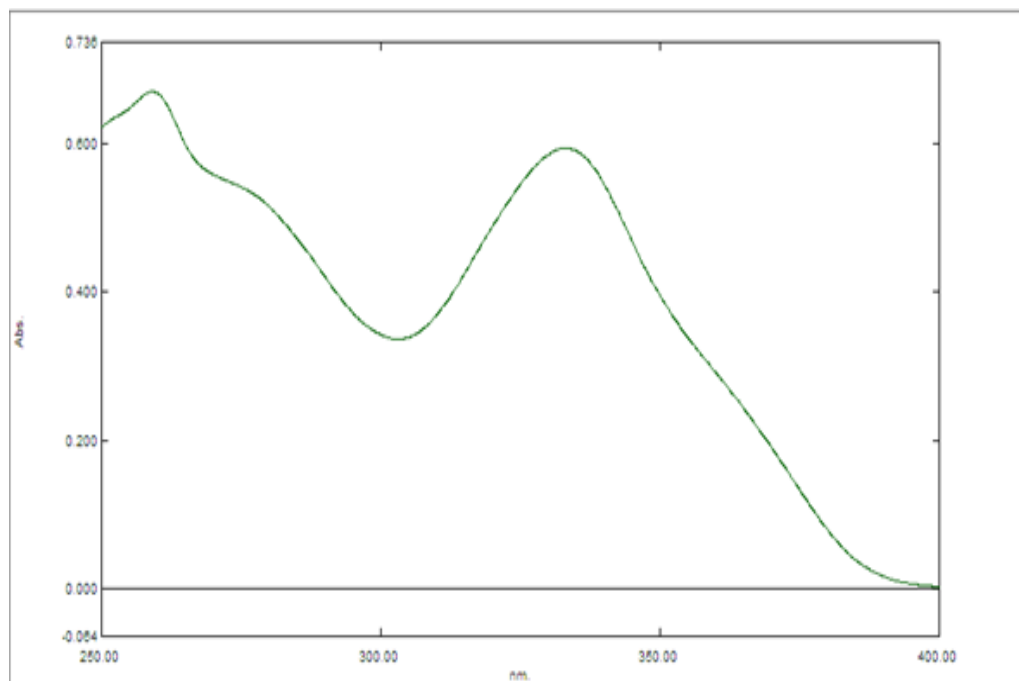


Figure 3.83: Maximum absorbance (λ_{max}) for Ledipasvir

3.3.14.2 Validation of UV method

3.3.14.1 Specificity: The UV spectrum of the blank, placebo, standard and sample were evaluated and all the peaks were found well resolved (figure 3.84).

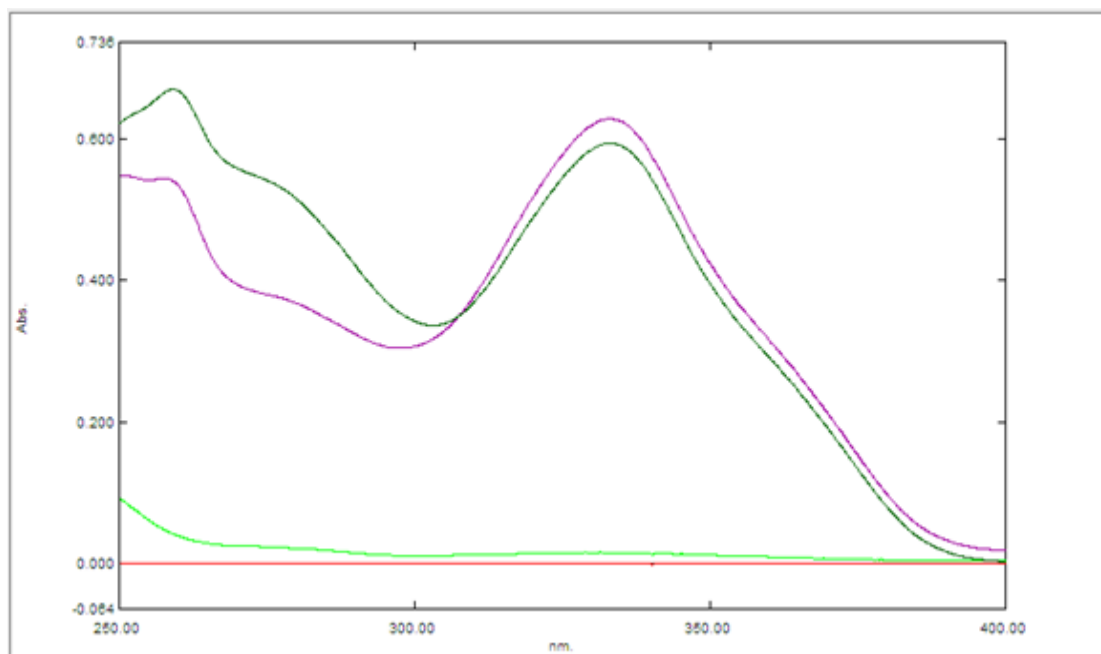


Figure 3.84: Specificity of blank, placebo, standard and sample (from bottom to upwards)

3.3.14.2 Linearity and Range: The method was found linear with a correlation coefficient (R^2) of 0.9996 and a % of Y-intercept of 0.0166 which is 2.80% compared to absorbance of standard at nominal concentration (10 $\mu\text{g/mL}$) (table 3.108, figure 3.85). The lower limit of quantitation (LLOQ) was defined as the lowest concentration within the linear range (5.0 $\mu\text{g/mL}$). The upper limit of quantitation (ULOQ) was defined as the highest concentration within the linear range (16.2 $\mu\text{g/mL}$).

Table 3.108: Result of Linearity and Range

% of Nominal value	Conc. of Std ($\mu\text{g/mL}$)	Abs.	Regression coefficient (R^2)		y-intercept	Slope of regression line
			Limit	Result		
50%	5.0	0.289	NLT 0.985	0.9996	0.003	0.0544
60%	6.4	0.359				
70%	7.5	0.418				
80%	8.6	0.469				
90%	9.6	0.543				
100%	10.8	0.593				
110%	11.8	0.645				
120%	12.8	0.704				
130%	13.9	0.774				
140%	15.0	0.823				
150%	16.2	0.882				
Lower limit of quantitation (LLOQ)					5.0 $\mu\text{g/mL}$	
Upper limit of quantitation (ULOQ)					16.2 $\mu\text{g/mL}$	

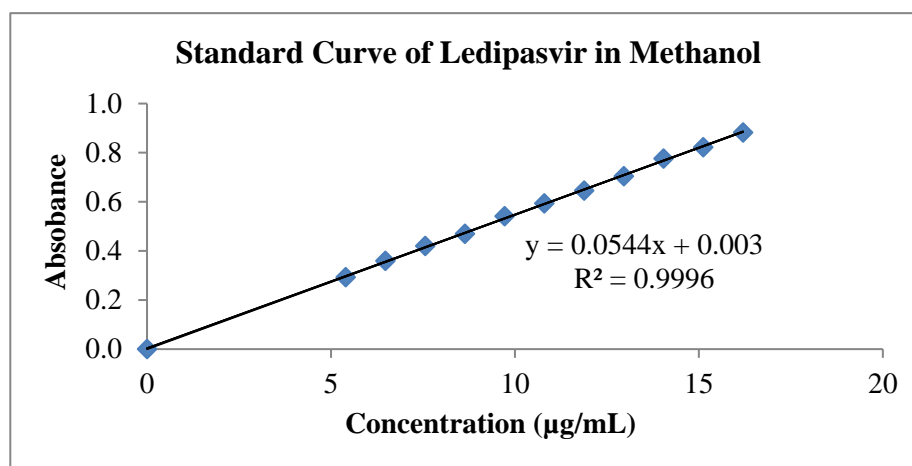


Figure 3.85: Linearity and Range study of Ledipasvir for UV method validation

3.3.14.3 Precision:

Repeatability: The data of repeatability study is presented in table 3.109. The % RSD of repeatability of the method was found to be 1.61%.

Table 3.109: Result of repeatability study for UV method validation

Sample	STD (mg)	Abs. of sample	Abs. of Std	Dissolution (%)	%RSD	Limit (%)
1	10.8	0.583	0.593	99.16	1.61	NMT 10.0
2		0.564		95.93		
3		0.579		98.48		
4		0.559		95.08		
5		0.573		97.46		
6		0.567		96.44		
Average of dissolution (%)				97.09%		

Intermediate Precision: The intermediate precision of the method was found to be 1.74%. The data is presented in Table 3.110 with acceptance criteria.

Table 3.110: Result of intermediate precision study for UV method validation

Sample		STD (mg)	Abs. of sample	Abs. of Std	Dissolution (%)	%RSD	%RSD of 12 sample	Limit (%)
Analyst 1	1	10.8	0.583	0.593	99.16	1.61	1.74	NMT 10.0
	2		0.564		95.93			
	3		0.579		98.48			
	4		0.559		95.08			
	5		0.573		97.46			
	6		0.567		96.44			
Analyst 2	1	9.6	0.566	0.533	95.21	2.01		
	2		0.574		96.55			
	3		0.570		95.88			
	4		0.591		99.41			
	5		0.578		97.22			
	6		0.595		100.08			

3.3.14.4 Accuracy:

The data of accuracy study is presented in Table 3.111 with acceptance criteria. The accuracy was found to be 99.87%.

Table 3.111: Result of accuracy study for UV method validation

% of Q value (Nominal Concentration)	Weight		Abs. of Sample	Weight of standard (mg)	Abs. of standard	% Recovery	Recovery (mg)	Limit
	API (mg)	Placebo (mg)						
80%	9.10	112.5	0.505	10.800	0.593	101.07	9.20	95.0% to 105.0%
	9.05	113.1	0.498			100.22	9.07	
	9.13	112.8	0.501			99.94	9.12	
100%	11.39	140.6	0.628			100.42	11.44	
	11.20	141.0	0.608			98.87	11.07	
	11.14	141.1	0.604			98.75	11.00	
120%	13.71	169.2	0.752			99.90	13.70	
	13.66	168.4	0.747			99.60	13.60	
	13.87	168.7	0.762			100.06	13.88	
Mean						99.87		
SD						0.73		
RSD						0.73		

3.3.14.5 Robustness: The data of robustness study is presented in Table 3.112 below which indicates that the method is robust within a range 331 nm to 335 nm of λ_{max} .

Table 3.112: Result of Robustness study for UV method validation

Test	$\lambda_{max} =$ 331 nm	$\lambda_{max} =$ 333nm	$\lambda_{max} =$ 335 nm	Limit
Abs. of Std.	0.589	0.593	0.590	≥ 75% dissolution within 30 minutes
Abs. of sample	0.569	0.573	0.569	
Dissolution (%)	97.44	97.46	97.27	

3.3.14.6 Solution stability study: The data is presented in table 3.113 (for standard) and table 3.114 (for sample). From the results, it can be comprehended that the solution exhibited stability for 24 hours at room temperature as well as refrigerator and no significant changes were observed with the exposure of light.

Table 3.113: Result of solution stability study (standard) for UV method validation

Time (hr)	Condition	Weight of Initial standard (mg)	Absorbance	Average Absorbance	Recovery	% Recovery	Limit
0	Initial	10.1	0.556	0.556			99.0 – 101.0%
			0.557				
			0.556				
12	Clear Vial Ambient		0.554	0.557	10.12	100.24	
			0.556				
			0.557				
	Amber Vial Ambient		0.559	0.556	10.11	100.06	
			0.556				
			0.554				
	Refrigerated		0.557	0.555	10.09	99.88	
			0.555				
			0.554				
24	Clear Vial Ambient	0.552	0.552	10.02	99.22		
		0.551					
		0.552					
	Amber Vial Ambient	0.553	0.555	10.08	99.76		
		0.555					
		0.556					
	Refrigerated	0.556	0.557	10.11	100.12		
		0.556					
		0.558					

Table 3.114: Result of solution stability study (sample) for UV method validation

Time (hr)	Condition	Weight of Initial standard	Absorbance	Average absorbance	Dissolution (%)	% Recovery	Limit
0	Initial (standard)	10.1	0.556	0.556	99.07	99.37	99.5 – 101.5%
			0.557				
			0.556				
	Initial (sample)		0.584	0.584			
			0.583				
			0.584				
12	Clear Vial Ambient	0.578	0.580	98.45	99.37		
		0.58					
		0.583					
	Amber Vial Ambient	0.587	0.587	99.52	100.46		
		0.586					
		0.587					
	Refrigerated	0.583	0.585	99.18	100.11		
		0.585					
		0.586					
24	Clear Vial Ambient	0.579	0.580	98.33	99.26		
		0.582					
		0.578					
	Amber Vial Ambient	0.591	0.589	99.86	100.80		
		0.588					
		0.587					
	Refrigerated	0.589	0.592	100.37	101.31		
		0.592					
		0.594					

3.3.15 Equivalency between UV and HPLC method

3.3.15.1 Comparison of standard calibration curves: Regression analysis of standard calibration curves of both methods are presented in table 3.115. The data expressed that correlation coefficient (R^2) is greater than 0.999 for both methods indicating strong linearity of the standard curves for both HPLC and UV assay methods.

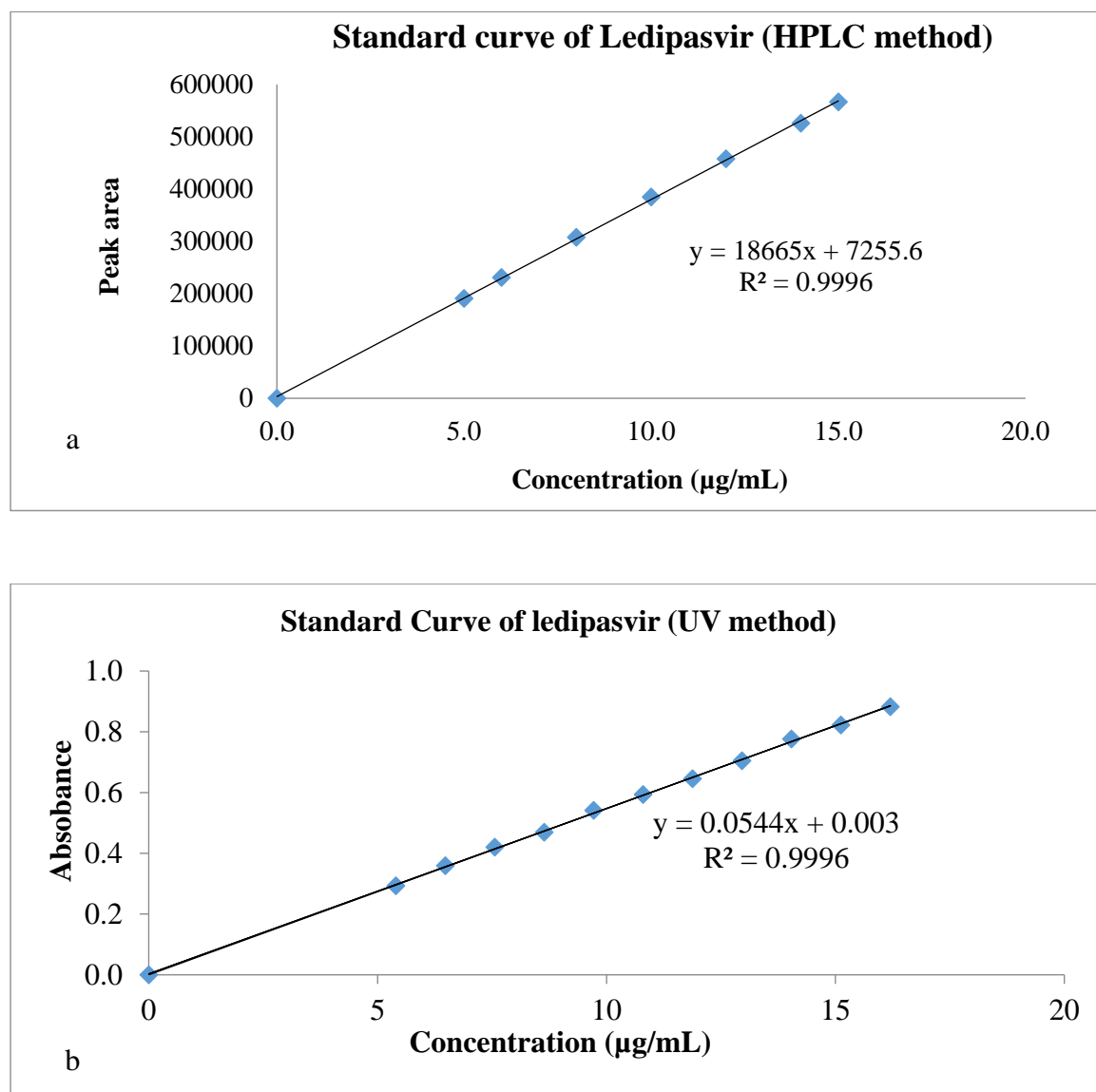


Figure 3.86: (a) Standard calibration curve of ledipasvir for HPLC method; (b) Standard calibration curve of ledipasvir for UV method

Table 3.115: Results of the regression analysis of data for the quantitation of Ledipasvir

Statistical parameters	HPLC method	UV method
Regression equation	$y = 18665x + 7255.6$	$y = 0.0544x + 0.003$
Correlation coefficient (r ²)	0.9996	0.9996
Y-intercept	7255.6	0.003
Slope of regression line	18665	0.544
Concentration range (µg/mL)	5.0 - 15.0	5.4 - 16.2

3.3.15.2 Comparison of repeatability and intermediate precision: Repeatability and intermediate precision for both HPLC and UV method are presented in table 3.116. From the results, it can be comprehended that % RSD for repeatability and intermediate precision for both methods were within limit (not more than 2%) and highly comparable.

3.3.15.3 Comparison of accuracy: Results of accuracy study for both HPLC and UV methods are presented in table 3.117. From the results, it can be seen that % RSD for accuracy for both methods were within limit (NMT 2%) and highly comparable.

3.3.15.4 Comparison of solution stability study: Results of solution stability studies of Ledipasvir working standard and test samples for both HPLC and UV methods are presented in table 3.118 and 3.119 respectively. From the results, it can be said that both methods are able to demonstrate that the solutions exhibit stability for 24 hours at room temperature as well as refrigerator and no significant changes are observed with the exposure of light.

Table 3.116: Comparison of repeatability and intermediate precision for HPLC and UV assay method

Parameters	% Assay				Limit
	Repeatability	% RSD	Intermediate precision	% RSD	
HPLC method	100.23	0.05	100.58	0.23	% RSD NMT 2%
	100.21		100.14		
	100.20		100.19		
	100.31		100.06		
	100.23		100.89		
	100.18		100.24		
UV method	99.91	0.68	99.03	0.68	
	99.22		100.59		
	100.25		99.40		
	100.75		99.25		
	99.79		98.72		
	98.88		99.08		

Table 3.117: Comparison of accuracy for HPLC and UV assay methods

% of Q value (Nominal Concentration)	%Recovery		Limit
	HPLC	UV	
80%	99.38	101.07	98.0% - 102.0%
	99.82	100.22	
	100.13	99.94	
100%	101.08	100.42	
	99.81	98.87	
	100.15	98.75	
120%	100.17	99.90	
	100.06	99.60	
	100.13	100.06	

Table 3.118: Comparison of solution stability study for HPLC and UV assay methods (standard solution)

Time (hour)	Conditions	% Recovery		Limit
		HPLC	UV	
0	Initial			98.0% to 102.0%
24	Clear vial ambient	99.65	99.26	
	Amber vial ambient	99.82	99.57	
	Refrigerated	100.43	100.31	

Table 3.119: Comparison of solution stability study for HPLC and UV assay methods (sample solution)

Time (hour)	Conditions	% Recovery		Limit
		HPLC	UV	
0	Initial			98.0% to 102.0%
24	Clear vial ambient	99.87	100.40	
	Amber vial ambient	101.77	99.37	
	Refrigerated	99.45	99.26	

3.3.15.5 % Recovery from HPLC and UV method: The %recovery of standard and samples are presented in table 3.120. The results showed that the %RSD of assay results between HPLC and UV was 0.44% which demonstrate the equivalency between HPLC and UV method for assay determination of Ledipasvir in pharmaceutical dosage forms.

Table 3.120: % Recovery of Ledipasvir from HPLC and UV method

Replicate	HPLC	UV	%RSD between HPLC and UV (Limit: NMT 2%)
1	100.23	99.88	0.44
2	100.21	101.45	
3	100.20	100.26	
4	100.31	100.10	
5	100.23	99.57	
6	100.18	99.93	
%RSD (Limit: NMT 2%)	0.05	0.65	

Furthermore, analysis of variance (ANOVA) (table 3.121), paired t-test (table 3.122) and paired equivalence test (table 3.123) were applied to statistically compare these two analytical methods at 95 % confidence interval level. In case of ANOVA (Zou et al., 2017) and paired t-test (Singh et al., 2019), P values were greater than 0.05 which indicates the

equivalency between HPLC and UV method for assay determination of Ledipasvir in pharmaceutical dosage forms. At the same time, the P value for paired equivalence test was smaller than 0.05 which also demonstrates equivalence between both methods (Mara and Cribbie, 2012).

Table 3.121: ANOVA table for comparing % recovery of Ledipasvir from HPLC and UV method

Method					
Null hypothesis			All means are equal		
Alternative hypothesis			At least one mean is different		
Significance level			$\alpha = 0.05$		
Equal variances were assumed for the analysis.					
Factor Information					
Factor Levels			Values		
Factor			2 (HPLC, UV)		
Analysis of Variance					
Source	DF	Adj-SS	Adj-MS	F-value	P-value
Factor	1	0.00241	0.002408	0.01	0.918
Error	10	2.15842	0.215842		
Total	11	2.16083			
Model Summary					
S	R-sq	R-sq (adj)		R-sq (pred)	
0.464588	0.11%	0.00%		0.00%	
Means					
Factor	N	Mean	St-Dev	95% CI	
HPLC	6	100.227	0.045	(99.804, 100.649)	
UV	6	100.198	0.655	(99.776, 100.621)	
Pooled StDev				0.464588	

Table 3.122: Paired t-test for comparing % recovery of Ledipasvir from HPLC and UV method

Paired T for HPLC - UV				
	N	Mean	StDev	SE Mean
HPLC	6	100.227	0.045	0.018
UV	6	100.198	0.655	0.268
Difference	6	0.028	0.663	0.271
95% CI for mean difference: (-0.668, 0.725)				
T-Test of mean difference = 0 (vs \neq 0): T-Value = 0.10 P-Value = 0.921				

Table 3.123: Paired equivalence test for comparing % recovery of Ledipasvir from HPLC and UV method

Method				Parameters
Test mean				mean of HPLC
Reference mean				mean of UV
Descriptive Statistics				
Variable	N	Mean	Std-Dev	SE Mean
HPLC	6	100.23	0.045019	0.018379
UV	6	100.20	0.65548	0.26760
Difference				Mean(HPLC) - Mean(UV)
Difference	StDev	SE	95% CI	Equivalence Interval
0.028333	0.663488	0.27087	(-0.51748, 0.57415)	(-1.24, 0.66)
CI is within the equivalence interval. Can claim equivalence.				
Test				Values
Null hypothesis				Difference \leq -1.24 or Difference \geq 0.66
Alternative hypothesis				-1.24 < Difference < 0.66
α level				0.05
Null Hypothesis	DF	T-Value	P-Value	
Difference \leq -1.24	5	4.6825	0.003	
Difference \geq 0.66	5	-2.3320	0.034	
The greater of the two P-Values is 0.034. Can claim equivalence.				

3.3.16 Development of GC method

Based on 3^2 full factorial design, nine experimental runs were generated using Design Expert® (version 13) software. Increment of temperature (degree Celsius) and split flow rate (ml/min) were taken as independent variables. Both the variables were studied at three level low, mid and high during designing of experiment. Retention time (min), tailing factor and theoretical plate count were regarded as dependent variables or responses of the study. After experimentation, observed values for responses were plotted in the software for analysis.

Run	Factor 1 A:Increment of T... degree celcius	Factor 2 B:Split Flow ml/min	Response 1 RT min	Response 2 TF	Response 3 TP
1	15	45	3.24	0.89	13659
2	5	50	3.29	1.36	13132
3	15	50	2.39	0.68	13748
4	5	45	3.88	1.08	12988
5	10	50	3.17	0.92	13476
6	5	40	3.92	0.86	13289
7	10	45	3.85	1.12	13036
8	10	40	3.73	1.16	12589
9	15	40	3.58	1.24	11790

Analysis of response 1 (Retention time, min):

Table 3.124: Fit summary for response 1 for GC method development

Source	Sequential p-value	Adjusted R ²	Predicted R ²	Remarks
Linear	0.0088	0.7243	0.5287	
2FI	0.3196	0.7341	0.2359	
Quadratic	0.0597	0.9323	0.7104	Suggested
Cubic	0.4063	0.9665	0.2362	Aliased

Table 3.125: ANOVA for quadratic model for response 1 (Retention time) GC method development

Source	Sum of Squares	df	Mean Square	F-value	p-value	Remarks
Model	1.88	5	0.3767	23.03	0.0134	significant
A-Increment of Temp	0.5891	1	0.5891	36.02	0.0093	
B-Split Flow	0.9441	1	0.9441	57.72	0.0047	
AB	0.0784	1	0.0784	4.79	0.1163	
A ²	0.0800	1	0.0800	4.89	0.1139	
B ²	0.1922	1	0.1922	11.75	0.0416	
Residual	0.0491	3	0.0164			
Cor Total	1.93	8				

The Model F-value of 23.03 implies the model is significant. There is only a 1.34% chance that an F-value this large could occur due to noise. P-values less than 0.0500 indicate model terms are significant. In this case A, B, B² are significant model terms.

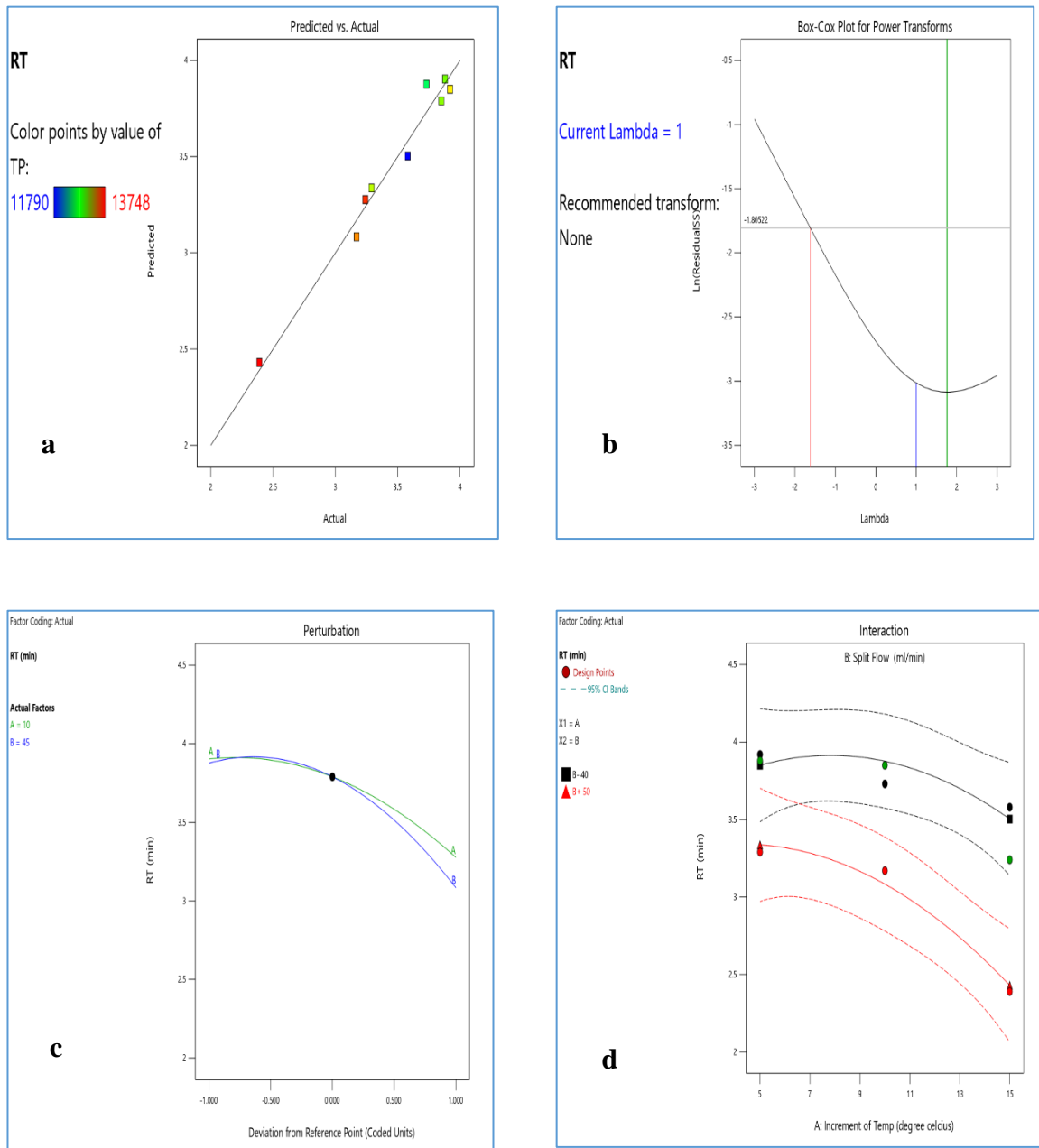


Figure 3.87: (a) Predicted vs actual plot; (b) Box-Cox plot; (c) Perturbation plot; (d) Interaction plot for response 1 (Retention time) of GC method development

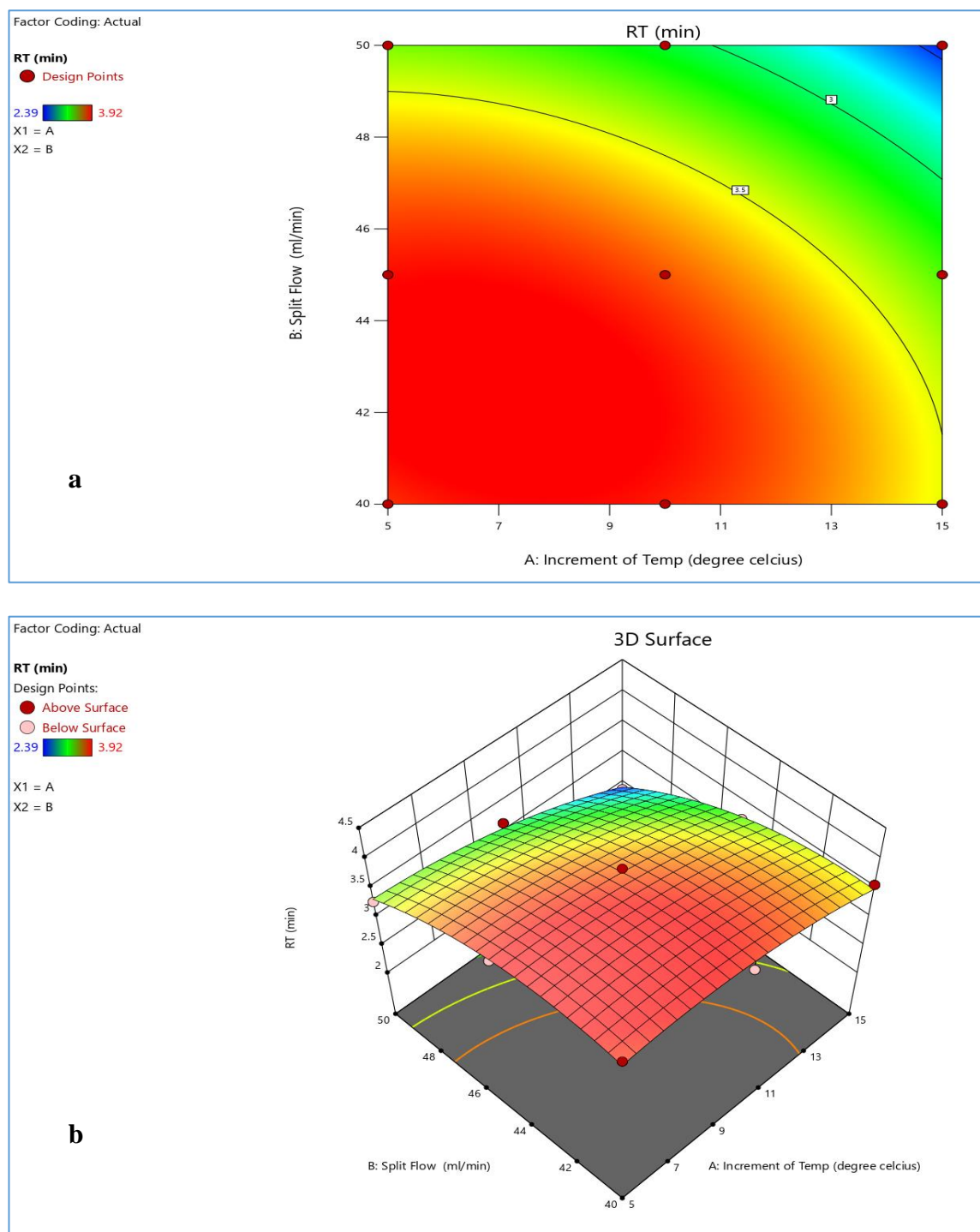


Figure 3.88: (a) Contour plot; (b) 3D response surface plot for response 1 (Retention time) of GC method development

Analysis of response 2 (Tailing factor):**Table 3.126:** Fit summary for response 2 (Tailing factor) for GC method development

Source	Sequential p-value	Adjusted R ²	Predicted R ²	Remarks
Linear	0.6111	-0.1315	-1.6548	
2FI	0.0008	0.8789	0.7451	Suggested
Quadratic	0.7519	0.8331	0.3352	
Cubic	0.5747	0.8347	-2.7667	Aliased

Table 3.127: ANOVA for 2FI model for response 2 (Tailing factor) for GC method development

Source	Sum of Squares	df	Mean Square	F-value	p-value	Remarks
Model	0.3359	3	0.1120	20.35	0.0031	significant
A-Increment of Temp	0.0400	1	0.0400	7.27	0.0429	
B-Split Flow	0.0150	1	0.0150	2.73	0.1596	
AB	0.2809	1	0.2809	51.06	0.0008	
Residual	0.0275	5	0.0055			
Cor Total	0.3634	8				

The Model F-value of 20.35 implies the model is significant. There is only a 0.31% chance that an F-value this large could occur due to noise. P-values less than 0.0500 indicate model terms are significant. In this case A, AB are significant model terms.

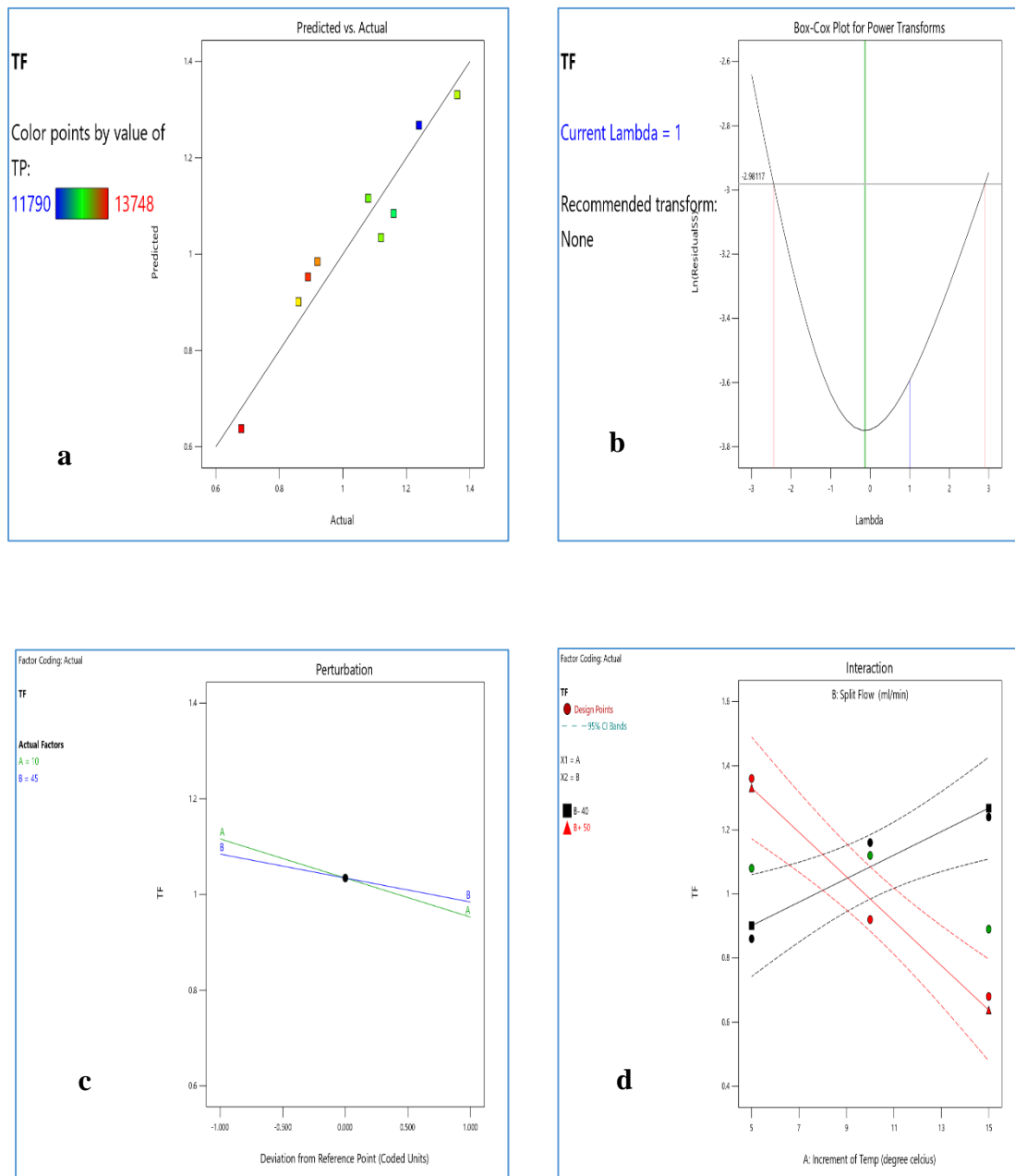


Figure 3.89: (a) Predicted vs actual plot; (b) Box-Cox plot; (c) Perturbation plot; (d) Interaction plot for response 2 (Tailing factor) of GC method development

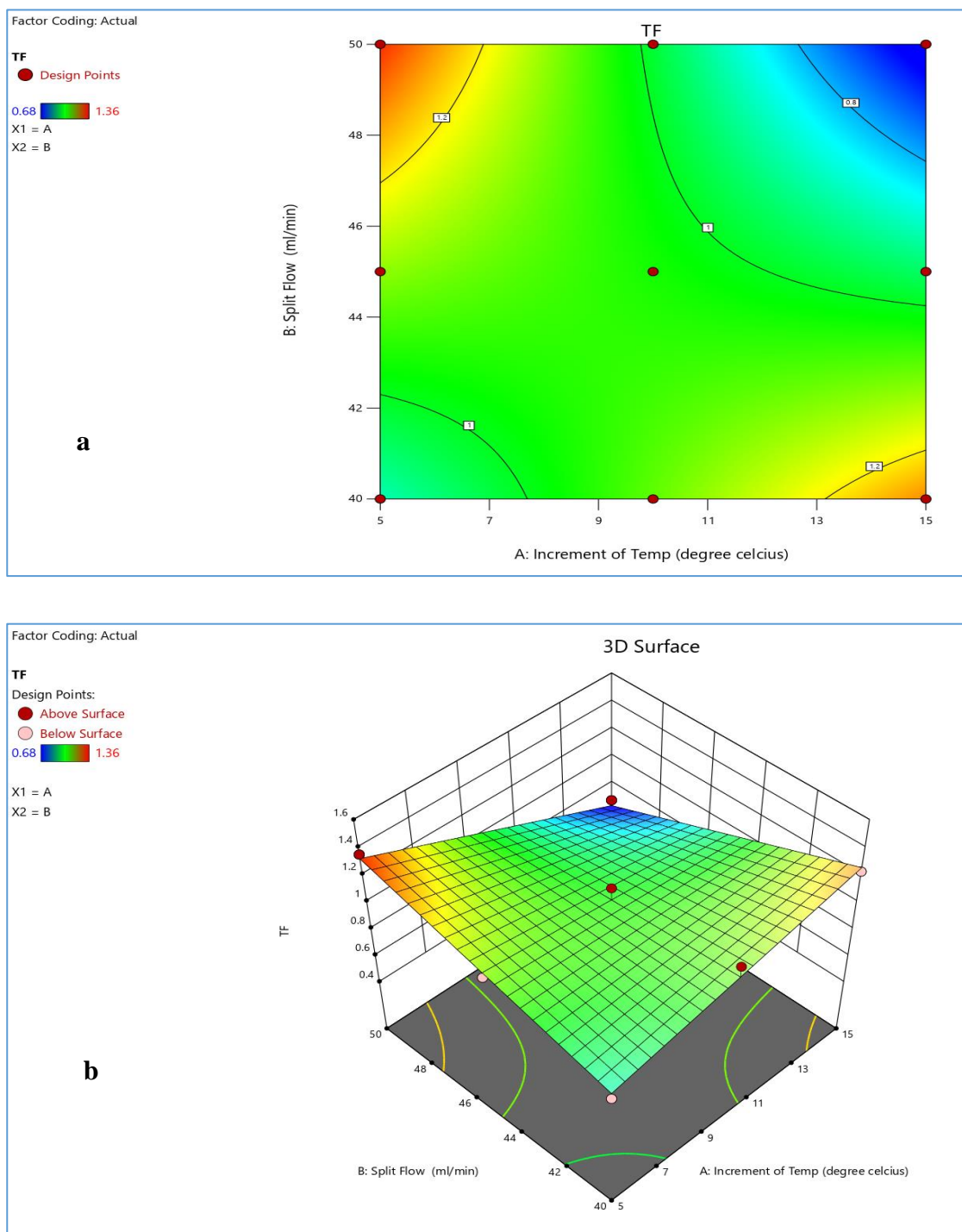


Figure 3.90: (a) Contour plot; (b) 3D response surface plot for response 2 (Tailing factor) of GC method development

*Analysis of response 3 (Theoretical plate count):***Table 3.128:** Fit summary for response 3 (Theoretical plate count) for GC method development

Source	Sequential p-value	Adjusted R ²	Predicted R ²	
Linear	0.1973	0.2237	-0.7030	
2FI	0.0259	0.6854	0.1108	Suggested
Quadratic	0.7272	0.5760	-0.8588	
Cubic	0.3242	0.8663	-2.0461	Aliased

Table 3.129: ANOVA for 2FI model for response 3 (Theoretical plate count) for GC method development

Source	Sum of Squares	df	Mean Square	F-value	p-value	
Model	2.330E+06	3	7.767E+05	6.81	0.0324	significant
A-Increment of Temp	7490.67	1	7490.67	0.0657	0.8079	
B-Split Flow	1.204E+06	1	1.204E+06	10.56	0.0227	
AB	1.118E+06	1	1.118E+06	9.81	0.0259	
Residual	5.702E+05	5	1.140E+05			
Cor Total	2.900E+06	8				

The Model F-value of 6.81 implies the model is significant. There is only a 3.24% chance that an F-value this large could occur due to noise. P-values less than 0.0500 indicate model terms are significant. In this case B, AB are significant model terms.

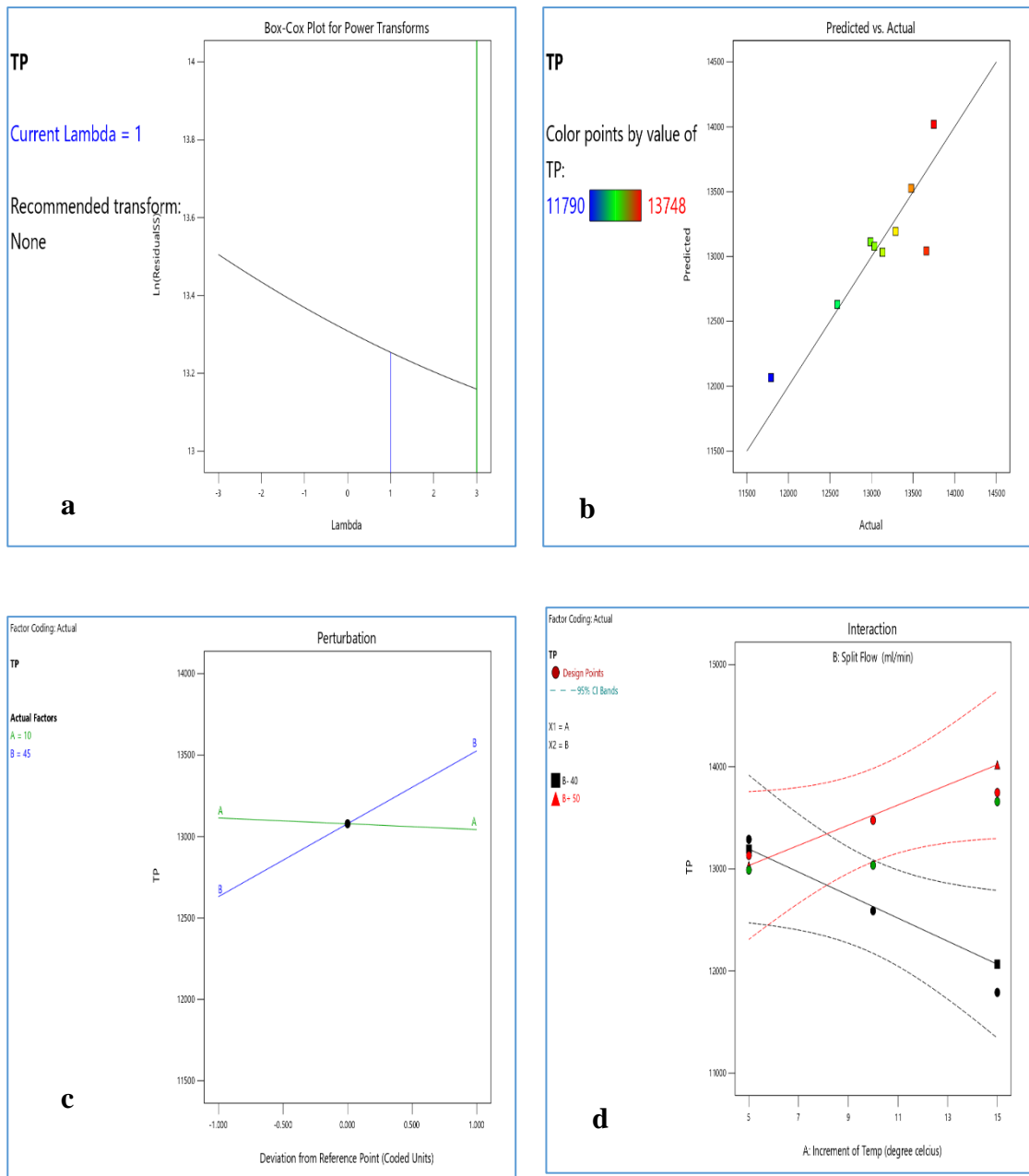


Figure 3.91: (a) Predicted vs actual plot; (b) Box-Cox plot; (c) Perturbation plot; (d) Interaction plot for response 3 (*Theoretical plate count*) of GC method development

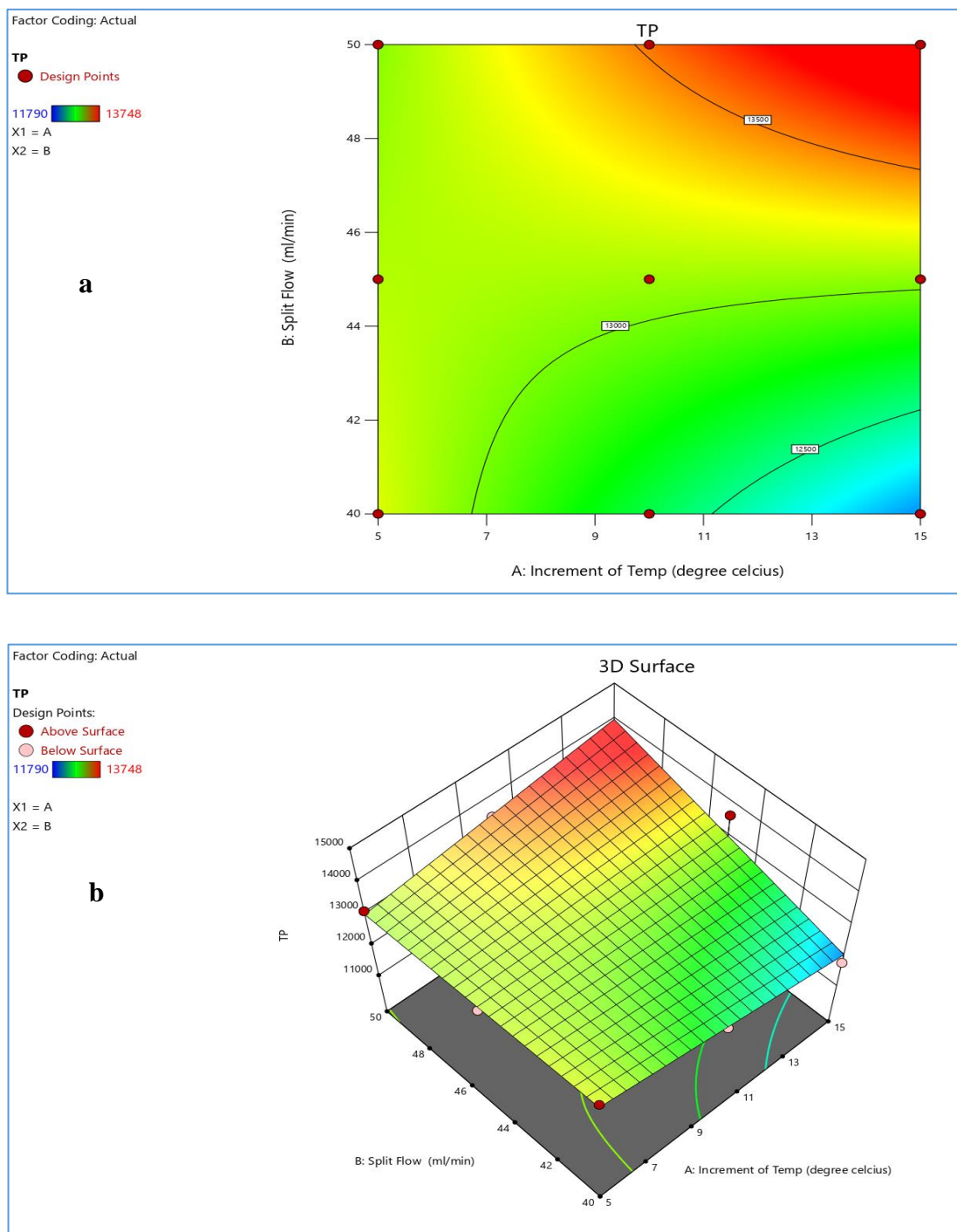


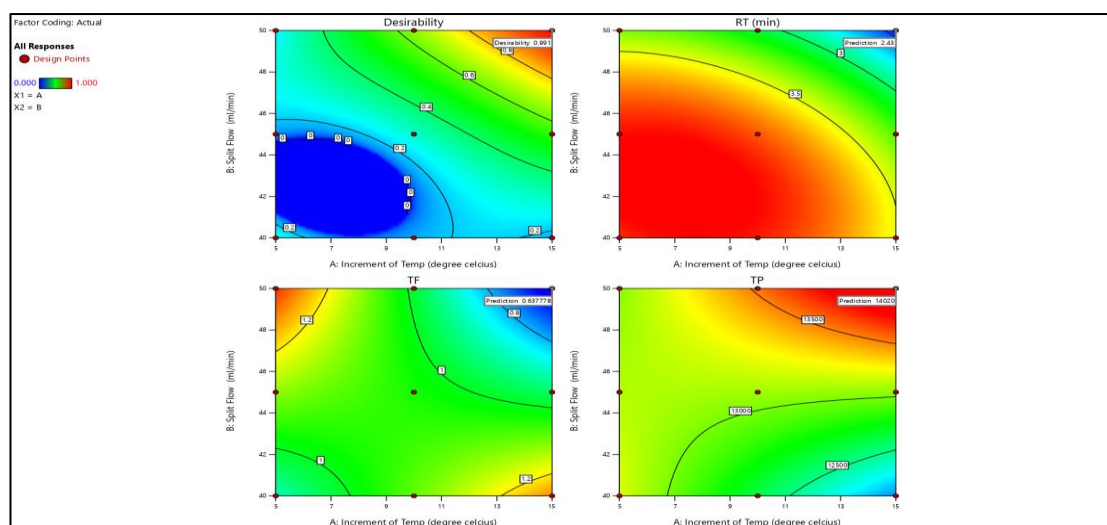
Figure 3.92: (a) Contour plot; (b) 3D response surface plot for response 3 (*Theoretical plate count*) of GC method development

*Optimization of experimental design:***Table 3.130:** Constraints for optimization of developed GC method

Name	Goal	Lower Limit	Upper Limit	Lower Weight	Upper Weight	Importance
A:Increment of Temp	is in range	5	15	1	1	3
B:Split Flow	is in range	40	50	1	1	3
RT	minimize	2.39	3.92	1	1	3
TF	minimize	0.68	1.36	1	1	3
TP	maximize	11790	13748	1	1	3

Table 3.131: Solutions for optimization of developed GC method

Number	Increment of Temp	Split Flow	RT	TF	TP	Desirability	
1	15.000	50.000	2.430	0.638	14019.972	0.991	Selected
2	15.000	49.853	2.464	0.647	13991.249	0.984	
3	14.751	50.000	2.472	0.655	13995.380	0.982	
4	15.000	49.704	2.497	0.656	13962.216	0.976	
5	14.424	50.000	2.526	0.678	13963.127	0.970	
6	5.000	40.000	3.850	0.901	13194.639	0.281	
7	15.000	40.931	3.508	1.209	12248.415	0.241	

**Figure 3.93:** 3D response surface plot for optimization of developed GC method

3.3.17 Validation of developed GC method

3.3.17.1 Linearity and range: A plot of the data as well as the correlation coefficient, y-intercept and slope of the regression line are included below and presented in table 3.132. The lower limit of quantitation was defined as the lowest concentration within the linear range (4.88 ppm). The upper limit of quantitation was defined as the highest concentration within the linear range (1460 ppm for dichloromethane).

Table 3.132: Result of linearity and range for GC method validation

% of Nominal Value		Dichloromethane	
		Concentration (ppm)	Peak areas
50%		49.0	173979
60%		59.0	202231
80%		78.0	263876
100%		98.0	309574
120%		117.0	364560
150%		146.0	457642
R ²	Limit	NLT 0.990	
	Result	0.9957	
Y–Intercept		13635	
Slope of regression line		3064.7	
% of y-intercept compared to 100% area (NMT 5.0%)		4.40	

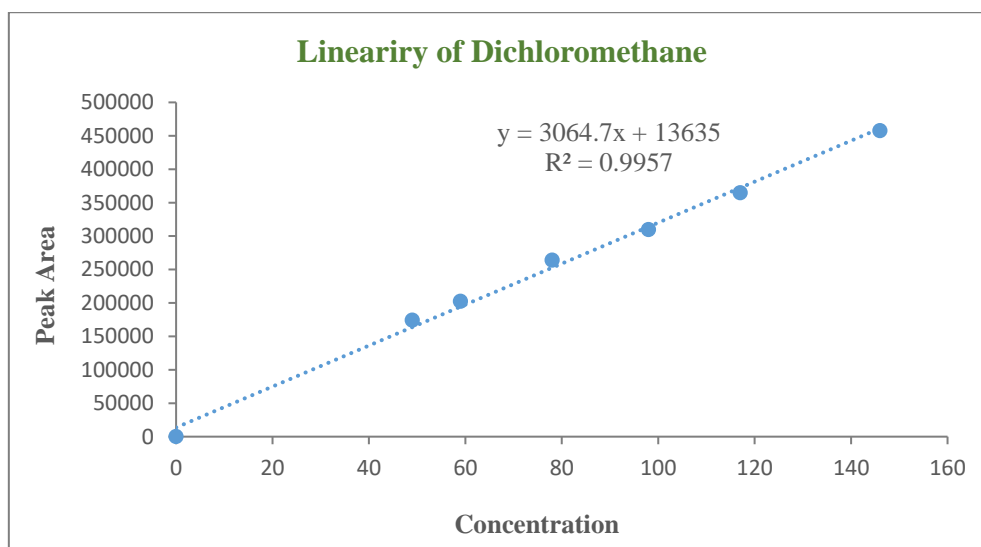


Figure 3.94: Linearity and range study for GC method validation

3.3.17.2 Precision:

Repeatability: The data of repeatability study is presented in table 3.133 below -

Table 3.133: Repeatability result of dichloromethane for GC method validation

Sample	Sample		Peak area of Dichloromethane in Standard	Content (ppm)	%RSD	Limit
	Weight (mg)	Peak area of Dichloromethane				
1	2009	189621	309574	40.337	2.1	RSD NMT 10.0%
2	2001	187394		40.022		
3	2022	190333		40.228		
4	2043	202047		42.265		
5	2024	191108		40.352		
6	2027	190766		40.220		
Average of content (ppm)				40.571		

Intermediate precision: The data of intermediate precision study is presented in table 3.134 below -

Table 3.134: Intermediate precision result of dichloromethane for GC method validation

Sample	Sample		Peak area of Dichloromethane in Standard	Content (ppm)	%RSD	%RSD of 12 samples	Limit
	Weight (mg)	Peak area of Dichloromethane					
Analyst 1	1	2009	309574	40.337	2.1	2.3	RSD NMT 10.0%
	2	2001		40.022			
	3	2022		40.228			
	4	2043		42.265			
	5	2024		40.352			
	6	2027		40.220			
Analyst 2	1	2016	336302	41.068	1.9		
	2	1912		43.177			
	3	1982		41.952			
	4	1998		41.464			
	5	2037		41.337			
	6	2058		41.152			
Average of content (ppm)				41.692			

3.3.17.3 Accuracy: The data of accuracy study is presented in table 3.135 where the accuracy of the method has been found to be 101.12%.

Table 3.135: Accuracy result of dichloromethane for GC method validation

% of Nominal Value	Dichloromethane for spiking			Placebo (mg)	Peak area of Dichloromethane	Recovery	% Recovery	Limit
	Weight (mg)	Concentration ($\mu\text{g/mL}$)	Peak area		Standard			
80%	83.1	83.1	233997	2098	309574	89.14	107.27	80.0% to 120.0%
	82.4	82.4	232342	2022		89.26	108.33	
	80.9	80.9	229338	2059		89.74	110.93	
100%	103.2	103.2	325623	2061		99.88	96.79	
	100.8	100.8	313846	2013		98.56	97.78	
	100.6	100.6	312287	2065		98.27	97.68	
120%	120.2	120.2	442926	2001		116.65	97.05	
	119.7	119.7	441791	2080		116.84	97.61	
	120.6	120.6	443934	1990		116.53	96.62	
Mean							101.12	
SD							5.88	
%RSD							5.82	

3.3.17.4 Specificity: The chromatograms of blank, placebo, standard and test samples shown that all the peaks were all resolved (Figure 3.95).

3.3.17.5 Robustness: The data of robustness study is presented in table 3.136 (Figure 3.96) which indicates that the method is robust.

3.3.17.6 System suitability: The data with acceptance criteria is presented in table 3.137.

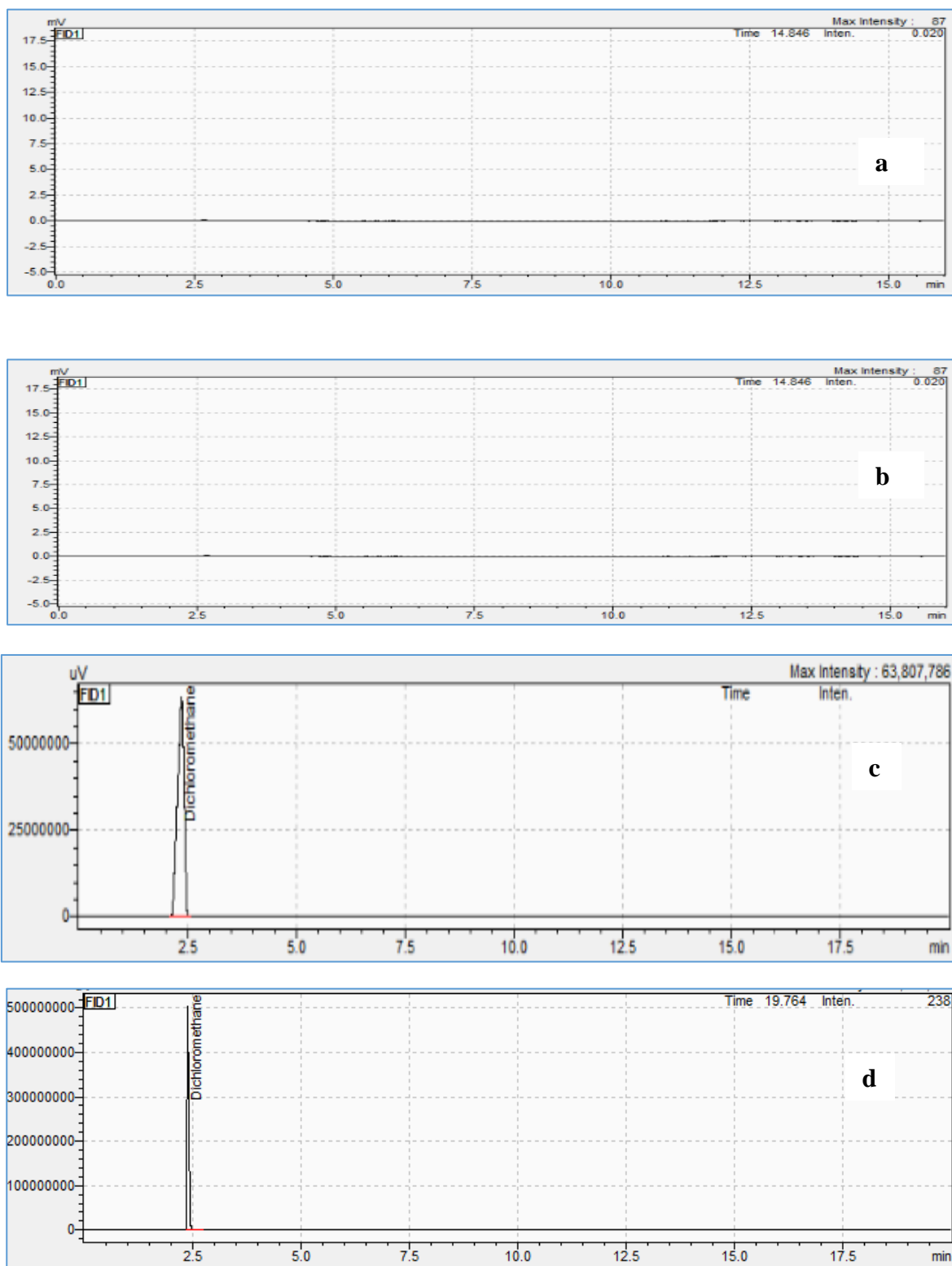


Figure 3.95: Chromatograms for specificity study of GC method (a) Blank; (b) Placebo; (c) Standard; (d) Sample

Table 3.136: Result of robustness study for GC method validation

Test	Result from system suitability		Changed condition of Detector Temperature		Changed condition of hold time at 120°C temperature		Limit
	Detector temp. (250°C)	Column temp. program (as per method)	Detector temp. (245°C)	Detector temp. (255°C)	Detector temp. (250°C)	Column temp. program changed	
Substance	Dichloromethane		Dichloromethane	Dichloromethane	Dichloromethane		
%RSD	2.34		5.32	2.48	3.52		NMT 10%
Tailing factor	0.68		1.491	1.238	1.324		NMT 1.5
Theoretical plates	14019		12617	14141	14139		NLT 5000

Table 3.137: Result of system suitability for GC method validation

Replicate	Peak area of Dichloromethane during system suitability and robustness study					
	Detector temp. (250°C)	Column temp. program (as per method)	Detector temp. (245°C)	Detector temp. (255°C)	Detector temp. (250°C)	Column temp. program changed
1	244154		251992	250035	243386	
2	241328		274576	259810	247349	
3	240869		249237	261380	241560	
4	250167		246620	247841	251178	
5	252886		258349	245563	243552	
6	256037		240173	262780	261025	
Average of area	247574		253491	254568	244337	
SD	63597.1		10901.84	6930.72	6761.09	
%RSD (NMT 10%)	2.34		4.30	2.72	2.77	
Tailing factor (NMT 1.5)	0.68		1.491	1.238	1.324	

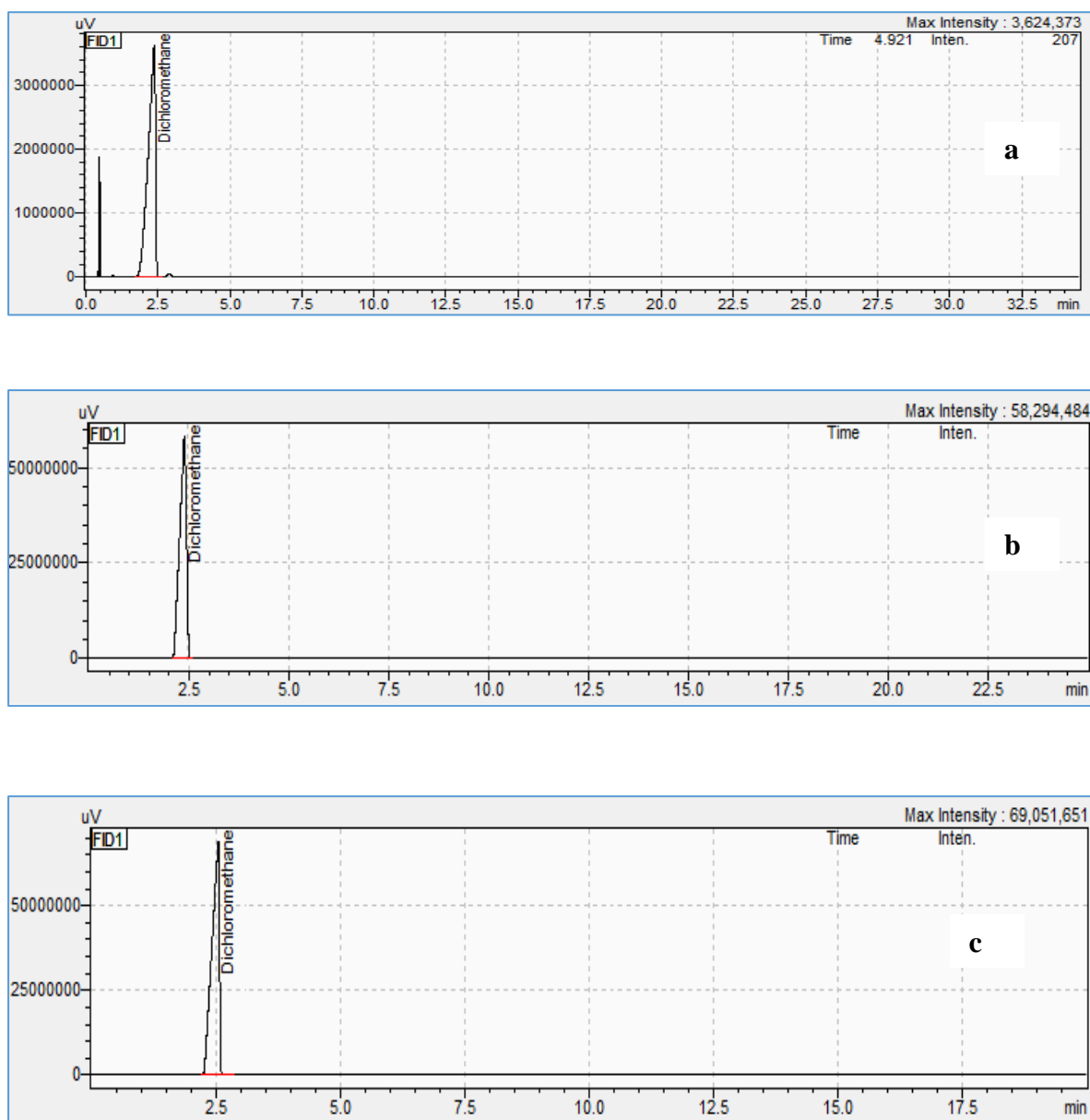


Figure 3.96: Chromatograms for robustness study for GC method validation (a) at Detector Temperature 245°C; (b) at Detector Temperature 255°C; (c) at Changed of Column Temperature Program

From the above test parameters, it can be observed that the linearity and range, precision (repeatability, intermediate), accuracy, specificity, robustness and system suitability of the developed GC method for analysis of residual solvent from the preparation of ledipasvir solid dispersions were found within the required limits. Therefore, as per ICH Q2 (R1) guideline, it can be declared that the developed method is validated and can be applied for the analysis of residual solvents of ledipasvir in dosage forms.

3.3.18 Residual solvent determination of SD formulations

3.3.18.1 Residual ethanol determination of Ledipasvir SD

At first, the residual ethanol of the Ledipasvir solid dispersions F1SD, F2SD, F3SD, F4SD, F5SD, F6SD, F7SD and F8SD were determined after 1 hour of secondary drying at 60°C using loss on drying method (LOD) and the results are presented in the table below:

Table 3.138: % LODs for of F1SD, F2SD, F3SD, F4SD, F5SD, F6SD, F7SD and F8SD after 1 hour of secondary drying

Formulation	%LOD
F1SD	10.0
F2SD	10.8
F3SD	11.40
F4SD	9.7
F5SD	8.5
F6SD	9.3
F7SD	10.6
F8SD	8.9

From the above table 3.138, it was found that F3SD had the highest LOD. It was taken as a representative to optimize the drying time to achieve LOD within limit. Then the drying was continued overnight and samples were taken at 3 hours, 6 hours, 12 hours and 24 hours intervals for LOD checking. The results are listed in the table 3.139 below:

Table 3.139: % LODs of F3SD after different hours of secondary drying

Drying time (hour)	% LOD
1	11.40
3	10.80
6	7.40
12	4.10
24	0.43

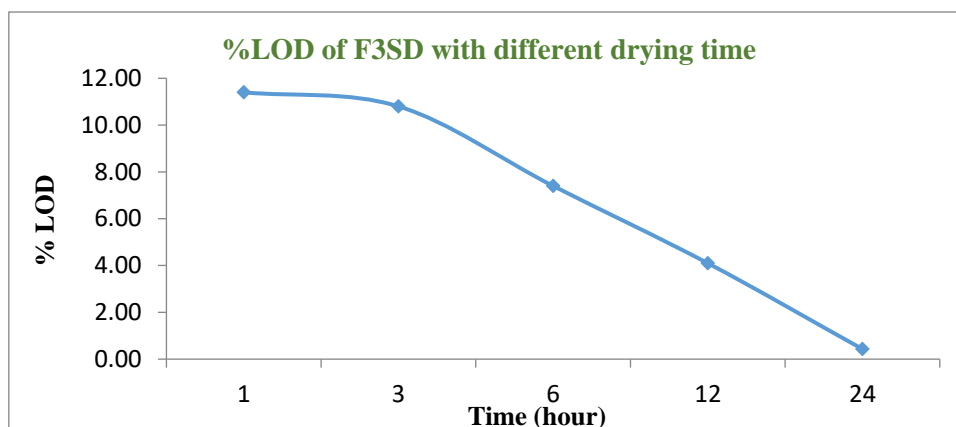


Figure 3.97: % LODs of F3 after different hours of secondary drying

Based on the optimized drying time found for F3SD from above table 3.139, remaining SDs were dried in the vacuum oven for 24 hours at 60°C and the LODs were recorded in the table 3.140.

Table 3.140: % LODs of F1SD, F2SD, F3SD, F4SD, F5SD, F6SD, F7SD and F8SD after 24 hours of secondary drying

Formulation	% LOD	
	1 hour	24 hours
F1SD	10.0	0.41
F2SD	10.8	0.39
F3SD	11.0	0.43
F4SD	9.7	0.29
F5SD	8.5	0.31
F6SD	9.3	0.38
F7SD	10.6	0.46
F8SD	8.9	0.38

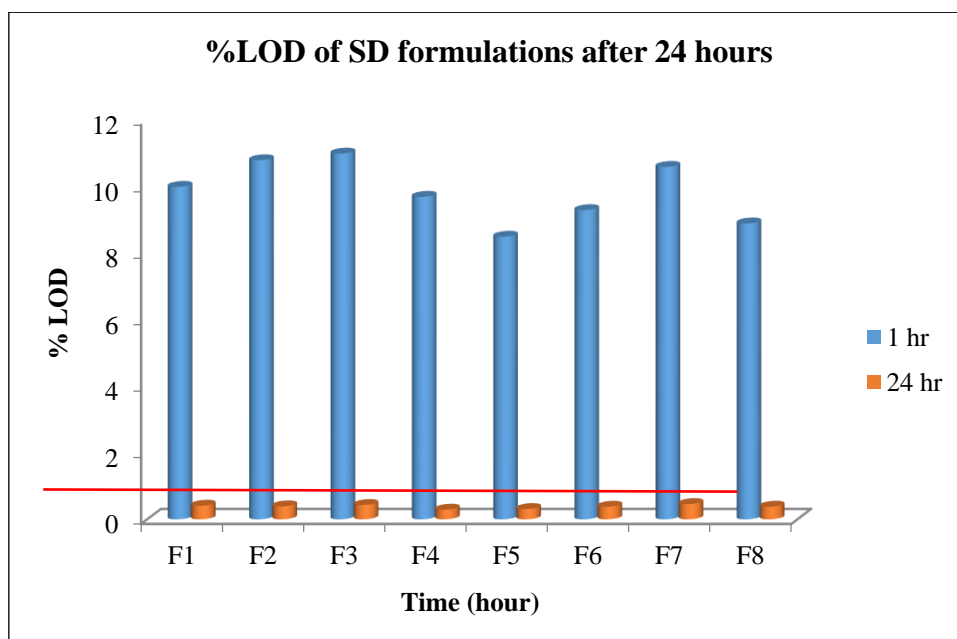


Figure 3.98: % LODs of F1SD, F2SD, F3SD, F4SD F5SD, F6SD, F7SD and F8SD after 24 hours of secondary drying

3.3.18.2 Residual dichloromethane determination of Ledipasvir SD

Initially the contents of Dichloromethane (DCM) were determined after 1 hour and following results were obtained:

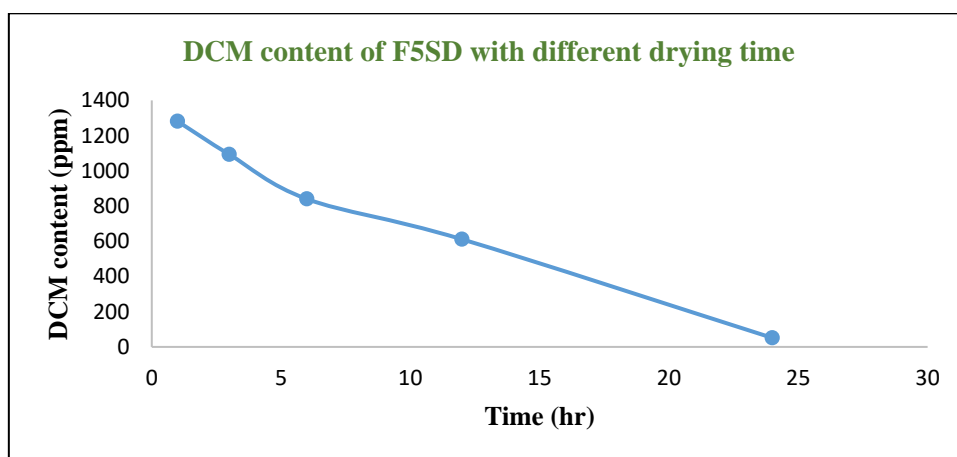
Table 3.141: Dichloromethane content of F5SD and F8SD after 1 hour of secondary drying

Formulation	Dichloromethane (ppm)
F5	1281
F6	1108

From the above table it was found that F5SD had the highest dichloromethane (DCM) content. It was taken as a representative to optimize the drying time to achieve the dichloromethane content within limit. Then the drying was continued overnight in a vacuum oven at 60°C and samples were taken at 3 hours, 6 hours, 12 hours and 24 hours intervals for residual dichloromethane content checking. The results are listed in the Table 3.142 below:

Table 3.142: Dichloromethane content of F5SD after different hours of secondary drying

Drying time (hour)	Dichloromethane (ppm)
1	1281
3	1093
6	840
12	611
24	51

**Figure 3.99:** Dichloromethane content of F5SD after different hours of secondary drying

Based on the optimized drying time found for F5SD from above table 3.142, remaining F8SD was dried in the vacuum oven for 24 hours at 40°C and the DCM contents were recorded in the table 3.143.

Table 3.143: Dichloromethane content of F5SD and F8SD after 24 hours of secondary drying

Formulation	DCM content (ppm)	
	1 hour	24 hour
F5SD	1281	51.0
F6SD	1108	47.6

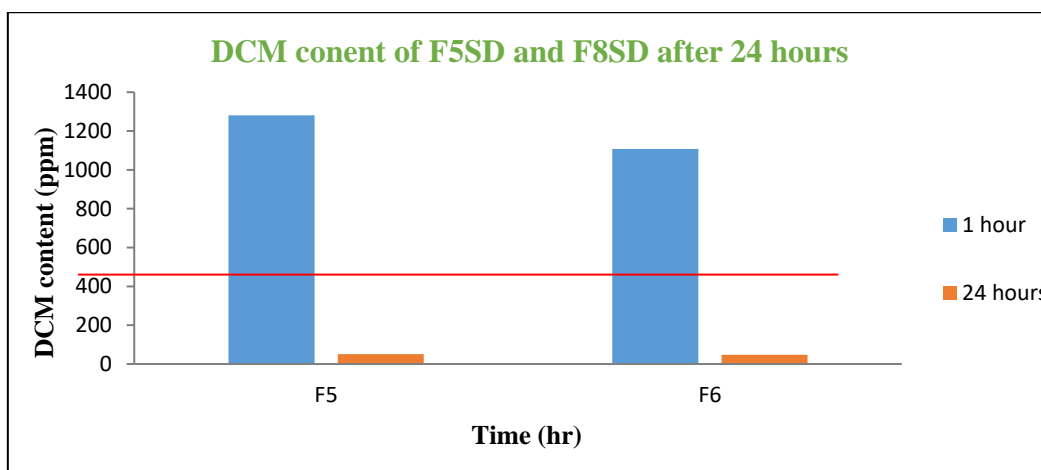


Figure 3.100: Dichloromethane content of F5SD and F8SD after 24 hours of secondary drying

From the results of the residual solvent study, it can be said that after 24 hours of drying at 60°C in a vacuum oven, the residual solvent level of all the SD formulations were found within the acceptable limit.

3.3.18.2 Residual ethanol determination of Velpatasvir SD

The residual ethanol of Velpatasvir solid dispersion, VF1SD was determined after 1 hour of secondary drying at 60°C using loss on drying method (LOD) method. The sample was taken after 24 hours of drying and the result was found 0.39% which is within the limit.

Chapter 4: Overall Discussion and Future Direction

4.1 Discussion on formulation

Inherent properties of Ledipasvir, Daclatasvir and Velpatasvir are their poorly water-soluble natures. Ledipasvir and Daclatasvir belong to BCS class 2 whereas Velpatasvir is a BCS class 4 drugs. Both Ledipasvir and Daclatasvir show high absorption but low dissolution rates. Dissolution is the rate limiting step for oral absorption of these drugs. As Velpatasvir is a BCS class 4 drug, it exhibits a low dissolution and low absorption rate. The bioavailability of Velpatasvir after oral administration is limited owing to its poor dissolution with gradual increment in pH of dissolution media which could limit its bioavailability after oral administration. These drugs exhibit variable bioavailability and need the enhancement in dissolution for increasing the bioavailability.

Currently two dosage forms of Ledipasvir, tablet and pellets, are available in the market. The tablets can be taken with or without food. Pellets can be taken in pediatric patients who cannot swallow the tablet formulation. But the administration of the pellets is complicated. It is indicated to sprinkle the pellets on one or more spoonful of non-acidic soft food at or below room temperature. Examples of non-acidic foods include pudding, chocolate syrup, mashed potato, and ice cream. And then it is advised to take pellets within 30 minutes of mild mixing with food and to swallow the entire contents without chewing to avoid a bitter aftertaste. Therefore, this process is really complicated for those who are unable to swallow tablets.

Currently, Daclatasvir is available in the market as tablet dosage forms only. Velpatasvir is available as tablets and pellets. However, the administration of the pellets is complicated in case of difficulty to swallow. Suitable dosage forms for children and elderly population or patients having difficulty with swallowing are not available at this moment for these drugs.

Therefore, Ledipasvir, Daclatasvir and Velpatasvir are suitable candidates for developing oral liquid suspension dosage forms with improved dissolution and hence, bioavailability. With a view to achieve this objective, solid dispersion based nanosuspensions were prepared and finally stabilized as oral liquid suspensions which can be conveniently administered by geriatric and pediatric population or patients having difficulty with swallowing.

At first, it was tried to prepare simple conventional oral suspensions with micronized and non-micronized Ledipasvir. However, the dissolution studies of these suspensions revealed

that they had poor and incomplete dissolution. Therefore, it was needed to apply advanced solubility enhancement technique to obtain improved and complete dissolution of Ledipasvir in the drug product.

At next, solid dispersions (SD) of Ledipasvir were prepared. To prepare the SDs, excipients like Poloxamer 188, Poloxamer 407, HPC (Klucel™ EF), HPC (Klucel™ EXF), HPMC 5cps, Povidone K17, Povidone K30 and CMC Sodium were selected based on their compatibility studies with Ledipasvir using FTIR and DSC in 1:1 physical binary mixture with each polymer. Afterwards, SDs were prepared for 1:1 drug-polymer ratio. Poloxamer 188, Poloxamer 407, HPC (Klucel™ EXF) and HPMC 5cps were selected for the preparation of nanosuspensions, as Ledipasvir was converted to amorphous form from the crystalline form in the SDs prepared with these polymers. In order to prepare the nanosuspensions, at first, SDs were prepared with different ratio of Ledipasvir and selected polymers following QBD approach using D-optimal design. Then the prepared nanosuspensions were evaluated for viscosity, zeta potential, particle size distribution (PSD), polydispersity index (PDI) and redispersibility. From the PSD and PDI studies, it was found that preparations with different ratios of Poloxamer 188 and Poloxamer 407 produced acceptable results i.e. they produced nanosuspensions. From the viscosity, zeta potential and redispersibility studies, it was found that all the prepared nanosuspensions were physically unstable due to very low viscosity, zeta potential and hardening of sediment resulting in inability to redisperse. However, the best results were found with Poloxamer 188 (NSF1a) and Poloxamer 407 (NFS2a) at a ratio of 0.7:1.3 for API:polymer in terms of PSD and PDI. Then best prepared nanosuspensions, NSF1a and NFS2a were stabilized by increasing viscosity, incorporating a gel network and altering the surface activity i.e. zeta potential through inclusion of a suspension vehicle. The suspension vehicle was developed using Box-Behnken design. Unstable nanosuspensions, NSF1a and NFS2a were incorporated in the optimized suspension vehicle. Formulated suspensions of Ledipasvir, FNSF1a and FNFS2a were evaluated for viscosity, zeta potential, assay, dissolution and all the test results were satisfactory. Comparative dissolution profiling was done for FNSF1a, FNFS2a, market product 2 (MP1), suspensions with micronized and non-micronized Ledipasvir against the market product 1 (MP1). The results were evaluated for difference factor (f_1), similarity factor (f_2) and dissolution efficiency (% DE) and all of them had different dissolution profiles compared to the market product 1. Formulated

suspensions, FNSF1a and FNSF2a had significantly faster dissolution rate whereas market product 2 (MP2), suspension with micronized and non-micronized Ledipasvir had substantially slower dissolution rate compared to the market product 1 (MP1). Sedimentation volume of the Formulated suspensions, FNSF1a and FNSF2a were checked and it was found that they were highly flocculated suspensions with excellent redispersibility up to 6 months. At the same time, *in-vivo* simulation was done with the help of PKSolver[®] it was found that the absorption of Ledipasvir was similar to that of the market product 1 (MP1) for a dose of 90mg whereas its absorption increased 1.65 fold for formulated suspensions, FNSF1a and 1.31 fold for FNSF2a compared to the market product, MP1 for a dose of 270mg. Finally, stability study was conducted for FNSF1a and FNSF2a at accelerated conditions up to six months and samples were picked at 3 months and 6 months timepoints to check zeta potential, redispersibility, assay and dissolution. Both the suspensions had satisfactory zeta potential for a stable suspension and good redispersibility even after 6 months. Similar dissolution profiles were found for both FNSF1a and FNSF2a suspensions after 3 months and 6 months time points when compared to the initial test results using difference factor (f_1), similarity factor (f_2) and dissolution efficiency (% DE). The assay content of Ledipasvir was found satisfactory after 3 and 6 months for both FNSF1a and FNSF2a suspensions with no significant change in the assay as per ICH Q1 (R2) guideline. The assay results of both the formulated suspensions at all time points (initial, 3 and 6 months) were also statistically evaluated by ANOVA and paired t-test. For both statistical tests, the p values were higher than 0.05 which indicates that there were no significant differences between the assay results of Ledipasvir i.e. they were similar.

At next, solid dispersion of Daclatasvir and Velpatasvir were prepared by same process that was used for preparing the solid dispersions of Ledipasvir where Poloxamer 188 was selected as polymer because the formulated suspension, FNSF1a produced best results in the *in-vivo* simulation study. Both Daclatasvir and Velpatasvir were compatible with Poloxamer 188 based on the FTIR and DSC study in 1:1 binary physical mixture. Afterwards, solid dispersions of Daclatasvir and Velpatasvir were prepared with Poloxamer 188 in a 1:1 ratio of API and polymer for both drugs separately. In case of Daclatasvir, the drug failed to produce amorphous solid dispersion and hence, was not further evaluated for nanosuspension preparation as amorphous form gives higher dissolution than the

crystalline form. On the other hand, Velpatasvir produced amorphous solid dispersion and therefore, was selected for the preparation of nanosuspension. To prepare the Velpatasvir nanosuspension VNSF1a, the same polymer and same process that was used for the preparation of Ledipasvir nanosuspension NSF1a, was followed. Then the prepared nanosuspension was evaluated for viscosity, zeta potential, particle size distribution (PSD), polydispersity index (PDI) and redispersibility. The outcome of PSD and PDI studies revealed that VNSF1a was a nanosuspension. From the viscosity, zeta potential and redispersibility studies, it was found that all the prepared nanosuspensions were physically unstable due to very low viscosity, zeta potential and hard cake formation resulting in inability to redisperse. Then the prepared nanosuspension of Velpatasvir, VNSF1a was stabilized by the same manner through incorporation into the same optimized suspension vehicle that was used to stabilize the Ledipasvir nanosuspension. The formulated suspension of Velpatasvir was evaluated for viscosity, zeta potential, assay, dissolution and all the test results were satisfactory. Comparative dissolution profiling was done for VFNSF1a against the market product 3 (MP3). The results were evaluated for difference factor (f_1), similarity factor (f_2) and dissolution efficiency (% DE) and it was found that the formulated suspension of Velpatasvir, VNSF1a had different dissolution profile than the market product 3 (MP3). VFNSF1a had significantly faster dissolution rate than market product 3 (MP3). The study of the pharmacokinetic parameters (C_{max} , AUC) using PKSolver[®] pointed that in case of single dose study (100mg dose), the absorption of Velpatasvir increased around 3 fold for the formulated suspension, VFNSF1a compared to the market product 3 (MP3).

4.2 Discussion on analytical methods

A RP-HPLC method was developed using 3^2 full factorial design to analyze Ledipasvir content in pharmaceutical dosage forms which consisted of buffer:acetonitrile as 48:52 ratio and a flow rate of 1.7 ml/min. Later on, a simple UV method was developed for the compound using Methanol blank at 333 nm wavelength which was also found equivalent to the developed RP-HPLC method where the equivalency was established using ANOVA, paired t-test and paired equivalence tests. A UV dissolution method was developed using Methanol as blank at 333 nm. A GC method was developed during the study to detect the amount of residual solvent in the preparations using 3^2 full factorial design. All the developed methods were validated using ICH Q2 (R1) guidelines.

4.3 Future Direction

The data of *in-vivo* simulation and *in-vitro* dissolution can be used for future dose adjustment of Ledipasvir and Velpatasvir. However, these predictions were based on computer generated simulation studies and more insights are needed on this topic based on actual *in-vivo* study. As the developed suspensions for Ledipasvir and Velpatasvir exhibited promising characteristics, these can be further recommended for *in vivo* studies.

5. References

- . T. C., . D. S., . N., & . D. S. (2012). A Review on Nanosuspensionspromising Drug Delivery Strategy. *Journal of Current Pharma Research*, 3(1).
- AAT Bioquest, I. (2020). *Citrate Buffer (pH 3.0 to 6.2) Preparation*.
- Abdul-Fattah, A. M., & Bhargava, H. N. (2002). Preparation and in vitro evaluation of solid dispersions of halofantrine. *International Journal of Pharmaceutics*, 235(1–2).
- Abood, A. N. (2016). Preparation and in vitro Evaluation of Acyclovir Suspension. *Kerbala Journal of Pharmaceutical Sciences*, 11.
- Agilent Technologies. (2018). *Application Specific GC Columns DB-624 Columns*. <https://www.agilent.com/en/product/gc-columns/application-specific-gc-columns/db-624-columns#features>
- Agrawal, Y., & Patel, V. (2011). Nanosuspension: An approach to enhance solubility of drugs. *Journal of Advanced Pharmaceutical Technology & Research*, 2(2).
- Allam, A. N., El gamal, S. S., & Naggar, V. F. (2011). Bioavailability : A Pharmaceutical Review Bioavailability. *Novel Drug Deliv Tech*, 1(1).
- Anderson, N. H., Bauer, M., Boussac, N., Khan-Malek, R., Munden, P., & Sardaro, M. (1998). An evaluation of fit factors and dissolution efficiency for the comparison of in vitro dissolution profiles. *Journal of Pharmaceutical and Biomedical Analysis*, 17(4–5).
- Anne Marie Helmenstine. (2019). *Definition of Zeta Potential*. Science, Tech, Math. <https://www.thoughtco.com/definition-of-zeta-potential-605810>
- Asawahame, C., Sutjarittangtham, K., Eitssayeam, S., Tragoolpua, Y., Sirithunyalug, B., & Sirithunyalug, J. (2015). Formation of orally fast dissolving fibers containing propolis by electrospinning technique. *Chiang Mai Journal of Science*, 42(2).
- Ashland. (2017). *KlucelTM hydroxypropylcellulose Physical and chemical properties*.
- Attari, Z., Kalvakuntla, S., Reddy, M. S., Deshpande, M., Rao, C. M., & Koteswara, K. B. (2016). Formulation and characterisation of nanosuspensions of BCS class II and IV drugs by combinative method. *Journal of Experimental Nanoscience*, 11(4).
- Bagaglio, S., Uberti-Foppa, C., & Morsica, G. (2017). Resistance Mechanisms in Hepatitis C Virus: implications for Direct-Acting Antiviral Use. *Drugs*, 77(10).
- Baishya, H. (2017). Application of Mathematical Models in Drug Release Kinetics of Carbidopa and Levodopa ER Tablets. *Journal of Developing Drugs*, 06(02).
- Batchelor, H. K., & Marriott, J. F. (2015). Formulations for children: Problems and solutions.

References

- British Journal of Clinical Pharmacology*, 79(3).
- Battu, P. R., & Reddy, M. S. (2009). Residual solvents determination by HS-GC with flame ionization detector in Omeprazole pharmaceutical formulations. *International Journal of PharmTech Research*, 1(2).
- Behera, S. (2012). UV-Visible Spectrophotometric Method Development and Validation of Assay of Paracetamol Tablet Formulation. *Journal of Analytical & Bioanalytical Techniques*, 03(06).
- Bharate, S. S. (2021). Recent developments in pharmaceutical salts: FDA approvals from 2015 to 2019. In *Drug Discovery Today* (Vol. 26, Issue 2).
- Bosselmann, S., & Williams, R. O. (2012). Has nanotechnology led to improved therapeutic outcomes? In *Drug Development and Industrial Pharmacy* (Vol. 38, Issue 2).
- Bristol-Myers Squibb Company. (2017). *DAKLINZA™ (Daclatasvir) tablets, for oral use*.
- Broman, E., Khoo, C., & Taylor, L. S. (2001). A comparison of alternative polymer excipients and processing methods for making solid dispersions of a poorly water soluble drug. *International Journal of Pharmaceutics*, 222(1).
- Bugay, D. E. (2001). Characterization of the solid-state: Spectroscopic techniques. *Advanced Drug Delivery Reviews*, 48(1).
- Cada, D. J., Baker, D. E., & Bindler, R. J. (2015). Ledipasvir/sofosbuvir. In *Hospital Pharmacy* (Vol. 50, Issue 3).
- CDER/FDA. (2014). *APPLICATION NUMBER: 205834Orig1s000 CLINICAL PHARMACOLOGY AND BIOPHARMACEUTICS REVIEW(S)*.
- CDER/FDA. (2015). Guidance for Industry, Waiver of in vivo bioavailability and bioequivalence studies for immediate release solid oral dosage forms based on a biopharmaceutics classification system. *Center for Drug Evaluation and Research*, May.
- Chasteen, T. G. (2000). Split / Splitless Gas Chromatography Injection. *Department of Chemistry, Sam Houston State University*.
- Chouhan, P., & Saini, T. R. (2016). D-optimal design and development of microemulsion based transungual drug delivery formulation of ciclopirox olamine for treatment of onychomycosis. *Indian Journal of Pharmaceutical Sciences*, 78(4).
- Chow, S. C. (2014). Bioavailability and bioequivalence in drug development. *Wiley Interdisciplinary Reviews: Computational Statistics*, 6(4).
- Chrominfo. (2020). *Advantages and disadvantages of solid dosage form*.

References

- <https://chrominfo.blogspot.com/2020/07/advantages-and-disadvantages-of-solid.html>
- Das, V., Bhairav, B., & Saudagar, R. B. (2017). Quality by design approaches to analytical method development. In *Research Journal of Pharmacy and Technology* (Vol. 10, Issue 9).
- Deicke, A., & Süverkrüp, R. (1999). Dose uniformity and redispersibility of pharmaceutical suspensions. I: Quantification and mechanical modelling of human shaking behaviour. *European Journal of Pharmaceutics and Biopharmaceutics*, 48(3).
- Deshiikan, S. R., & Papadopoulos, K. D. (1998). Modified Booth equation for the calculation of zeta potential. *Colloid and Polymer Science*, 276(2).
- Dey, R., & Chowdhury, D. R. (2020). Review of Pharmaceutical Solid Polymorphism: Preparation, Characterization and Influence on Performance of Drugs. *Journal of Advances in Bio- Pharmaceutics and Pharmacovigilance*, 2(1).
- Dheyab, M. A., Aziz, A. A., Jameel, M. S., Noqta, O. A., Khaniabadi, P. M., & Mehrdel, B. (2020). Simple rapid stabilization method through citric acid modification for magnetite nanoparticles. *Scientific Reports*, 10(1).
- DOW. (2002). METHOCEL Cellulose Ethers. *Technical Handbook*.
- Drugbank. (2014a). *Ledipasvir*. <https://go.drugbank.com/drugs/DB09027>
- Drugbank. (2014b). *Ledipasvir*.
- Drugbank. (2015a). *Daclatasvir*. <https://go.drugbank.com/drugs/DB09102>
- Drugbank. (2015b). *Daclatasvir*.
- Drugbank. (2016a). *Velptatasvir*. <https://go.drugbank.com/drugs/DB11613>
- Drugbank. (2016b). *Velptatasvir*.
- Eguchi, N., Kawabata, K., & Goto, H. (2017). Electrochemical Polymerization of 4,4-Dimethyl-2,2'-Bithiophene in Concentrated Polymer Liquid Crystal Solution. *Journal of Materials Science and Chemical Engineering*, 05(02).
- El-Say, K., Refaey, T., Samy, A., & Badawi, A. (2011). Box-Behnken Design For Optimization Of Formulation Variables To Improve The Flowability And Compressibility Of Bezafibrate. *Arizona Journal of Pharmaceutical Science*, 43(January).
- Elliott, J. P., McConaha, J., Cornish, N., Bunk, E., Hilton, L., Modany, A., & Bucker, I. (2014). Influence of viscosity and consumer use on accuracy of oral medication dosing devices. *Journal of Pharmacy Technology*, 30(4).
- EMA. (2014). *Human medicines European public assessment report (EPAR): Harvoni*,

References

- ledipasvir 90 mg / sofosbuvir 400 mg, Hepatitis C, Chronic, Date of authorisation: 17/11/2014, Revision: 16, Status: Authorised.*
- EMA/CHMP/VWP/164653/2005. (2010). Committee for Medicinal Products for Human Use - Remdesivir. *Emea*, 44(December).
- European Medicines Agency. (2014). *Assessment Report Harvoni*.
- European Medicines Agency. (2015). *Assessment report Daklinza*.
- European Medicines Agency. (2016). *Assessment Report Epclusa*.
- Factorial designs.* (n.d.). <https://www.fox.temple.edu/wp-content/uploads/2016/05/Factorial-Designs.pdf>
- FACTORS AFFECTING DRUG ABSORPTION.* (n.d.).
- Fakes, M. G., Vakkalagadda, B. J., Qian, F., Desikan, S., Gandhi, R. B., Lai, C., Hsieh, A., Franchini, M. K., Toale, H., & Brown, J. (2009). Enhancement of oral bioavailability of an HIV-attachment inhibitor by nanosizing and amorphous formulation approaches. *International Journal of Pharmaceutics*, 370(1–2).
- Ferreira, S. L. C., Bruns, R. E., Ferreira, H. S., Matos, G. D., David, J. M., Brandão, G. C., da Silva, E. G. P., Portugal, L. A., dos Reis, P. S., Souza, A. S., & dos Santos, W. N. L. (2007). Box-Behnken design: An alternative for the optimization of analytical methods. In *Analytica Chimica Acta* (Vol. 597, Issue 2).
- FMC. (2003). *PRODUCT OVERVIEW: Avicel® RC-591*.
- Forster, A., Hemenstall, J., & Rades, T. (2010). Characterization of glass solutions of poorly water-soluble drugs produced by melt extrusion with hydrophilic amorphous polymers. *Journal of Pharmacy and Pharmacology*, 53(3).
- Gao, L., Zhang, D., & Chen, M. (2008). Drug nanocrystals for the formulation of poorly soluble drugs and its application as a potential drug delivery system. In *Journal of Nanoparticle Research* (Vol. 10, Issue 5).
- Gassmann, P., List, M., Schweitzer, A., & Sucker, H. (1994). Hydrosols - Alternatives for the parenteral application of poorly water soluble drugs. *European Journal of Pharmaceutics and Biopharmaceutics*, 40(2).
- Gaumet, M., Vargas, A., Gurny, R., & Delie, F. (2008). Nanoparticles for drug delivery: The need for precision in reporting particle size parameters. In *European Journal of Pharmaceutics and Biopharmaceutics* (Vol. 69, Issue 1).
- Gilead Sciences, I. (2014). *Harvoni (ledipasvir and sofosbuvir) tablets, for oral use. US prescribing information*.

References

- Gilead Sciences, I. (2016). *EPCLUSA® (sofosbuvir and velpatasvir) tablets, for oral use*.
- Gillespie, W. R. (1997). Convolution-based approaches for in vivo-in vitro correlation modeling. *Advances in Experimental Medicine and Biology*, 423.
- Graeser, K. A., Patterson, J. E., Zeitler, J. A., & Rades, T. (2010). The role of configurational entropy in amorphous systems. *Pharmaceutics*, 2(2).
- Gras, K., Lee, C. G., & Vickers, A. (2014). Agilent J&W DB-624 UI Ultra Inert GC Capillary Column for Challenging Industrial Applications. *Agilent Technologies*.
- Grodowska, K., & Parczewski, A. (2010). Analytical methods for residual solvents determination in pharmaceutical products. In *Acta Poloniae Pharmaceutica - Drug Research* (Vol. 67, Issue 1).
- Gumustas, M., Sengel-Turk, C. T., Gumustas, A., Ozkan, S. A., & Uslu, B. (2017). Effect of Polymer-Based Nanoparticles on the Assay of Antimicrobial Drug Delivery Systems. In *Multifunctional Systems for Combined Delivery, Biosensing and Diagnostics*.
- Gupta, P., Kakumanu, V. K., & Bansal, A. K. (2004). Stability and solubility of celecoxib-PVP amorphous dispersions: A molecular perspective. *Pharmaceutical Research*,
- Gustafsson, C., Nyström, C., Lennholm, H., Bonferoni, M. C., & Caramella, C. M. (2003). Characteristics of hydroxypropyl methylcellulose influencing compactibility and prediction of particle and tablet properties by infrared spectroscopy. *Journal of Pharmaceutical Sciences*, 92(3).
- Hasan, M. N., Shahriar, S. M. S., Mondal, J., Nurunnabi, M., & Lee, Y. (2021). Bioinspired and biomimetic materials for oral drug delivery. In *Bioinspired and Biomimetic Materials for Drug Delivery*.
- Hashim, H. O. (2019). *chromatography and HPLC principles*.
- Heimbach, T., Fleisher, D., & Kaddoumi, A. (2007). Overcoming Poor Aqueous Solubility of Drugs for Oral Delivery. In *Prodrugs*.
- Hercules. (1999). *AQUALON® Sodium Carboxymethylcellulose Physical and Chemical Properties*.
- Hercules. (2001). *Klucel® Hydroxypropylcellulose*.
- Hörter, D., & Dressman, J. B. (1997). Influence of physicochemical properties on dissolution of drugs in the gastrointestinal tract. In *Advanced Drug Delivery Reviews* (Vol. 25, Issue 1).
- Howlader, M. S. I., Chakrabarty, J. K., Faisal, K. S., Kumar, U., Sarkar, M. R., & Khan, M. F. (2012). Enhancing dissolution profile of diazepam using hydrophilic polymers by

References

- solid dispersion technique. *International Current Pharmaceutical Journal*, 1(12).
- Hughes, B. L., Page, C. M., & Kuller, J. A. (2017). Hepatitis C in pregnancy: screening, treatment, and management. *American Journal of Obstetrics and Gynecology*, 217(5).
- Hughes, D. L. (2016). Patent Highlights: Recently Approved HCV NS5a Drugs. *Organic Process Research and Development*, 20(8).
- ICH. (2019). ICH guideline Q3C (R6) on impurities: Guideline for Residual Solvents. *International Conference on Harmonization of Technical Requirements for Registration of Pharmaceuticals for Human Use*, 31(August).
- ICH guideline Q1A(R2). (2003). ICH Harmonised Tripartite Guideline, Stability Testing of New Drug Substances and Products. *Current Step 4, February*.
- Islam, S., Dey, L. R., Shahriar, M., Dewan, I., & Islam, S. A. (2013). Enhancement of Dissolution Rate of Gliclazide Using Solid Dispersions: Characterization and Dissolution Rate Comparison. *Bangladesh Pharmaceutical Journal*, 16(1).
- Ita, K. (2020). Microemulsions. In *Transdermal Drug Delivery*.
- Jacob, S., Nair, A. B., & Shah, J. (2020). Emerging role of nanosuspensions in drug delivery systems. In *Biomaterials Research* (Vol. 24, Issue 1).
- Jacobs, C., & Müller, R. H. (2002). Production and characterization of a budesonide nanosuspension for pulmonary administration. *Pharmaceutical Research*, 19(2).
- Jagadeesan, R., & Radhakrishnan, M. (2013). Novel approaches in the preparation of solid dispersion on solubility: A review. In *International Journal of Pharmacy and Pharmaceutical Sciences* (Vol. 5, Issue 3).
- Jena, B. R., Panda, S. P., Umasankar, K., Swain, S., Koteswara Rao, G. S. N., Damayanthi, D., Ghose, D., & Pradhan, D. P. (2020). Applications of QbD-based Software's in Analytical Research and Development. *Current Pharmaceutical Analysis*, 17(4).
- Kachrimanis, K., Fucke, K., Noisternig, M., Siebenhaar, B., & Griesser, U. J. (2008). Effects of moisture and residual solvent on the phase stability of orthorhombic paracetamol. *Pharmaceutical Research*, 25(6).
- Kannao, S. U. B. B. (2014). SOLID DISPERSION – A TECHNIQUE FOR SOLUBILITY ENHANCEMENT OF WEAKLY WATER SOLUBLE DRUG –A REVIEW. *Indo American Journal of Pharmaceutical Research*, 04(06).
- Kaplan, S. A. (1972). Biopharmaceutical considerations in drug formulation design and evaluation. *Drug Metabolism Reviews*, 1(1).
- Karant, H., Shenoy, V. S., & Murthy, R. R. (2006). Industrially feasible alternative

References

- approaches in the manufacture of solid dispersions: A technical report. *AAPS PharmSciTech*, 7(4).
- Karmoker, J. R., Priya, R. J., Sarkar, S., & Islam, S. (2017). Comparative in vitro equivalence evaluation of some local Gliclazide brands of Bangladesh. *The Pharma Innovation Journal TPI*, 6(3).
- Kerč, J., & Srčič, S. (1995). Thermal analysis of glassy pharmaceuticals. *Thermochimica Acta*, 248(C).
- Kocbek, P., Baumgartner, S., & Kristl, J. (2006). Preparation and evaluation of nanosuspensions for enhancing the dissolution of poorly soluble drugs. *International Journal of Pharmaceutics*, 312(1–2).
- Kumar, A., Sharma, S., & Kamble, R. (2010). Self emulsifying drug delivery system (SEDDS): Future aspects. *International Journal of Pharmacy and Pharmaceutical Sciences*, 2(SUPPL. 4).
- Kumar Sarangi, M., Singh, N., & Bhagwan Singh, S. P. (2018). A Comparative Study of Solubility Enhancement of Aceclofenac by Solid Dispersion Technique Using Several Polymers. *J Appl Pharm*, 10.
- Larsson, M., Hill, A., & Duffy, J. (2012). Suspension stability: Why particle size, zeta potential and rheology are important Product Technical Specialists Rheometry Products Malvern Instruments Limited. *Annual Transactions of the Nordic Rheology Society*, 20(1988).
- Leuner, C., & Dressman, J. (2000). Improving drug solubility for oral delivery using solid dispersions. In *European Journal of Pharmaceutics and Biopharmaceutics* (Vol. 50, Issue 1).
- Liversidge, G. G., Cundy, K. C., Bishop, J. F., & Czekai, D. A. (1992). *Surface modified drug nanoparticles* (Patent No. US5145684).
- M Manohar, Jomy Joseph, T. S. (2013). Application of Box Behnken design to optimize the parameters for turning Inconel 718 using coated carbide tools. *International Journal of Scientific and Engineering Research*, 4(4).
- Mahato, R. I., & Narang, A. S. (2011). *Pharmaceutical Dosage Forms and Drug Delivery*. In *Pharmaceutical Dosage Forms and Drug Delivery*.
- Mahdavinia, G. R., Ettehadi, S., Amini, M., & Sabzi, M. (2015). Synthesis and characterization of hydroxypropyl methylcellulose-g-poly(acrylamide)/LAPONITE® RD nanocomposites as novel magnetic- and pH-sensitive carriers for controlled drug

References

- release. *RSC Advances*, 5(55).
- Malakar, J., & Nayak, A. K. (2012). Formulation and statistical optimization of multiple-unit ibuprofen-loaded buoyant system using 23-factorial design. *Chemical Engineering Research and Design*, 90(11), 1834–1846.
- Malinowski, H., Marroum, P., Uppoor, V. R., Gillespie, W., Ahn, H. Y., Lockwood, P., Henderson, J., Baweja, R., Hossain, M., Fleischer, N., Tillman, L., Hussain, A., Shah, V., Dorantes, A., Zhu, R., Sun, H., Kumi, K., Machado, S., Tammara, V., ... Williams, R. (1997). FDA guidance for industry extended release solid oral dosage forms: Development, evaluation, and application of in vitro/in vivo correlations. *Dissolution Technologies*, 4(4).
- Mara, C. A., & Cribbie, R. A. (2012). Paired-samples tests of equivalence. *Communications in Statistics: Simulation and Computation*, 41(10).
- Mastanamma, S. K., Chandini, S. K., Reehana, S. K., & Saidulu, P. (2018). Development and validation of stability indicating RP-HPLC method for the simultaneous estimation of Sofosbuvir and Ledipasvir in bulk and their combined dosage form. *Future Journal of Pharmaceutical Sciences*, 4(2).
- Mathematical models of drug release. (2015). In *Strategies to Modify the Drug Release from Pharmaceutical Systems*.
- McEwan, P., Bennett, H., Ward, T., Webster, S., Gordon, J., Kalsekar, A., Yuan, Y., & Brenner, M. (2016). The cost-effectiveness of daclatasvir-based regimens for the treatment of hepatitis C virus genotypes 1 and 4 in the UK. *European Journal of Gastroenterology and Hepatology*, 28(2).
- Mehmood, Y., Khan, I. U., Shahzad, Y., Khan, R. U., Iqbal, M. S., Khan, H. A., Khalid, I., Yousaf, A. M., Khalid, S. H., Asghar, S., Asif, M., Hussain, T., & Shah, S. U. (2020). In-vitro and in-vivo evaluation of velpatasvir-loaded mesoporous silica scaffolds. A prospective carrier for drug bioavailability enhancement. *Pharmaceutics*, 12(4).
- Michael E. Aulton, & Kevin M. G. Taylor. (2017). Aulton's Pharmaceutics The Design and Manufacture of Medicines. In *BMC Public Health* (Vol. 5, Issue 1).
- Mirza R Baig, A. S. and S. K. (2018). Sensible use of technologies to increase solubility and bioavailability in formulation development. *Advancements In Bioequivalence & Bioavailability*.
- Mohamad Zen, N. I., Abd Gani, S. S., Shamsudin, R., & Fard Masoumi, H. R. (2015). The use of D-optimal mixture design in optimizing development of okara tablet formulation

References

- as a dietary supplement. *Scientific World Journal*, 2015.
- Mohammed, N. N., Majumdar, S., Singh, A., Deng, W., Murthy, N. S., Pinto, E., Tewari, D., Durig, T., & Repka, M. A. (2012). Kluce1™ EF and ELF polymers for immediate-release oral dosage forms prepared by melt extrusion technology. *AAPS PharmSciTech*, 13(4).
- Müller, R. H., Peters, K., Becker, R., & Kruss, B. (1995). Nanosuspensions for the iv administration of poorly soluble drugs-stability during sterilization and long-term storage. *Proceedings of the 22nd International Symposium on Controlled Release of Bioactive Materials*, 574–575.
- Müller, R. H., Jacobs, C., & Kayser, O. (2001). Nanosuspensions as particulate drug formulations in therapy: Rationale for development and what we can expect for the future. *Advanced Drug Delivery Reviews*, 47(1). Müller, R. H., & Keck, C. M. (2004). Challenges and solutions for the delivery of biotech drugs - A review of drug nanocrystal technology and lipid nanoparticles. *Journal of Biotechnology*, 113(1–3).
- Naeem Aamir, M., Ahmad, M., Akhtar, N., Murtaza, G., Khan, S. A., Shahiq-Uz-Zaman, & Nokhodchi, A. (2011). Development and in vitro-in vivo relationship of controlled-release microparticles loaded with tramadol hydrochloride. *International Journal of Pharmaceutics*, 407(1–2).
- Naturespharmacy. (2018). *Oral dosage forms advantages, disadvantages, and classification*. <http://naturespharmacy.biz/oral-dosage-forms.html>
- Nawal, A. (2018). Review on preparation, characterization, and pharmaceutical application of nanosuspension as an approach of solubility and dissolution enhancement. *Journal of Pharmacy Research*, 12(5).
- Nayon, A. U., Nesa, J.-U., Uddin, N., Amran, S., & Bushra, U. (2013). Development and validation of UV Spectrometric Method for the Determination of Cefixime trihydrate in Bulk and Pharmaceutical Formulation. *Asian Journal of Biomedical and Pharmaceutical Sciences*, 3(22).
- Newey-Keane, L., & Carrington, S. (2016). Controlling the Stability of Medicinal Suspensions. *American Pharmaceutical Review*.
- Nogueira, R., Queiroz, S. M., Silva, G. E. B., Rocha, W. F. C., Sarmanho, G. F., Almeida, R. R. R., & Moreira, G. F. (2012). Determination of volatiles in pharmaceutical certified reference materials. *Journal of the Brazilian Chemical Society*, 23(9).
- Pandey, S., Pandey, P., Kumar, R., & Singh, N. P. (2011). Residual solvent determination

References

- by head space gas chromatography with flame ionization detector in omeprazole API. *Brazilian Journal of Pharmaceutical Sciences*, 47(2).
- Park, Y. J., Ryu, D. S., Li, D. X., Quan, Q. Z., Oh, D. H., Kim, J. O., Seo, Y. G., Lee, Y. I., Yong, C. S., Woo, J. S., & Choi, H. G. (2009). Physicochemical characterization of tacrolimus-loaded solid dispersion with sodium carboxymethyl cellulose and sodium lauryl sulfate. *Archives of Pharmacal Research*, 32(6).
- Patel, D. K., Kesharwani, R., & Kumar, V. (2019). Lipid Nanoparticle Topical and Transdermal Delivery: A Review on Production, Penetration Mechanism to Skin. *International Journal of Pharmaceutical Investigation*, 9(4).
- Patel, R. (2010). Parenteral suspension: an overview. *Int J Curr Pharm Res*, 2(3).
- Patil, A. N., Shinkar, D. M., & Saudagar, R. B. (2017). REVIEW ARTICLE: SOLUBILITY ENHANCEMENT BY SOLID DISPERSION. *International Journal of Current Pharmaceutical Research*, 9(3).
- Patil, M. P., More, M. K., Chhajed, S. S., Bhambere, D. S., & Kshirsagar, S. J. (2020). Synthesis and characterization of mesoporous silica nanoparticles loaded with repaglinide for dissolution enhancement. *Indian Journal of Pharmaceutical Sciences*, 82(4).
- Patil, M. V., Bhise, S., & Kandhare, A. (2011). Pharmacological evaluation of ameliorative effect of aqueous extract of Cucumis sativus L. fruit formulation on wound healing in Wistar rats. *Chronicles of Young Scientists*, 2(4).
- Patravale, V. B., Date, A. A., & Kulkarni, R. M. (2010). Nanosuspensions: a promising drug delivery strategy. *Journal of Pharmacy and Pharmacology*, 56(7).
- Penton, Z. (1992). Determination of residual solvent in pharmaceutical preparations by static headspace GC. *Journal of High Resolution Chromatography*, 15(5).
- PerkinElmer®. (2018). *DSC 4000 Installation and Hardware Guide*.
- pharmacy180.com. (2019). *Complexation and protein binding*.
- Pharmapproach. (2020). Oral Administration of Drugs: Advantages and Disadvantages. In *Pharmapproach.com* (pp. 2–3). <https://www.pharmapproach.com/oral-administration-of-drugs-advantages-and-disadvantages/>
- Pragati S. Dubey, Ganesh S. Bangale, N. M. (2020). ESTIMATION AND VALIDATION OF RESIDUAL SOLVENTS IN MARKETED FORMULATION OF ANTI-HYPERTENSIVE DRUG BY GAS CHROMATOGRAPHIC METHOD. *Indian Research Journal of Pharmacy and Science*.

References

- Prakash, K., Raju, P. N., Kumari, K. S., & Narasu, M. L. (2008). Solubility and dissolution rate determination of different antiretroviral drugs in different pH media using UV visible spectrophotometer. *E-Journal of Chemistry*, 5(SUPPL. 2).
- Purna Chandra Reddy Guntaka, S. L. (2018). A COMPARATIVE STUDY OF LEDIPASVIR SOLID DISPERSION TECHNIQUE USING SPRAY DRYING AND HOT-MELT EXTRUSION. *International Journal of Pharmaceutical Sciences and Research*, 9 (12).
- Quintanar-Guerrero, D., Ganem-Quintanar, A., Allémann, E., Fessi, H., & Doelker, E. (1998). Influence of the stabilizer coating layer on the purification and freeze-drying of poly(D,L-lactic acid) nanoparticles prepared by an emulsion-diffusion technique. *Journal of Microencapsulation*, 15(1).
- Qureshi, S. A. (2010). In vitro-in vivo correlation (ivivc) and determining drug concentrations in blood from dissolution testing - a simple and practical approach. *Open Drug Delivery Journal*, 4(SPEC. ISSUE 1).
- R. Santosh, K., & T. Naga Satya, Y. (2016). (PDF) Pharmaceutical Suspensions: Patient Compliance Oral Dosage Forms. *World Journal of Pharmacy and Pharmaceutical Sciences*, 5(12).
- Raja, P. M. V., & Barron, A. R. (2021). Dynamic Headspace Gas Chromatography Analysis. Rice University. *Rice University*.
- Rane, Y., Mashru, R., Sankalia, M., & Sankalia, J. (2007). Effect of hydrophilic swellable polymers on dissolution enhancement of carbamazepine solid dispersions studied using response surface methodology. *AAPS PharmSciTech*, 8(2).
- Rao, G. C. S., Kumar, M. S., Mathivanan, N., & Rao, M. E. B. (2004). Nanosuspensions as the most promising approach in nanoparticulate drug delivery systems. In *Pharmazie* (Vol. 59, Issue 1).
- Raphael, B. (1999). Statistical evaluation of stability data for assessing variability of an analytical method. *Accreditation and Quality Assurance*, 4(6).
- Rastogi, V., Yadav, P., Lal, N., Rastogi, P., Singh, B. K., Verma, N., & Verma, A. (2018). Mathematical prediction of pharmacokinetic parameters-an in-vitro approach for investigating pharmaceutical products for IVIVC. *Future Journal of Pharmaceutical Sciences*, 4(2).
- Reeves, Philip T., Camille Roesch, M. N. R. (2017). *Routes of Administration and Dosage Forms. MSD Veterinary Manual*.

References

- <https://www.msdrvmanual.com/pharmacology/pharmacology-introduction/routes-of-administration-and-dosage-forms>
- Rote, A. P., Alhat, J., & Kulkarni, A. A. (2017). Development and Validation of RP-HPLC Method for the Simultaneous Estimation of Ledipasvir and Sofosbuvir in Bulk and Pharmaceutical Dosage Form. *International Journal of Pharmaceutical Sciences and Drug Research*, 9(06).
- Rowe, R. C., Sheskey, P. J., & Quinn, M. E. (2018). Handbook of Pharmaceutical Excipients Sixth Edition. *Revue Des Nouvelles Technologies de l'Information, sixth edit.*
- Sareen, S., Joseph, L., & Mathew, G. (2012). Improvement in solubility of poor water-soluble drugs by solid dispersion. *International Journal of Pharmaceutical Investigation*, 2(1).
- Savolainen, M., Kogermann, K., Heinz, A., Aaltonen, J., Peltonen, L., Strachan, C., & Yliruusi, J. (2009). Better understanding of dissolution behaviour of amorphous drugs by in situ solid-state analysis using Raman spectroscopy. *European Journal of Pharmaceutics and Biopharmaceutics*, 71(1).
- Sekiguchi, K., & Obi, N. (1961). Studies on Absorption of Eutectic Mixture. I. A Comparison of the Behavior of Eutectic Mixture of Sulfathiazole and that of Ordinary Sulfathiazole in Man. *Chemical and Pharmaceutical Bulletin*, 9(11).
- Shams, T., Sayeed, M. S. Bin, Kadir, M. F., Khan, R. I., Jalil, R. U., & Islam, M. S. (2011). Thermal, infrared characterization and in vitro evaluation of Repaglinide solid dispersion. *Der Pharmacia Lettre*, 3(6).
- Sharma, A., Jain, C. P., & Tanwar, Y. S. (2013). Preparation and characterization of solid dispersions of carvedilol with poloxamer 188. *Journal of the Chilean Chemical Society*, 58(1).
- Shid, R. L., Dhole, S. N., Kulkarni, N., & Shid, S. L. (2013). Nanosuspension: A review. In *International Journal of Pharmaceutical Sciences Review and Research* (Vol. 22, Issue 1).
- Shinohara, S., Eom, N., Teh, E. J., Tamada, K., Parsons, D., & Craig, V. S. J. (2018). The Role of Citric Acid in the Stabilization of Nanoparticles and Colloidal Particles in the Environment: Measurement of Surface Forces between Hafnium Oxide Surfaces in the Presence of Citric Acid. *Langmuir*, 34(8).
- Sigma-Aldrich Co. LLC. (2017). *SUPELCOSIL™ LC-DP HPLC Column*. https://www.sigmaaldrich.com/BD/en/product/supelco/58842?cm_sp=Insite--

References

- caContent_prodMerch_gruCrossEntropy_-_prodMerch10-4
- Singh, P., & Sinha, M. (2013). Determination of Residual Solvents In Bulk Drug and Formulations. *Am. J. PharmTech Res*, 3(4).
- Sinha, S., Ali, M., Baboota, S., Ahuja, A., Kumar, A., & Ali, J. (2010). Solid dispersion as an approach for bioavailability enhancement of poorly water-soluble drug ritonavir. *AAPS PharmSciTech*, 11(2).
- Sojitra, C., Tehare, A., Dholakia, C., Sudhakar, P., Agarwal, S., & Singh, K. K. (2019). Development and validation of residual solvent determination by headspace gas chromatography in Imatinib Mesylate API. *SN Applied Sciences*, 1(3).
- Somia Gul et al. (2018). DEVELOPMENT AND VALIDATION OF UV-SPECTROPHOTOMETRIC METHOD FOR ESTIMATION OF VELPATASVIR IN BULK FORM BY ABSORBANCE MAXIMA METHOD. *International Journal of Pharmacy*, 2249–1848.
- Taylor, L. S., & Zografis, G. (1997). Spectroscopic characterization of interactions between PVP and indomethacin in amorphous molecular dispersions. *Pharmaceutical Research*, 14(12).
- Teeranachaideekul, V., Junyaprasert, V. B., Souto, E. B., & Müller, R. H. (2008). Development of ascorbyl palmitate nanocrystals applying the nanosuspension technology. *International Journal of Pharmaceutics*, 354(1–2).
- TGA. (2017). *Australian Public Assessment Report for: Sofosbuvir / Velpatasvir*.
- The Product Makers (Australia) Pty Ltd. (2019). *Safety Data Sheet of Mango Flavor Natural*.
- Thermoscientific. (2018). *Routine-grade performance of a new static headspace autosampler for the analysis of residual solvents according to USP< 467> method* (Application Note 10676).
- Tomassetti, M., Catalani, A., Rossi, V., & Vecchio, S. (2005). Thermal analysis study of the interactions between acetaminophen and excipients in solid dosage forms and in some binary mixtures. *Journal of Pharmaceutical and Biomedical Analysis*, 37(5).
- Tran, P., Pyo, Y. C., Kim, D. H., Lee, S. E., Kim, J. K., & Park, J. S. (2019). Overview of the manufacturing methods of solid dispersion technology for improving the solubility of poorly water-soluble drugs and application to anticancer drugs. In *Pharmaceutics* (Vol. 11, Issue 3).
- Urbanetz, N. A. (2006). Stabilization of solid dispersions of nimodipine and polyethylene glycol 2000. *European Journal of Pharmaceutical Sciences*, 28(1–2).
- USP. (2012). Solutions / Buffer Solutions. In *USP* (pp. 5773–5774).

References

- USP. (2016). *Dissolution <711>*.
- USP. (2021). *Pharmaceutical dosage forms*. USP General Chapter <1151>.
- Van Eerdenbrugh, B., Froyen, L., Martens, J. A., Bleton, N., Augustijns, P., Brewster, M., & Van den Mooter, G. (2007). Characterization of physico-chemical properties and pharmaceutical performance of sucrose co-freeze-dried solid nanoparticulate powders of the anti-HIV agent loviride prepared by media milling. *International Journal of Pharmaceutics*, 338(1–2).
- Walsh, A. M., Mustafi, D., Makinen, M. W., & Lee, R. C. (2006). A surfactant copolymer facilitates functional recovery of heat-denatured lysozyme. *Annals of the New York Academy of Sciences*, 1066.
- Wang, J., & Somasundaran, P. (2005). Adsorption and conformation of carboxymethyl cellulose at solid-liquid interfaces using spectroscopic, AFM and allied techniques. *Journal of Colloid and Interface Science*, 291(1).
- Wang, Y., Zheng, Y., Zhang, L., Wang, Q., & Zhang, D. (2013). Stability of nanosuspensions in drug delivery. In *Journal of Controlled Release* (Vol. 172, Issue 3).
- WHO. (2009). Stability testing of active pharmaceutical ingredients and finished pharmaceutical products. WHO Technical Report Series, No. 953, Annex 2. In *World Health Organ Tech Rep Ser* (Vol. 6, Issue 953).
- WHO. (2021). *Hepatitis C*.
- Yadollahi, R., Vasilev, K., & Simovic, S. (2015). Nanosuspension technologies for delivery of poorly soluble drugs. In *Journal of Nanomaterials* (Vol. 2015).
- Yu, L. (2001). Amorphous pharmaceutical solids: Preparation, characterization and stabilization. *Advanced Drug Delivery Reviews*, 48(1).
- Zamani, F., Jahanmard, F., Ghasemkhah, F., Amjad-Iranagh, S., Bagherzadeh, R., Amani-Tehran, M., & Latifi, M. (2017). Nanofibrous and nanoparticle materials as drug-delivery systems. In *Nanostructures for Drug Delivery*.
- Zhang, D., Tan, T., Gao, L., Zhao, W., & Wang, P. (2007). Preparation of azithromycin nanosuspensions by high pressure homogenization and its physicochemical characteristics studies. *Drug Development and Industrial Pharmacy*, 33(5).
- Zhang, Y., Huo, M., Zhou, J., & Xie, S. (2010). PKSolver: An add-in program for pharmacokinetic and pharmacodynamic data analysis in Microsoft Excel. *Computer Methods and Programs in Biomedicine*, 99(3).
- Zhang, Y., Huo, M., Zhou, J., Zou, A., Li, W., Yao, C., & Xie, S. (2010). DDSolver: An

References

- add-in program for modeling and comparison of drug dissolution profiles. *AAPS Journal*, 12(3).
- Zhao, G. H., Kapur, N., Carlin, B., Selinger, E., & Guthrie, J. T. (2011). Characterisation of the interactive properties of microcrystalline cellulose-carboxymethyl cellulose hydrogels. *International Journal of Pharmaceutics*, 415(1–2).
- Zishan, M., Amir, M., Ahmad, Z., Hussain, M. W., Singh, P., & Idris, S. (2017). REVIEW ON APPLICATION AND FACTOR AFFECTING AND OFFICIAL MONOGRAPHS IN DISSOLUTION PROCESS. *Journal of Drug Delivery and Therapeutics*, 7(3).
- Zou, X., Sha, A., Ding, B., Tan, Y., & Huang, X. (2017). Evaluation and Analysis of Variance of Storage Stability of Asphalt Binder Modified by Nanotitanium Dioxide. *Advances in Materials Science and Engineering*, 2017.